Diss. ETH No. 15970

Molecular interactions along the ion pathway of the F_1F_0 ATP synthase

A dissertation submitted to the

FEDERAL INSTITUTE OF TECHNOLOGY ZÜRICH

For the degree of

DOCTOR OF NATURAL SCIENCES

Presented by

CHRISTOPH VON BALLMOOS

Dipl. Natw. ETH

Born July, 26, 1974

From Heimiswil (BE)

Accepted on the recommendation of

Prof. Dr. Peter Dimroth, examiner

Prof. Dr. Josef Brunner, co-examiner

Zürich 2005

Table of contents

Summary

Adenosine triphosphate (ATP) is the main carrier of free energy in living cells. A variety of molecular processes like biosynthesis, transport, or mobility are catalyzed by enzymes, which are fueled by ATP. A major proportion of ATP is synthesized by a single enzyme, the F_1F_0 ATP synthase. This membrane bound protein complex is found in bacteria, the chloroplasts of plants and in the inner membrane of mitochondria. As indicated by the name, the enzyme consists of two subcomplexes. The water soluble F_1 complex harbors the nucleotide binding sites and is responsible for the chemical coupling of ADP and inorganic phosphate to ATP. This reaction is catalyzed by a rotary mechanism, which induces conformational changes within F_1 driving the synthesis of ATP. The rotation energy for this process is supplied by a torque, which is generated in the membrane embedded F_0 part, utilizing a transmembrane electrochemical gradient. Compared to the F_1 part, from which a high resolution structure as well as many functional details are known, knowledge about the membrane embedded F_0 part trails behind.

The presented work is divided into nine chapters, which are dealing with different aspects of torque generation in the F_0 motor. The second chapter is written in German, and describes the applied technique of photocrosslinking to an audience of non specialists. Chapters three und four are dealing with the localization of the ion binding site in the F_0 motor relative to the membrane bilayer. The first approach describes the use of a photocrosslinking compound, which specifically interacts with the ion binding site. After illumination, the compound reacts with the lipids of the surrounding bilayer. The second approach uses fluorescence quenching to quantitatively determine the depth of a fluorescently labeled binding site in the membrane harboring spin-labeled phospholipids. Both experiments clearly show that the ion binding site is deeply embedded in the membrane and is located close to the centre of the bilayer. The fifth chapter describes the identification of the site of interaction within the ATP synthase of strongly toxic organotin compounds. A radioactively labeled organotin was equipped with a photoactivatable moiety and allowed the unambiguous identification of subunit a as the target of organotin compounds. The sixth chapter delineates the development of a novel approach to measure Na^+ uptake into liposomes. A fluorescent compound, which specifically complexes with Na^+ ions, is enclosed into proteoliposomes during reconstitution and the Na^+-transport can subsequently be monitored by means of fluorescence spectroscopy. The seventh chapter describes an experimental approach to characterize the ion binding site of the ATP synthase

from different organisms. The pH-dependent modification with the specific inhibitor dicyclohexylcarbodiimide (DCCD) of the ATP synthases from *Ilyobacter tartaricus, Escherichia coli*, spinach chloroplast and bovine mitochondria was measured and compared. Data analysis of such experiments is usually very laborious and the use of MALDI mass spectroscopy for facilitated data analysis is described. The results are subsequently interpreted in respect to an alternative coupling ion mechanism, in which a coordinated hydronium ion (H_3O^+) replaces the group protonation of an acidic residue thus far proposed. The eighth chapter describes a novel purification method for the hydrophobic a subunit of the F_0 part by means of mixed organic solvents. This kind of purification for the first time allowed the characterization of the entire a subunit by MALDI mass spectroscopy.

Finally, the discussion introduces the actual mechanistic models of the F_0 motor from different research groups. They are compared in respect to several critical aspects. Potential discrepancies between H^+ and Na^+ dependent enzymes are addressed and experiments towards their clarification are proposed.

Zusammenfassung

ATP ist die universelle Energieform in allen lebenden Zellen und ist verantwortlich für den Antrieb von vielen lebenswichtigen Prozessen sowie für die Synthese aller zellulären Bestandteile. Ein Grossteil des ATP wird von einem einzigen Enzym hergestellt, der F_1F_0 ATP Synthase. Dieses findet sich sowohl in den Membranen von Bakterien und Pflanzen, wie auch in tierischen Zellen. Wie der Name verrät, ist das Protein aus zwei Einheiten aufgebaut. Der wasserlösliche F_1 Teil ist für die chemische Kopplung von ADP mit anorganischem Phosphat zum energiereichen Phosphat verantwortlich. Die Reaktion wird von einem Rotationsmechanismus katalysiert, welcher durch konformationelle Änderungen im F_1 Teil die Herstellung von ATP ermöglicht. Der Antrieb für diese Rotationsbewegung stammt aus dem in der Membran eingebetteten F_0 Teil, welcher in der Lage ist, ein elektrochemisches Potential in eine Drehbewegung umzuwandeln. Während vom F_1 Teil sowohl die atomare Struktur wie auch viele funktionelle Eigenschaften bekannt sind, sind die Kenntnisse über den F_0 Teil weit weniger ausgeprägt.

Die vorliegende Arbeit befasst sich mit verschiedenen Aspekten der Antriebsbewegung im F_0 Teil. Das zweite Kapitel beschäftigt sich in einer Sprache, die sich an nicht Spezialisten wendet, mit der Technik des chemischen Photocrosslinking, welche in den folgenden Kapiteln zum Tragen kommt. Die Kapitel drei und vier beschäftigen sich mit der relativen und absoluten Lokalisierung der Ionenbindungsstelle des c-Rings der ATP Synthase in der Membran. Der erste Ansatz bedient sich eines photoaktivierbaren Crosslinkers, welcher kovalent mit der Bindestelle reagiert und nach Belichtung eine Quervernetzung mit Membranlipiden eingeht. Der zweite Ansatz beschreibt eine genauere quantitative Bestimmung der Ionenbindestelle mit Hilfe von einem Fluoreszenzmarker und spin-gelabelten Phospholipiden. Beide Ansätze führen zum eindeutigen Ergebnis, dass die Ionenbindestelle tief in der Membran eingebettet liegt. Im fünften Kapitel wird mit Hilfe eines photoaktivierbaren Derivativs die Bindestelle des Umweltgiftes Tributylzinnchlorid (TBT) an der ATP Synthase untersucht. Mit Hilfe einer radioaktiven Markierung kann die spezifische Bindung an die a-Untereinheit des F_0 Teils sichtbar gemacht werden. Das sechste Kapitel befasst sich mit einer neuartigen Methode zur Bestimmung von Na^+ Ionen in Lipidvesikeln (Liposomen). Die Technik bedient sich eines Fluoreszenzfarbstoffes, welcher spezifisch mit Na^+ interagiert. Der Farbstoff wird in die Liposomen eingeschlossen und der Transport kann kontinuierlich mittels Fluoreszenzspektroskopie nachgewiesen werden. Das siebte Kapitel

beschreibt einen experimentellen Ansatz zur Untersuchung der Ionenbindestelle der ATP Synthase aus verschiedenen Organismen. Dabei wird die pH abhängige Markierung des Inhibitors Dicyclohexylcarbodiimid (DCCD) an die ATP Synthase von *Ilyobacter tartaricus*, *Escherichia coli*, Chlorplasten aus Spinat und den Mitochondrien aus Rinderherz verglichen. Der Einsatz von Massenspektroskopie erleichtert dabei die Auswertung der Daten, welche durch konventionelle Methoden sehr aufwändig wäre. Die Ergebnisse werden danach im Hinblick auf ein koordiniertes Hydroniumion (H_3O^+) als alternatives Kopplungsion statt einer Punktprotonierung diskutiert. Das achte Kapitel beschreibt eine neue Methode zur Reinigung der stark hydrophoben a-Untereinheit des F_0 Teils mittels organischen Lösungsmitteln. Diese Art der Reinigung ermöglichte die erstmalige Identifikation der Untereinheit mittels Massenspektroskopie.

Die abschliessende Diskussion vergleicht die aktuellen Modelle zum Mechanismus der Ionentranslokation durch den F_0-Teil von verschiedenen Arbeitsgruppen. Die entsprechenden Modelle werden kurz vorgestellt und hinterher kritisch diskutiert. Mögliche Diskrepanzen zwischen den Mechanismen von H^+ und Na^+ abhängigen Enzymen werden angesprochen und Experimente zu deren Klärung vorgeschlagen.

1. General introduction

Adenosine triphosphate (ATP) is the main carrier of free energy in living cells. A variety of molecular processes like biosynthesis, transport, or mobility are catalyzed by enzymes, which consume the chemical energy stored in the terminal anhydride bond of the molecule. ATP is membrane impermeable and must therefore be permanently synthesized within the cell with a very high turn over rate. In an active human being, the total amount of ATP synthesis can reach the body weight of the human per day.

To accomplish the endergonic synthesis of ATP from adenosine diphosphate (ADP) and inorganic phosphate, an external energy source is required. Depending on the ATP synthesis mechanism one distinguishes between substrate chain phosphorylation and oxidative or light driven phosphorylation. The two latter processes use an electrochemical gradient across a biological membrane to store the energy derived from the degradation of nutrients, or light, respectively. The electrochemical gradient is then used by the F_1F_0 ATP synthase to generate ATP from its precursors. This ubiquitous enzyme is found in almost all organisms, e.g. in the cytoplasmic bacterial membrane, the thylakoid membrane of chloroplast and in the inner membrane of mitochondria (Figure 1-1).

1.1 F_1F_0 ATP synthases

F_1F_0 ATP synthase, also called F-type ATPase, is a multi subunit enzyme complex which is found in almost every living cell. Its overall structure is conserved among all species. The enzyme is anchored within the biological membrane with the F_0 part and it harbours a soluble peripheral F_1 part, which is exposed to the compartment, where ATP is synthesized.

The basic working principle involves a catalytic rotational mechanism to drive ATP synthesis. In the membrane embedded F_0 part, the electrochemical gradient is used to drive ions across the membrane. This ion flux is converted into rotational movement, which is transmitted to the soluble F_1 part via the mobile central stalk connected with the c ring. Within the F_1 part, the rotation induces conformational changes in the nucleotide binding site, allowing ATP synthesis.
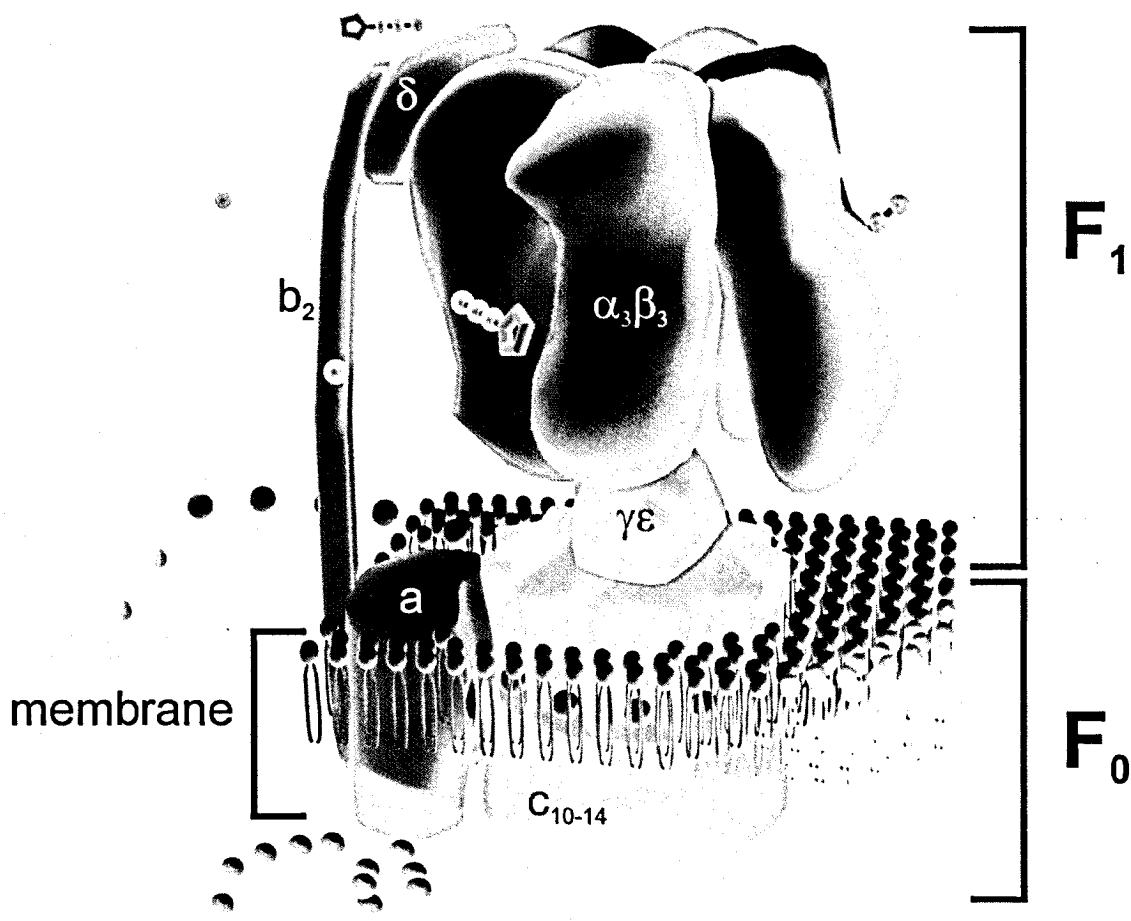
Figure 1-1. The overall structure of the ATP synthase in a biological membrane. F_1 and F_0 represent two motors, which exchange energy with each other through rotational coupling. The rotary subunits ($\gamma\varepsilon c_{10-14}$) are centrally localized and depicted in light grey, whereas the membrane anchored and cytoplasmic stator subunits ($ab_2\alpha\beta\delta$) are drawn in dark grey. During ATP synthesis, the coupling ions pass the membrane through the membrane embedded subunits.

Under anaerobic conditions, when the respiratory enzymes are not active, the F-ATPase can be used as an ion pump to establish the indispensable membrane potential under the cost of ATP. In this context, the two parts can be assumed as independent motors, which are able to exchange energy with each other.

The F_1F_0 complex from all sources can be dissociated under mild conditions into the two component parts, with the F_1 still functioning as an ATPase, and the membranous F_0 retaining the ion translocation function, although this is now passive and bidirectional. Only when the two parts are linked is ATP synthesized with the energy derived from vectorial ion translocation. Similarly, ATP hydrolysis can only be used to generate an ion motive force in the intact enzyme. This linkage of endergonic and exergonic reactions in F_1F_0 is called coupling. When the interaction between F_1 and F_0 is disrupted so that energy transduction is lost, the system is said to be uncoupled.

The enzyme has been particularly intensively studied over the past decades by many scientists. It is therefore not surprising, that the actual understanding of this enzyme derives from investigations, performed with a broad variety of systems and organisms. With respect to molecular biology, the enzyme of *E. coli* has been most intensively investigated and much important functional information was elucidated from this organism. The enzyme from bovine mitochondria played a crucial role in early and present structural investigations of the soluble F_1 part. In addition, ATP synthases from plant chloroplast or a variety of other bacteria have complemented the actual picture of this enzyme.

The catalytic F_1 domain, harbouring the nucleotide binding sites, has the universal subunit composition $\alpha_3\beta_3\gamma\delta\epsilon$, with a molecular mass ranging around 350 kDa. In bacteria, the F_0 contains the subunits ab_2c_{10-14}, making up a molecular mass of about 150 kDa.
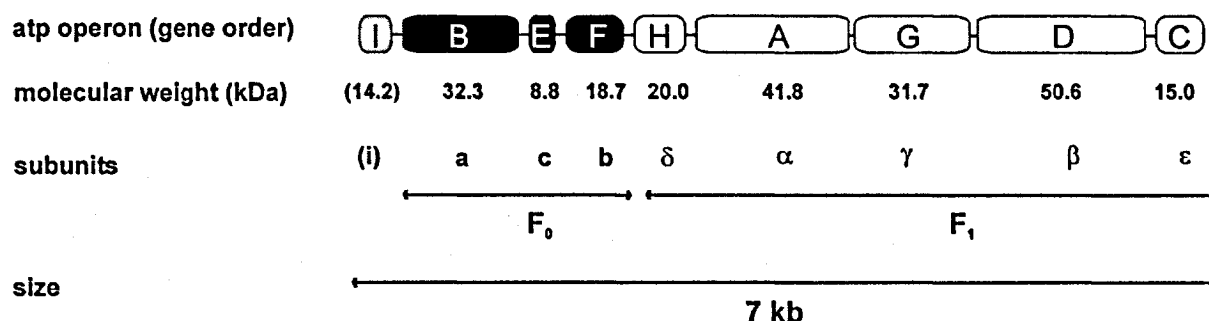
Figure 1-2 Organization of the *Ilyobacter tartaricus* atp operon.Genes encoding F_0 are colored black and genes encoding F_1 subunits are depicted in white. The gene encoding the i-protein is drawn in light grey.

In the bacterial genome, the coding regions for the eight subunits are clustered in a single operon, termed *unc* (*unc*oupled) or *atp*. The genes are arranged in the sequence *uncIBEFHAGDC*, transcribed and further translated into the i-protein, the F_0 subunits a, c and b and the F_1 subunits δ, γ, α, β, and ε, respectively (Figure 1-2). The role of the i-gene is still speculative. It codes for a small, most likely hairpin structured, membrane protein. During purification of the intact enzyme only substoichiometric amounts of the i protein are copurified. The deletion of the *uncI* gene does not affect a functional assembly of the enzyme complex; growth yield and ATP hydrolysis activity in isolated membranes are however decreased in the deletion mutant (Gay, 1984; von Meyenburg *et al.*, 1985). A recent work points to its possible function in Mg^{2+} uptake, by forming channel like structures with *atpZ*, a gene found in some bacterial *unc* operons (Hicks *et al.*, 2003). For ancient and recent reviews, see Boyer and Capaldi and Aggeler (Boyer, 1997; Capaldi and Aggeler, 2002).

1.1.1 Rotational energy drives ATP synthesis in the F_1 part

The F_1 part is effectively a complex of three α and three β subunits that displays strong negative cooperativity of substrate binding and, at the same time, strong positive cooperativity of enzymatic activity. To explain these unusual properties, Boyer proposed what has become known as the 'binding change' or 'alternating site' hypothesis (Figure 1-4). The key feature of this hypothesis is that the three catalytic sites, and therefore the three αβ subunit pairs containing these sites, are each in a different conformation at any one time. One is open and ready for ATP (or ADP + P_i) binding, while the second and third are partly open or closed, respectively, around bound nucleotide. ATP binding, and the resulting closure of the open site, produces a cooperative conformational change in which the other two sites are altered, so that the closed one becomes partly open and the partly open one becomes fully open. Thus, each site alternates between the three states as ATP hydrolysis or, in the reverse direction, as ATP synthesis, proceeds.

Obvious questions raised by any binding change mechanism are how the conformational changes are propagated between the three catalytic sites in F_1F_0, and how the catalytic site events are coupled to proton translocation. Boyer suggested that both could occur by rotation of one or more of the single copy subunits in F_1 (Boyer, 1993; Boyer, 2000). We now know that it is the γ, ε and c_{11} subunits that provide the rotor. Even earlier, the idea of subunit rotation was also developed independently by Cox and colleagues (Cox *et al.*, 1984), who proposed a c ring rotation against subunits a and b during proton translocation.

First hints for a rotational mechanism on an experimental basis were found, when it proved possible to visualize the F_1 part of the *E. coli* complex using cryoelectron microscopy. These analyses showed convincingly that the α and β subunits alternate around a hexagon containing a central mass that could be identified as the γ subunit.

When the individual images were classified on the basis of their dominant features, they fell into three classes, with the γ subunit being located at a different $\alpha\beta$ pair in each (Gogol *et al.*, 1990).

In 1994 the high-resolution (2.8 Å) structure of a major part of the bovine heart F_1, including $\alpha_3\beta_3$ and part of the γ subunit (Abrahams *et al.*, 1994) showed an enzyme in which the three catalytic sites had different conformations: one open, one closed for ongoing bond cleavage, and the third partly open for imminent release of product ADP and P_i (Figure 1-3, A and B). The limited contacts between γ and $\alpha_3\beta_3$ included a hydrophobic or greasy sleeve, provided by the N-terminal domains of the α and β subunits, an ideal structure for efficient rotation of the γ subunit. In the following years, it had been shown that crosslinking of γ to the C-terminal domain of β blocked activity (Aggeler *et al.*, 1995). Cross and colleagues extended this work by showing that, if the crosslink was subsequently released and reformed, γ became attached to a different β subunit (Duncan *et al.*, 1995).

It was three years after the high resolution structure, when this hypothesized rotation was visualized for the first time by Noji and coworkers (Noji *et al.*, 1997). They had the idea of attaching a fluorescently labeled actin filament to the γ subunit and watching the movements of this filament by video fluorescence microscopy. This group saw that ATP hydrolysis drove a 360° rotation of the actin filament in three 120° steps in one direction, although at a very slow rate (3%). More recently, the heavy actin filament has been replaced by small gold particles, allowing observation of the ATP hydrolysis reaction without notable delay (Yasuda *et al.*, 2001).

Although, a large body of information was won through the following structures of the other subunits of the F_1 part and their different combinations (Gibbons *et al.*, 2000; Lill *et al.*, 1996; Ogilvie *et al.*, 1997; Rodgers and Wilce, 2000; Uhlin *et al.*, 1997; Wilkens and Capaldi, 1998; Wilkens *et al.*, 1995; Wilkens *et al.*, 1997a; Wilkens *et al.*, 1997b), the interest shifted to the question, how rotation is accomplished in terms of ion transport and how the system is regulated.
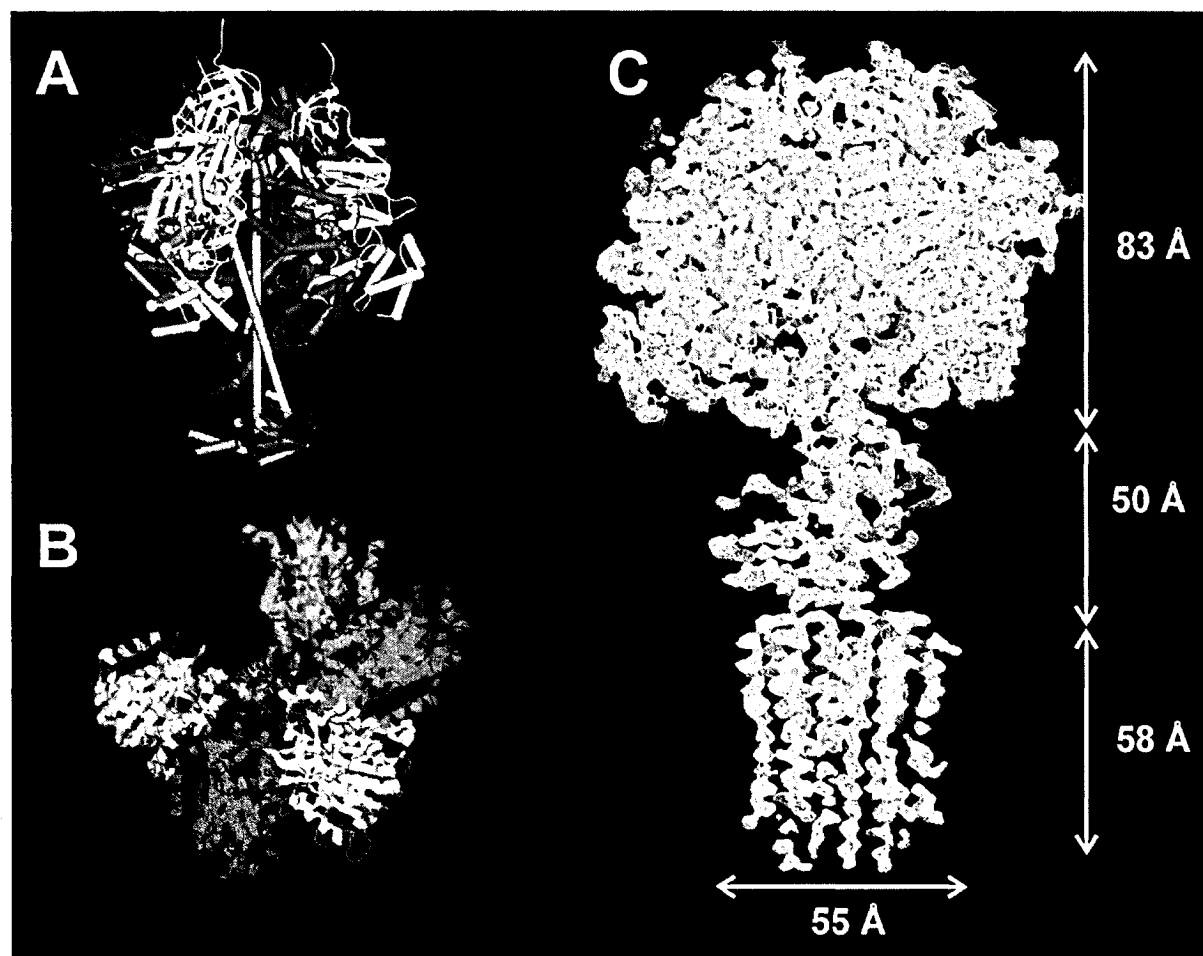
Figure 1-3. Structure of the F₁-ATPase from bovine mitochondria and yeast. A.) Side view of the F₁ ATPase from bovine mitochondria taken from (Menz *et al.*, 2001), showing the central arrangement of the γ subunit as a long bihelical structure with a beta-barreled socket docking onto the F₀ part. **B.)** The top view from the same enzyme is taken from (Abrahams *et al.*, 1994) and shows the central arrangement of α₃β₃ around the central γ-subunit. The β subunit carrying the empty nucleotide binding pocket is drawn in mint green. **C.)** Electron density map of the F₁c₁₀ complex from *S. cervisiae* at 3.9 Å, solved by X-ray crystallography taken from (Stock *et al.*, 1999). The structure allows an impression about the spatial arrangement of the intact enzyme. Subunit a, b and δ were lost during crystallization. Furthermore, the prediction of the c oligomer as ring like arrangement of hairpin structure could be confirmed. No side chain assignment was possible at this resolution, however.

An immediately arising question in a rotational system is what is rotating and what is not, in other terms, what is the rotor and what is the stator. In this perspective, crosslinking studies have been important for our present pictures of ATP synthase structure and function. The earliest experiments used chemical modifying reagents to induce crosslinking (Aggeler *et al.*, 1992), but these were soon superseded by genetic incorporation of pairs of cysteine residues into parts of the complex (for example, see Ref. (Aggeler *et al.*, 1995)). It is these

crosslinking studies that first defined the rotor composition fully by showing that γ, ε and the c subunit ring must rotate together: they can be covalently interconnected without loss of ATP hydrolysis-driven proton pumping or ATP synthesis (Schulenberg *et al.*, 1999; Tsunoda *et al.*, 2001). The groups of Fillingame and Cross conducted extensive crosslinking studies within the F_0 part, all of which are consistent with a rotation of the c ring against the ab_2 subcomplex (Fillingame *et al.*, 2000; Hutcheon *et al.*, 2001).
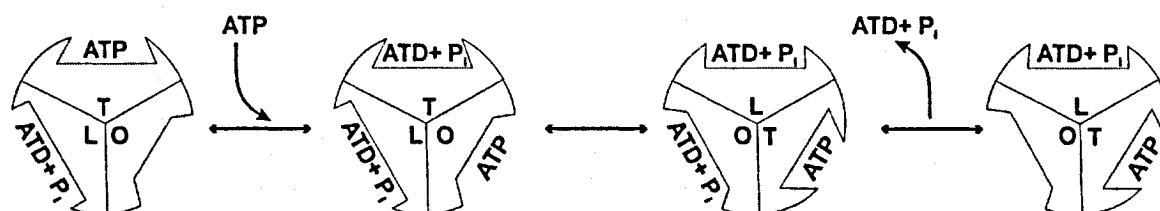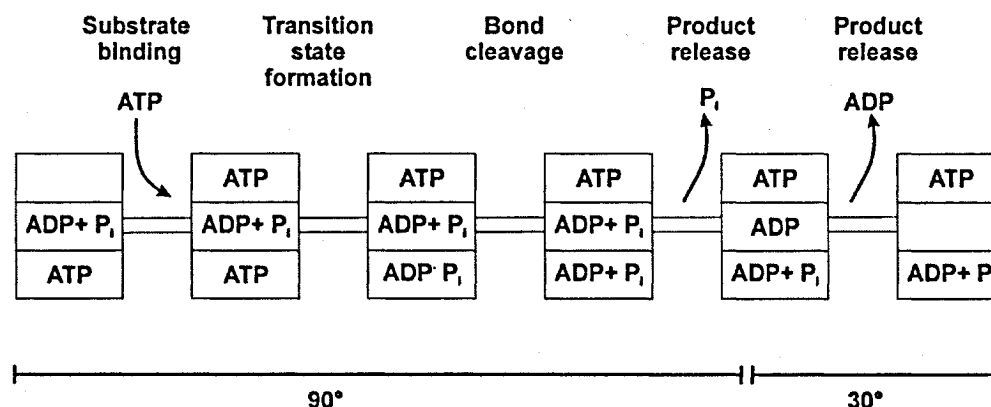
Figure 1-4. Binding change mechanism during ATP hydrolysis taken from (Capaldi and Aggeler, 2002). A.) Each catalytic site cycles through three states: T, L and O. ATP binds to the O (open and empty) site-to convert it into a T (tight and ATP-occupied) site. After bond cleavage, the T site is converted into the L (loose and ADP + P_i-occupied) site, from which the products can escape to recover the O state. At any one time, the three catalytic sites are in the O, T and L states, respectively. The concerted switching of states in each of the sites results in the hydrolysis (or synthesis) of one ATP molecule, and a rotation of the γ–ε rotor of 120°. B.) Substeps in the hydrolysis or synthesis of one ATP molecule based on kinetic and inhibitor studies (reviewed in (Weber and Senior, 2000)) are shown for a three site mechanism. Thus, ATP binding in the open site (top) leads to transition state formation and then bond cleavage in a closed site (bottom), followed by P_i release from a partly open site as it opens fully and then releases ADP (middle). Each step in (b) could produce a substep in the rotation of the γ subunit, so that the 90° rotation seen by Yasuda *et al.* (Yasuda *et al.*, 2001) is broken up into several steps.

A different question is how the rotations of $\gamma-\varepsilon$ and the c ring are coupled to ATP hydrolysis. As pointed out by Oster and Wang (Oster *et al.*, 2000), efficiency increases if energetic transactions proceed in small steps and, according to thermodynamic principles, the more the better. The implication is that for each 120° turn (needed for the synthesis or hydrolysis of 1 ATP), there must be several substeps linked to the catalytic site reaction, each conveyed to the γ subunit by a different conformational change in the $\alpha_3\beta_3$ ring. Consideration of the reaction scheme (Figure 1-4) for ATP hydrolysis indicates several possible mechanochemical steps: ATP binding, transition state formation, bond cleavage, Pi release and ADP release. Several or all of these steps can alter the conformation of $\alpha\beta$ pairs to drive or facilitate rotation of the γ subunit. In 2001, Yasuda *et al.* (Yasuda *et al.*, 2001) were able to resolve two substeps – a 90° (ATP binding) and a 30° (ADP release) rotation of γ – in their latest experiments. There is evidence for other substeps involving bond cleavage (Turina and Capaldi, 1994) and P_i binding (Weber and Senior, 2000) and it is therefore suggested that there are at least four conformational states to provide substeps in the overall 120° rotation (Figure 1-4). Insights into the conformational changes involved in the movements of the rotor within F_1 can be obtained from comparisons of recently reported structures of the enzyme (Gibbons *et al.*, 2000; Hausrath *et al.*, 2001). Evidence that the different arrangements of γ and ε seen in the X-ray studies are functionally relevant and not caused by crystallization artifacts comes from cryoelectron microscopy (Wilkens and Capaldi, 1994) and crosslinking studies (Aggeler and Capaldi, 1996).

1.1.2 The ion motive force is converted into mechanical rotation in the F_0 part

Structurally, the least well-defined part of the ATP synthase is F_0, composed of the three subunits a, b, and c. So far no high resolution structures of this domain are known, which would undoubtedly be needed to explain the energy transduction mechanism in molecular terms. The electron density map at 3.9 Å of the F_1c_{10} complex from *S. cervisiae* is the only structure in which the connection between the F_1 and F_0 parts can be seen (Stock *et al.*, 1999) (Figure 1-3). The interaction region between $\gamma\varepsilon$ and c_{10} was, however, poorly resolved, so that no interaction sites could be predicted. Subunits a, b and δ were lost during the crystallization process. However, a large body of biochemical knowledge about the driving forces used for rotation, the ion path across the membrane and the function of key amino acid residues is available to draw a good picture of the F_0 motor. Based on moderate-resolution structural data the overall architecture of F_0 consists of an oligomeric ring of c subunits that is flanked

laterally by a single a subunit (Mellwig and Bottcher, 2003). Subunit a is connected by the peripheral stalk b_2 subunits to F_1 and the c ring is linked at the cytoplasmic surface to the central stalk subunits γ and ε which, as mentioned above, together build the rotor.

1.1.2.1 Subunit a

Subunit a is the largest polypeptide of the F_0 sector and it has been proposed to consist of 5 or 6 membrane spanning α-helices (Jäger et al., 1998; Long et al., 1998; Valiyaveetil and Fillingame, 1998; Yamada et al., 1996). Whereas there is general agreement about the topology for the two C-terminal helices, different results have were obtained concerning the loop regions and in the localization of the N-terminus. There seems to be no direct interaction with the F_1 part, but only with the two other membranous subunits b and c. Together with the c-ring, subunit a plays a key role in the ion translocation mechanism (Deckers-Hebestreit and Altendorf, 1996; Fillingame, 1990; Howitt et al., 1996). The amino-terminal domain seems not to be directly involved in transport but required for assembly of the F_0-moiety or for membrane insertion (Lewis and Simoni, 1992). Extensive crosslinking studied from Jiang and Fillingame showed a neat interaction of the two C-terminal helices with the c-ring (Jiang and Fillingame, 1998). Together with a series of second site suppressor mutations, that restore function of primary mutants, the group of Fillingame has proposed a model for helical arrangement in subunit a (Fillingame et al., 2003). Therein, aR210 (E. coli numbering) is an essential residue directly involved in ion translocation (Cain and Simoni, 1989; Eya et al., 1991; Lightowlers et al., 1988). Recent mutational investigations on the equivalent residue in the P. modestum enzyme shed light into its pivotal role during transport (Wehrle et al., 2002). Besides aR210, site directed mutagenesis has revealed Glu219 and His245 to be important, but not essential in the E. coli subunit a (Cain and Simoni, 1986; Cain and Simoni, 1988; Cain and Simoni, 1989; Eya et al., 1991; Hartzog and Cain, 1994; Howitt et al., 1990; Lightowlers et al., 1988). Only few structural information about subunit a is available, since the particular hydrophobicity of the protein severely complicates the handling of this protein. In a recent approach, Dmitriev and Fillingame have successfully purified subunit a in mixed polar organic solvents. A subsequent structural investigation by NMR analogously to subunit c, however, was not successful (Dmitriev et al., 2004). The intriguing interaction of subunit a with the oligomeric c-ring displays one of the remaining mysteries of the ATP synthase. On one hand, there is a neat interaction of the subunits during ion transport; on the other hand, they rapidly rotate against each other during catalysis. If the interaction between the two is lost, which is easily achieved by addition of detergent, rotation is no longer coupled to ion

transport (uncoupled enzyme). It is therefore not surprising, that in the crystallographic analysis of the entire complex from yeast mitochondria, subunit a was lost during crystallization (Stock et al., 1999).

1.1.2.2 Subunit b

In the enzyme complex, two identical b subunits make up the peripheral stalk as a parallel dimer. Dimerization of the b subunits is thought to be an early event necessary for enzyme assembly and function (Sorgen et al., 1998a; Sorgen et al., 1998b). The two b subunits exist in an extended α-helical conformation, spanning from the periplasmic side of the membrane to near the top of F_1. Detailed structural information of the entire b subunit is not available so far. In recent electron microscopy studies, it was possible to distinguish the peripheral stalk from the remainder of the enzyme (Mellwig and Bottcher, 2003). In the amino-terminal membrane spanning region, the peripheral stalk contacts a single a subunit. Similarly, at the carboxyl end of the peripheral stalk, the two b subunits interact with a single δ subunit. The b dimer has been studied by a variety of traditional biochemical approaches such as CD spectroscopy, cross-linking, and sedimentation experiments (Dunn, 1992; Futai et al., 1989; Greie et al., 2000; McCormick et al., 1993; Revington et al., 1999). NMR studies with the membrane spanning part in mixed polar solvents and a systematic mutagenesis approach supported a model suggesting that the amino-termini of the two b subunits were in close contact and then the subunits diverge as they traverse the membrane (Dmitriev et al., 1999; Hardy et al., 2003). X-ray crystallography of a model polypeptide reflecting residues 62-122, corresponding to the dimerization domain, showed an extended, highly α-helical structure (Del Rizzo et al., 2002). The two monomers were shown to interact with their C-terminal regions, even in the absence of the other ATPase subunits (Dunn and Chandler, 1998; McLachlin et al., 1998; Rodgers et al., 1997; Sawada et al., 1997). Therefore the $b_2\delta$ complex seems to have a shape consistent with its role to act as the peripheral stalk of ATP synthase and linking subunit a to $\alpha_3\beta_3$ (Dunn et al., 2000). Further evidence for the long extension of subunit b from the bilayer to the top of the F_1 moiety derived from crosslinking studies (Rodgers and Capaldi, 1998). A disulfide crosslink was formed between residue 156 of subunit b to the N-terminal region of subunit α. This linkage between α and b did not affect ATPase activity, but proton pumping was markedly reduced. An explanation for this finding would be, that the torque generated by rotation of the γε domain within the $\alpha_3\beta_3$ hexamer could require compensation by conformational flexibility presented by the connection between the peripheral stalk and F_1 (Rodgers and Capaldi, 1998). Although the

two b subunits have long been viewed as a single functional unit, the asymmetric nature of the enzyme complex suggests that the functional roles of each b subunit should not necessarily be considered equivalent (Grabar and Cain, 2004). The role of subunit b as elastic energy storage has been raised and different models are discussed (Blum *et al.*, 2001). Recent work on subunit b is also done by Weber and Senior and the group of Gräber, which are investigating the strength of the $b_2\delta\alpha_3\beta_3$ complex by fluorescent methods (Diez *et al.*, 2004; Weber *et al.*, 2004). Thereby, Diez *et al.* point out, that the interaction of b_2 to F_1 is not strong enough to support models, in which the free energy for ATP synthesis is accumulated in the elastic strain between stator and rotor and then transduced to the catalytic site in one single step.

Although, subunit b has been shown to be indispensable for ion transport (Schneider and Altendorf, 1985), no direct participation could be found. In a recent work it was shown, that the helical part of subunit b is sufficient to drive coupling ion transport across the membrane, although not at full speed (Greie *et al.*, 2004).

1.1.2.3 Subunit c

Subunit c of *E. coli* consists of 79 mostly hydrophobic amino acids. It plays a key role in the ion translocation mechanism. A conserved carboxyl group (Asp61 in *E. coli*) serves as binding site for the protons during their translocation across the membrane. In the sodium-dependent F-type ATPase of *Propionigenium modestum* the equivalent residue is Glu65. Additional ligands for sodium binding are Ser66 and Gln32 (Kaim *et al.*, 1997). The protein folds like a hairpin with two transmembrane-spanning α-helices separated by a polar loop region, which is exposed to the cytoplasm. Such an arrangement is supported by biochemical and genetic experiments (reviewed in (Deckers-Hebestreit and Altendorf, 1996)) as well as by NMR data of subunit c monomers (see below). Structure determination of *P. modestum* subunit c was performed by NMR spectroscopy with protein solubilized in dodecyl sulfate micelles (Matthey *et al.*, 2002; Matthey *et al.*, 1999). The secondary structure was found to comprise four well defined α-helices connected by short loops. The helical structure is interrupted in the region of the Na^+ binding site. Due to the lack of long range NOEs, it was not possible to assign a tertiary structure. The solution structure of the *E. coli* c-monomer was determined using NMR in a chloroform/methanol/water (4:4:1) mixture at pH 8.0 and 5.0 (Rastogi and Girvin, 1999a; Rastogi and Girvin, 1999b). At these pH values the protein folds into two extended, slightly bent α-helices of 38 and 33 amino acids in length, which are connected by a polar loop. The two structures adopt different conformations at low or high pH, the major distinction being a 140° turn of helix II with respect to helix I. It is assumed

that this conformational change is elicited by the protonation or deprotonation of Asp61. With the aid of this structural basis, a mechanistic model was proposed describing how proton translocation across F_0 could be coupled to the generation of torque, which is essential for ATP synthesis (Rastogi and Girvin, 1999b). In this mechanism, torque generation is assumed to be driven by the clockwise rotation of helix II of subunit c (as viewed from the cytoplasm) when Asp61 becomes protonated. The interface between subunits a and c is stabilised *via* electrostatic interactions, and thus helix II of subunit c moves in a ratchet-like manner versus the penultimate helix of subunit a. This promotes the movement of the c-oligomer versus subunit a. After deprotonation of Asp61 from the following c subunit the starting position is regenerated. The idea of a protonation/ deprotonation mechanism for torque generation in F_0 has further been worked out by the group of Fillingame. They slightly modified the model of Rastogi and Girvin to explain discrepancies that have been arisen from crosslink experiments and mutagenesis studies, which questioned the physiological relevance of the pH-dependent conformational change of subunit c (Fillingame *et al.*, 2003).

1.1.2.4 Subunit c oligomer

It was supposed that the subunit c oligomer is arranged in F_0 as a ring-like structure. This assumption was based on crosslinking studies (Jones *et al.*, 1998), tryptophane scanning mutagenesis (Groth *et al.*, 1998; Schnick *et al.*, 2000), electron microscopy (Birkenhager *et al.*, 1995; Singh *et al.*, 1996; Takeyasu *et al.*, 1996) and X-ray crystallography (Stock *et al.*, 1999). However, the stoichiometry (Foster & Fillingame, 1982; Jones & Fillingame, 1998; Dmitriev *et al.*, 1999; Schnick *et al.*, 2000; Jiang *et al.*, 2001) and the helix packing were discussed controversially (Groth *et al.*, 1998; Jones & Fillingame, 1998). In the following years, the structure and the stoichiometry of c-oligomers from different organisms were elucidated. A first structural model was obtained from protein crystals of the F_1c_{10} complex from *S. cervisiae* (Stock *et al.*, 1999) (Figure 1-3).The electron densities of individual c subunits show that they consist of two α-helices, linked by a loop. However, the side chain orientation in the c-oligomer could not be resolved. Recently, the c-rings of chloroplast, *I. tartaricus* and *P. modestum* ATPase were analysed by atomic force microscopy and *cryo* electron microscopy of 2D-crystals (Meier *et al.*, 2003; Seelert *et al.*, 2000). Chloroplast c-oligomers are composed of 14 monomers, whereas the *I. tartaricus* and *P. modestum* ATPase comprises 11 c subunits. The stoichiometry of the *E. coli* ATP synthase is still under discussion, though recent experiments point to a preferred number of 10 subunits (Jiang *et al.*, 2001; Tomashek and Brusilow, 2000; J. C. Greie and K. Altendorf, unpublished

results), a value also found for the thermophilic bacterium *Bacillus* PS3 (Mitome *et al.*, 2004). In the structure of the *I. tartaricus* c-oligomer the two helices forming one c subunit are identified by the connecting loop (Vonck *et al.*, 2002). The inner helices are packed very tightly. This tight helix packing leaves no space for large side chains, and therefore the most likely residues at the helix interface are glycines. This allowed the assignment of the inner helices to the N-terminal half of the c subunit sequence.
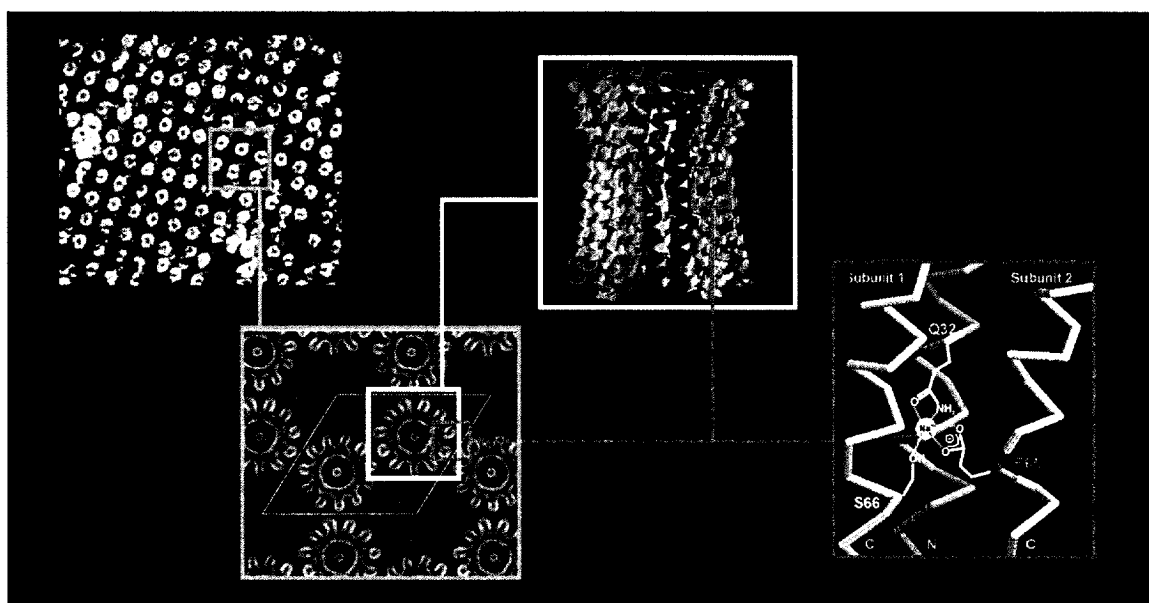
Figure 1-5. Structure of the c-ring of the ATP synthase from *I. tartaricus*. (From left to right). Atomic force microscopy analysis of 2D crystals of the isolated c-ring of *I. tartaricus* allowed determining the undecameric stoichiometry of this species. The analysis of the same crystals by cryo electron microscopy allowed resolving the turbine like structure of the c-ring. The 4.5 Å resolution was however insufficient to determine the orientation of the side chains. Various biochemical data allowed a prediction of the Na$^+$ binding site, which is localized in the center of the membrane bilayer. Pictures taken from (Meier and Dimroth, 2002; Meier *et al.*, 2003; Vonck *et al.*, 2002).

In this model a Na$^+$ binding pocket is formed in a space flanked by three helices and there may be left enough space between neighboring outer helices and the connecting inner helix for access channels from the cytoplasm to the binding sites in the center of the bilayer (von Ballmoos *et al.*, 2002a; von Ballmoos *et al.*, 2002b; Vonck *et al.*, 2002). The binding site includes Glu65 from one c subunit and Ser66 and Gln32 from the neighboring c subunit (Kaim *et al.*, 1997; Meier and Dimroth, 2002) (Figure 1-5).

Interestingly, the number of c subunits forming the ring is not fixed but varies among species. Hence, there is obviously a mismatch between the threefold symmetry of F_1 and the number

of c subunits in F_0. In one complete rotation of the rotor as many ions as c subunits present traverse the membrane and lead to the formation of three molecules of ATP. The H^+ (Na^+) to ATP stoichiometry is therefore not integer but varies between 3.3 (c_{10}) and 4.7 (c_{14}). The physiological relevance of the different ratios and the obvious prerequisite of a mismatch are topics of actual discussions.

1.1.3 Na^+ dependent F_1F_0 ATP synthases

1.1.3.1 *Propionigenium modestum* and *Ilyobacter tartaricus*

Although most organisms are featuring an ATP synthase, which uses protons as coupling ions, this is not true for every organism. In the early 1980's, Schink and coworkers could isolate and characterize marine bacteria from anoxic brackwater in Venice (Schink, 1984; Schink and Pfennig, 1982).

Propionigenium modestum is a rod shaped, strictly anaerobic, non motile gram negative bacterium, which grows on the fermentation of succinate to propionate and CO_2 (Hilpert *et al.*, 1984). The only exergonic reaction in the energy-metabolism from *P. modestum* is the decarboxylation of (S)-methylmalonyl-CoA to propionyl-CoA and carbon dioxide. During this decarboxylation reaction sodium ions are translocated across the lipid membrane and generate an electrochemical Na^+-gradient. This gradient can be used by the Na^+ translocating F_1F_0 ATP synthase to synthesize ATP (Hilpert *et al.*, 1984;. Laubinger and Dimroth, 1987; Laubinger and Dimroth, 1988).

The close relative *Ilyobacter tartaricus* features the same morphological and physiological properties as *P. modestum*. Besides L-tartrate, *I. tartaricus* degrades citrate, pyruvate, glucose and fructose with fermentation products formiate, acetate and probably CO_2. *I. tartaricus* also uses a Na^+ gradient as driving force for its ATP synthase. This could be generated by an oxaloacetate decarboxylase Na^+ pump, as tartrate is most likely converted to oxaloacetate and further degraded *via* its decarboxylation to pyruvate. However, *I. tartaricus* is easier to cultivate, and the better yields and the extremely high similarity to *P. modestum* in respect to the ATP synthase makes it an ideal working organism (Neumann *et al.*, 1998). A third bacterium, *Acetobacter woodi*, is also known to rely on a Na^+-dependent ATP synthase (Heise *et al.*, 1992).

1.1.4 General features of the *P. modestum* ATP synthase

The *P. modestum* F_1F_0 ATP synthase is homologous to other F-type ATPases (Dimroth, 1997). The eight different subunits are organized in a single operon on the chromosome. Compared to *E. coli*, the sequence conservation within subunits is rather low; exceptions are the nucleotide binding subunits α and β, which show high homology in most species. The most striking feature is the selectivity of the enzyme for sodium ions. In the absence of sodium ions, no hydrolysis activity can be measured. Only within a narrow pH range around 6.5, the enzyme can alternatively pump protons across the membrane. Under more physiological condition, the enzyme shows a strong dependency on sodium ion concentration and exhibits a functional pH range from 7 to 9. Li^+ can act as an alternative coupling ion, however with a K_m which is about ten-times higher than for Na^+ (Kluge and Dimroth, 1993a; Kluge and Dimroth, 1993b). As expected, the ion specificity is determined by the F_0 part alone. This allowed the construction of *E. coli* (F_1 part) and *P. modestum* (F_0 part) hybrid enzymes, showing ATP hydrolysis dependent Na^+ transport (Gerike *et al.*, 1995; Kaim and Dimroth, 1993; Kaim and Dimroth, 1994). Important properties of the coupling ion were deduced from kinetic studies with the covalent inhibitor dicyclohexylcarbodiimide (DCCD) by Kluge *et al.* (Kluge and Dimroth, 1993a). Similar to the H^+ translocating enzymes, DCCD covalently interacts with the conserved acidic residue of the c-subunit (Asp61 in *E. coli*, Glu65 in *P modestum*). As expected for an acid catalyzed reaction, the velocity shows a strong pH dependency with an inflection point at pH 6.5-6.8, representing the p_K of the glutamate in the hydrophobic environment of the membrane. If Na^+ is added to the solution, the dependency is shifted towards the acidic range (Kluge and Dimroth, 1993b). This reflects a competition of the two ions for the binding site. More insights in the coordination of the Na^+ ions were obtained in 1997, when Kaim *et al.* showed, that two further residues, Gln32 and Ser66, are required for successful coordination of the Na^+ ion within the binding site (Kaim *et al.*, 1997).

1.1.5 The ion pathway through the membrane

Both the ATP synthesis and hydrolysis are intimately coupled to ion transport across the membrane, which is accomplished by the membrane embedded F_0 part. There is general agreement, that during ATP synthesis, the coupling ions enter the membrane from the periplasm through a half channel in subunit a, from where they are dislodged to subunit c in the middle of the membrane. The ions are kept on their binding sites, until they are released to

the cytoplasm through intrinsic half channels within the c-ring (Meier *et al.*, 2003; von Ballmoos *et al.*, 2002a; von Ballmoos *et al.*, 2002b). In contrary to this model, a second half channel within the a subunit is proposed for H^+-translocating enzymes. Whereas there is clear evidence for the existence of the periplasmic channel of subunit a, the experimental data for a cytoplasmic half channel within subunit a are rather poor (Angevine *et al.*, 2003; Kaim *et al.*, 1998). It might however be that the two types of enzymes do slightly differ in the structure of their and a and c subunits, which will be discussed in more detail in the last chapter of this work.

1.1.6 The role of the membrane potential during ATP synthesis

According to Mitchell's chemiosmotic model energy stored in a transmembrane electrochemical ion gradient is utilized by the ATP synthase to produce ATP from ADP and phosphate. A long-standing tenet of this model is the assumption that membrane potential ($\Delta\psi$) and transmembrane ion gradients are thermodynamically equivalent:

Proton motive force (Δp) = $\Delta\psi$ + (2.3 RT/F) x ΔpH

While this relationship accurately describes the equilibrium energetic coupling, there is evidence that the transmembrane electrical potential controls the kinetics of the rotary motion in a manner that is independent from the ion gradient (Kaim and Dimroth, 1999). In the absence of the electrical driving force the F_0 motor is in an idling mode, which allows sodium ions to exchange across the membrane. The idling mode persists in the presence of a transmembrane Na^+ gradient (ΔpNa), but is converted into unidirectional Na^+ transport if a membrane potential $\Delta\psi$> -40 mV is applied. The pivotal role of the membrane potential as driving force for the ATP synthase is reinforced in ATP synthesis experiments with the reconstituted enzymes from *P. modestum*, *E. coli*, or spinach chloroplasts. These do not show any ATP formation in the absence of $\Delta\psi$ (Kaim and Dimroth, 1999).

These coherent results demand to revisit the classical acid base transition experiment performed almost 40 years ago (Jagendorf and Uribe, 1966). Thylakoids equilibrated with succinate buffer pH 5 synthesize ATP, when the outside pH is increased rapidly to pH 8. It was therefore concluded that ATP synthesis could be driven by ΔpH only. However, in more recent investigations the succinate monoanion, which is the most abundant form at pH 5, is shown to be membrane permeable generating a diffusion potential of approximately 140 mV

under the experimental conditions employed. ATP synthesis is only observed when the diffusion potential is created, but not in parallel experiments with membrane-impermeable buffers creating ΔpH only. The rationale for the permeability of the succinate monoanion is a delocalized and therefore shielded negative charge shared by both carboxylic groups in an energetically favored ring structure. Accordingly, maleinate (cis) but not fumarate (trans) induces a diffusion potential and supports ATP synthesis in similar experiments (Kaim and Dimroth, 1999).

1.1.7 Model of the F_0 motor

Without energization, the F_1F_0 ATP synthase is resting in its idling mode and catalyzes Na^+-exchange across the membrane. The rotor is not locked in a fixed position but performs thermal fluctuations in both directions against the stator within a narrow angle (Kaim and Dimroth, 1998) (Figure 1-6, top).

The fundamental question that has to be answered is how the electric potential drives the ions through the F_0 motor components and how this ion flux is linked to the generation of torque. It is important to recognize that the rotor sites switch between the empty and the ion bound states, which endow them with strikingly different properties. It can be assumed, that the binding sites outside of the a-c interface are occupied by Na^+ ions. Within the interface, however, the empty binding site is negatively charged and therefore electrostatically attracted by the universally conserved stator arginine (R227 in *P. modestum*) or by the membrane potential. After ion binding from the periplasmic channel the net charge of the site is reduced. This lowers the energy barrier for its diffusion through the hydrophobic rotor-stator part and prevents it from getting attracted backwards by the arginine.

The positive stator charge (R227) plays a fundamental role in the function of the F_0 motor. Any mutation of this residue even the most conservative exchange to a lysine abolishes the function of the *E. coli* enzyme completely (Vik and Antonio, 1994). The key role of R227 is strongly supported by mutational investigations with the *P. modestum* ATP synthase, which further establish its necessity for the dissociation of ions from approaching rotor sites (Wehrle et el., 2002).

When driving ATP synthesis, an ion arrives from the periplasm via the stator channel at an empty rotor site and binds to it (Figure 1-6, left). The intrinsic rotor channel is closed at this position to prevent ion leakage through the membrane along this route. After the site has moved out of the interface with the stator, the rotor channel reopens and allows the bound ion

to freely exchange with the cytoplasmic reservoir. However, at physiological pH and Na^+ concentrations, the site is occupied until it reaches the stator from the opposite side, where it encounters the positive stator charge causing dissociation of the ion and release through its intrinsic rotor channel into the cytoplasm. Now negatively charged, the site is electrostatically attracted by the stator charge and guided into the a-c interface. Without an external driving force there is an equal probability for the rotor site to move in either direction and the motor resides in its idling mode. After applying sufficient transmembrane voltage, however, the diffusion becomes biased towards the stator channel. Attraction of the site towards the channel can be rationalized by a horizontal component of the membrane potential (Dimroth *et al.*, 1999; Xing *et al.*, 2004). This will be present between two aqueous channels reaching the center of the membrane from opposing sides. Given that the conductive channels have essentially the same potential as the connected reservoirs, the potential drop will occur laterally between them if their termini overlap in the center of the bilayer. When the rotor site has picked up an ion from the stator channel reducing its net charge to that of a dipole, it moves onward through the hydrophobic part of the stator, while the arginine attracts the next empty rotor site.
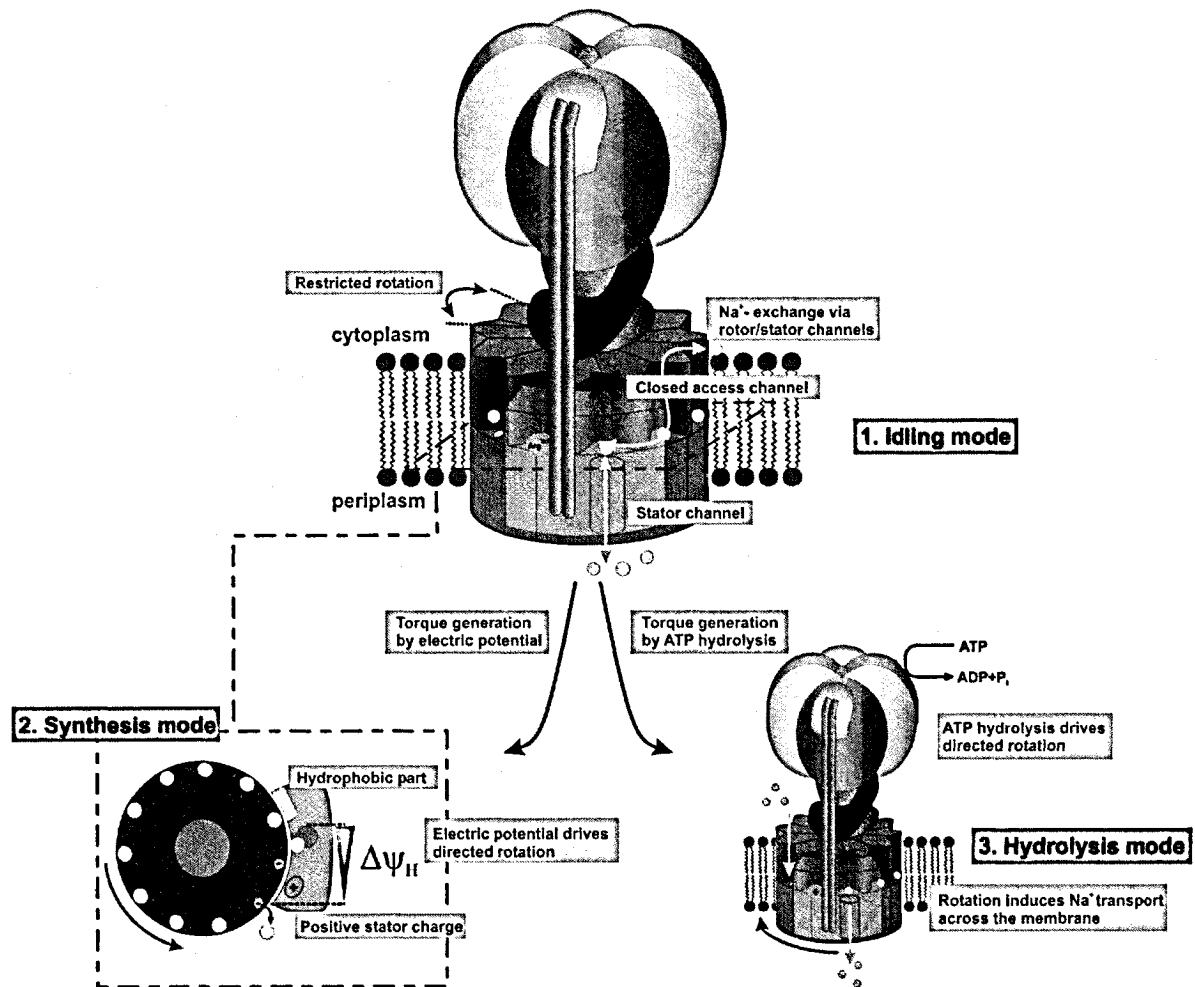
Figure 1-6. Model of three operation modes of the ATP synthase.

1.Idling mode In the absence of a suitable energy source the ATP synthase is in an idling mode. The rotor moves back and forth against the stator within a narrow angle, exchanging Na^+ ions between the cytoplasmic and periplasmic reservoirs. A rotor site at the stator channel exchanges Na^+ with the periplasm and a rotor site outside the a-c interface exchanges Na^+ with the cytoplasm. Upon moving the occupied site from the stator channel through the hydrophobic part to the outside of the a-c interface and backwards, Na^+ ions exchange across the membrane. Please note that the rotor channel within the a-c interface is blocked to avoid leakage across the membrane. Rotor sites moving through the Arg227 containing part are obligatory empty and therefore do not contribute to the exchange of Na^+ ions.

2. Synthesis mode Top view on the section through the ac_{11} assembly at the level of the binding sites. The positive stator charge (Arg227) is known to trigger the dissociation of an ion from the binding site approaching the a-c interface. The ion is subsequently released through the appropriate rotor channel into the cytoplasm. Now negatively charged, the ion binding site is electrostatically attracted by the positive stator charge and moves into the a-c interface. In the absence of a membrane potential the binding site performs thermal fluctuations into either direction from the stator charge with equal

probability (idling mode). During respiration a membrane potential $\Delta\psi$ is generated which is positive at the periplasmic surface. We envision a horizontal component of the potential $\Delta\psi$ between a water-filled inlet and outlet channel within the center of the membrane. This component pulls the negatively charged rotor site towards the stator channel where it quickly picks up a Na^+ ion. Now neutralized to a dipole the site is no longer attracted backwards by the stator charge but continues its movement through the hydrophobic part of the stator while the next empty rotor site is attracted by the membrane potential. Hence the membrane potential is the crucial driving force to induce the torque required for ATP synthesis.

3. Hydrolysis mode At low electrochemical potential the ATP synthase can operate in reverse as an ATPase whereupon it functions as an electrogenic ion pump. ATP hydrolysis by the F_1 motor induces torque that drives the rotor into the opposite direction. Hence, rotor sites approach the stator channel form the hydrophobic portion of the a subunit. The sites must be occupied since an unbalanced negative charge is unable to penetrate. Upon approaching Arg227, the ion dissociates and diffuses through the stator channel into the periplasm. The torque derived from ATP hydrolysis easily rotates the negatively charged site through the hydrophilic portion of the stator passing Arg227. Outside the a-c interface the site quickly picks up a Na^+ form the cytoplasm through its rotor channel.

1.2 Photoactivatable compounds as affinity probes

In contrary to classical chemical reagents, the reactivity of photochemical probes takes the route over an electronically excited state. The absorption of a photon leads to an electron shift from a low to a high energy orbital. The excess energy generates a far more reactive molecule compared to the ground state molecule.

The classical photochemical reaction can be divided into three processes:

1. A photon is absorbed and the molecule is shifted to a high energy level
2. Primary photochemical processes convert the excited molecule to a reactive intermediate.
3. Secondary or dark processes which are driven by the generated intermediates in the primary processes.

The use of photoactivatable compounds has developed over the past 40 years to a variety of methods, which are used for the functional and the structural analysis of all kinds of biomolecules. Their widespread use can be rationalized by two major advances. The first arises from the reasonable chemical stability of most photochemical reagents in the absence of light, which allows a compartment or component localization of the photo-compound prior to activation. The second results from the exceptional reactivity of many photochemically generated intermediates and their ability to attack essentially all kinds of biomolecules (Brunner, 1993). In the presented work, two derivatives of aryldiazirines were used to answer

specific questions and their mechanism is described briefly. 3*H*,3-Aryldiazirines were first reported in 1973 and also suggested to be valuable photocrosslinking agents (Smith and Knowles, 1973). They are indeed stable to a variety of chemical conditions and are easily photolyzed at around 360 nm, a relatively mild wavelength for biological samples. Upon photolysis, they are converted into an extremely reactive carbene, which can insert into almost all kinds of chemical bonds. However, during photolysis, also semi stable diazo-isomers are generated, which are strong alkylating agents that are responsible for undesired dark reactions. This drawback was mainly circumvented by the introduction of a trifluoromethyl group, which stabilized the diazo-compounds through its strong electron-withdrawing effect (Brunner *et al.*, 1980). An overview reaction scheme of a light activated trifluoromethylated aryldiazirine is shown in Figure 1-7. Although there is a natural preference for functional groups, the carbene can also easily interact with C-H bonds, thereby covering the whole spectrum of biomolecules.
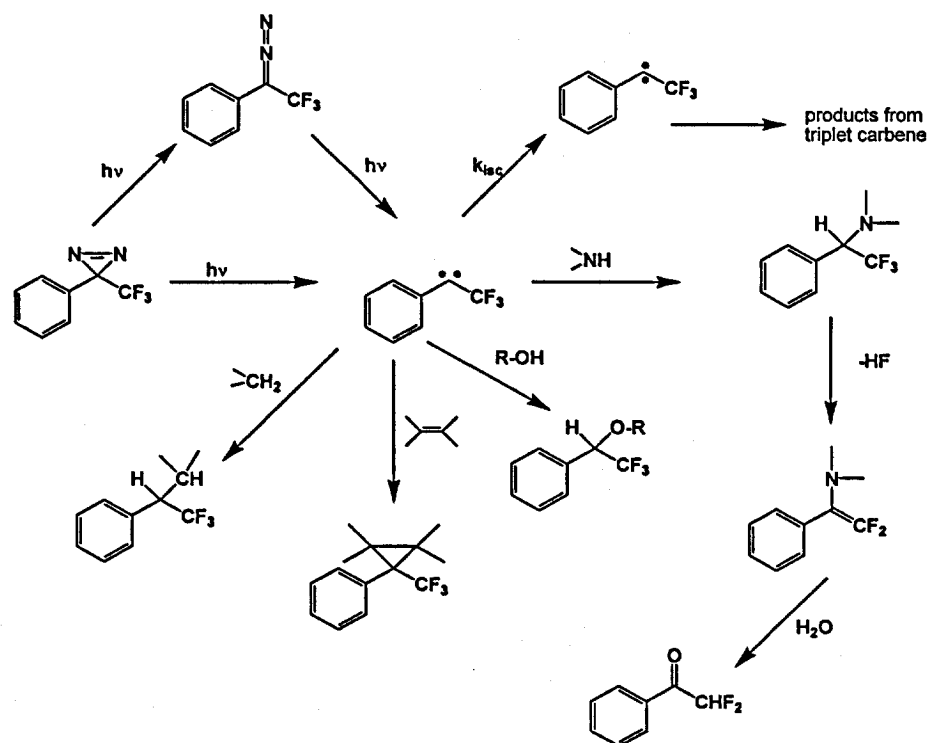
Figure 1-7. Photolysis scheme of 3-trifluoromethyl-3-phenyl-diazirine, showing the formation of the diazoisomer and the singlet and triplet carbene. Reactions of the singlet carbene with various functional groups frequently occurring in biomolecules are shown. The products from reaction with amines can eliminate hydrogen fluoride and in turn hydrolyze to regenerate the starting amine; k_{isc} refers to intersystem crossing of the singlet to the triplet carbene.

1.3 Aim of this work

The central metabolic role of ATP has stimulated much interest in how it is formed using the energy of oxidations or light. Peter Mitchell's unprecedented recognition that energy derived from light or oxidation could create an electrochemical proton gradient across the chloroplast or mitochondrial membrane in which the enzymes are embedded shifted the focus to the question of how the movement of protons across the coupling membrane induced the formation of ATP. The Na^+-dependent ATP synthase from the anaerobic bacteria *P. modestum* and *I. tartaricus* provide unique experimental advantages over the proton dependent enzymes in respect to the investigation of the coupling ion mode in the enzyme. We tried to exploit these properties by means of affinity and crosslinking studies with photoactivatable compounds to gain insight into the mode of action of the enzyme. Further investigations are addressing the chemical environment of the critical functional parts of the enzyme in absence of a high resolution structure.

1.4 References

Abrahams, J.P., Leslie, A.G., Lutter, R. and Walker, J.E. (1994) Structure at 2.8 A resolution of F_1-ATPase from bovine heart mitochondria. *Nature*, **370**, 621-628.

Aggeler, R. and Capaldi, R.A. (1996) Nucleotide-dependent movement of the epsilon subunit between alpha and beta subunits in the *Escherichia coli* F_1F_0-type ATPase. *J. Biol. Chem.*, **271**, 13888-13891.

Aggeler, R., Chicas Cruz, K., Cai, S.X., Keana, J.F. and Capaldi, R.A. (1992) Introduction of reactive cysteine residues in the epsilon subunit of *Escherichia coli* F_1 ATPase, modification of these sites with tetrafluorophenyl azide-maleimides, and examination of changes in the binding of the epsilon subunit when different nucleotides are in catalytic sites. *Biochemistry*, **31**, 2956-2961.

Aggeler, R., Haughton, M.A. and Capaldi, R.A. (1995) Disulfide bond formation between the COOH-terminal domain of the β subunits and the γ and ε subunits of the *Escherichia coli* F_1-ATPase. Structural implications and functional consequences. *J. Biol. Chem.*, **270**, 9185-9191.

Angevine, C.M., Herold, K.A. and Fillingame, R.H. (2003) Aqueous access pathways in subunit a of rotary ATP synthase extend to both sides of the membrane. *Proc. Natl. Acad. Sci. U.S.A.*, **100**, 13179-13183.

Birkenhager, R., Hoppert, M., Deckers-Hebestreit, G., Mayer, F. and Altendorf, K. (1995) The F_0 complex of the *Escherichia coli* ATP synthase. Investigation by electron spectroscopic imaging and immunoelectron microscopy. *Eur. J. Biochem.*, **230**, 58-67.

Blum, D.J., Ko, Y.H., Hong, S., Rini, D.A. and Pedersen, P.L. (2001) ATP synthase motor components: proposal and animation of two dynamic models for stator function. *Biochem. Biophys. Res. Commun.*, **287**, 801-807.

Boyer, P.D. (1993) The binding change mechanism for ATP synthase - some probabilities and possibilities. *Biochim. Biophys. Acta*, **1140**, 215-250.

Boyer, P.D. (1997) The ATP synthase- a splendid molecular machine. *Annu. Rev. Biochem.*, **66**, 717-749.

Boyer, P.D. (2000) Catalytic site forms and controls in ATP synthase catalysis. *Biochim. Biophys. Acta*, **1458**, 252-262.

Brunner, J. (1993) New photolabeling and crosslinking methods. *Annu. Rev. Biochem.*, **62**, 483-514.

Brunner, J., Senn, H. and Richards, F.M. (1980) 3-Trifluoromethyl-3-phenyldiazirine. A new carbene generating group for photolabeling reagents. *J. Biol. Chem.*, **255**, 3313-3318.

Cain, B.D. and Simoni, R.D. (1986) Impaired proton conductivity resulting from mutations in the a subunit of F_1F_0 ATPase in *Escherichia coli*. *J. Biol. Chem.*, **261**, 10043-10050.

Cain, B.D. and Simoni, R.D. (1988) Interaction between Glu-219 and His-245 within the a subunit of F_1F_0-ATPase in *Escherichia coli*. *J. Biol. Chem.*, **263**, 6606-6612.

Cain, B.D. and Simoni, R.D. (1989) Proton translocation by the F_1F_0 ATPase of *Escherichia coli*. Mutagenic analysis of the a subunit. *J. Biol. Chem.*, **264**, 3292-3300.

Capaldi, R.A. and Aggeler, R. (2002) Mechanism of the F_1F_0-type ATP synthase, a biological rotary motor. *Trends. Biochem. Sci.*, **27**, 154-160.

Cox, G.B., Jans, D.A., Fimmel, A.L., Gibson, F. and Hatch, L. (1984) Hypothesis. The mechanism of ATP synthase. Conformational change by rotation of the beta-subunit. *Biochim. Biophys. Acta*, **768**, 201-208.

Deckers-Hebestreit, G. and Altendorf, K. (1996) The F_0F_1-type ATP synthase of bacteria: Structure and funcion of the F_0 complex. *Annu. Rev. Microbiol.*, **50**, 791-824.

Del Rizzo, P.A., Bi, Y., Dunn, S.D. and Shilton, B.H. (2002) The "second stalk" of *Escherichia coli* ATP synthase: structure of the isolated dimerization domain. *Biochemistry*, **41**, 6875-6884.

Diez, M., Börsch, M., Zimmermann, B., Turina, P., Dunn, S.D. and Graber, P. (2004) Binding of the b-subunit in the ATP synthase from *Escherichia coli*. *Biochemistry*, **43**, 1054-1064.

Dimroth, P., Wang, H., Grabe, M. and Oster, G. (1999) Energy transduction in the sodium F-ATPase of *Propionigenium modestum*. *Proc. Natl. Acad. Sci. U.S.A.*, **96**, 4924-4929.

Dmitriev, O., Jones, P.C., Jiang, W. and Fillingame, R.H. (1999) Structure of the membrane domain of subunit b of the *Escherichia coli* F_0F_1 ATP synthase. *J. Biol. Chem.*, **274**, 15598-15604.

Dmitriev, O.Y., Altendorf, K. and Fillingame, R.H. (2004) Subunit A of the *E. coli* ATP synthase: reconstitution and high resolution NMR with protein purified in a mixed polarity solvent. *FEBS Lett.*, **556**, 35-38.

Duncan, T.M., Bulygin, V.V., Zhou, Y., Hutcheon, M.L. and Cross, R.L. (1995) Rotation of subunits during catalysis by *Escherichia coli* F_1-ATPase. *Proc. Natl. Acad. Sci. USA*, **92**, 10964-10968.

Dunn, S., Revington, M., Cipriano, D. and Shilton, B. (2000) The b subunit of *Escherichia coli* ATP synthase. *J. Bioenerg. Biomembr.*, **32**, 347-355.

Dunn, S.D. (1992) The polar domain of the b subunit of *Escherichia coli* F_1F_0-ATPase forms an elongated dimer that interacts with the F_1 sector. *J. Biol. Chem.*, **267**, 7630-7636.

Dunn, S.D. and Chandler, J. (1998) Characterization of a $b_2\delta$ complex from *Escherichia coli* ATP synthase. *J. Biol. Chem.*, **273**, 8646-8651.

Eya, S., Maeda, M. and Futai, M. (1991) Role of the carboxy terminal region of H^+-ATPase (F_0F_1) a subunit from *Escherichia coli*. *Arch. Biochem. Biophys.*, **284**, 71-77.

Fillingame, R.H. (1990) Molecular mechanism of ATP synthesis by F_1F_0- Type H^+-transporting ATP synthases. In *The Bacteria*, Vol. XII, pp. 345-391.

Fillingame, R.H., Angevine, C.M. and Dmitriev, O.Y. (2003) Mechanics of coupling proton movements to c-ring rotation in ATP synthase. *FEBS Lett.*, **555**, 29-34.

Fillingame, R.H., Jiang, W. and Dmitriev, O.Y. (2000) Coupling H(+) transport to rotary catalysis in F-type ATP synthases: structure and organization of the transmembrane rotary motor. *J. Exp. Biol.*, **203** Pt 1, 9-17.

Futai, M., Noumi, T. and Maeda, M. (1989) ATP synthase (H+-ATPase): results by combined biochemical and molecular biological approaches. *Annual Review of Biochemistry*, **58**, 111-136.

Gay, N.J. (1984) Construction and characterisation of an *Escherichia coli* strain with a *uncI* mutation. *J. Bacteriol.*, **158**, 820-825.

Gerike, U., Kaim, G. and Dimroth, P. (1995) In vivo synthesis of ATPase complexes of *Propionigenium modestum* and *Escherichia coli* and analysis of their function. *Eur. J. Biochem.*, **232**, 496-602.

Gibbons, C., Montgomery, M.G., Leslie, A.G. and Walker, J.E. (2000) The structure of the central stalk in bovine F_1-ATPase at 2.4 A resolution. *Nat. Struct. Biol.*, **7**, 1055-1061.

Gogol, E.P., Johnston, E., Aggeler, R. and Capaldi, R.A. (1990) Ligand-dependent structural variations in *Escherichia coli* F_1 ATPase revealed by cryoelectron microscopy. *Proc. Natl. Acad. Sci. USA*, **87**, 9585-9589.

Grabar, T.B. and Cain, B.D. (2004) Genetic complementation between mutant b subunits in F_1F_0 ATP synthase. *J. Biol. Chem.*

Greie, J.C., Deckers-Hebestreit, G. and Altendorf, K. (2000) Secondary structure composition of reconstituted subunit b of the *Escherichia coli* ATP synthase. *Eur. J. Biochem.*, **267**, 3040-3048.

Greie, J.C., Heitkamp, T. and Altendorf, K. (2004) The transmembrane domain of subunit b of the *Escherichia coli* F_1F_0 ATP synthase is sufficient for H^+-translocating activity together with subunits a and c. *Eur. J. Biochem.*, **271**, 3036-3042.

Groth, G., Tilg, Y. and Schirwitz, K. (1998) Molecular architecture of the c-subunit oligomer in the membrane domain of F-ATPases probed by tryptophan substitution mutagenesis. *J. Mol. Biol.*, **281**, 49-59.

Hardy, A.W., Grabar, T.B., Bhatt, D. and Cain, B.D. (2003) Mutagenesis studies of the F_1F_0 ATP synthase b subunit membrane domain. *J. Bioenerg. Biomembr.*, **35**, 389-397.

Hartzog, P.E. and Cain, B.D. (1994) Second-site supressor mutations at Glycine 218 and Histidine 245 in the a subunit of F_1F_0 ATP synthase in *Escherichia coli*. *J. Biol. Chem.*, **269**, 32313-32317.

Hausrath, A.C., Capaldi, R.A. and Matthews, B.W. (2001) The conformation of the ε and γ subunits within the *E. coli* F_1 ATPase. *J. Biol. Chem.*, **276**, 47227-32.

Heise, R., Müller, V. and Gottschalk, G. (1992) Presence of a sodium-translocating ATPase in membrane vesicles of the homoacetogenic *Acetobacterium woodii*. *Eur. J. Biochem.*, **206**, 553-557.

Hicks, D.B., Wang, Z., Wei, Y., Kent, R., Guffanti, A.A., Banciu, H., Bechhofer, D.H. and Krulwich, T.A. (2003) A tenth atp gene and the conserved atpI gene of a *Bacillus* atp operon have a role in Mg^{2+} uptake. *Proc. Natl. Acad. Sci. U.S.A.*, **100**, 10213-10218.

Hilpert, W., Schink, B. and Dimroth, P. (1984) Life by a new decarboxylation-dependent energy conservation mechanism with Na^+ as coupling ion. *EMBO J.*, **3**, 1665-1670.

Howitt, S.M., Lightowlers, R.N., Gibson, F. and Cox, G.B. (1990) Mutational analysis of the function of the a-subunit of the F_0F_1-ATPase of *Escherichia coli*. *Biochim. Biophys. Acta*, **1015**, 264-268.

Howitt, S.M., Rodgers, A.J., Jeffrey, P.D. and Cox, G.B. (1996) A mutation in which alanine 128 Is replaced by aspartic acid abolishes dimerization of the b-subunit of the F_0F_1-ATPase from *Escherichia coli*. *J. Biol. Chem.*, **271**, 7038-7042.

Hutcheon, M.L., Duncan, T.M., Ngai, H. and Cross, R.L. (2001) Energy-driven subunit rotation at the interface between subunit a and the c oligomer in the F(O) sector of *Escherichia coli* ATP synthase. *Proc. Natl. Acad. Sci. U.S.A.*, **98**, 8519-8524.

Jagendorf, A.T. and Uribe, E. (1966) ATP formation caused by acid-base transition of spinach chloroplasts. *Proc. Natl. Acad. Sci. USA*, **55**, 170-177.

Jäger, H., Birkenhäger, R., Stalz, W.-D., Altendorf, K. and Deckers-Hebestreit, G. (1998) Topology of subunit a of the *Escherichia coli* ATP synthase. *Eur. J. Biochem.*, **251**, 122-132.

Jiang, W. and Fillingame, R.H. (1998) Interacting helical faces of subunits a and c in the F_1F_0 ATP synthase of *Escherichia coli* defined by disulfide cross-linking. *Proc. Natl. Acad. Sci. U.S.A.*, **95**, 6607-6612.

Jiang, W., Hermolin, J. and Fillingame, R.H. (2001) The preferred stoichiometry of c subunits in the rotary motor sector of *Escherichia coli* ATP synthase is 10. *Proc. Natl. Acad. Sci. U.S.A.*, **98**, 4966-4971.

Jones, P.C., Jiang, W. and Fillingame, R.H. (1998) Arrangement of the multicopy H^+-translocating subunit c in the membrane sector of the *Escherichia coli* F_1F_0 ATP synthase. *J. Biol. Chem.*, **273**, 17178-17185.

Kaim, G. and Dimroth, P. (1993) Formation of a functionally active sodium-translocating hybrid F_1F_0 ATPase in *Escherichia coli* by homologous recombination. *Eur. J. Biochem.*, **218**, 937-944.

Kaim, G. and Dimroth, P. (1994) Construction, expression and characterization of a plasmid-encoded Na^+-specific ATPase hybrid consisting of *Propionigenium modestum* F_0-ATPase and *Escherichia coli* F_1-ATPase. *Eur. J. Biochem.*, **222**, 615-623.

Kaim, G. and Dimroth, P. (1998) Voltage-generated torque drives the motor of the ATP synthase. *EMBO J.*, **17**, 5887-5895.

Kaim, G. and Dimroth, P. (1999) ATP synthesis by F-type ATP synthase is obligatorily dependent on the transmembrane voltage. *EMBO J*, **18**, 4118-4827.

Kaim, G., Matthey, U. and Dimroth, P. (1998) Mode of interaction of the single a subunit with the multimeric c subunits during the translocation of the coupling ions by F_1F_0 ATPases. *EMBO J.*, **17**, 688-695.

Kaim, G., Wehrle, F., Gerike, U. and Dimroth, P. (1997) Molecular basis for the coupling ion selectivity of F_1F_0 ATP synthases: probing the liganding groups for Na^+ and Li^+ in the c subunit of the ATP synthase from *Propionigenium modestum*. *Biochemistry*, **36**, 9185-9194.

Kluge, C. and Dimroth, P. (1993a) Kinetics of inactivation of the F_1F_0 ATPase of *Propionigenium modestum* by dicyclohexylcarbodiimide in relationship to H^+ and Na^+ concentration: probing the binding site for the coupling ions. *Biochemistry*, **32**, 10378-10386.

Kluge, C. and Dimroth, P. (1993b) Specific protection by Na^+ or Li^+ of the F_1F_0-ATPase of *Propionigenium modestum* from the reaction with dicyclohexylcarbodiimide. *J. Biol. Chem.*, **268**, 14557-14560.

Laubinger, W. and Dimroth, P. (1987) Characterization of the Na^+-stimulated ATPase of *Propionigenium modestum* as an enzyme of the F_1F_0 type. *Eur. J. Biochem.*, **168**, 475-480.

Laubinger, W. and Dimroth, P. (1988) Characterization of the ATP synthase of *Propionigenium modestum* as a primary sodium pump. *Biochemistry*, **27**, 7531-7537.

Lewis, M.J. and Simoni, R.D. (1992) Deletions in hydrophilic domains of subunit a from the *Escherichia coli* F_1F_0-ATP synthase interfere with membrane insertion or F_0 assembly. *J. Biol. Chem.*, **267**, 3482-3489.

Lightowlers, R.N., Howitt, S.M., Hatch, L., Gibson, F. and Cox, G. (1988) The proton pore in the *Escherichia coli* F_0F_1-ATPase: Substitution of glutamate by glutamine at position 219 of the alpha-subunit prevents F_0-mediated proton permeability. *Biochim. Biophys. Acta*, **933**, 241-248.

Lill, H., Hensel, F., Junge, W. and Engelbrecht, S. (1996) Cross-linking of Engineered Subunit δ to $(\alpha\beta)_3$ in Chloroplast F-ATPase. *J. Biol. Chem.*, **271**, 32737-32742.

Long, J.C., Wang, S. and Vik, S.B. (1998) Membrane topology of subunit a of the F_1F_0 ATP synthase as determined by labelling of unique cysteine residues. *J. Biol. Chem.*, **273**, 16235-16240.

Matthey, U., Braun, D. and Dimroth, P. (2002) NMR investigations of subunit c of the ATP synthase from Propionigenium modestum in chloroform/methanol/water (4: 4: 1). *Eur J Biochem*, **269**, 1942-1946.

Matthey, U., Kaim, G., Braun, D., Wüthrich, K. and Dimroth, P. (1999) NMR studies of subunit c of the ATP synthase from *Propionigenium modestum* in dodecylsulfate micelles. *Eur. J. Biochem.*, **261**, 459-467.

McCormick, K.A., Deckers-Hebestreit, G., Altendorf, K. and Cain, B.D. (1993) Characterization of mutations in the b subunit of F_1F_0 ATP synthase in *Escherichia coli*. *J. Biol. Chem.*, **268**, 24683-24691.

McLachlin, D.T., Bestard, J.A. and Dunn, S.D. (1998) The b and δ subunits of the *Escherichia coli* ATP synthase interact via residues in their C-terminal regions. *J. Biol. Chem.*, **273**, 15162-15168.

Meier, T. and Dimroth, P. (2002) Intersubunit bridging by Na^+ ions as a rationale for the unusual stability of the c-rings of Na^+-translocating F_1F_0 ATP synthases. *EMBO Rep.*, **3**, 1094-1098.

Meier, T., Matthey, U., von Ballmoos, C., Vonck, J., Krug von Nidda, T., Kühlbrandt, W. and Dimroth, P. (2003) Evidence for structural integrity in the undecameric c-rings isolated from sodium ATP synthases. *J. Mol. Biol.*, **325**, 389-397.

Mellwig, C. and Böttcher, B. (2003) A unique resting position of the ATP-synthase from chloroplasts. *J. Biol. Chem.*, **278**, 18544-18549.

Menz, R.I., Walker, J.E. and Leslie, A.G. (2001) Structure of bovine mitochondrial F^1-ATPase with nucleotide bound to all three catalytic sites: implications for the mechanism of rotary catalysis. *Cell*, **106**, 331-341.

Mitome, N., Suzuki, T., Hayashi, S. and Yoshida, M. (2004) Thermophilic ATP synthase has a decamer c-ring: indication of noninteger 10:3 H^+/ATP ratio and permissive elastic coupling. *Proc. Natl. Acad. Sci. U.S.A.*, **101**, 12159-12164.

Neumann, S., Matthey, U., Kaim, G. and Dimroth, P. (1998) Purification and properties of the F_1F_0 ATPase of *Ilyobacter tartaricus*, a sodium ion pump. *J. Bacteriol.*, **180**, 3312-3316.

Noji, H., Yasuda, R., Yoshida, M. and Kinosita, K., Jr. (1997) Direct observation of the rotation of F_1-ATPase. *Nature*, **386**, 299-302.

Ogilvie, I., Aggeler, R. and Capaldi, R.A. (1997) Cross-linking of the delta subunit to one of the three alpha subunits has no effect on functioning, as expected if delta is a part of the stator that links the F_1 and F_0 parts of the *Escherichia coli* ATP synthase. *J. Biol. Chem.*, **272**, 16652-16656.

Oster, G., Wang, H. and Grabe, M. (2000) How F_0-ATPase generates rotary torque. *Philo. Trans. R. Soc. Lond.*, **355**, 523-528.

Rastogi, V.K. and Girvin, M.E. (1999a) ^1H, ^{13}C, and ^{15}N assignments and secondary structure of the high pH form of subunit c of the F_1F_0 ATP synthase. *J. Biomol. NMR*, **13**, 91-92.

Rastogi, V.K. and Girvin, M.E. (1999b) Structural changes linked to proton translocation by subunit c of the ATP synthase. *Nature*, **402**, 263-268.

Revington, M., McLachlin, D.T., Shaw, G.S. and Dunn, S.D. (1999) The dimerization domain of the b subunit of the *Escherichia coli* F_1F_0-ATPase. *J. Biol. Chem.*, **274**, 31094-31101.

Rodgers, A.J. and Wilce, M.C. (2000) Structure of the γ-ε complex of ATP synthase. *Nat. Struct. Biol.*, **7**, 1051-1054.

Rodgers, A.J., Wilkens, S., Aggeler, R., Morris, M.B., Howitt, S.M. and Capaldi, R.A. (1997) The subunit delta-subunit b domain of the *Escherichia coli* F_1F_0 ATPase. The b subunits interact with F_1 as a dimer and through the δ subunit. *J. Biol. Chem.*, **272**, 31058-31064.

Rodgers, A.J.W. and Capaldi, R.A. (1998) The second stalk composed of the b- and δ-subunits connects F_0 to F_1 via an α-subunit in the *Escherichia coli* ATP synthase. *J. Biol. Chem.*, **273**, 29406-29410.

Sawada, K., Kuroda, N., Watanabe, H., Moritani-Otsuka, C. and Kanazawa, H. (1997) Interaction of the δ and b subunits contributes to F_1 and F_0 interaction in *Escherichia coli* F_1F_0-ATPase. *J. Biol. Chem.*, **272**, 30047-30053.

Schink, B. (1984) Fermentation of tartrate enantiomers by anaerobic bacteria, and description of two new species of strict anaerobes, *Ruminococcus pasteurii* and *Ilyobacter tartaricus*. *Arch. Microbiol.*, **139**, 409-414.

Schink, B. and Pfennig, N. (1982) *Propionigenium modestum* gen. nov. sp. nov. a new strictly anaerobic, nonsporing bacterium growing on succinate. *Arch. Microbiol.*, **133**, 209-216.

Schneider, E. and Altendorf, K. (1985) All three subunits are required for the reconstitution of an active proton channel (F_0) of *Escherichia coli* ATP synthase (F_1F_0). *EMBO J.*, **4(2)**, 515-518.

Schnick, C., Forrest, L.R., Sansom, M.S. and Groth, G. (2000) Molecular contacts in the transmembrane c-subunit oligomer of F-ATPases identified by tryptophan substitution mutagenesis. *Biochim. Biophys. Acta*, **1459**, 49-60.

Schulenberg, B., Aggeler, R., Murray, J. and Capaldi, R.A. (1999) The γε-c subunit interface in the ATP synthase of *Escherichia coli*. *J. Biol. Chem.*, **274**, 34233-34237.

Seelert, H., Poetsch, A., Dencher, N.A., Engel, A., Stahlberg, H. and Muller, D.J. (2000) Structural biology. Proton-powered turbine of a plant motor. *Nature*, **405**, 418-419.

Singh, S., Turina, P., Bustamante, C.J., Keller, D.J. and Capaldi, R. (1996) Topographical structure of membrane-bound *Escherichia coli* F_1F_0 ATP synthase in aqueous buffer. *FEBS Lett.*, **397**, 30-34.

Smith, R.A. and Knowles, J.R. (1973) Letter: Aryldiazirines. Potential reagents for photolabeling of biological receptor sites. *J. Am. Chem. Soc.*, **95**, 5072-5073.

Sorgen, P.L., Bubb, M.R., McCromick, K.A., Edison, A.S. and Cain, B.D. (1998a) Formation of the b sububit dimer is necessary for interaction with F_1-ATPase. *Biochemistry*, 37, 923-932.

Sorgen, P.L., Caviston, T.L., Perry, R.C. and Cain, B.D. (1998b) Deletions in the second stalk of the F_1F_0-ATPase in *Escherichia coli*. *J. Biol. Chem.*, 1998, 27873-27878.

Stock, D., Leslie, A.G. and Walker, J.E. (1999) Molecular architecture of the rotary motor in ATP synthase. *Science*, 286, 1700-1705.

Takeyasu, K., Omote, H., Nettikadan, S., Tokumasu, F., Iwamoto-Kihara, A. and Futai, M. (1996) Molecular imaging of *Escherichia coli* F_0F_1-ATPase in reconstituted membranes using atomic force microscopy. *FEBS Lett.*, 392, 110-113.

Tomashek, J.J. and Brusilow, W.S. (2000) Stoichiometry of Energy Coupling by Proton-Translocating ATPases: A History of Variability. *J. Bioenerg. Biomembr.*, 32, 493-500.

Tsunoda, S.P., Aggeler, R., Yoshida, M. and Capaldi, R.A. (2001) Rotation of the c subunit oligomer in fully functional F_1F_0 ATP synthase. *Proc. Natl. Acad. Sci. U.S.A.*, 98, 898-902.

Turina, P. and Capaldi, R.A. (1994) ATP binding causes a conformational change in the gamma subunit of the *Escherichia coli* F_1ATPase which is reversed on bond cleavage. *Biochemistry*, 33, 14275-14280.

Uhlin, U., Cox, G.B. and Guss, J.M. (1997) Crystal structure of the epsilon subunit of the proton-translocating ATP synthase from *Escherichia coli*. *Structure*, 5, 1219-1230.

Valiyaveetil, F.I. and Fillingame, R.H. (1998) Transmembrane topography of subunit a in the *Escherichia coli* F_1F_0 ATP synthase. *J. Biol. Chem.*, 273, 16241-16247.

Vik, S.B. and Antonio, B.J. (1994) A mechanism of proton translocation by F_1F_0 ATP synthases suggested by double mutants of the a subunit. *J. Biol. Chem.*, 269, 30364-30369.

von Ballmoos, C., Appoldt, Y., Brunner, J., Granier, T., Vasella, A. and Dimroth, P. (2002a) Membrane topography of the coupling ion binding site in Na^+-translocating F_1F_0 ATP synthase. *J. Biol. Chem.*, 277, 3504-3510.

von Ballmoos, C., Meier, T. and Dimroth, P. (2002b) Membrane embedded location of Na^+ or H^+ binding sites on the rotor ring of F_1F_0 ATP synthases. *Eur. J. Biochem.*, 269, 5581-5589.

von Meyenburg, K., Jorgensen, B.B., Michelsen, O., Sorensen, L. and McCarthy, J.E.G. (1985) Proton conduction by subunit a of the membrane-bound ATP synthase of Escherichia coli revealed after induced overproduction. *Embo J.*, 4, 2357-2363.

Vonck, J., von Nidda, T.K., Meier, T., Matthey, U., Mills, D.J., Kuhlbrandt, W. and Dimroth, P. (2002) Molecular architecture of the undecameric rotor of a bacterial Na^+-ATP synthase. 321, 307-316.

Weber, J. and Senior, A.E. (2000) ATP synthase: what we know about ATP hydrolysis and what we do not know about ATP synthesis. *Biochim. Biophys. Acta*, 1458, 300-309.

Weber, J., Wilke-Mounts, S., Nadanaciva, S. and Senior, A.E. (2004) Quantitative determination of direct binding of b subunit to F_1 in *Escherichia coli* F_1F_0-ATP synthase. *J. Biol. Chem.*, 279, 11253-11258.

Wehrle, F., Kaim, G. and Dimroth, P. (2002) Molecular mechanism of the ATP synthase's F_0 motor probed by mutational analyses of subunit a. *J. Mol. Biol.*, 322, 369-381.

Wilkens, S. and Capaldi, R.A. (1994) Asymmetry and structural changes in ECF_1 examined by cryoelectronmicroscopy. *Biol. Chem. Hoppe Seyler*, 375, 43-51.

Wilkens, S. and Capaldi, R.A. (1998) ATP synthase's second stalk comes into focus. *Nature*, 393, 29.

Wilkens, S., Dahlquist, F.W., McIntosh, L.P., Donaldson, L.W. and Capaldi, R.A. (1995) Structural features of the epsilon subunit of the *Escherichia coli* ATP synthase determined by NMR spectroscopy. *Nat. Struct. Biol.*, 2, 961-967.

Wilkens, S., Dunn, S.D., Chandler, J., Dahlquist, F.W. and Capaldi, R.A. (1997a) Solution structure of the N-terminal domain of the delta subunit of the *E. coli* ATP synthase. *Nat. Struct. Biol.*, 4, 198-201.

Wilkens, S., Rodgers, A., Ogilvie, I. and Capaldi, R.A. (1997b) Structure and arrangement of the δ subunit in the *Escherichia coli* ATP synthase (ECF_1F_0). *Biophys. Chem.*, 68, 95-102.

Xing, J., Wang, H., von Ballmoos, C., Dimroth, P. and Oster, G. (2004) Torque Generation by the F_0 motor of the Sodium ATPase. *Biophys. J.*, 87, 2148-2163.

Yamada, H., Moriyama, Y., Maeda, M. and Futai, M. (1996) Transmembrane topology of *Escherichia coli* H^+-ATPase (ATP synthase) subunit a. *FEBS Lett.*, 390, 34-38.

Yasuda, R., Noji, H., Yoshida, M., Kinosita, K., Jr. and Itoh, H. (2001) Resolution of distinct rotational substeps by submillisecond kinetic analysis of F_1-ATPase. *Nature*, 410, 898-904.

2. Partnersuche im Energiekraftwerk der Zelle

Christoph von Ballmoos und Peter Dimroth

Institut für Mikrobiologie der Eidgenössischen Technischen Hochschule, ETH Zentrum, CH-8092 Zürich,
Switzerland

Tief im Innern funktionieren biologische Zellen nach ganz ähnlichen Prinzipien wie unsere makroskopische Welt. Um in der Zelle eine Leistung zu erbringen, wird Energie gebraucht, ähnlich einer vom Mensch hergestellten Maschine, die Strom benötigt. Diese Energie wird in Miniaturkraftwerken hergestellt, die so klein sind, dass sie nicht einmal mit dem Mikroskop erkannt werden können. Mit ausgeklügelten Methoden sind Wissenschaftler den Geheimnissen dieser Kraftwerke auf der Spur. Wir haben chemische Sonden ins Zentrum der Fabrik eingeschleust und so Einblicke in ihre Funktion erhalten.

Das 20. Jahrhundert war geprägt von zahlreichen Entdeckungen, die unser heutiges Leben nachhaltig verändert haben. Ein grosser Teil dieser technischen Errungenschaften hat eines gemeinsam: Sie werden mit Strom betrieben. Obwohl wir verschiedene Energieformen kennen, war die Bereitstellung von Elektrizität die entscheidende Voraussetzung für das Jahrhundert der Technologie. Die Welt hatte eine Energieform gefunden, die fast grenzenlos kompatibel mit allen Anwendungen ist, vom kleinsten Hörgerät bis hin zum elektrisch betriebenen Auto.

Der Strom in der Zelle

Wer hätte gedacht, dass sich in allen biologischen Zellen bereits vor Urzeiten eine universelle Energieform entwickelt hat. Auch die Zelle kennt verschiedene Energieträger, aber keiner ist so vielfältig verwendbar, so effizient, so allgemeingültig wie ATP. ATP steht für Adenosintriphosphat und ist ein chemisches Molekül, das aus aus einem Nukleinsäure-Baustein (Nukleotid), der mit zwei zusätzlichen Phosphatresten verknüpft ist, besteht. Bei der Abspaltung des letzten Phosphatrestes wird Energie freisetzt, die für andere Prozesse in der Zelle verwendet werden kann. Dabei entstehen Adenosindiphosphat (ADP) und anorganisches Phosphat (P_i) (Abbildung 2-1).

Der menschliche Körper verwendet ATP zur Kontraktion der Muskeln, zur Nervenleitung, zur exakten Steuerung von unzähligen biochemischen Prozessen und nicht zuletzt zum Aufbau seiner eigenen Körpersubstanz. Dementsprechend gross ist auch der tägliche Umsatz von ATP, der bei einem erwachsenen Menschen problemlos die Hälfte seines Körpergewichts betragen kann. Um diesen Umsatz zu gewährleisten, benötigt die Zelle eine effiziente Maschine (Enzym), die das ADP wieder mit Phosphat zu ATP verbindet (Abbildung 2-1). Dieses als ATP Synthase bezeichnete Enzym verbraucht einen grossen Teil der Energie, welche im Stoffwechsel aus der Verbrennung der Nahrungsstoffe bereitgestellt wird.
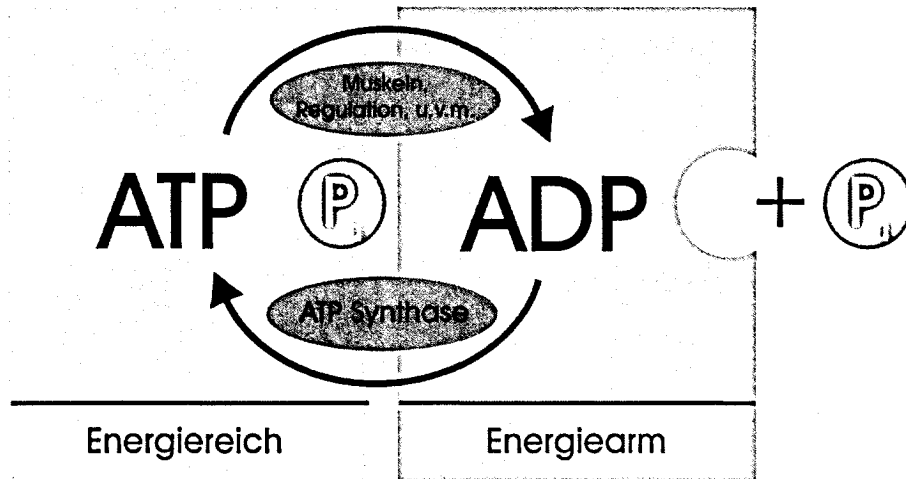
Abbildung 2-1. Zellinterner Energiekreislauf. Von der ATP-Synthase wird ATP unter Energiezufuhr aus ADP und Phosphat (Pi) synthetisiert und unter Verrichtung von Arbeit wieder in diese Produkte gespalten.

Die ATP Synthase – Energiekraftwerk des Lebens

Als man erkannte, dass die ATP Synthase für fast die ganze Produktion des zellulären ATP verantwortlich ist, rückte sie in den Blickpunkt der wissenschaftlichen Forschung. Die Erfolge dieser Forschung sind beachtlich und das Ergebnis erstaunt. Das pilzförmige Enzym ist aus vielen Einzelteilen zusammengesetzt und funktioniert verblüffend ähnlich wie ein Kraftwerk, das vom Menschen erbaut wurde (Abbildung 2-2 B).

Die Energie, welche in einem Wasserkraftwerk zu Elektrizität umgewandelt wird, ist im Steigungsgefälle (Gradienten) des Wassers eines Stausees gespeichert. Dabei verhindert die Staumauer, dass das Wasser ungenutzt seinen Weg ins Tal fliesst. In der Zelle wird die Funktion der Staumauer von einer biologischen Trennschicht, der Membran, übernommen, die aus fettähnlichen Stoffen (Lipiden) besteht. Lipide sind Moleküle, die aus einem langen, wasserunlöslichen Teil (hydrophob) und einer wasserlöslichen Kopfgruppe (hydrophil) bestehen. In Wasser lagern sich die Lipide spontan zu Doppelschichten zusammen, so dass die hydrophoben Teile miteinander in Kontakt treten und nur die hydrophilen Kopfgruppen dem Wasser zugewandt sind (Abbildung 2-2A). Membranen umschliessen biologische Systeme und ermöglichen dadurch verschiedene chemische Zusammensetzungen in den gebildeten Kompartimenten. So ist es für wasserlösliche Kationen (H^+, Na^+, K^+, Mg^{2+}) unmöglich, die Membran frei zu passieren. Häuft sich nun auf der einen Seite der Membran eine Sorte von Ionen an, so entsteht ein Konzentrationsgefälle (chemischer Gradient) zwischen den Kompartimenten. Die Membran wirkt damit auch als elektrischer Isolator und verhindert den Ausgleich von Ladungen. Dadurch bildet sich eine Spannung über die

Membran (Mebranpotential), welche für die Funktionsfähigkeit der Zellen unentbehrlich ist. Zusammen mit dem chemischen Gradienten bildet das Membranpotential die so genannte ionenmotorische Kraft, eine Art biologische Batterie, die für den Antrieb der ATP Synthase zuständig ist. Wie dieser Energiespeicher vom Enzym genutzt wird, wird seit langem intensiv untersucht, wobei einige äusserst spektakuläre und unerwartete Ergebnisse erzielt wurden. Unser gegenwärtiger Wissensstand über den Enzymmechanismus soll im Folgenden stark vereinfacht erklärt werden.
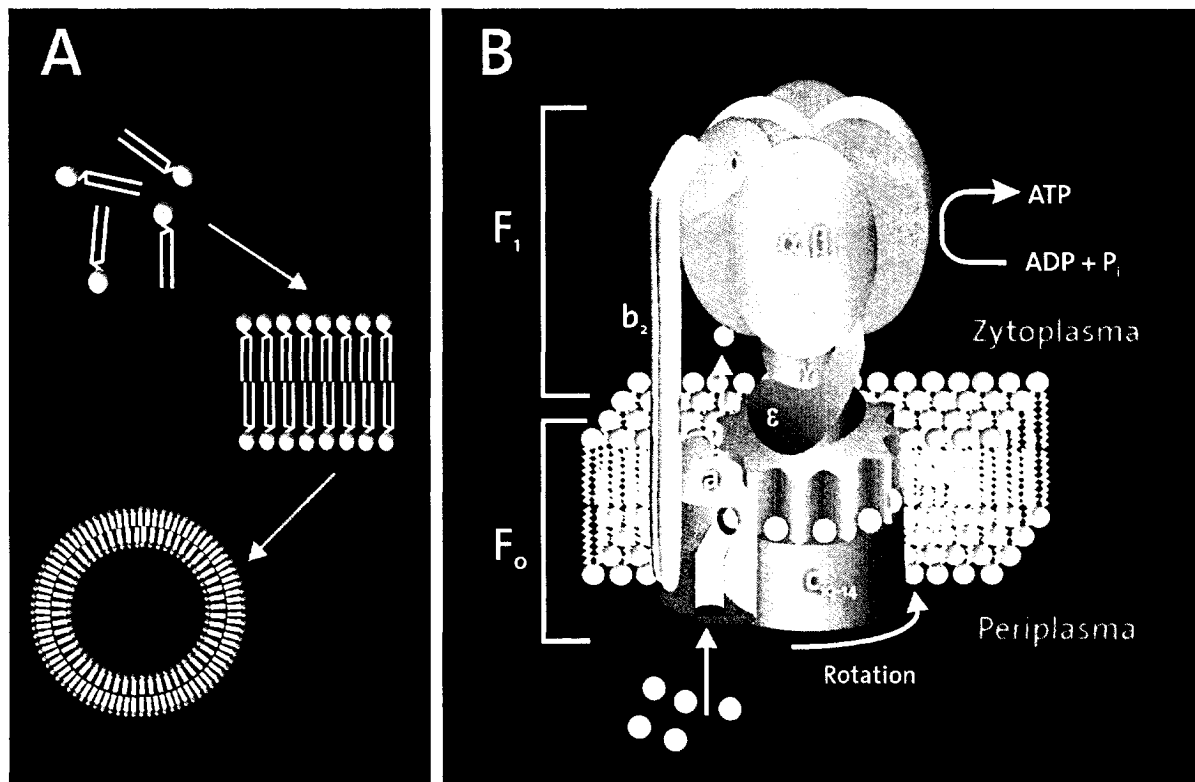
Abbildung 2-2. A. Bildung von Lipidvesikeln.. In wässriger Umgebung lagern sich Lipidmoleküle spontan zu Doppelschichten zusammen. Bei Verbindung dieser Schichten werden Kompartimente voneinander getrennt, die eine unterschiedliche chemische Zusammensetzung aufweisen können, da die Doppelschicht für viele Stoffe undurchlässig ist. **B. Molekulare Architektur und Funktion der ATP-Synthase.** Beim Ionendurchgang durch den F_0-Teil wird die Turbine in Rotation versetzt. Die mechanische Bewegung löst Strukturänderungen aus, die im F_1-Teil zur Synthese von ATP führen. (Abbildung 2-2.)

Wie aus Abbildung 2-2B ersichtlich ist, kann die ATP Synthase in zwei Teile unterteilt werden. Der in der Membran eingebettete F_0-Teil transportiert Ionen über die Membran und nutzt die ionenmotorische Kraft, um eine mechanische Drehbewegung der Turbine (c_{10-14}) in Gang zu setzen. Die Drehbewegung wird von einer zentralen Welle ($\gamma\epsilon$) übernommen, die

fest mit der Turbine verbunden ist und bis in den Innenraum des Enzymkopfes ($\alpha_3\beta_3$) hereinragt (F_1-Teil). Dort löst sie Strukturänderungen aus, die zur Verknüpfung von ADP und P_i zum energiereichen ATP führen. Der Beweis, dass dieses Kraftwerk aus dem Mikrokosmos (das Enzym hat ungefähr die Höhe von zwei Millionstel Millimeter) tatsächlich dreht (bis zu 400 Umdrehungen pro Sekunde), gelang 1996 einer japanischen Forschergruppe: Indem sie ein grosses leuchtendes Molekül an das Enzym befestigten, konnte die Rotation mittels eines Fluoreszenz-Mikroskops beobachtet werden. Ein grober Eindruck von der Gestalt des Enzyms wurde mit Hilfe der Elektronenmikroskopie erhalten, und durch Bestrahlung von Enzymkristallen mit Röntgenstrahlen konnte gar die atomare Struktur des zytoplasmatischen F_1-Teils geklärt werden. Grosse Anstrengungen werden unternommen, um auch die atomare Struktur des gesamten Enzyms aufzuklären, da über die Anordnung und die Funktion des in der Membran gelegenen F_0-Teils noch sehr wenig bekannt ist.

Dunkelheit im verborgenen Teil des Kraftwerks

Der F_0-Teil besteht aus den drei in der Membran verankerten Untereinheiten a, b und c (Abbildung 2-2B). Innerhalb der a-Untereinheit befindet sich ein Kanal, der den Fluss der Ionen vom Zelläusseren (Periplasma) bis zur Mitte der Membran ermöglicht, wo sie auf eine der Bindungsstellen der Turbine (c_{10-14}) übertragen werden. Ein vollständiger Ionendurchgang durch die Membran kommt erst zustande, nachdem sich die Turbine fast vollständig gedreht hat und das Ion über einen Turbinenkanal auf die zytoplasmatische Seite entlassen wurde. Im Gegensatz zur Turbine, die zusammen mit der zentralen Welle den Rotor des Enzyms darstellt, sind die restlichen Teile unbeweglich und werden deshalb als Stator bezeichnet. Der Stator wird fixiert, indem die in der Membran liegende a-Untereinheit über die b-Untereinheiten (b_2) mit dem F_1-Teil verbunden wird.

An der Drehbewegung sind zahlreiche Interaktionen zwischen den einzelnen Aminosäuren der Untereinheiten beteiligt. Um diese zu verstehen, bedient sich die moderne Wissenschaft vieler verschiedener Techniken. So werden mit Hilfe von molekularbiologischen Methoden einzelne Aminosäuren ausgetauscht (mutiert) und die Auswirkungen dieser Mutationen auf die Funktion des Enzyms verfolgt. Die atomare Strukturaufklärung gewinnt immer mehr an Bedeutung, doch sind Untersuchungen dieser Art äusserst aufwändig. Besonders aussagekräftige Methoden sind im letzten Jahrzehnt im Bereich der Nanotechnologie entwickelt worden. Mit Hilfe von leistungsstarken Mikroskopen und Lasertechnologie ist es möglich, einzelne Moleküle zu beobachten, was zu einem völlig neuen Verständnis ihres dynamischen Verhaltens geführt hat.

In unserem Labor verwenden wir zusätzlich massgeschneiderte organische Moleküle als Sonden, um zielgenau in die funktionellen Zentren des Enzyms vorzudringen und dort durch Licht induzierte chemische Bindungen herzustellen. Die Analyse des so veränderten Enzyms erlaubt Rückschlüsse auf seinen strukturellen Aufbau und auf seine Funktion.

Mit Licht auf Partnersuche

Unter diesen licht-(photo)aktivierbaren Substanzen verstehen wir organische Moleküle, die mit einer speziellen funktionellen chemischen Gruppe ausgestattet sind. Diese funktionelle Gruppe ist unter üblichen Bedingungen chemisch stabil, reagiert aber sensitiv gegenüber Bestrahlung mit Licht einer bestimmen Wellenlänge. Unter dieser Lichteinwirkung entsteht eine unstabile, höchst reaktive Zwischenstufe, welche die sofortige Reaktion mit einem Partnermolekül sucht. Diese Reaktion führt zu einer stabilen Bindung zwischen der photoaktivierbaren Substanz und dem Molekül, das sich während der Belichtung unmittelbar in seiner Nähe befindet. In Abbildung 2-3 ist dieser Vorgang am Beispiel einer Aryldiazirin-Gruppe gezeigt. Das eingestrahlte Licht wird dabei von dem Dreiring absorbiert, was die Abspaltung von Stickstoff (N_2) zur Folge hat, eine Reaktion, die energetisch äusserst günstig, und deshalb nicht umkehrbar (irreversibel) ist. Dabei entsteht ein so genanntes Carben, eine sehr reaktive Form eines Kohlenstoffatoms, die sich sofort einen neuen Bindungspartner sucht.

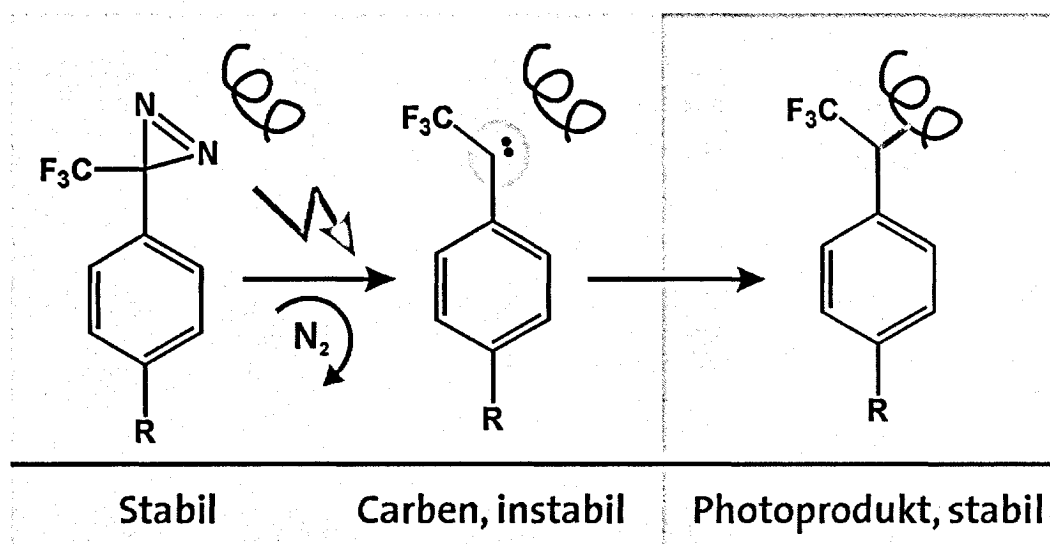Stabil   Carben, instabil   Photoprodukt, stabil

Abbildung 2-3. Prinzip der von Licht induzierten Knüpfung einer stabilen chemischen Bindung. Aus dem Photomolekül wird bei Bestrahlung zunächst eine instabile, sehr reaktive Zwischenform gebildet, die dann mit einem Partnermolekül in unmittelbarer Umgebung eine stabile chemische Bindung eingeht.

Die entstandene Bindung ist chemisch robust und kann hinterher mit diversen Methoden analysiert werden. Wie solche Experimente zum Gewinn von funktionellen und strukturellen Information verwendet werden können, möchten wir im Folgenden erläutern.

In den Tiefen der Membran

Die ATP Synthase ist ein grosser Enzymkomplex, der beim Menschen aus mehr als einem Dutzend Untereinheiten und damit aus tausenden von Aminosäuren besteht. Trotz der Ähnlichkeit, welche die grobe Organisation der einzelnen Untereinheiten von verschiedenen Organismen untereinander aufweisen, ist in der Abfolge der Aminosäuren eine grosse Variation zu beobachten. Eine erwähnenswerte Ausnahme bildet dabei eine negativ geladene Aminosäure, die sich auf jeder Untereinheit der Turbine (c_{10-14}) befindet. Ohne Ausnahme wird sie in jedem Organismus gefunden, und ohne Ausnahme bringt eine Variation zu einer Aminosäure ohne die negative Ladung einen Funktionsverlust des Gesamtenzyms mit sich. Sie bildet zusammen mit anderen Aminosäuren die so genannte Ionen-Bindungsstelle auf der Turbine und empfängt die ankommenden Ionen aus der a-Untereinheit, um sie durch die Membran zu transportieren (Abbildung 2-2). Es war daher von Interesse, in welcher Tiefe der Membran sich diese wichtige Aminosäure befindet, d.h. wir wollten herausfinden, ob sie sich an der Oberfläche oder im Innern der Membran befindet.

Um dieses Problem zu lösen, haben wir uns zu Nutze gemacht, dass diese negative Aminosäure mit dem organischen Molekül Dicyclohexylcarbodiimid eine spezifische Bindung eingeht. Sobald dieser Hemmstoff (Inhibitor) gebunden hat, wird die Rotation der Turbine und damit die Funktion der ATP Synthase blockiert. Wir haben den Inhibitor mit einer photoaktivierbaren Gruppe verbunden, ohne dadurch seine ursprünglichen, hemmenden Eigenschaften zu verändern. Die isolierte ATP Synthase wurde in eine künstliche Membran eingebettet, der modifizierte Inhibitor zugesetzt und die Probe mit einer starken Lichtquelle bestrahlt. Bei der anschliessenden Analyse stellten wir fest, dass sich die photoaktivierbare Gruppe ein Lipidmolekül der Membran als Bindungspartner ausgewählt hatte. Die weitere Analyse des neuen Komplexes aus Protein, Inhibitor und Lipid ergab, dass die Quervernetzung am hydrophoben Ende des Lipids stattgefunden hat und dass die negativ geladene Aminosäure deshalb tief in der Membran verankert vorliegt.

In einem aktuellen Projekt kümmern wir uns um eine ganz ähnliche Fragestellung. Aus elektronenmikroskopischen Daten ist bekannt, dass die aus c-Untereinheiten bestehende Turbine einen zylindrischen Hohlraum besitzt. Wir stellten uns die Frage, was sich im Inneren dieses Hohlraums befindet. Um dieses Problem zu lösen haben wir eine einzelne Aminosäure

im Innern des Hohlraums so verändert, dass wir sie anschliessend gezielt chemisch modifizieren konnten. Dazu wurde ein Molekül hergestellt, das auf der einen Seite die photoaktivierbare Gruppe trägt und auf der anderen Seite eine funktionelle Gruppe, die mit der modifizierten Aminosäure reagiert. Wir errichteten somit eine Art chemische Falle, um den Partner im Inneren der Turbine einzufangen und zu identifizieren. Dabei ist es wichtig, dass man die ATP Synthase möglichst in ihrer natürlichen Umgebung lässt. Wir haben deshalb ganze Bakterienzellen bestrahlt und die Probe erst hinterher aufgearbeitet und massenspektroskopisch analysiert. Dabei konnten wir feststellen, dass der Innenraum der Turbine mit Lipiden gefüllt ist.

Umweltgift blockiert das Zentrum der Fabrik

Eine ganz andere Fragestellung möchten wir in unserem letzten Beispiel erläutern. Die Voraussetzung für eine erfolgreiche Funktion der ATP Synthase ist ein reibungsloses Zusammenspiel aller Untereinheiten und derer Teilfunktionen. Durch diese Vielfältigkeit ist die ATP Synthase allerdings auch ein Ziel für Inhibitoren aller Art. Viele dieser Inhibitoren sind auf den Gebrauch im Labor beschränkt und sind nur von geringem Interesse für eine breitere Öffentlichkeit. Eine Ausnahme bilden Organozinn-Substanzen, die jährlich in Tausenden von Tonnen hergestellt werden. Ihre Verwendung als hochkonzentrierter Zusatz in Schiffsfarben hat den Zweck, störende Wasserorganismen abzutöten und zu vermeiden, dass sich Muscheln und Algen am Schiffsrumpf festsetzen. Der Einsatz von solchen Anti-Fouling Wirkstoffen hat daher einen drastischen Einfluss auf den Treibstoffverbrauch eines Tankschiffes und ist deshalb von grossem wirtschaftlichen Interesse. Dass diese Substanzen in bereits sehr geringen Mengen die ATP Synthase effektiv hemmen, ist seit mehr als 30 Jahren bekannt. Der Angriffspunkt und die Art der Wirkung konnten jedoch nicht bestimmt werden, da die Interaktion mit dem Enzym nicht zu einer stabilen Bindung führt. Wir haben deshalb ein Molekül synthetisiert, das dem Inhibitor sehr ähnlich ist, aber eine lichtreaktive Gruppe trägt. Um feststellen zu können, welche Untereinheit der Bindungspartner für den Inhibitor ist, haben wir unser Molekül zusätzlich mit einer radioaktiven Sonde versetzt. Nach Belichtung und Analyse der Probe gelangten wir zu dem eindeutigen Ergebnis, dass sich die Angriffstelle des Inhibitors auf der a-Untereinheit befindet. Mit diesem und weiteren Resultaten konnten wir nachweisen, dass Organozinn-Substanzen den Eingang des Kanals in der a-Untereinheit blockieren und so die Funktion der ATP Synthase zerstören.

Die Nadel im Heuhaufen finden

In diesem Artikel wird am Beispiel der ATP Synthase in drei verschiedenen Beispielen gezeigt, wie mit photoaktivierbaren Reagenzien gezielt Problemstellungen untersucht werden können. Die chemischen Werkzeuge werden dabei so entworfen, dass sie nur an einer ganz bestimmten Stelle im Enzym binden. Die Fähigkeit, die photoaktivierbare Substanz massgeschneidert herstellen und präzise einsetzen zu können, ist deshalb eine Voraussetzung für die erfolgreiche Verwendung dieser Technik. Das anschliessende einfache experimentelle Vorgehen mit einer Aktivierung auf Knopfdruck (Bestrahlung mit Licht) ermöglicht eine gezielte, örtlich beschränkte Untersuchung der Bindungspartner in einem komplexen biologischen System. Die hier beschriebene Technik erfordert keinen grossen technischen Aufwand und stellt daher ein wertvolles Werkzeug dar, um komplexe biologische Zusammenhänge mit einfachen experimentellen Mitteln erkennen zu können.

3. Membrane topography of the coupling ion binding site in Na$^+$-translocating F$_1$F$_0$ ATP synthase

Christoph von Ballmoos[1], Yvonne Appoldt[1], Josef Brunner[2], Thierry Granier[3], Andrea Vasella[3], and Peter Dimroth[1]

[1]Institut für Mikrobiologie der Eidgenössischen Technischen Hochschule, ETH Zentrum, CH-8092 Zürich, Switzerland, [2]Institut für Biochemie der Eidgenössischen Technischen Hochschule, ETH-Zentrum, CH-8092 Zürich, Switzerland, [3]Laboratorium für Organische Chemie der Eidgenössischen Technischen Hochschule, ETH-Hönggerberg, CH-8093 Zürich, Switzerland

[1] The abbreviations used are: NMR, nuclear magnetic resonance; DCCD, dicyclohexylcarbodiimide; POPC, 1-palmitoyl-2-oleyl-*sn*-glycero-3-phosphocholine; HPLC, high-pressure liquid chromatography; Diazirine-BCCD, *N*-4-[3-(trifluoromethyl)-3H-diazirin-3-yl]benzyl-*N'*-cyclohexyl-carbodiimide; DEAE, diethylaminoethyl; ACMA, 9-amino-6-chloro-2-methoxyacridine; MALDI-TOF-MS, matrix assisted laser desorption and ionization time of flight mass spectroscopy; SDS-PAGE, sodium dodecyl sulfate polyacrylamide gel electrophoresis.

3.1 Abstract

A carbodiimide with a photoactivatable diazirine substituent was synthesized and incubated with the Na$^+$-translocating F$_1$F$_0$ ATP synthase from both *Propionigenium modestum* and *Ilyobacter tartaricus*. This caused severe inhibition of ATP hydrolysis activity in the absence of Na$^+$ ions but not in its presence, indicating the specific reaction with the Na$^+$-binding cE65 residue. Photocrosslinking was investigated with the substituted ATP synthase from both bacteria in reconstituted 1-palmitoyl-2-oleyl-*sn*-glycero-3-phosphocholine (POPC)-containing proteoliposomes. A subunit c/POPC conjugate was found in the illuminated samples but no a-c crosslinks were observed, not even after ATP-induced rotation of the c-ring. Our substituted diazirine moiety on cE65 was therefore in close contact with phospholipid but does not contact subunit a. Na$^+_{in}$ /^{22}Na$^+_{out}$ exchange activity of the ATP synthase was not affected by modifying the cE65 sites with the carbodiimide, but upon photoinduced crosslinking, this activity was abolished. Crosslinking the rotor to lipids apparently arrested rotational mobility required for moving Na$^+$ ions back and forth across the membrane. The site of crosslinking was analyzed by digestions of the substituted POPC using phospolipases C and A$_2$, and by mass spectroscopy. The substitutions were found exclusively at the fatty acid side chains, which indicates that cE65 is located within the core of the membrane.

3.2 Introduction

F$_1$F$_0$ ATP synthases are large protein complexes within the membranes of mitochondria, chloroplasts, or bacteria that use an electrochemical H$^+$ or Na$^+$ gradient across the membrane to synthesize ATP. The F$_1$ portion harboring the catalytic sites for ATP synthesis protrudes from the membrane and has the universal subunit composition $\alpha_3\beta_3\gamma\delta\epsilon$. Its high-resolution crystal structure from bovine mitochondria (Abrahams *et al.*, 1994) was in remarkable agreement with the binding change mechanism (Boyer, 1997) suggesting a rotary catalytic mechanism, which was proven experimentally (Noji *et al.*, 1997). The γ and ϵ subunits form the central stalk protruding from the more compact $\alpha_3\beta_3$ cylinder and make a connection with the oligomeric c-ring of the membrane-intrinsic F$_0$-moiety (Gibbons *et al.*, 2000; Stock *et al.*, 1999). Subunits γ, ϵ, and c$_n$ could be crosslinked without loss of function (Tsunoda *et al.*, 2001) and were shown to represent the rotor by direct visualization of rotation with an attached actin filament (Elston *et al.*, 1998; Noji *et al.*, 1997; Pänke *et al.*, 2000).

Besides c_n, the membrane-bound subunit a is part of the F_0-motor which is thought to use the electrochemical ion gradient to generate rotary torque (Dimroth et al., 1999; Elston et al., 1998; Junge et al., 1997). As the structure of the a subunit is not known in any detail, its role in the ion translocation and torque-generating mechanism remains speculative. The a subunit is connected laterally with the c_n-ring (Birkenhager et al., 1995; Jiang and Fillingame, 1998; Singh et al., 1996; Takeyasu et al., 1996), where it is held in place by the two b subunits which form the peripheral stalk connecting subunit a with an α subunit of F_1 with the help of the δ subunit (Dunn and Chandler, 1998; Rodgers and Capaldi, 1998).

Recent structural data have shown that the number of c subunits forming the rotor ring varies among species, being 10 for yeast mitochondria (Stock et al., 1999), 14 for spinach chloroplasts (Seelert et al., 2000) and 11 for the Na$^+$-translocating ATP synthase from the bacterium Ilyobacter tartaricus (Stahlberg et al., 2001). The c oligomer plays a profound role in the ion translocation and hence, its structure is of primary importance to understand the function of the rotary F_0-motor. In the Na$^+$-translocating ATP synthases from Ilyobacter tartaricus (Neumann et al., 1998) and Propionigenium modestum (Laubinger and Dimroth, 1988), Q32, E65 and S66 of the c subunits serve as Na$^+$ binding ligands (Kaim et al., 1997), while equivalents of cE65 serve as proton binding sites in H$^+$-translocating ATP synthases (Miller et al., 1990). This acidic residue has been implicated from an NMR[1] structure of monomeric subunit c of E. coli in an organic solvent mixture to be located in the core of the membrane (Girvin et al., 1998). In a model derived from a secondary NMR structure of subunit c from P. modestum (Matthey et al., 1999), cE65 was placed closer to the membrane surface, explaining numerous data on the direct accessibility of this Na$^+$ binding residue from the aqueous environment (Kaim and Dimroth, 1998a; Kaim and Dimroth, 1999; Kaim et al., 1998).

In order to test these two hypotheses experimentally we took advantage of the fact that cE65 is specifically modified with dicyclohexylcarbodiimide (DCCD). We have chemically synthesized a carbodiimide derivative with a photoactivatable diazirine ring, modified cE65 accordingly and analyzed the crosslink products formed upon illumination in reconstituted proteoliposomes. We show here that crosslinking occurs specifically with the fatty acid side chains of the phospholipids, demonstrating the location of cE65 to be in the core of the cytoplasmic membrane.

3.3 Experimental Procedures

Materials

Solvents and chemicals were purchased from Fluka, Switzerland. 4-[3-(trifluoromethyl)-3H-diazirin-3-yl]benzyliodide was prepared as described (Baldini *et al.*, 1988). Di-bis-phenylmethylcarbodiimide was a gift from Brian Beechey.

POPC was purchased from Avanti Polar Lipids (Alabaster, AL). HPLC grade chloroform was supplied by Amtech-Chemie, Switzerland. Fractogel TSK-DEAE-650 column material was purchased from Merck. Bio-Beads SM-2 (polystyrene beads) were from Biorad. Phospholipase C and phospholipase A_2 were purchased from Sigma.

General methods

Thin layer chromatography was performed on Merck silica gel 60F-254 plates. Intermediates and carbodiimides were detected by fluorescence quenching in UV-light (254 nm) or with a carbodiimide reaction spray (Kohn and Wilchek, 1982). Flash chromatography was performed with Merck 60 (0.04-0.063 mm) silica gel in various solvent mixtures. UV spectra (λ_{max} in nm (log ε)) were recorded in a 1 cm quartz cell. IR spectra were recorded from a 3% $CHCl_3$ solution. ^{1}H-NMR (300MHz) and ^{13}C-NMR(75MHz) were recorded on a Varian Gemini system. Chemical shifts δ are in ppm and coupling constants J in Hz.

Chemical synthesis of carbodiimides

All the applied carbodiimides were synthesized by reaction of iminophosphoranes with isocyanates (Molina and Vilaplana, 1994; Staudinger and Hauser, 1921). *N, N'*-Dibenzylcarbodiimide (Jászay *et al.*, 1987) and *N*-benzyl-*N'*-cyclohexylcarbodiimide (Zetzsche and Fredrich, 1940) have already been described. The synthesis of the diazirine derivative of *N*-benzyl-*N'*-cyclohexylcarbodiimide (4, Diazirine-BCCD) is shown in Figure 3-1 and described in detail below.
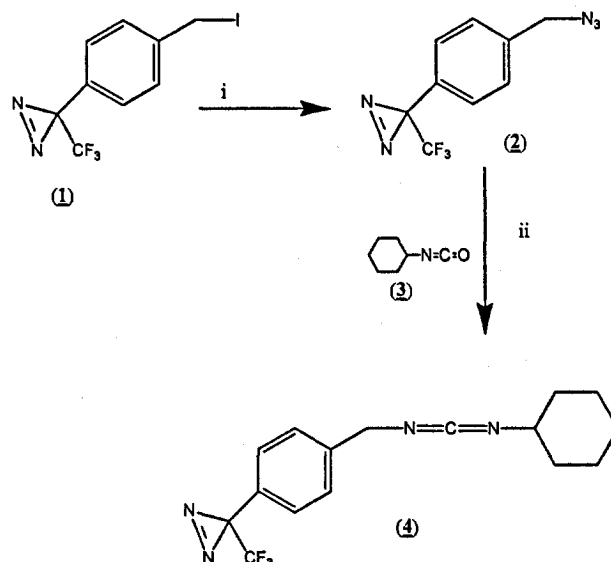
Figure 3-1. Synthesis of Diazirine-BCCD (4). Synthesis of N-4-[3-(trifluoromethyl)-3H-diazirin-3-yl]benzyl-N'-cyclohexyl-carbodiimide (4) from 4-[3-(trifluoromethyl)-3H-diazirin-3-yl]benzyl iodide (1) via 4-[3-(trifluoromethyl)-3H-diazirin-3-yl]benzyl azide (2). i) NaN₃, MeOH, 4h, 40°C; ii) PPh₃, cyclohexylisocyanate (3), CHCl₃, 16h, 40°C; 4-phenyl-3H-1,2,4-triazolin-3,5-dione, RT.

Synthesis of 4-[3-(trifluoromethyl)-3H-diazirin-3-yl]benzyl azide (2)

A solution of 4-[3-(trifluoromethyl)-3H-diazirin-3-yl]benzyliodide (1, 200 mg, 0.613 mmol) in 6 ml MeOH was treated with NaN₃ (87 mg, 1.38 mmol) and stirred for 4 h at 40°C in a water bath. The reaction mixture was allowed to cool to room temperature and the solvent was evaporated *in vacuo* at a temperature below 30°C. Flash chromatography was performed in hexane:ethylacetate (6:1). The residue was briefly dried *in vacuo* to yield 140 mg (95%) of (2).

R$_f$(hexane)= 0.3. UV (CHCl₃): 247 (3.2), 270 (2.7), 353 (2.5). IR (CHCl₃): 2927 m, 2855 m, 2103 s, 1613 w, 1520 w, 1456 w, 1344 m, 1178 s, 1161 s, 1099 w, 1054 m, 1013 m, 939 s. ^{1}H-NMR (CDCl₃): 4.36 (s, ArCH₂); 7.21 (d, J= 8.1, 2H); 7.35 (d, J= 8.1, 2H). ^{19}F-NMR (CDCl₃): -65.0 (s, CF₃). ^{13}C-NMR (CDCl₃): 54.15; 127.19; 128.7; 129.38; 137.5. HR-MS (EI) calcd for C₉H₆F₃N₃: [M – N₂]$^+$=213.0509 found 213.0509.

Synthesis of N-4-[3-(trifluoromethyl)-3H-diazirin-3-yl]benzyl-N'-cyclohexyl-carbodiimide (4)

A solution of 4-[3-(trifluoromethyl)-3H-diazirin-3-yl]benzyl azide (2, 130 mg, 0.539 mol) in 4 ml CHCl₃ was mixed with triphenylphosphine (152 mg, 0.575 mmol) and cyclohexylisocyanate (3, 0.095 ml, 0.740 mmol), and stirred for 12 h at 40° C. The reaction mixture was cooled to room temperature and 4-phenyl-3H-1,2,4-triazolin-3,5-dione was

added until a red color persisted, and then evaporated *in vacuo*. Flash chromatography was performed in hexane:ethylacetate (6:1, 1% triethylamine). The residue was dried *in vacuo* to yield 70 mg (40%) of (4).

R$_f$ (hexane)=0.1. UV (CH$_2$Cl$_2$): 247 (3.2), 270 (2.5), 371 (2.1). IR (CHCl$_3$): 3059 w, 2934 m, 2857 w, 2124 s, 1689 w, 1611 w, 1517 w, 1439 m, 1344 m, 1261 w, 1161 m, 1117 w, 1017 w. ^{1}H-NMR (CDCl$_3$): 1.05-1.35 (m, 5H); 1.45-1.85 (m, 5H); 3.10-3.26 (m, NCH); 4.38 (s, ArCH$_2$N); 7.20 (d, J= 7.3, 2H); 7.37 (d, J= 8.7, 2H). ^{19}F-NMR (CDCl$_3$): -65.1 (s, CF$_3$). ^{13}C-NMR (CDCl$_3$): 24.42; 25.33; 50.11; 126.76; 128.03; 140.3. HR-MS (EI) calcd for C$_{16}$H$_6$F$_3$N$_3$: [M $-$ N$_2$]$^+$=294.1339 found 294.1339.

Purification of F$_1$F$_0$ ATP synthase from Propionigenium modestum and Ilyobacter tartaricus

The F$_1$F$_0$ ATP synthase was purified from whole cells of *P. modestum* or *I. tartaricus* by fractionated polyethyleneglycol precipitation (Laubinger and Dimroth, 1988; Neumann *et al.*, 1998). The ATP synthase was resuspended in 5mM potassium phosphate buffer, pH 8.0, and stored in liquid N$_2$.

Labeling of cE65 from purified F$_1$F$_0$ ATP synthase with carbodiimide derivatives

Typically, 20-30 µg purified ATP synthase in 20 µl 5 mM potassium phosphate, pH 7.0, 5 mM MgCl$_2$ was incubated with 10-50 µM carbodiimide derivative from a 20 mM stock solution in MeOH. The endogenous Na$^+$ content of the buffer was ≤4 µM. For kinetic inhibition measurements, samples were taken at various times and diluted to 1 ml of the assay mixture.

Determination of ATP hydrolyzing activity

ATP hydrolyzing activity was determined with the coupled enzyme assay and followed spectrophotometrically as described (Laubinger and Dimroth, 1988).

Preparation of lipid vesicles

Medium-sized, 100 nm unilamellar vesicles were made from synthetic POPC by the extrusion method (Hope *et al.*, 1985). Typically, 20 mg of POPC in CHCl$_3$:MeOH (2:1, v:v) in a round-bottomed 10 ml flask were flushed with argon, dried as a thin film under reduced pressure in a rotary evaporator for 20 min, and dried in high vacuum for 4 h. The dried lipids were resuspended in 2 ml buffer (50 mM potassium phosphate, pH 7.0, 100 mM K$_2$SO$_4$) and

subjected to seven freeze-thaw cycles in liquid N_2 and at 37°C with short vigorous shaking after each cycle. In order to gain unilamellar vesicles of defined size, the suspension was passed 20 times through a 100 nm membrane using a liposome extruder (LiposoFast Pneumatic, Avestin, Canada). After this procedure, the completely clarified solution was stored at 4°C.

Reconstitution of purified F_1F_0 ATP synthase in POPC vesicles

For the reconstitution, the preformed liposomes were treated with Triton X-100 to favor the insertion of the ATP synthase into the vesicle membrane. Afterwards, the detergent was removed by adsorption to polystyrene beads. Typically, 2 ml of the liposome suspension (10 mg/ml) was mixed with Triton X-100 and $MgCl_2$ to yield final concentrations of 0.25% and 5 mM, respectively. After adding 400 µg purified ATP synthase (lipid:protein ratio (50:1, w:w)), the suspension was incubated for 45 min at room temperature with gentle stirring. To remove the detergent, three portions of wet polystyrene beads (50, 50, 80 mg) were added at 0 min, 45 min and 90 min. The suspension was then carefully separated from the beads and the proteoliposomes collected by ultracentrifugation (50 min, 200'000 g, 4°C). The supernatant was removed and the pellet resuspended in 400 µl of reconstitution buffer (50 mM potassium phosphate, pH 7.0, containing 100 mM K_2SO_4 and 5 mM $MgCl_2$) and stored at 4°C.

ATP-dependent H⁺-uptake into proteoliposomes

ATP-dependent H⁺-transport into proteoliposomes by reconstituted *P. modestum* ATP synthase was measured as described (Laubinger and Dimroth, 1989). The quenching of ACMA fluorescence was monitored with a RF-5001PC spectrofluorometer (Shimadzu) using excitation and emission wavelengths of 410 nm and 480 nm, respectively.

Labeling of the F_1F_0 ATP synthase reconstituted in POPC vesicles with Diazirine-BCCD (4) and crosslinking

A suspension of the F_1F_0 ATP synthase (350 µl, 350 µg protein) was incubated with 200 µM Diazirine-BCCD (4) (20 mM stock solution in MeOH) for 30 min at room temperature to attach this molecule to Glu65 of the c-oligomer. The proteoliposomes were diluted to 2 ml with reconstitution buffer, centrifuged (50 min, 200'000 g, 4°C), and resuspended in 300 µl reconstitution buffer. A sample of 240 µl was then mounted 10 cm in front of a Hg-lamp and irradiated for 40 s at λ> 320 nm and 280 W (350 W Hg-Lamp, SUSS LH 1000 lamp house). One portion (80 µl) was kept at 4°C as a control. A second 80 µl portion was mixed with 650

μl 100 mM potassium phosphate, pH 7.3, 21 μl Triton X-100 (20%) and 12.4 U phospholipase C and incubated at 37°C overnight. The third 80 μl portion was added to 650 μl 100 mM Tricine/KOH buffer, pH 8.9, 21 μl Triton X-100 (20%), 5 mM $CaCl_2$ and 14.5 U phospholipase A_2 and incubated at room temperature overnight.

Na⁺-exchange experiments

The Na⁺-exchange measurements were performed as described (Kluge and Dimroth, 1992).

Preparation of subunit c and derivatives for MALDI analysis

Subunit c of the ATP synthase of *I. tartaricus* was extracted with organic solvents as described (Matthey *et al.*, 1997). Typically, a proteoliposome sample (80 μl, 80 μg protein) was mixed with a tenfold excess of $CHCl_3$:MeOH (1:1, v:v) to precipitate insoluble proteins. After centrifugation, 160 μl water was added to achieve phase separation. The lower organic phase containing the hydrophobic c-subunits and POPC was collected and an equal volume of MeOH was added. In order to remove the lipids, the sample was applied to a Fractogel TSK-DEAE column (1.5 cm x 0.3 cm), equilibrated with $CHCl_3$:MeOH (1:1, v:v). The column was washed with $CHCl_3$:MeOH:H_2O (4:4:1, v:v:v), and subunit c and derivatives were subsequently eluted with 50 mM ammonium acetate in $CHCl_3$:MeOH:H_2O (4:4:1, v:v:v). The sample was then evaporated to dryness in a Speed-Vac and stored at –20°C.

MALDI analysis

Molecular masses were determined on a Perseptive Biosystems Voyager Elite System, a MALDI-TOF instrument with reflector. The measurements were made in the linear positive mode to avoid decomposition of the crosslinker in the reflector mode. The instrument has an accuracy of ± 0.1% in the linear mode. Immediately prior to use, the dried samples were redissolved in $CHCl_3$:HCOOH (1:1, v:v), and placed on the target onto a layer of sinapinic acid, which was deposited before from a saturated stock solution in acetonitrile:water (2:1, v:v), containing 0.1% trifluoroacetic acid. The samples were dried under a stream of nitrogen and directly subjected to measurement.

3.4 Results

Reaction of carbodiimide derivatives with Na$^+$-translocating F$_1$F$_0$ ATP synthase

Work described below was carried out initially with the Na$^+$-translocating F$_1$F$_0$ ATP synthase from *Propionigenium modestum*, but as the very closely related ATP synthase from *Ilyobacter tartaricus* is much easier to prepare we switched later to this enzyme; in fact the c subunits from these two enzymes, which are the topic of this investigation, are identical except for four conservative amino acid exchanges.

<div align="center">

TABLE 3.1:

Inhibition of the ATPase activity of *P. modestum* by different carbodiimide derivatives

</div>

		% ATPase activity after 2 min	
Derivative	c (µM)	- NaCl	+ NaCl
N, N'-Dicyclohexylcarbodiimide	100	12	75
N, N'-Diphenylcarbodiimide	200	55	30
N, N'-Bis-dimethylphenylcarbodiimide	20	20	95
N, N'- Dibenzylcarbodiimide	50	22	96
N-Benzyl-*N'*-cyclohexylcarbodiimide	50	11	75
N-4-[3-(Trifluoromethyl)-3H-diazirine-3-yl]benzyl-*N'*-cyclohexylcarbodiimide (**4**)	50	6	77

Incubation mixtures contained 30 µg protein in 5 mM potassium phosphate, pH 7.0, 5 mM MgCl$_2$ and 20- 200 µM carbodiimide derivative with or without 50 mM NaCl.
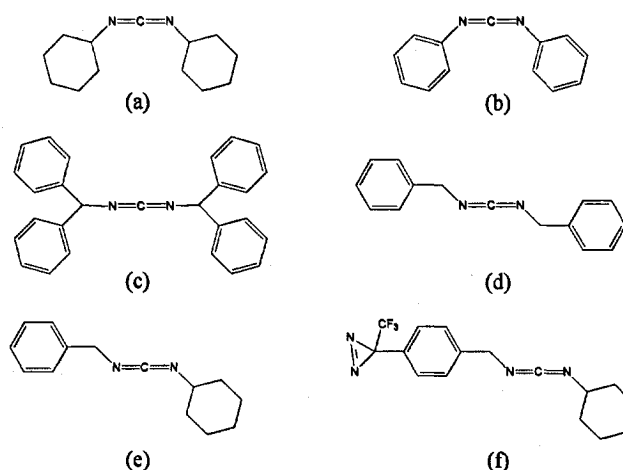

Figure 3-2. Structures of DCCD and carbodiimide derivatives used in this study. (a) *N, N'*-dicyclohexylcarbodiimide; (b) *N, N'*-diphenylcarbodiimide; (c) *N, N'*-bis-dimethylphenylcarbodiimide; (d) *N, N'*- dibenzylcarbodiimide; (e) *N*-benzyl-*N'*-cyclohexylcarbodiimide; (f) *N*-4-[3-(trifluoromethyl)-3H-diazirine-3-yl]benzyl-*N'*-cyclohexylcarbodiimide (**4**).

N, N'-Dicyclohexylcarbodiimide (DCCD) specifically modifies glutamate 65 of subunit c of the Na$^+$-translocating ATP synthases of *P. modestum* (Laubinger and Dimroth, 1988) or *I. tartaricus* (Neumann *et al.*, 1998). This modification inhibits ATP hydrolysis activity of the enzyme, and Na$^+$ ions provide protection from DCCD labeling (Kluge and Dimroth, 1993a; Kluge and Dimroth, 1993b). Hence, the Na$^+$-protected inhibition of the ATPase by carbodiimides provides a convenient assay to monitor their specific reaction with cE65. Treatment of ATP synthase with 100 µM DCCD showed rapid inactivation of ATP hydrolysis and effective protection from this inhibition was observed in presence of 50 mM NaCl (a,b, Table 3.1). *N, N'*-Diphenylcarbodiimide (for structures, see Figure 3-2) inhibited the enzyme at 200 µM but this inhibition was not protected by Na$^+$, indicating that cE65 was not a specific target for this compound. With 20 µM *N, N'*-di-bis-phenylmethylcarbodiimide, ATP hydrolysis was inhibited in a Na$^+$-protectable manner indicating its reaction with cE65. It appears therefore that the substituents on the carbodiimide nitrogens must be flexible enough to permit a reaction with cE65 (Table 3.1).

Based on these observations, a number of carbodiimide derivatives, including one with a photoactivatable diazirine ring were synthesized and assayed for specific interaction with cE65. As summarized in Table 3.1, the *N*-benzyl-*N'*-cyclohexylcarbodiimide derived Diazirine-BCCD (**4**) inhibited the ATPase in a Na$^+$-protectable manner, similarly as *N, N'*-dibenzylcarbodiimide and *N*-benzyl-*N'*-cyclohexylcarbodiimide, indicating that these compounds react specifically with cE65. All the following crosslinking experiments were accomplished with Diazirine-BCCD (**4**).

Crosslink formation between substituted cE65 with subunits a or c

Subunit c substituted with a carbodiimide is expected to rotate by ATP hydrolysis until this is blocked by steric interferences with the a subunit. Hence, if a diazirine substituent on cE65 came into close contact with subunit a, an a-c crosslink product should be formed upon illumination. This was first analyzed with the modified ATP synthase in Triton X-100 micelles by SDS-PAGE and Western blotting with polyclonal antibodies against subunits a or c. The main crosslinking products that specifically formed upon illumination were a c-multimer, probably a dimer, and an a-c adduct. However, formation of the a-c adduct was independent of ATP addition. This situation did not change by varying the concentration of the crosslinker, the incubation time, or the temperature during incubation or illumination, which indicates that the diazirine substituent on cE65 does not form close intramolecular contacts with subunit a, following ATP-driven rotation of the c-ring (data not shown). We

attribute the a-c products to temporary intermolecular interactions between a and c subunits of two different ATP synthases. This conclusion was corroborated by the lack of any a-c crosslink formation if the same experiments were performed with ATP synthase reconstituted into proteoliposomes (see below).

Reconstitution of the ATP synthase from *P. modestum* into liposomes prepared from synthetic phospholipids

To investigate crosslinking between the substituted subunit c and phospholipids it was advantageous to use phospholipids with defined chemical structures. The F_1F_0 ATP synthase was therefore reconstituted into proteoliposomes consisting of POPC. Retention of enzyme function during reconstitution was shown by measuring ATP hydrolysis (data not shown) and proton pumping activities (Figure 3-3).
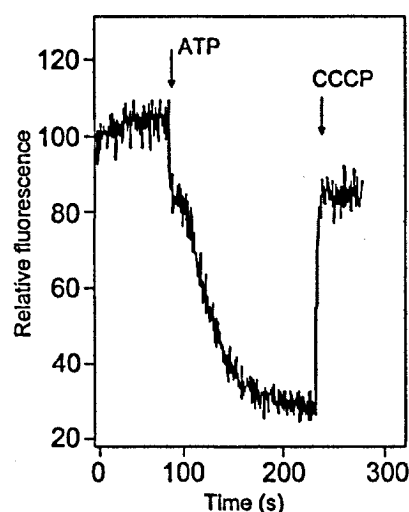
Figure 3-3. ATP-dependent ACMA fluorescence quenching of POPC-liposomes containing *P. modestum* ATP synthase. 10-20 µl (1-2 mg lipid) of reconstituted proteoliposomes in 50 mM potassium phosphate, pH 7.0, 5 mM $MgCl_2$ and 100 mM K_2SO_4 were diluted into 1.5 ml 5 mM potassium phosphate, pH 7.0, 5 mM $MgCl_2$, 100 mM K_2SO_4 and 2 µM valinomycin was added. The quenching of florescence was initiated by adding 2.5 mM K-ATP and abolished wit 2 µM CCCP. Fluorescence was measured using excitation and emission wavelengths of 410 and 480 nm, respectively.

The ATPase activity of reconstituted proteoliposomes was severely inhibited after modifying part of the cE65 sites with the photoactivatable Diazirine-BCCD (4), quite similar to the inhibition of the detergent-solubilized enzyme (Table 3.1). The modification was without effect on the $Na^+_{in}/$ $^{22}Na^+_{out}$ exchange activity in accordance with previous results with the

DCCD-modified enzyme (Kaim and Dimroth, 1999). After irradiation of the sample, however, the sodium exchange activity decreased significantly to levels that are typically found in control liposomes without enzyme (Figure 3-4). The Na$^+_{in}$/ ^{22}Na$^+_{out}$ exchange activity has been attributed to the "idling" mode of the F$_0$ motor performing back and forth rotations of the rotor versus the stator within a narrow angle and thereby moving Na$^+$ ions back and forth across the membrane (Kaim and Dimroth, 1998b). This explanation is corroborated by our present data: crosslinking a modified c subunit with phospholipid (see below) abolishes the rotational motions of the rotor versus the stator that are obligatory for the exchange between internal and external Na$^+$ ions.
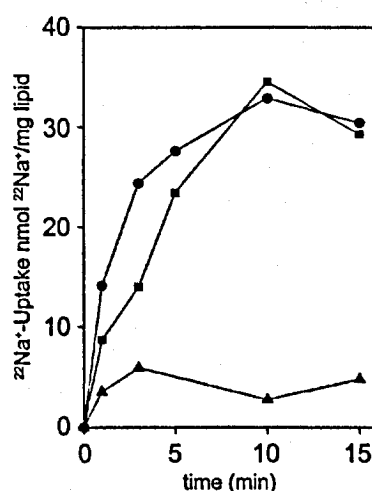
Figure 3-4. ^{22}Na$^+_{in}$/Na$^+_{out}$-exchange by reconstituted _P. modestum_ F$_1$F$_0$-ATP synthase in POPC-liposomes. 50 µl F$_1$F$_0$-liposomes (4 mg lipid) in 50 mM potassium phosphate, pH 7.0, 100 mM K$_2$SO$_4$, 5 mM MgCl$_2$, 100 mM NaCl were diluted into 1 ml 2 mM Tricine/KOH, pH 7.4 buffer containing 5 mM MgCl$_2$, 100 mM K$_2$SO$_4$, 100 mM choline chloride and 1 µCi carrier-free ^{22}NaCl to generate a ΔpNa$^+$ of ~90 mV. The mixture was incubated at room temperature and samples were taken at the indicated times. After separating external ^{22}Na$^+$ by cation exchange chromatography, internal ^{22}Na$^+$ was analyzed by γ-counting (●). ^{22}Na$^+$-uptake after treatment of the F$_1$F$_0$-liposomes with 100 µM cross-linker (4) for 30 min (■); ^{22}Na$^+$-uptake after illumination (30 sec) of the cross-linker (4) treated F$_1$F$_0$-liposomes (▲).

Identification of crosslinked products with the modified subunit c

Crosslinked products were identified after removal of excess phospholipids by SDS-PAGE and Western blotting using polyclonal antibody against subunit c. Most of the subunit c-containing material moved as a broad zone in the area of the monomer (6.5 kDa). A second distinct band of lower intensity was seen with the mobility expected for the dimer. No other crosslinking products containing subunit c became visible, notably none with the mobility

expected for an a-c product (~32 kDa). This was independent from the addition of either ADP or ATP to the reaction mixtures (data not shown). Hence, a-c crosslinks are not formed with ATP synthase reconstituted into proteoliposomes and inhibition of Na$^+_{in}$/ ^{22}Na$^+_{out}$ exchange after photo-induction must be due to crosslink formation of subunit c with another nearby molecule, most probably a phospholipid. This was investigated by SDS-PAGE using 16.5 % acrylamide for better separation of small size proteins. Very similar results were obtained with the ATPase from *P. modestum* or *I. tartaricus*, and the *P. modestum* data are exemplarily shown in Figure 3-5. In the sample treated with Diazirine-BCCD (4), a band moving somewhat slower than subunit c was found in addition to the subunit c band. After illumination, a third band of a c subunit derivative with even lower mobility became apparent indicating the formation of a crosslinked product. Its size is too small for a conjugate with another subunit, but compatible with the one for a conjugate with a phospholipid molecule.
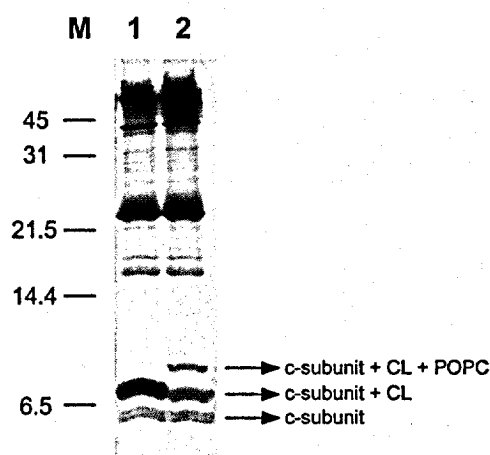
Figure 3-5. Separation of c subunit derivatives by SDS-PAGE. The *P. modestum* ATP synthase was reconstituted into POPC liposomes and modified with 250 µM crosslinker (4). Samples containing 25 µg protein were then applied to SDS gel electrophoresis on a 16.5 % gel (45). Lane 1 shows the sample prior to illumination and lane 2 shows the sample after 40 s illumination with UV light (λ>320nm at 280 W). Arrows indicate the different subunit c products. M: protein marker (sizes are given in kDa).

MALDI analysis of crosslink products

To identify crosslink products containing subunit c, mass spectroscopic analysis was applied. These experiments were performed with the ATP synthase of *I. tartaricus,* which is easier to purify but closely related to the *P. modestum* enzyme (see above). The ATP synthase was reconstituted into POPC-containing liposomes and modified at cE65 with the Diazirine-BCCD (4). Samples were either untreated or irradiated with UV light. The modified c

subunits were then isolated by extraction with chloroform/methanol (1:1, v:v), separated from excess phospholipids by ion exchange chromatography in organic solvents, and analyzed by MALDI.
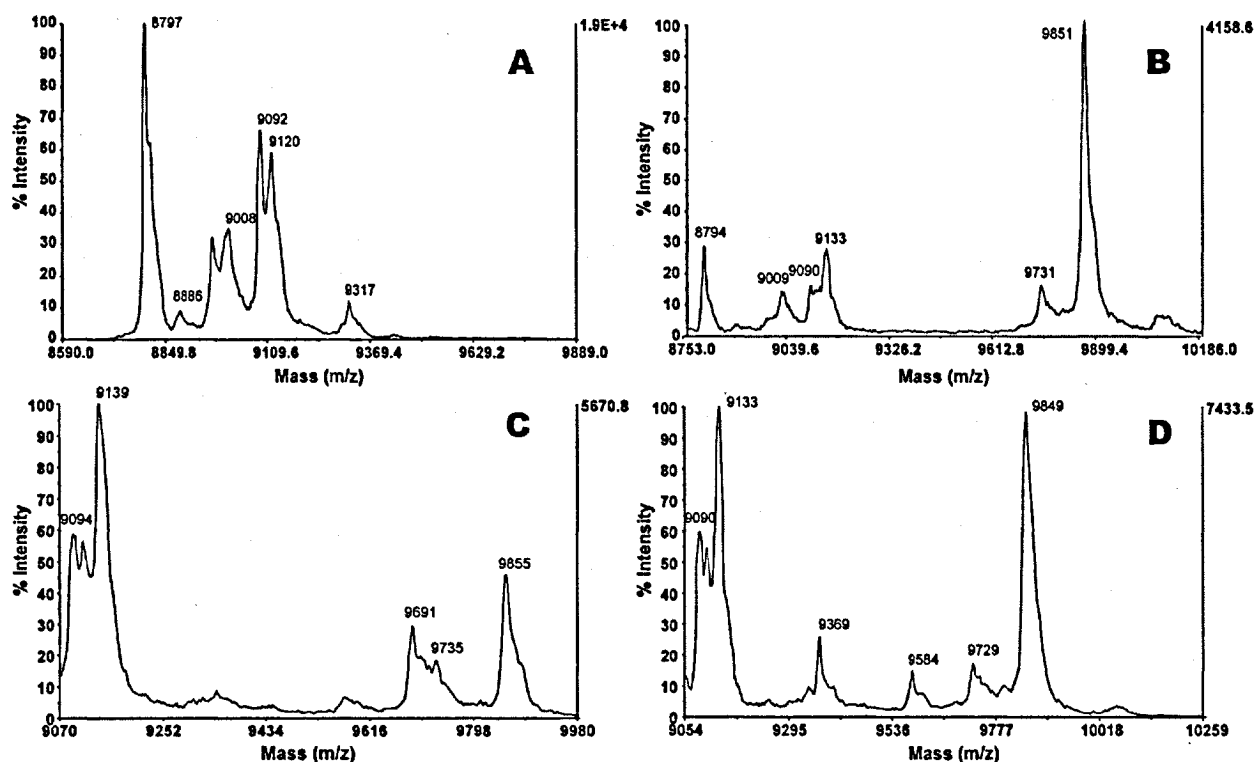
Figure 3-6. MALDI analysis of subunit c modified at E65 with Diazirine-BCCD (4) and of crosslink products. (A) The c subunit of the F_1F_0 ATP synthase from *Ilyobacter tartaricus* reconstituted into POPC liposomes were specifically modified at E65 by 30 min incubation with 200 µM Diazirine-BCCD (4) at 25°C. Excess crosslinker was then removed by ultracentrifugation and resolubilization. (B) like (A), but with subsequent irradiation (λ>320 nm) for 40 sec; (C) like (B), but with subsequent digestion at 37°C overnight with phospholipase C; (D) like (B), but with subsequent digestion at 25°C overnight with phospolipase A_2. The modified c subunits and crosslink products were isolated by extracting the samples with 10 volumes $CHCl_3$:MeOH (1:1, v:v) and subsequent phase separation by adding 2 volumes of water. The lower organic phase was subjected to weak anion exchange chromatography to separate the c subunit derivatives from excess phospholipids. The fractions with the c subunit derivatives were dried in a Speed-Vac. Immediately prior to MALDI analysis, samples were resolubilized in $CHCl_3$:MeOH (1:1, v:v).

The results of Figure 3-6 show mass spectra of modified c subunits without (A) and after irradiation (B); and assignments of the masses are given in Table 3.2. Subunit c modified with Diazirine-BCCD (4) has a calculated mass of 9119 Da and a corresponding peak at m/z = 9120 is clearly observable in the non-irradiated sample. Other peaks that could be assigned in this sample are the unmodified c subunit (m/z = 8797), the modified c subunit linked to the

sinapinic acid matrix (m/z = 9317), and putative degradation products arising during mass spectroscopy (m/z = 9092; m/z = 9008). This phenomenon can be assured by measurements in the reflector mode, where a complete degradation of the subunit c/crosslink occurs, showing a product arising from a fragmentation of the crosslinker attached to subunit c (data not shown).

TABLE 3.2:

Assignment of the masses recorded in MALDI spectra (Figure 3-6)

Identified product	Calculated mass	Mass found in MALDI (m/z)
A		
c subunit, unlabeled	8795	8797
c subunit, labeled with Diazirine-BCCD (4)	9119	9120
c subunit, labeled with (4), N2-cleavage during MALDI	9091	9092
c subunit, labeled with (4), partial label cleavage during MALDI (- 115 m/z)	9004	9009
c subunit, labeled with (4), sinapinic acid (Matrix-Peak)	9315	9317
B		
c subunit, labeled with (4), crosslinked to water, reaction with formic acid	9137	9133
c subunit, labeled with (4), crosslinked with POPC	9851	9851
c subunit, labeled with (4), crosslinked with POPC, partial label cleavage during MALDI (- 115 m/z)	9736	9731
C		
c subunit, labeled with (4), crosslinked with POPC, PLC digest	9685 (diacyl-glycerol)	9691
	9275 (phospho-choline)	none
D		
c subunit, labeled with (4), crosslinked with POPC, PLA₂ digest	9587 (minus oleic acid)	9584
	9373 (oleic acid only)	9369

Abbreviations: Diazirine-BCCD (4), N-4-[3-(trifluoromethyl)-3H-diazirin-3-yl]benzyl-N'-cyclohexyl-carbodiimide; POPC, 1-palmitoyl-2-oleyl-sn-glycero-3-phosphocholine; PLC, phospholipase C; PLA₂, phospholipase A₂

In the irradiated sample, the main peak is of m/z = 9851, corresponding to the mass calculated for subunit c modified with Diazirine-BCCD (4) crosslinked with POPC. Upon irradiation, the diazirine group was apparently completely decomposed because no peak with m/z = 9119 corresponding to subunit c with attached Diazirine-BCCD (4) was found and instead the peak with m/z = 9133 could indicate photoinduced addition products with H_2O and/or formic acid. The small peak at m/z = 9731 is likely to arise by degradation of the subunit c/POPC conjugate during MALDI. These results thus indicate that in the membrane-

bound ATP synthase the cE65 residues within the c subunit ring which are accessible to the Diazirine-BCCD (4) are exposed towards the phospholipid environment.

Crosslink formation of the modified subunit c with POPC could involve either the fatty acid side chains, the glycerol moiety or phosphocholine depending on the membrane topography of cE65. The approach used to discriminate between these possibilities is illustrated in Figure 3-7. For this purpose, the crosslinked product was digested with either phospholipase C or phospholipase A_2. Then, the modified c subunits were isolated as usual and subjected to MALDI analysis. The results shown in Figure 3-6C and Table 3.2C indicate that digestion with phospholipase C converted the crosslinked subunit c/POPC product (m/z = 9851) into a new product with m/z = 9691, corresponding to the mass expected for a crosslink product with the diacylglycerol moiety of POPC. A peak at the mass of a crosslink product with the phosphocholine group (m/z = 9275) was not found, however.
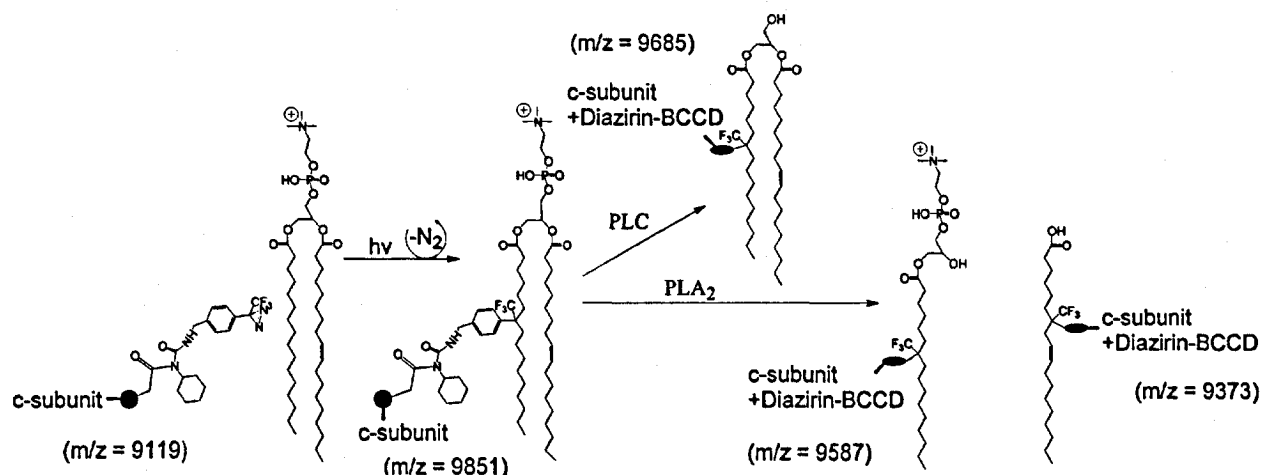
Figure 3-7. Model for crosslink formation between Diazirine-BCCD (4) bound to E65 of subunit c and phospholipids. Upon irradiation with UV light the diazirine group is converted into a highly reactive carbene, which immediately reacts with any neighbouring molecule. To illustrate this reaction, crosslink formation with the fatty acid portion of POPC is shown. Subsequent digestion with phospholipase C or phospholipase A_2 would yield crosslink products of molecular mass m/z = 9685 or 9587 and 9373, respectively. Note that crosslink formation with the glycerol moiety or phosphocholine would yield different products with different masses after digestion with the phospholipases.

The mass spectrum after digestion of the crosslinked subunit c/POPC product with phospholipase A_2 was also analyzed. Two new peaks (m/z = 9584 and m/z = 9369) appeared (Figure 3-6 D, Table 3.2D), which match the mass of the modified c subunit bound to POPC lacking one fatty acid (oleic acid) and the mass of the modified c subunit bound to the free fatty acid (oleic acid), respectively.

These results show clearly that the crosslinking occurs exclusively with the fatty acid side chains of the phospholipids and hence that cE65 is localized within the fatty acid-containing core of the membrane (Figure 3-8A).
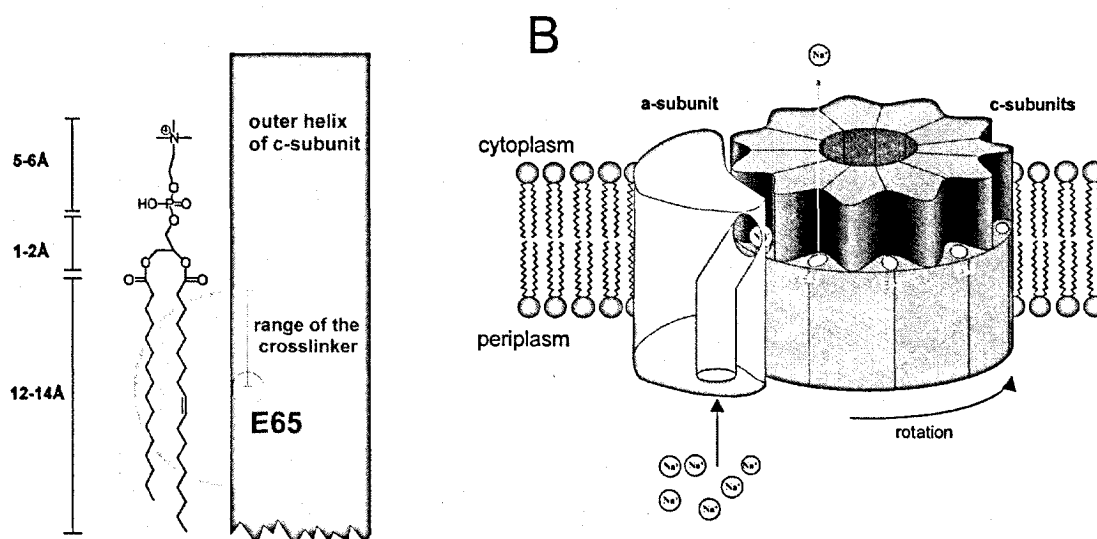
Figure 3-8 A. Approximate topography of glutamate 65 of subunit c in the lipid bilayer. The left part shows a POPC molecule with approximate dimensions and the right part shows glutamate 65 with the dimension of the attached carbodiimide crosslinker within the outer helix of subunit c. According to our results, the crosslinker reacts exclusively with the fatty acid side chains of POPC. As indicated by the yellow circle, E65 should thus be located at the level of ≥ C8 of the fatty acid side chains within the membrane.**B.) Schematic diagram on structural features of the F$_0$ part of the Na$^+$-ATP synthase and the path of Na$^+$ ions through the membrane.** The rotor consists of 11 c subunits and the stator consists of subunit a which is laterally connected to the rotor. The eleven Na$^+$ binding sites on the rotor are formed with ligands from Q32 on the inner helix and E65 and S66 on outer helices. These sites are located within the core of the membrane. Subunit a contains a Na$^+$ access channel which connects the periplasm with the c subunit binding site at the a/c interface. All other sites of the c ring are in contact through access channels inherent in c$_{11}$ with the cytoplasm.In ATP synthesis, Na$^+$ ions following their electrochemical potential pass through the subunit a channel onto an empty rotor site at the a/c interface. Through the potential, rotation is biased to the right. After exiting the rotor/stator interface, the Na$^+$ ion dissociates through its individual rotor channel into the cytoplasm.

3.5 Discussion

Considerable data accumulated over the years that the F$_0$ subunits a and c$_n$ together make up the membrane embedded rotary motor of the ATP synthase with the c$_n$ ring rotating versus subunit a (Hutcheon *et al.*, 2001; Kaim and Dimroth, 1998a; Kaim *et al.*, 1998; Tsunoda *et*

al., 2001). Evidence is also available that this rotation and the translocation of the coupling ions across the membrane are intimately associated events so that one cannot occur without the other. Essential insights into this model have been derived from the Na$^+$ translocating F$_1$F$_0$ ATP synthase from *Propionigenium modestum*, which provides unique experimental approaches to follow the translocation of the coupling ions across the cytoplasmic membrane. Each c subunit of the *P. modestum* ATP synthase carries a Na$^+$ binding site with ligands contributed by Q32, E65, and S66 (Kaim *et al.*, 1997). This site becomes transiently occupied with Na$^+$ during its translocation across the membrane. Evidence indicates a Na$^+$-selective subunit a channel, which connects the adjacent rotor site of c$_{11}$ with the periplasmic surface, whereas rotor sites not in contact with subunit a have direct access from the cytoplasmic compartment (one channel model, (Dimroth *et al.*, 1999). This view is consistent with the ATP-dependent occlusion of 1 Na$^+$ per ATP synthase with a Na$^+$-impermeable a subunit channel (Kaim and Dimroth, 1998a; Kaim and Dimroth, 1998b; Kaim *et al.*, 1998) and it is also consistent with the catalysis of Na$^+_{in}$/^{22}Na$^+_{out}$ exchange by F$_1$F$_0$ of *P. modestum*. As has been pointed out previously (Dimroth *et al.*, 2000a), these observations are not compatible, however, with models proposing two half channels in subunit a (two channel model, (Junge *et al.*, 1997)) through which the rotor sites communicate with the two different sites of the membrane. Another important difference is that the model for torque generation by the F$_0$ motor proposed in (Dimroth *et al.*, 1999) is the only one which takes the essential role of the membrane potential into account (Kaim and Dimroth, 1998b; Kaim and Dimroth, 1999).

Here, we synthesized a photoactivatable carbodiimide (Diazirine-BCCD, $\underline{4}$), which reacted specifically with cE65. Partial modification of the rotor sites with this compound blocked ATP hydrolysis and Na$^+$ pumping but not Na$^+_{in}$/^{22}Na$^+_{out}$ exchange, as expected. Upon illumination, however, the exchange activity was abolished which suggests that the rotor becomes immobilized through crosslinking to phospholipids. These proved to be the targets of the photochemical reaction and hence, the cE65 site which carries the photocrosslinker must be exposed towards the phospholipids. This is in accord with models in which the C-terminal helices of the c-subunits are on the outside of the ring (Dmitriev *et al.*, 1999; Stock *et al.*, 1999).

We clearly demonstrate that the crosslinker reacted exclusively with the fatty acid side chains of the phospholipids. This indicates that the topography of cE65 is within the core of the membrane. The length of the attached crosslinker is about 8 Å when fully extended and therefore the distance of cE65 to the glycerol moiety of POPC must be at least in the same range to explain the absence of crosslink formation with this portion of the molecule (Figure

3-8A). This result is astonishing given the overwhelming evidence for direct access of cE65 from the aqueous compartment by Na$^+$ (Dimroth *et al.*, 2000b). It is in good agreement, however, with an *E. coli* model of the topography of subunit c within the membrane (Dmitriev *et al.*, 1999), which is compatible with the structure of the c oligomer from yeast (Stock *et al.*, 1999).

The location of the c subunit binding sites within the membrane core is also compatible with unpublished structural data on the c_{11} oligomer from *I. tartaricus*. In this structure, a tightly associated inner ring comprising the N-terminal helices is surrounded by an outer ring comprising the C-terminal helices. The outer helices are positioned within the grooves formed by the inner ring of helices leaving enough space between them to form access channels for the coupling ions to reach the membrane buried cE65 residue from the aqueous compartment. Hence, agreement has now been reached on the position of cE65 near the center of the membrane. This location however, by no means, decides in favor of the two-channel model. Our evidence for the direct accessibility of cE65 in case of the Na$^+$ translocating ATP synthase (see above) rather warrants a modification of the one-channel model as shown in Figure 3-8B. Based on the findings presented here and elsewhere we propose that Na$^+$ ions enter the a subunit channel from the periplasmic reservoir and pass through it onto the adjacent rotor site which is near the center of the membrane. From this position, the ion passes towards the cytoplasmic surface through a channel formed between an inner and two outer helices of the c_{11} ring after the rotor has turned the site out of the interface with the a channel. According to this new concept, one may want to term our model the 1a+11c-channel-model rather than the one-channel-model.

Acknowledgements

3.6 References

Abrahams, J.P., Leslie, A.G., Lutter, R. and Walker, J.E. (1994) Structure at 2.8 A resolution of F$_1$-ATPase from bovine heart mitochondria. *Nature*, 370, 621-628.

Baldini, G., Martoglio, B., Schachenmann, A., Zugliani, C. and Brunner, J. (1988) Mischarging Escherichia coli tRNAPhe with L-4'-[3-(trifluoromethyl)-3H- diazirin-3-yl]phenylalanine, a photoactivatable analogue of phenylalanine. *Biochemistry*, 27, 7951-7959.

Birkenhager, R., Hoppert, M., Deckers-Hebestreit, G., Mayer, F. and Altendorf, K. (1995) The F$_0$ complex of the *Escherichia coli* ATP synthase. Investigation by electron spectroscopic imaging and immunoelectron microscopy. *Eur. J. Biochem.*, 230, 58-67.

Boyer, P.D. (1997) The ATP synthase- a splendid molecular machine. *Annu. Rev. Biochem.*, 66, 717-749.

Dimroth, P., Matthey, U. and Kaim, G. (2000a) Critical evaluation of the one- versus the two-channel model for the operation of the ATP synthase's F(o) motor. *Biochim. Biophys. Acta*, 1459, 506-513.

Dimroth, P., Matthey, U. and Kaim, G. (2000b) Osmomechanics of the *Propionigenium modestum* F$_0$ motor. *Journal of Bioenergetics And Biomembranes*, 32, 449-458.

Dimroth, P., Wang, H., Grabe, M. and Oster, G. (1999) Energy transduction in the sodium F-ATPase of *Propionigenium modestum. Proc. Natl. Acad. Sci. U.S.A.*, 96, 4924-4929.

Dmitriev, O.Y., Jones, P.C. and Fillingame, R.H. (1999) Structure of the subunit c oligomer in the F$_1$Fo ATP synthase: model derived from solution structure of the monomer and cross-linking in the native enzyme. *Proc. Natl. Acad. Sci. USA*, 96, 7785-7790.

Dunn, S.D. and Chandler, J. (1998) Characterization of a b$_2$δ complex from *Escherichia coli* ATP synthase. *J. Biol. Chem.*, 273, 8646-8651.

Elston, T., Wang, H. and Oster, G. (1998) Energy transduction in ATP synthase. *Nature*, 391, 510-513.

Gibbons, C., Montgomery, M.G., Leslie, A.G. and Walker, J.E. (2000) The structure of the central stalk in bovine F$_1$-ATPase at 2.4 A resolution. *Nat. Struct. Biol.*, 7, 1055-1061.

Girvin, M.E., Rastogi, V.K., Abildgaard, F., Markley, J.L. and Fillingame, R.H. (1998) Solution structure of the transmembrane H⁺-transporting subunit c of the F$_1$F$_0$ ATP synthase. *Biochemistry*, 37, 8817-8824.

Hope, M.J., Bally, M.B., Webb, G. and Cullis, P.R. (1985) Production of large unilamellar vesicles by a rapid extrusion procedure – characterization of size distribution, trapped volume and ability to maintain a membrane potential. *Biochim. Biophys. Acta*, 812, 55-65.

Hutcheon, M.L., Duncan, T.M., Ngai, H. and Cross, R.L. (2001) Energy-driven subunit rotation at the interface between subunit a and the c oligomer in the F(O) sector of *Escherichia coli* ATP synthase. *Proc. Natl. Acad. Sci. U.S.A.*, 98, 8519-8524.

Jászay, Z.M., Petneházy, L., Töke, L. and Szajánii, B. (1987) Preparation of carbodiimides using phage transfer catalysis. *Synthesis*, 520.

Jiang, W. and Fillingame, R.H. (1998) Interacting helical faces of subunits a and c in the F$_1$Fo ATP synthase of *Escherichia coli* defined by disulfide cross-linking. *Proc. Natl. Acad. Sci. U.S.A.*, 95, 6607-6612.

Junge, W., Lill, H. and Engelbrecht, S. (1997) ATP synthase: an electrochemical transducer with rotatory mechanics. *Trends Biochem. Sci.*, 22, 420-423.

Kaim, G. and Dimroth, P. (1998a) A triple mutation in the a subunit of the *Escherichia coli/Propionigenium modestum* F$_1$F$_0$ ATPase hybrid causes a switch from Na⁺ stimulation to Na⁺ inhibition. *Biochemistry*, 37, 4626-4634.

Kaim, G. and Dimroth, P. (1998b) Voltage-generated torque drives the motor of the ATP synthase. *EMBO J.*, 17, 5887-5895.

Kaim, G. and Dimroth, P. (1999) ATP synthesis by F-type ATP synthase is obligatorily dependent on the transmembrane voltage. *EMBO J*, 18, 4118-4827.

Kaim, G., Matthey, U. and Dimroth, P. (1998) Mode of interaction of the single a subunit with the multimeric c subunits during the translocation of the coupling ions by F$_1$F$_0$ ATPases. *EMBO J.*, 17, 688-695.

Kaim, G., Wehrle, F., Gerike, U. and Dimroth, P. (1997) Molecular basis for the coupling ion selectivity of F$_1$F$_0$ ATP synthases: probing the liganding groups for Na⁺ and Li⁺ in the c subunit of the ATP synthase from *Propionigenium modestum. Biochemistry*, 36, 9185-9194.

Kluge, C. and Dimroth, P. (1992) Studies on Na⁺ and H⁺ translocation through the F$_0$ part of the Na⁺-translocating F$_1$F$_0$ ATPase from *Propionigenium modestum*: discovery of a membrane potential dependent step. *Biochemistry*, 31, 12665-12672.

Kluge, C. and Dimroth, P. (1993a) Kinetics of inactivation of the F$_1$F$_0$ ATPase of *Propionigenium modestum* by dicyclohexylcarbodiimide in relationship to H+ and Na+ concentration: probing the binding site for the coupling ions. *Biochemistry*, 32, 10378-10386.

Kluge, C. and Dimroth, P. (1993b) Specific protection by Na⁺ or Li⁺ of the F$_1$F$_0$-ATPase of *Propionigenium modestum* from the reaction with dicyclohexylcarbodiimide. *J. Biol. Chem.*, 268, 14557-14560.

Kohn, J. and Wilchek, M. (1982) Selective And Highly Sensitive Spray Reagent For Detection Of Nanomolar Quantities Of Carbodiimides On Thin Layer Plates. *J. Chromatography*, **240**, 262-263.

Laubinger, W. and Dimroth, P. (1988) Characterization of the ATP synthase of *Propionigenium modestum* as a primary sodium pump. *Biochemistry*, **27**, 7531-7537.

Laubinger, W. and Dimroth, P. (1989) The sodium ion translocating adenosinetriphosphatase of *Propionigenium modestum* pumps protons at low sodium ion concentrations. *Biochemistry*, **28**, 7194-7198.

Matthey, U., Kaim, G., Braun, D., Wüthrich, K. and Dimroth, P. (1999) NMR studies of subunit c of the ATP synthase from *Propionigenium modestum* in dodecylsulfate micelles. *Eur. J. Biochem.*, **261**, 459-467.

Matthey, U., Kaim, G. and Dimroth, P. (1997) Subunit c from the sodium-ion-translocating F_1F_0-ATPase of *Propionigenium modestum*-production, purification and properties of the protein in dodecylsulfate solution. *Eur. J. Biochem.*, **247**, 820-825.

Miller, M.J., Oldenburg, M. and Fillingame, R.H. (1990) The essential carboxyl group in subunit c of the F_1F_0 ATP synthase can be moved and H(+)-translocating function retained. *Proc. Natl2 Acad. Sci. U.S.A.*, **87**, 4900-4904.

Molina, P. and Vilaplana, M. (1994) Iminophosphoranes - useful building blocks for the praparation of nitrogen-containing heterocycles. *Synthesis*, 1197-1218.

Neumann, S., Matthey, U., Kaim, G. and Dimroth, P. (1998) Purification and properties of the F_1F_0 ATPase of *Ilyobacter tartaricus*, a sodium ion pump. *J. Bacteriol.*, **180**, 3312-3316.

Noji, H., Yasuda, R., Yoshida, M. and Kinosita, K., Jr. (1997) Direct observation of the rotation of F_1-ATPase. *Nature*, **386**, 299-302.

Pänke, O., Gumbiowski, K., Junge, W. and Engelbrecht, S. (2000) F-ATPase: specific observation of the rotating c subunit oligomer of EF_0EF_1. *FEBS Lett.*, **472**, 34-38.

Rodgers, A.J.W. and Capaldi, R.A. (1998) The second stalk composed of the b- and δ-subunits connects F_0 to F_1 via an α-subunit in the *Escherichia coli* ATP synthase. *J. Biol. Chem.*, **273**, 29406-29410.

Seelert, H., Poetsch, A., Dencher, N.A., Engel, A., Stahlberg, H. and Muller, D.J. (2000) Structural biology. Proton-powered turbine of a plant motor. *Nature*, **405**, 418-419.

Singh, S., Turina, P., Bustamante, C.J., Keller, D.J. and Capaldi, R. (1996) Topographical structure of membrane-bound *Escherichia coli* F_1F_0 ATP synthase in aqueous buffer. *FEBS Lett.*, **397**, 30-34.

Stahlberg, H., Muller, D.J., Suda, K., Fotiadis, D., Engel, A., Meier, T., Matthey, U. and Dimroth, P. (2001) Bacterial Na⁺-ATP synthase has an undecameric rotor. *EMBO Rep.*, **2**, 229-233.

Staudinger, H. and Hauser, E. (1921) *Helv. Chim. Acta*, **4**, 861.

Stock, D., Leslie, A.G. and Walker, J.E. (1999) Molecular architecture of the rotary motor in ATP synthase. *Science*, **286**, 1700-1705.

Takeyasu, K., Omote, H., Nettikadan, S., Tokumasu, F., Iwamoto-Kihara, A. and Futai, M. (1996) Molecular imaging of *Escherichia coli* F_0F_1-ATPase in reconstituted membranes using atomic force microscopy. *FEBS Lett.*, **392**, 110-113.

Tsunoda, S.P., Aggeler, R., Yoshida, M. and Capaldi, R.A. (2001) Rotation of the c subunit oligomer in fully functional F_1F_0 ATP synthase. *Proc. Natl. Acad. Sci. U.S.A.*, **98**, 898-902.

Zetzsche and Fredrich. (1940) *Chem. Ber.*, **73**, 114-1123.

4. Membrane embedded location of Na$^+$ or H$^+$ binding sites on the rotor ring of F$_1$F$_0$ ATP synthases

Christoph von Ballmoos, Thomas Meier, and Peter Dimroth

Institut für Mikrobiologie der Eidgenössischen Technischen Hochschule, ETH Zentrum, CH-8092 Zürich, Switzerland

Abbreviations: DCCD, dicyclohexylcarbodiimide; POPC, 1-palmitoyl-2-oleyl-*sn*-glycero-3-phosphocholine; HPLC, high-pressure liquid chromatography; ACMA, 9-amino-6-chloro-2-methoxyacridine; MALDI-TOF-MS, matrix assisted laser desorption and ionization time of flight mass spectroscopy; SLPC, 1-palmitoyl-2-stearoyl-(n-doxyl)-*sn*-glycero-3-phosphatidylcholine; PCD, *N*-cyclohexyl-*N'*-(1-pyrenyl)carbodiimide; TEMPO, 2,2,6,6-tetramethylpiperidin-1-yloxy (TEMPO)

4.1 Abstract

Recent crosslinking studies indicated the localization of the coupling ion binding site in the Na^+-translocating F_1F_0 ATP synthase of *Ilyobacter tartaricus* within the hydrophobic part of the bilayer. Similarly, a membrane embedded H^+-binding site is accepted for the H^+-translocating F_1F_0 ATP synthase of *Escherichia coli*. For a more definite analysis, we performed parallax analysis of fluorescence quenching with ATP synthases from both *I. tartaricus* and *E. coli*. Both ATP synthases were specifically labelled at their c subunit sites with *N*-cyclohexyl-*N'*-(1-pyrenyl)carbodiimide, a fluorescent analogue of dicyclohexylcarbodiimide and the enzymes were reconstituted into proteoliposomes. Using either soluble quenchers or spinlabelled phospholipids, we observed a deeply membrane embedded binding site, which was quantitatively determined for *I. tartaricus* and *E. coli* to be 1.3 ± 2.4 Å and 1.3 ± 2.4 Å from the bilayer center apart, respectively. These data show a conserved topology among enzymes of different species. We further demonstrated the direct accessibility for Na^+ ions to the binding sites in the reconstituted *I. tartaricus* c_{11} oligomer in the absence of any other subunits, pointing to intrinsic rotor channels. The common membrane embedded location of the binding site of ATP synthases suggest a common mechanism for ion transfer across the membrane.

4.2 Introduction

Structurally similar F_1F_0 ATP synthases are present in mitochondria, chloroplasts or eubacteria, where they catalyze ATP formation with the energy stored in a transmembrane electrochemical gradient of protons or Na^+ ions (for a recent review, see Capaldi and Aggeler) (Capaldi and Aggeler, 2002). The enzyme is composed of an extrinsic membrane domain, F_1, which harbors the catalytic sites for ATP synthesis. The subunit composition of F_1 is $\alpha_3\beta_3\gamma\delta\epsilon$ (Weber and Senior, 1997; Yoshida *et al.*, 2001). Alternating α and β subunits form a cylinder around a central α-helical stalk of the γ subunit (Abrahams *et al.*, 1994; Groth and Pohl, 2001; Stock *et al.*, 1999). Rotation of the γ subunit with respect to the $\alpha_3\beta_3$ subcomplex has been directly observed (Noji *et al.*, 1997). There is strong evidence to support a mechanism in which the central stalk of the soluble F_1 domain, together with the oligomeric c-ring in the membrane domain, rotates as an assembly coupling ion movement with ATP synthesis or hydrolysis (Pänke *et al.*, 2000; Sambongi *et al.*, 1999; Tsunoda *et al.*, 2001). The F_0 membrane domain consists of three different subunits in the stoichiometry ab_2c_n (n=10-14) (for review see (Deckers-Hebestreit *et al.*, 2000). The single a subunit and the two b subunits

are supposed to contact the c-ring laterally (Birkenhager *et al.*, 1995; Jiang and Fillingame, 1998; Singh *et al.*, 1996; Takeyasu *et al.*, 1996). The number of c subunits forming the ring varies among species, being 10 for yeast mitochondria (Stock *et al.*, 1999), 14 for spinach chloroplasts (Seelert *et al.*, 2000) and 11 for the Na⁺ translocating F_1F_0 ATP synthase from *Ilyobacter tartaricus* (Stahlberg *et al.*, 2001). Each monomeric unit folds as a helical hairpin. The N-terminal helices form a tightly packed inner ring and the C-terminal helices form a more loosely packed outer ring (Stock *et al.*, 1999; Vonck *et al.*, 2002). Cavities between neighbouring outer helices and the inner ring were suggested to act as Na⁺ access channels to the binding sites, which are located in the middle of the membrane (von Ballmoos *et al.*, 2002; Vonck *et al.*, 2002). In the binding site, the Na⁺ ion is coordinated by residues Gln32, Glu65, and Ser66 (Kaim *et al.*, 1997), while equivalents of Glu65 are thought to serve as proton binding sites in H⁺-translocating enzymes (e.g. Asp61 in *E. coli*) (Miller *et al.*, 1990). This acidic residue is also known to be the dicyclohexylcarbodiimide (DCCD) binding site in subunit c. In a recent study, using crosslinking with a photoactivatable derivative of DCCD, we were able to show that the binding site is surrounded by the fatty acid parts of the lipids and hence located in the hydrophobic part of the membrane (von Ballmoos *et al.*, 2002).

To validate and extend this new finding we investigated the localization of the binding site both for the Na⁺-translocating ATP synthase of *I. tartaricus* and for the H⁺-translocating ATP synthase of *E. coli* by parallax analysis of fluorescence quenching. The method was originally described by Chattopadhyay and London (Chattopadhyay and London, 1987) and has been applied successfully for the localization of the DCCD binding residues in bovine F_1F_0 ATP synthase (Pringle and Taber, 1985), vacuolar H⁺-ATPase (Harrison *et al.*, 2000) and other proteins (Velasco-Guillen *et al.*, 1998; Zucker *et al.*, 2001). We show here a conserved localization of the binding site in Na⁺- or H⁺-translocating ATP synthases. We confirm the direct accessibility of the binding site in native membranes and we show that this accessibility is an intrinsic property of the oligomeric c-ring. Significance of these findings, which were so far attributed as a special feature of Na⁺-dependent enzymes, in respect to a similar mechanism in H⁺-dependent enzymes is discussed.

4.3 Material and Methods

Materials

Solvents and chemicals were purchased from Fluka, Buchs, Switzerland. 1-palmitoyl-2-oleyl-*sn*-glycero-3-phosphatidylcholine (POPC) and spinlabelled phosphatidylcholines (n-SLPC) 1-

palmitoyl-2-stearoyl-(n-doxyl)-*sn*-glycero-3-phosphatidylcholine (n=5, 7, 10, 12, 14, 16) were purchased from Avanti Polar Lipids (Alabaster, AL). *N*-cyclohexyl-*N'*-(1-pyrenyl)carbodiimide (PCD) was purchased from Molecular Probes, Leiden, The Netherlands. The membrane permeable quencher 2,2,6,6-tetramethylpiperidin-1-yloxy (TEMPO) and 4-hydroxy-TEMPO were from Sigma-Aldrich, Steinheim, Germany. HPLC grade chloroform was supplied by Amtech-Chemie, Kölliken, Switzerland. Biobeads SM-2 (polystyrene beads) were from Bio-Rad.

Purification of F$_1$F$_0$ ATP synthase from *Ilyobacter tartaricus*

The F$_1$F$_0$ ATP synthase was purified from whole cells of *I. tartaricus* by fractionated precipitation with polyethyleneglycol (Neumann *et al.*, 1998). The ATP synthase was resuspended in 5 mM potassium phosphate buffer, pH 8.0, and stored in liquid N$_2$.

Purification of c$_{11}$ oligomer of the F$_1$F$_0$ ATP synthase from Ilyobacter tartaricus-The purification of the highly stable c-oligomer was performed as described (Stahlberg *et al.*, 2001).

Enrichment of F$_1$F$_0$ ATP synthase from *E. coli*

A protocol similar to the purification procedure of the ATP synthase of *I. tartaricus* was used to enrich the F$_1$F$_0$ ATP synthase from *E. coli*. Cells, grown as described (Moriyama *et al.*, 1991), were suspended in a buffer containing 5 mM Tris-HCl, pH 8.0, 0.5 mM EDTA and 10% glycerol. The cells were disrupted in a French pressure cell (1x18'000 psi, 1.2 x10^8 Pa) and the suspension was centrifuged at 12'000 g for 40 minutes to remove cell debris. The membranes were collected by ultracentrifugation (210'000 g, 2 h, 4 °C) and resuspended in a small volume of the same buffer. The inner membranes were subsequently separated from the outer membranes by a sucrose gradient as described (Ward *et al.*, 2000). Fractions with a golden appearance containing the inner membranes were centrifuged (210'000 g, 90 min, 4 °C), resuspended in solubilization buffer (50 mM MOPS, pH 7.0 containing 1% Triton X-100) and slightly stirred for 30 min at 4 °C. Insoluble material was removed by centrifugation (210'000 g, 60 min, 4 °C) and the ATPase was purified by fractionated precipitation with PEG-6000. For this purpose, after addition of 50 mM MgCl$_2$, a 50% solution of PEG-6000 was slowly added to the enzyme solution. When approximately 75% of the activity was still present in the supernatant, the suspension was centrifuged (39'000 g, 15 min, 4 °C). The ATPase was then precipitated with additional PEG-6000 until the residual activity in the supernatant was approximately 15%. The ATPase was collected by centrifugation (39'000 g,

15 min, 4 °C) and carefully resuspended in a buffer containing 10 mM Tris-HCl, pH 8.0, 1 mM MgCl$_2$ and 10% glycerol. Insoluble material was removed by centrifugation (39'000 g, 15 min, 4 °C) and the enzyme stored in liquid N$_2$. Activity was shown to remain stable over several months.

Labeling of cE65 of purified F$_1$F$_0$ ATP synthase or purified c$_{11}$ oligomer with fluorescent PCD

A portion of 20-30 μg purified ATP synthase in 100 μl 5 mM potassium phosphate buffer, pH 7.5 was incubated with 50 μM PCD from a 10 mM stock solution in dimethylformamide. The c$_{11}$ ring was solubilized in 1% octylglucoside. The endogenous Na$^+$ content of the buffer was ≤10 μM. For kinetic inhibition measurements, samples of 5 μl were taken at various times and diluted into 1 ml of the assay mixture.

Determination of ATP hydrolyzing activity

The coupled enzyme assay was used to determine ATP hydrolyzing activity of the different samples (Laubinger and Dimroth, 1988).

Preparation of lipid vesicles

The preparation of medium-sized lipid vesicles was done as described (von Ballmoos *et al.*, 2002). For vesicles containing spin labelled phospholipids, the amount of unlabelled POPC was adjusted and the different lipids mixed prior to evacuation.

Reconstitution of PCD-labelled F$_1$F$_0$ ATP synthase and PCD-labelled c$_{11}$ in POPC and SLPC-containing vesicles

The reconstitution procedure used was first described in (Knol *et al.*, 1996) and recently successfully adapted to our protein (von Ballmoos *et al.*, 2002). The detergent removal step by polystyrene beads should also be efficient in the removal of unbound fluorescent probe.

Determination of binding site accessibility for Na$^+$ in reconstituted c$_{11}$ oligomer

The same reconstitution procedure was used. For better incorporation yields, soy bean phosphatidylcholine was used instead of pure POPC. The proteoliposomes were centrifuged and resuspended in the appropriate buffer for DCCD labelling. Then, 30 μM of DCCD from a 100 mM stock solution in ethanol was added. The reaction was stopped at different times by adding 10 volumes of CHCl$_3$:MeOH (1:1, v:v). Phase separation was induced by adding H$_2$O

to $CHCl_3:MeOH:H_2O$ (5:5:3, v:v:v) . The $CHCl_3$ phase was collected and analyzed by HPLC on a Synchropak WAX300 column (SynChrom, Inc.) at a flow rate of 1 ml/min. After applying the sample, the column was washed with 5 ml $CHCl_3/MeOH/H_2O$ (4:4:1) (solvent A) and proteins were eluted by a linear gradient of solvent A to 40% solvent B ($CHCl_3/MeOH/0.9$ M aqueous ammonium acetate (4:4:1)) applied within 25 min. Protein elution was monitored at 280 nm and peaks from DCCD labeled and unlabeled subunit c were integrated.

ATP-dependent H⁺-uptake into proteoliposomes

ATP-dependent H⁺-transport into proteoliposomes by reconstituted *E. coli* ATP synthase was measured as described (Laubinger and Dimroth, 1989). The quenching of ACMA fluorescence was monitored with a RF-5001PC spectrofluorometer (Shimadzu) using excitation and emission wavelengths of 410 nm and 480 nm, respectively.

MALDI analysis

Molecular masses were determined on a Perseptive Biosystems Voyager Elite System, a MALDI-TOF instrument with reflector. The measurements were made in the linear positive mode to avoid decomposition of the fluorescent probe in the reflector mode. The instrument has an accuracy of ± 0.1% in the linear mode. The samples were extracted with $CHCl_3:MeOH$ (1:1, v:v) and prepared for MALDI measurement as described (von Ballmoos *et al.*, 2002).

Fluorometric measurements

All measurements were performed on a RF-5001PC spectrofluorometer (Shimadzu) in a 300 μl quartz cuvette. Typically, about 250 μg of lipid or about 5 μg of protein was diluted into 300 μl of reconstitution buffer and used for a single measurement. An emission spectrum from 360 nm to 460 nm was recorded at room temperature using an excitation wavelength of 342 nm. The excitation and emission monochromator slit widths were set at 3 nm. For titration of fluorescence yield with different quencher concentrations, samples were incubated with quencher from stock solution (typically 1 M) and equilibrated 1 min prior to recording spectra. Emission was corrected for any background by performing a titration in the absence of protein.

Dynamic collisional quenching can be expressed in the Stern-Volmer Plot F_0/F_1-1 vs. [Q] and obeys the following equation:

$$\frac{F_0}{F_1} = 1 + K_D[Q]$$ (1)

where F_0 and F_1 are the fluorescence intensities in the absence and the presence of the quencher, respectively. K_D represents the Stern-Volmer constant and is a value for the quenching efficiency of a molecule.

Parallax method of depth dependent fluorescent quenching

The depth of the fluorophore coupled to cE65 was calculated by the parallax method (Chattopadhyay and London, 1987). Thereby the PCD-labelled ATP synthase is reconstituted into vesicles containing lipids harboring a spin label at different positions on the fatty acid chain. The fluorescence yields depend on the spinlabel position and the concentration of the labelled lipids. The relation of these results to the depth of the fluorophore can be expressed in the following equation:

$$Z_{cF} = L_{c1} + \frac{\left(\frac{-1}{\pi C}\right) \cdot \ln\left(\frac{F_1}{F_2}\right) - L_{21}^2}{2L_{21}}$$ (2)

where Z_{cf} is the distance of the fluorophore from the center of the bilayer, L_{c1} is the distance of the shallow quencher 1 from the bilayer center, and L_{21} is the distance between the shallow quencher 1 and the deep quencher 2. The two-dimensional quencher concentration in the bilayer is expressed as C, calculated as the ratio of the mole fraction of quencher in total lipid and the surface area of a lipid molecule (assumed as 70 Å²) (Chattopadhyay and London, 1987). F_1 and F_2 are the relative fluorescence intensities measured at the appropriate concentration of quencher 1 and quencher 2, respectively.

4.4 Results

Enrichment of F_1F_0 ATP synthase from E. coli

The recombinant plasmid pBWU13 carrying the entire atp operon from E. coli was introduced into the atp deletion strain E. coli DK8 and expressed as described by Moriyama (Moriyama et al., 1991). In our hands purification of the ATP synthase by published procedures was not satisfactory (Fillingame and Foster, 1986; Moriyama et al., 1991).

Therefore, the protocol used for purifying the ATP synthase from *I. tartaricus* was adapted to the *E. coli* enzyme and is described in detail in Material and Methods. Briefly, after cell rupture, the inner membranes were isolated, the ATP synthase extracted with Triton X-100 and purified by fractionated precipitation with polyethyleneglycol. The enzyme was obtained in ~50% yield compared to inner membrane activity with a specific activity of 7.3 U/ mg protein, corresponding to an about 20-fold enrichment from the inner membrane fraction and its purity was estimated on a silver stained SDS-electrophoresis (Fig 1).
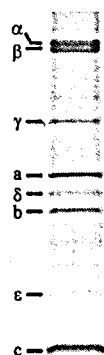
Figure 4-1. SDS polyacrylamide gel electrophoresis of purified *E. coli* ATP synthase. Purified ATP synthase (3 µg) was subjected to SDS-electrophoresis (12.7%, (Schägger and von Jagow, 1987)) and stained with silver.

As a measure for the retention of energy coupling the isolated enzyme was incubated with DCCD for 7 or 15 minutes and at pH 6.4 or 8.0, respectively. In both conditions, more than 95% of the activity became inhibited which indicates that the isolated ATP synthase has retained its energy coupling functions (Table 4.1).

TABLE 1:
ATP hydrolysis activities of various fractions during purification.

Fraction	U/ml	U/mg	% activity
Inner membranes	4.6	-	-
First PEG-precipitation	3.5	-	-
Last PEG-precipitation	0.6	-	-
Purified enzyme	48.3	7.3	100
50 µM DCCD, pH 6.4, 7 min			4.9
50 µM DCCD, pH 8, 15 min			4.5

Abbreviations: PEG, polyethyleneglycol

Specific labelling of ATP synthases with a fluorescent carbodiimide

Dicyclohexylcarbodiimide (DCCD) specifically modifies the coupling ion binding glutamate or aspartate in the c ring of F_1F_0 ATP synthases. Labelling of these sites with the fluorescent derivative N-cyclohexyl-N'-(1-pyrenyl)carbodiimide (PCD) provides unique options to monitor by fluorescence quenching the accessibility of these sites and their location within the membrane.
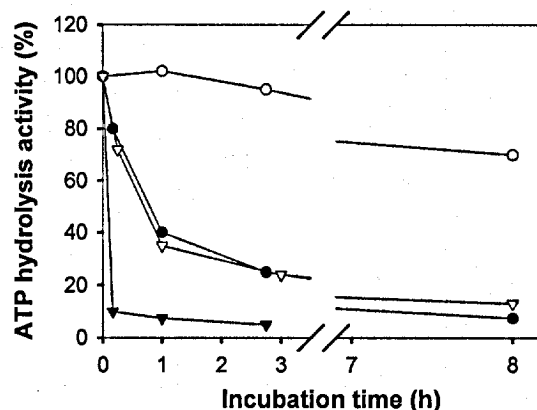

Figure 4-2. Inhibition of ATP hydrolysis activity by the fluorescent carbodiimide PCD. Purified ATP synthase from *I. tartaricus* (25 µg) in 100 µl 5 mM potassium phosphate buffer, pH 8 was incubated with 50 µM PCD at room temperature. Samples of 5 µl were taken at the times indicated and immediately diluted into 1 ml of the assay mixture and ATP hydrolysis activity was measured (•). An untreated sample was taken as a control for enzyme stability at (o); control with 50 µM DCCD instead of 50 µM PCD (▼); purified ATP synthase from *E. coli* was incubated with PCD as stated above (▽).

The results of Figure 4-2 show the inactivation kinetics of the *I. tartaricus* ATPase by DCCD or PCD. With DCCD more than 90% of the activity was lost within 15 minutes, while the inactivation with the more bulky PCD derivative was slower, yielding approximately 60% or 90% loss of activity after 1h or 8h, respectively. The reaction product of PCD with a carboxyl group shows a dramatic increase of the fluorescence compared to the reagent itself. The modification reaction was therefore also followed by measuring fluorescence emission spectra. The results of Figure 4-3 show a massive increase of the fluorescence after incubation of the ATP synthase with PCD. These enhanced fluorescence emission signals were not observed after preincubation with DCCD as one would expect if the two carbodiimides react with the same residue of the enzyme. This conclusion was corroborated by the inhibition of PCD labeling in the presence of Na^+ which resembles the effect of this coupling ion on the reaction of cE65 with DCCD (Kluge and Dimroth, 1993b).
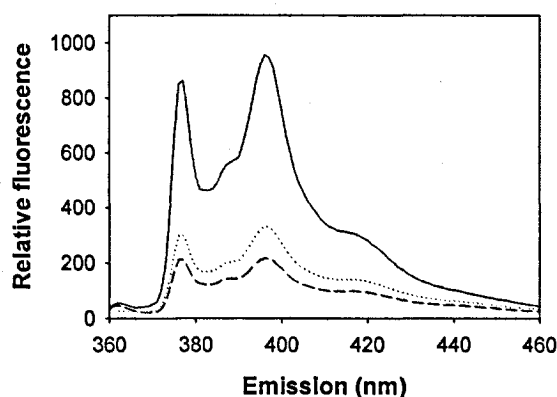
Figure 4-3. Specific modification of cGlu65 of *Ilyobacter tartaricus* **by fluorescent PCD.** Purified ATP synthase from *I. tartaricus* (10 µg) in 100 µl 5 mM potassium phosphate buffer, pH 8 was incubated with 50 µM PCD at room temperature for 5 hours. Samples were diluted with 200 µl of the same buffer and fluorescence emission spectra from 360 to 460 nm were recorded, using an excitation wavelength of 342 nm (——). To show the specific reaction with cGlu65, a sample was pretreated prior to PCD incubation for 1 hour with 50 µM DCCD (– – –) or 10 mM NaCl (··········), respectively.

Covalent modification of subunit c by PCD was verified with MALDI mass spectroscopy: the peak of m/z = 9120 found corresponded to the expected mass of 9119 Da of the PCD modified c subunit. The *E. coli* ATP synthase was similarly inhibited by PCD (data not sown) and the covalent modification of its c subunit was verified with mass spectroscopy (found m/z = 8606, expected 8608). Hence PCD reacts specifically and covalently with cGlu65 of the ATP synthase of *I. tartaricus* or cAsp61 of the ATP synthase of *E. coli* and is therefore suitable for fluorescence investigations.

Reconstitution of the *E. coli* ATP synthase into POPC-liposomes

To compare the two enzymes, the F_1F_0 ATP synthase from *E. coli* was reconstituted into liposomes consisting of POPC as described for the *I. tartaricus* enzyme (von Ballmoos *et al.*, 2002). The retention of the coupled enzyme activity was verified by ATP hydrolysis and DCCD inhibition (data not shown) and proton pumping activities monitored by ACMA quenching (Figure 4-4).
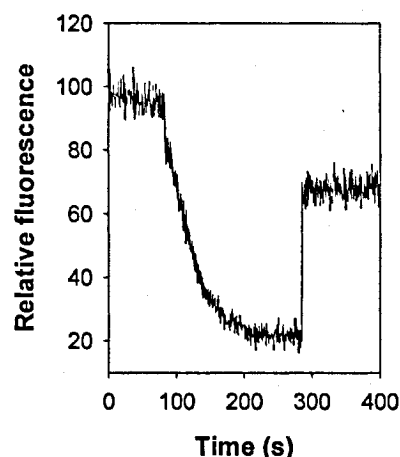
Figure 4-4. ATP-dependent ACMA fluorescence quenching of *E. coli* ATP synthase in POPC-liposomes. Purified *E. coli* ATP synthase was reconstituted into POPC liposomes. The proteoliposomes (75 µl, ~20 µg of protein , 1.5 mg lipid) were diluted in 1.5 ml 50 mM potassium phosphate, pH 7.5, 5 mM MgCl$_2$ and 100 mM were supplied with 2 µM valinomycin to avoid generation of an electric potential. The quenching of fluorescence was started by adding 2.5 mM Na-ATP and abolished with 2 µM carbonyl cyanide *p*-chlorophenylhydrazone. Fluorescence was measured using excitation and emission wavelengths of 410 and 480 nm, respectively.

Fluorescence quenching measurements of reconstituted F$_1$F$_0$ ATP synthases

Purified F$_1$F$_0$ ATP synthase from *I. tartaricus* was labelled with PCD and reconstituted into POPC vesicles as described under Material and Methods. Fluorescence emission spectra of PCD-labelled enzyme were similar to those reported (Harrison *et al.*, 2000; Narayanaswami *et al.*, 1993). The fluorophore is known to show an environment dependent spectrum, moving from a single maximum at 386 nm in a hydrophilic environment to two maxima at 377 nm and 396 nm in a more hydrophobic one. We found spectra with two maxima in the detergent-solubilized as well as in the reconstituted enzyme, with a increase at 377 nm upon reconstitution, indicating a hydrophobic environment in the detergent solubilized as well as in the lipid incorporated form of the enzyme.

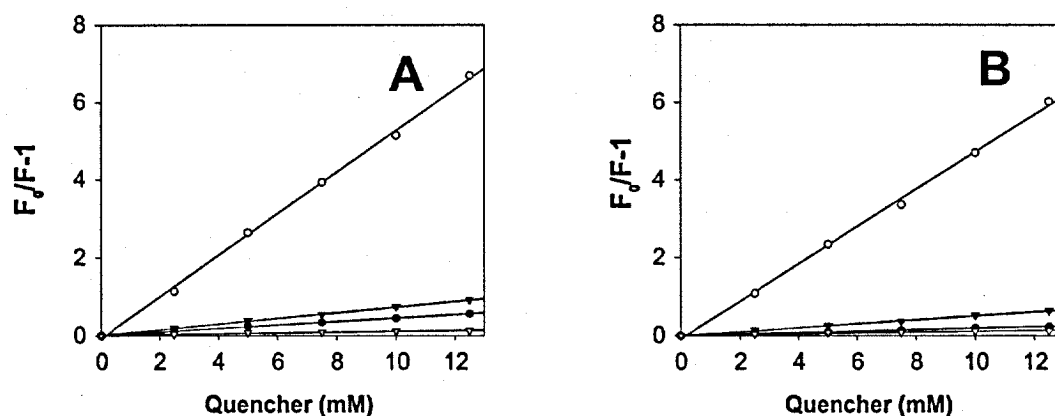**Figure 4-5. Fluorescence quenching of reconstituted ATP synthase from *I. tartaricus* with soluble quenchers.** Stern-Volmer plots of different quenchers are shown. *A*, proteoliposomes containing 250 µg of POPC and 5 µg of *I. tartaricus* ATP synthase were diluted into 300 µl of 50 mM potassium phosphate, pH 7.0, 5 mM MgCl$_2$ and 100 mM K$_2$SO$_4$ and used for a single measurement. For titration of fluorescence yield with different quencher concentrations, samples were incubated with a specific quencher for 1 min from a 1 M stock solution prior to recording spectra. Emission spectra were recorded from 360 nm to 460 nm, using an excitation wavelength of 342 nm. The values at 396 nm were taken for calculations. F$_0$ represents fluorescence yield in the absence, F in the presence of quencher. Acrylamide (cationic, ∇); potassium iodide (anionic, ●); TEMPO-OH (▼); TEMPO (o). *B* is like *A*, but F$_1$F$_0$ ATP synthase from *E. coli* was investigated, using 50 mM potassium phosphate, pH 7.5, 5 mM MgCl$_2$ and 100 mM K$_2$SO$_4$ as reconstitution buffer.

A first set of experiments was performed using soluble quenchers as indicator of the localization of the binding site. We titrated the fluorescence yield against the concentration of quenchers with different chemical properties. No quenching response was observed with the water soluble cationic quencher acrylamide and only marginal quenching was seen with the water soluble anionic quencher potassium iodide or with TEMPO-OH, which is also water soluble. In contrast, efficient quenching was observed with the hydrophobic quencher TEMPO. Hence the fluorophore attached at the coupling ion binding site can only be closely approached by hydrophobic compounds that partition into the lipid bilayer. This confirms the integral membrane location of the binding site (Figure 4-5A). Similar results were obtained from quenching experiments performed with the PCD-labelled *E. coli* ATP synthase reconstituted into POPC, indicating similar membrane embedded coupling ion binding sites on their enzyme (Figure 4-5B).

The fact, that the binding site of the *I. tartaricus* enzyme is embedded in the membrane permitted us to determine its precise localization by parallax analysis of fluorescence quenching. In these studies, we used spinlabelled phosphatidylcholines, harbouring a doxyl group at different positions along the acyl chain. The spinlabelled lipids were mixed in

different ratios with unlabelled POPC prior to the formation of liposomes. The incorporation of quencher lipids at the reconstitution stage avoids any problems arising from different membrane partitioning of the fatty acyl quencher. Spinlabelled fatty acids were used in former parallax experiments, but their detergent like structure and properties as well as their unpredictable positioning in the membrane made the experiments rather difficult to interpret. To obtain conclusive data, we used all commercially available phospholipids spinlabelled at positions 5, 7, 10, 12, 14 and 16 of the stearic acid chain. Either of these compounds was able to quench the pyrene fluorescence in a concentration dependent manner showing the successful introduction of the SLPC at the reconstitution stage. More interestingly, also a position dependent quenching was observed. The results of Figure 4-6A show a continuous increase of the quenching response if the spinlabel was moved successively from position 5 to position 14, close to the center of the membrane. With phospholipids carrying the spinlabel at position 16, the quenching efficiency dropped significantly reaching the level of the position-5-labelled species. These results resemble previous data obtained with this method and are therefore not unexpected (Velasco-Guillen *et al.*, 1998).
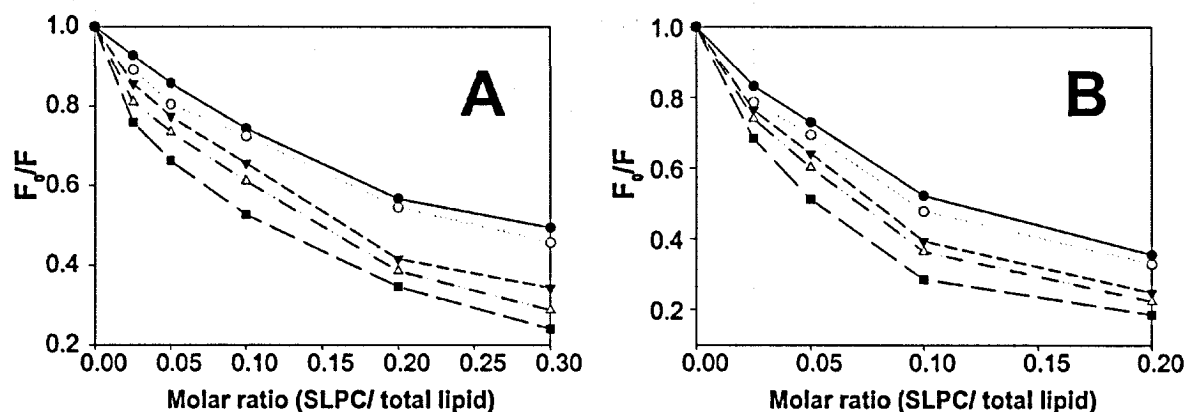
Figure 4-6. Fluorescence quenching of PCD labelled ATP synthases reconstituted in POPC vesicles containing spinlabelled phospholipids. *A*, purified F_1F_0 ATP synthase from *I. tartaricus* was labelled with 50 µM PCD for 6-8 hours at room temperature. Preformed vesicles containing different concentration of spinlabelled phospholipids were taken for reconstitution as described (von Ballmoos *et al.*, 2002). Polystyrene Bio-Beads were taken for removal of residual detergent and should also be helpful to remove unbound fluorophore. The liposomes were collected by ultracentrifugation and resuspended in 50 mM potassium phosphate, pH 7.0, 5 mM MgCl₂ and 100 mM K₂SO₄. Fluorescence emission spectra were recorded from 360 nm to 460 nm, using an excitation wavelength of 342 nm. The yields at 396 nm were taken for parallax analysis calculations. (———), 5-SLPC; (·········), 7-SLPC; (– – – –), 10-SLPC; (– ·· –·), 12-SLPC; (— — —), 14-SLPC. *B* is like *A*, but F_1F_0 ATP synthase from *E. coli* was investigated, using 50 mM potassium phosphate, pH 7.5, 5 mM MgCl₂ and 100 mM K₂SO₄ as reconstitution buffer.

A reasonable explanation for this behaviour may be that the modified end of 16-SLPC acyl chain forces the chain to bend backwards in the membrane, thereby moving the spinlabelled group to a localization closer to the membrane surface. Parallax analysis using different pairs of SLPC for the calculation of the distance between the fluorophore and the bilayer center gave according to equation (2) a value of 1.3 ± 2.4 Å for the *I. tartaricus* enzyme. Very similar results were obtained for the *E. coli* enzyme (Figure 4-6B), resulting in a fluorophore distance from the bilayer center of 1.8 ± 2.8 Å. Fluorescence quenching experiments were also performed with the isolated c_{11} ring after labelling with PCD and reconstitution into liposomes. The results obtained were very similar to those obtained with the labelled F_1F_0 ATP synthase (c.f. Figure 4-5), and therefore indicate proper incorporation of the c ring into the membrane. An important question is whether the c_{11} rotor sites are accessible from one aqueous surface through c_{11} intrinsic channels as proposed recently (von Ballmoos *et al.*, 2002). Another option, favoured vigorously for the *E. coli* ATP synthase, is that access to the membrane embedded rotor sites occurs exclusively via two oppositely oriented subunit a half channels (Fillingame *et al.*, 2000; Junge *et al.*, 1997).
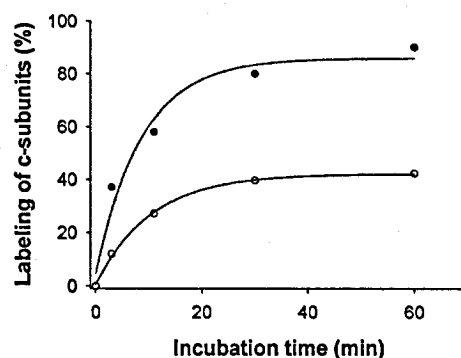
Figure 4-7. Specific labeling of the reconstituted c_{11} oligomer with DCCD and protection with Na^+ Ions. Purified c_{11}, solubilized in 10 mM Tris-HCl, pH 8.0, 1.5 % octylglucoside was reconstituted in preformed vesicles containing soy bean lipids (type II) in a lipid: protein ratio= 100:1 as described in Material and Methods. Proteoliposomes were collected by ultracentrifugation and resuspended in 5 mM MES/MOPS/TRICINE, pH 6.6 containing ≤ 15 µM Na^+. Half of the sample was treated with 5 mM NaCl from a 2 M stock solution. Samples were left for 2 hours at 4 °C for equilibration with the buffer. The samples were incubated with 30 µM DCCD at room temperature and aliquots of 100 µl were taken at the times indicated and diluted into 1 ml $CHCl_3$:MeOH =1:1 to stop the reaction. The modification was analyzed by HPLC as described in Material and Methods. Unmodified (17.78 min) and modified (13.45 min) c subunits were clearly separated on a weak anion exchange column in $CHCl_3$:MeOH:H_2O=4:4:1, using 0.1 M ammonium acetate in the same system as elution solvent. Reaction kinetics without Na^+ (•); or with 5 mM NaCl (o) in the incubation mixture.

To investigate these ambiguities, the accessibility of the binding sites for Na$^+$ or H$^+$ from the aqueous environment was probed with the reconstituted c$_{11}$ oligomer of *I. tartaricus*. In a first series of experiments, the labelling efficiency by PCD was investigated at different pH values and in presence or absence of Na$^+$. The results indicated increased labelling at decreasing pH and protection from the modification by Na$^+$, analogous to observations with the entire ATP synthase complex (Kluge and Dimroth, 1993a). We also measured the kinetics of the modification with DCCD, and the results in Figure 4-7 show a striking decrease in subunit c labelling in the presence of 5 mM NaCl compared to the sample without Na$^+$ addition. For the labelling with DCCD we have chosen a slightly acidic pH (6.6). This assures partial protonation of c65E which is the prerequisite for its reaction with DCCD (Kluge and Dimroth, 1993a). Please note that at this pH complete protection by Na$^+$ cannot be expected because Na$^+$ ion binding requires the deprotonated form of cE65 which is favoured at a more alkaline pH. Nevertheless, these results provide compelling evidence that Na$^+$ or H$^+$ have access to the membrane buried binding sites of the c$_{11}$ rotor ring within a lipid bilayer without the presence of subunit a.. These results therefore reinforce our model for the rotor ring with 11 intrinsic channels linking one aqueous surface with the 11 binding sites in the center of the membrane (von Ballmoos *et al.*, 2002).

4.5 Discussion

It is widely accepted that subunit a and the oligomeric c$_n$ rotor ring of F$_1$F$_0$ ATP synthases form the membrane embedded complex responsible for coupling ion transport across the membrane and that this transport requires rotation of c$_n$ versus subunit a and subunit b (Hutcheon *et al.*, 2001; Kaim and Dimroth, 1998a; Kaim *et al.*, 1998; Suzuki *et al.*, 2002; Tsunoda *et al.*, 2001). The Na$^+$-translocating F$_1$F$_0$ ATP synthases from *P. modestum* and *I. tartaricus* provide unique experimental approaches to investigate coupling ion transport across the membrane. Each c-subunit of the undecameric turbine contains a binding site for Na$^+$ built by two adjacent monomeric units with residues Gln32 and Ser66 on the first and Glu65 on the second (Kaim *et al.*, 1997; Vonck *et al.*, 2002). A large body of evidence is available, that the Na$^+$ binding site is reached from the periplasm via a half channel in subunit a and has free access to the cytoplasmic site outside the subunit a interface (Kaim and Dimroth, 1998a; Kaim and Dimroth, 1998b; Kaim *et al.*, 1998). With these data in mind, a model was proposed with one channel in subunit a and a location of the rotor sites near the membrane surface (Dimroth *et al.*, 1999). However, by crosslinking experiments with a

photoactivatable derivative of DCCD, we recently determined a more hydrophobic localization of the binding site (von Ballmoos *et al.*, 2002). To reach these deeply membrane embedded sites from the aqueous surface, access channels are obviously required. In our view which is based on many different biochemical approaches and on recent structural features of the undecameric rotor ring from *I. tartaricus* (Vonck *et al.*, 2002), the sites are connected to the cytoplasmic membrane surface via 11 rotor intrinsic access channels (von Ballmoos *et al.*, 2002). The rotor sites of the H$^+$-translocating ATP synthase from *E. coli* were proposed to reside in the center of the membrane (Girvin *et al.*, 1998; Hoppe and Sebald, 1984; Junge *et al.*, 1997; Lötscher *et al.*, 1984) and further experimental proof for this location is obtained from our present investigations. However, the model for H$^+$ translocation by the *E. coli* ATP synthase is seriously distinct from that of Na$^+$ translocation by the *I. tartaricus* or *P. modestum* enzymes. In the *E. coli* model, the rotor sites communicate with the two aqueous reservoirs separated by the membrane exclusively via two oppositely oriented half channels in subunit a and no channels have been envisaged within the rotor itself (Junge *et al.*, 1997). Hence, if the two different models reflected accurately natural conditions, the *E. coli* and *P. modestum* ATP synthases must have grossly different structures of the a and c subunits. Such a supposition, however, contrasts the generally accepted idea that structures have been conserved during evolution and is hardly compatible with the fact that hybrid *E. coli/ P. modestum* ATP synthases were fully functional (Kaim and Dimroth, 1994).

Here, we used parallax analysis of fluorescence quenching for a more precise localization of the binding site within the membrane. We covalently labelled the Glu65 of *I. tartaricus* and the analogue Asp61 in *E. coli* with a fluorescent analogue of DCCD. The labelled enzymes were reconstituted into preformed vesicles and were probed with different soluble quenchers. The quenching efficiency of acrylamide and potassium iodide was negligible compared to the membrane permeable compound TEMPO. This indication of a membrane embedded localization of the fluorophore was confirmed, when the labelled ATP synthases were reconstituted into vesicles containing spinlabelled phospholipids at different positions along their stearic acid chain. A conserved localization of 1.3± 2.4 Å and 1.8± 2.8 Å from the center of the bilayer was found for the ATP synthases of *I. tartaricus* and *E. coli*, respectively. These data correspond very well with a distance of 18 Å from the membrane surface in case of the mitochondrial enzyme (Pringle and Taber, 1985). Data supporting a membrane localization were also found for the chloroplast enzyme (Engelbrecht and Junge, 1997; Hutcheon *et al.*, 2001). This uniquely conserved location of the coupling ion binding site in the center of the membrane indicates additional common structural features among the c oligomers from

different species. It is clear from this location that the sites can only be reached via protein channels. It is therefore crucial to decide whether these channels are present in subunit a exclusively or whether each rotor site has its individual c ring intrinsic access channel from the cytoplasmic surface and the single a subunit channels functions in further transporting the ion to the periplasmic surface of the membrane.
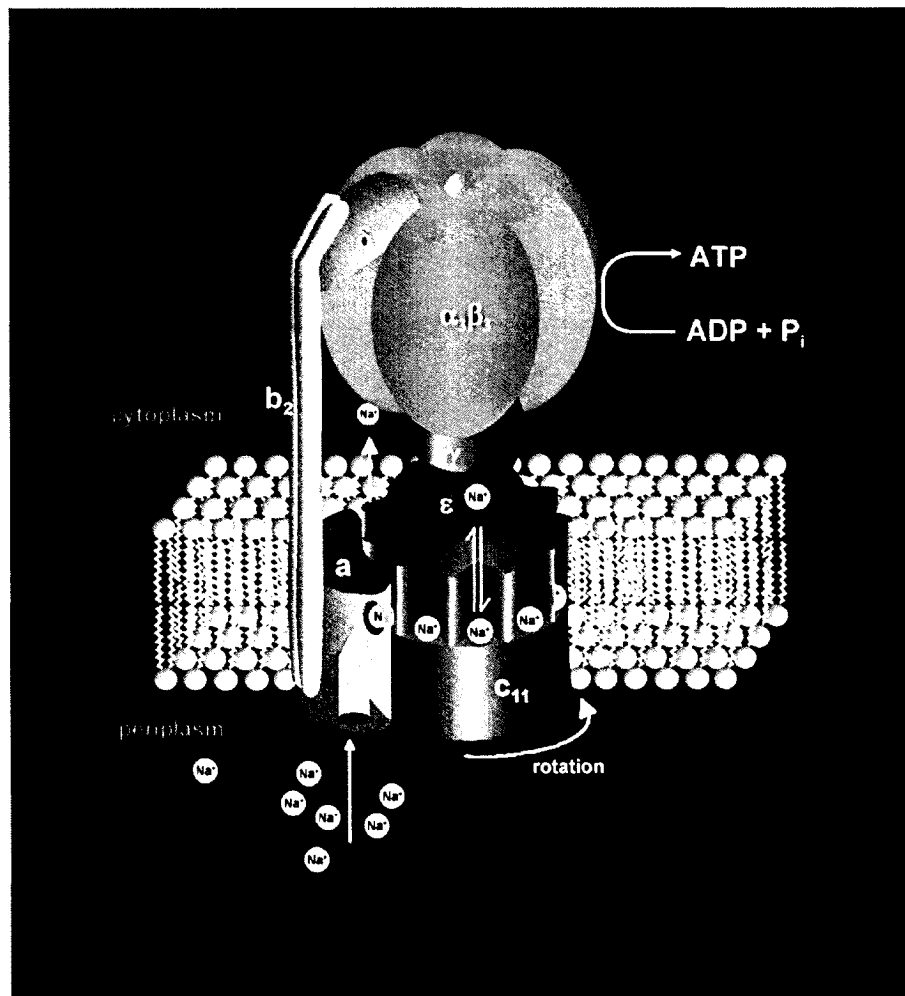
Figure 4-8. Model for Na^+ translocation through the F_0 sector of the F_1F_0 ATP synthase from *I. tartaricus*. During ATP synthesis, the Na^+ ions are envisaged to enter a channel from the periplasmic reservoir formed by subunit a. They pass through this channel approximately to the center of the membrane and bind an empty rotor site at the subunit a/c interface. The next empty rotor site is attracted to the a subunit channel by the membrane potential and the rotor site just occupied rotates out of the subunit a/c interface. The bound Na^+ ion is now accessible to the cytoplasmic reservoir by its rotor intrinsic channel and may dissociate into this reservoir at very low external Na^+ concentrations. Under physiological conditions, however, the site remains occupied until it approaches the a subunit from the other side. The universally conserved arginine (aArg[227] in *I. tartaricus*, aArg[210] in *E. coli*) has been shown to be responsible for facilitating the dissociation of Na^+ from an approaching rotor site (unpublished results).

For Na$^+$-dependent enzymes, it is known, that the specific reaction of cGlu65 with DCCD can be blocked by prior addition of Na$^+$-ions. It is accepted, that DCCD reaches the binding site via the hydrophobic part of the membrane (Engelbrecht and Junge, 1997; Hutcheon *et al.*, 2001), whereas Na$^+$ ions are not membrane permeable without channels. It is hard to imagine, how protection of several binding sites from reaction with DCCD by Na$^+$ ions can take place, if the only channels leading to this site reside on subunit a. Moreover, the binding site in close contact with subunit a is probably the least accessible for a DCCD molecule, because it is shielded from the lipid environment. To overcome any doubts, we reconstituted the native c-oligomer into lipid vesicles to probe the direct accessibility of the binding site from the aqueous environment. The modification of the binding sites by DCCD was specifically protected by Na$^+$ which proves the direct access of Na$^+$ to the c subunit sites by intrinsic access channels of the ring, because no other subunit was present in the reconstituted system. We already speculated about this intrinsic property of c$_{11}$ recently, when structural data of the c oligomer became available (Vonck *et al.*, 2002) and proposed the 1a + 11c channel model (Figure 4-8) (von Ballmoos *et al.*, 2002).

The recent finding of Fillingame and co-workers, that Asp61 of the *E. coli* c oligomer is only accessible in a detergent solubilized form is of course offensive for a common model of ion translocation among these species (Valiyaveetil *et al.*, 2002). Our initial findings of direct accessibility were recently confirmed with the ATP synthase embedded in the bacterial membranes or with the enzyme reconstituted into proteoliposomes (Meier *et al.*, 2003). Hence, this accessibility is not an artefact inherent to the ATP synthase in detergent micelles but an intrinsic property of the c ring.

The common membrane topography of the ion binding sites among different species reported in this work tempts to formulate also a common way of ion translocation across the membrane. For Na$^+$-translocating enzymes, accumulated data support the model proposed in (von Ballmoos *et al.*, 2002), where the binding sites are in direct contact with the cytoplasm through individual intrinsic channels in the c ring. It is therefore obvious to ask whether this model could also be valid for the H$^+$-translocating F$_1$F$_0$ ATP synthase, e.g. from *E. coli* or bovine mitochondria. Unfortunately, H$^+$-translocating enzymes are more difficult to analyze because of the ubiquitous abundance of H$^+$ and so far, no experimental evidence for the 2-channel model is available. Therefore, future investigations in the H$^+$-translocating enzymes possibly should consider the experimentally well documented model presented here.

4.6 References

Abrahams, J.P., Leslie, A.G., Lutter, R. and Walker, J.E. (1994) Structure at 2.8 A resolution of F₁-ATPase from bovine heart mitochondria. *Nature*, **370**, 621-628.

Birkenhager, R., Hoppert, M., Deckers-Hebestreit, G., Mayer, F. and Altendorf, K. (1995) The F₀ complex of the *Escherichia coli* ATP synthase. Investigation by electron spectroscopic imaging and immunoelectron microscopy. *Eur. J. Biochem.*, **230**, 58-67.

Capaldi, R.A. and Aggeler, R. (2002) Mechanism of the F₁F₀-type ATP synthase, a biological rotary motor. *Trends. Biochem. Sci.*, **27**, 154-160.

Chattopadhyay, A. and London, E. (1987) Parallax method for direct measurement of membrane penetration depth utilizing fluorescence quenching by spin-labeled phospholipids. *Biochemistry*, **26**, 39-45.

Deckers-Hebestreit, G., Greie, J., Stalz, W. and Altendorf, K. (2000) The ATP synthase of *Escherichia coli*: structure and function of F₀ subunits. *Biochim. Biophys. Acta*, **1458**, 364-373.

Dimroth, P., Wang, H., Grabe, M. and Oster, G. (1999) Energy transduction in the sodium F-ATPase of *Propionigenium modestum*. *Proc. Natl. Acad. Sci. U.S.A.*, **96**, 4924-4929.

Engelbrecht, S. and Junge, W. (1997) ATP synthase: a tentative structural model. *FEBS Lett.*, **414**, 485-491.

Fillingame, R.H. and Foster, D.L. (1986) Purification of F₁F₀ H(+)-ATPase from *Escherichia coli*. *Methods Enzymol.*, **126**, 545-557.

Fillingame, R.H., Jiang, W., Dmitriev, O.Y. and Jones, P.C. (2000) Structural interpretations of F(0) rotary function in the *Escherichia coli* F(1)F(0) ATP synthase. *Biochim. Biophys. Acta*, **1458**, 387-403.

Girvin, M.E., Rastogi, V.K., Abildgaard, F., Markley, J.L. and Fillingame, R.H. (1998) Solution structure of the transmembrane H⁺-transporting subunit c of the F₁F₀ ATP synthase. *Biochemistry*, **37**, 8817-8824.

Groth, G. and Pohl, E. (2001) The structure of the chloroplast F₁-ATPase at 3.2 A resolution. *J. Biol. Chem.*, **276**, 1345-1352.

Harrison, M., Powell, B., Finbow, M.E. and Findlay, J.B. (2000) Identification of lipid-accessible sites on the nephrops 16-kDa proteolipid incorporated into a hybrid vacuolar H(+)-ATPase: site-directed labeling with N-(1-Pyrenyl)cyclohexylcarbodiimide and fluorescence quenching analysis. *Biochemistry*, **39**, 7531-7537.

Hoppe, J. and Sebald, W. (1984) The proton conducting F₀-part of bacterial ATP synthases. *Biochim. Biophys. Acta*, **768**, 1-27.

Hutcheon, M.L., Duncan, T.M., Ngai, H. and Cross, R.L. (2001) Energy-driven subunit rotation at the interface between subunit a and the c oligomer in the F(O) sector of *Escherichia coli* ATP synthase. *Proc. Natl. Acad. Sci. U.S.A.*, **98**, 8519-8524.

Jiang, W. and Fillingame, R.H. (1998) Interacting helical faces of subunits a and c in the F₁F₀ ATP synthase of *Escherichia coli* defined by disulfide cross-linking. *Proc. Natl. Acad. Sci. U.S.A.*, **95**, 6607-6612.

Junge, W., Lill, H. and Engelbrecht, S. (1997) ATP synthase: an electrochemical transducer with rotatory mechanics. *Trends Biochem. Sci.*, **22**, 420-423.

Kaim, G. and Dimroth, P. (1994) Construction, expression and characterization of a plasmid-encoded Na⁺-specific ATPase hybrid consisting of *Propionigenium modestum* F₀-ATPase and *Escherichia coli* F₁-ATPase. *Eur. J. Biochem.*, **222**, 615-623.

Kaim, G. and Dimroth, P. (1998a) A triple mutation in the a subunit of the *Escherichia coli/Propionigenium modestum* F₁F₀ ATPase hybrid causes a switch from Na⁺ stimulation to Na⁺ inhibition. *Biochemistry*, **37**, 4626-4634.

Kaim, G. and Dimroth, P. (1998b) Voltage-generated torque drives the motor of the ATP synthase. *EMBO J.*, **17**, 5887-5895.

Kaim, G., Matthey, U. and Dimroth, P. (1998) Mode of interaction of the single a subunit with the multimeric c subunits during the translocation of the coupling ions by F₁F₀ ATPases. *EMBO J.*, **17**, 688-695.

Kaim, G., Wehrle, F., Gerike, U. and Dimroth, P. (1997) Molecular basis for the coupling ion selectivity of F₁F₀ ATP synthases: probing the liganding groups for Na⁺ and Li⁺ in the c subunit of the ATP synthase from *Propionigenium modestum*. *Biochemistry*, **36**, 9185-9194.

Kluge, C. and Dimroth, P. (1993a) Kinetics of inactivation of the F₁F₀ ATPase of *Propionigenium modestum* by dicyclohexylcarbodiimide in relationship to H⁺ and Na⁺ concentration: probing the binding site for the coupling ions. *Biochemistry*, **32**, 10378-10386.

Kluge, C. and Dimroth, P. (1993b) Specific protection by Na⁺ or Li⁺ of the F₁F₀-ATPase of *Propionigenium modestum* from the reaction with dicyclohexylcarbodiimide. *J. Biol. Chem.*, **268**, 14557-14560.

Knol, J., Veenhoff, L., Liang, W.J., Henderson, P.J., Leblanc, G. and Poolman, B. (1996) Unidirectional reconstitution into detergent-destabilized liposomes of the purified lactose transport system of *Streptococcus thermophilus*. *J. Biol. Chem.*, **271**, 15358-15366.

Laubinger, W. and Dimroth, P. (1988) Characterization of the ATP synthase of *Propionigenium modestum* as a primary sodium pump. *Biochemistry*, **27**, 7531-7537.

Laubinger, W. and Dimroth, P. (1989) The sodium ion translocating adenosinetriphosphatase of *Propionigenium modestum* pumps protons at low sodium ion concentrations. *Biochemistry*, 28, 7194-7198.

Lötscher, H.R., deJong, C. and Capaldi, R.A. (1984) Modification of the F_0 portion of the H^+-translocating adenosinetriphosphatase complex of Escherichia coli by the water-soluble carbodiimide 1-ethyl-3-[3-(dimethylamino)propyl]carbodiimide and effect on the proton channeling function. *Biochemistry*, 23, 4128-4134.

Meier, T., Matthey, U., von Ballmoos, C., Vonck, J., Krug von Nidda, T., Kühlbrandt, W. and Dimroth, P. (2003) Evidence for structural integrity in the undecameric c-rings isolated from sodium ATP synthases. *J. Mol. Biol.*, 325, 389-397.

Miller, M.J., Oldenburg, M. and Fillingame, R.H. (1990) The essential carboxyl group in subunit c of the F_1F_0 ATP synthase can be moved and H(+)-translocating function retained. *Proc. Natl2 Acad. Sci. U.S.A.*, 87, 4900-4904.

Moriyama, Y., Iwamoto, A., Hanada, H., Maeda, M. and Futai, M. (1991) One-step purification of Escherichia coli H(+)-ATPase (F_0F_1) and its reconstitution into liposomes with neurotransmitter transporters. *J. Biol. Chem.*, 266, 22141-22146.

Narayanaswami, V., Kim, J. and McNamee, M.G. (1993) Protein-lipid interactions and Torpedo californica nicotinic acetylcholine receptor function. 1. Spatial disposition of cysteine residues in the gamma subunit analyzed by fluorescence-quenching and energy-transfer measurements. *Biochemistry*, 32, 12413-12419.

Neumann, S., Matthey, U., Kaim, G. and Dimroth, P. (1998) Purification and properties of the F_1F_0 ATPase of *Ilyobacter tartaricus*, a sodium ion pump. *J. Bacteriol.*, 180, 3312-3316.

Noji, H., Yasuda, R., Yoshida, M. and Kinosita, K., Jr. (1997) Direct observation of the rotation of F_1-ATPase. *Nature*, 386, 299-302.

Pänke, O., Gumbiowski, K., Junge, W. and Engelbrecht, S. (2000) F-ATPase: specific observation of the rotating c subunit oligomer of EF_0EF_1. *FEBS Lett.*, 472, 34-38.

Pringle, M.J. and Taber, M. (1985) Fluorescent analogues of N,N'-dicyclohexylcarbodiimide as structural probes of the bovine mitochondrial proton channel. *Biochemistry*, 24, 7366-7371.

Sambongi, Y., Iko, Y., Tanabe, M., Omote, H., Iwamoto-Kihara, A., Ueda, I., Yanagida, T., Wada, Y. and Futai, M. (1999) Mechanical rotation of the c subunit oligomer in ATP synthase (F_0F_1): direct observation. *Science*, 286, 1722-1724.

Schägger, H. and von Jagow, G. (1987) Tricine-sodium dodecyl sulfate-polyacrylamide gel electrophoresis for the separation of proteins in the range from 1 to 100 kDa. *Anal. Biochem.*, 166, 368-379.

Seelert, H., Poetsch, A., Dencher, N.A., Engel, A., Stahlberg, H. and Muller, D.J. (2000) Structural biology. Proton-powered turbine of a plant motor. *Nature*, 405, 418-419.

Singh, S., Turina, P., Bustamante, C.J., Keller, D.J. and Capaldi, R. (1996) Topographical structure of membrane-bound *Escherichia coli* F_1F_0 ATP synthase in aqueous buffer. *FEBS Lett.*, 397, 30-34.

Stahlberg, H., Muller, D.J., Suda, K., Fotiadis, D., Engel, A., Meier, T., Matthey, U. and Dimroth, P. (2001) Bacterial Na⁺-ATP synthase has an undecameric rotor. *EMBO Rep.*, 2, 229-233.

Stock, D., Leslie, A.G. and Walker, J.E. (1999) Molecular architecture of the rotary motor in ATP synthase. *Science*, 286, 1700-1705.

Suzuki, T., Ueno, H., Mitome, N., Suzuki, J. and Yoshida, M. (2002) F_0 of ATP Synthase Is a Rotary Proton Channel. OBLIGATORY COUPLING OF PROTON TRANSLOCATION WITH ROTATION OF c-SUBUNIT RING. *J. Biol. Chem.*, 277, 13281-13285.

Takeyasu, K., Omote, H., Nettikadan, S., Tokumasu, F., Iwamoto-Kihara, A. and Futai, M. (1996) Molecular imaging of *Escherichia coli* F_0F_1-ATPase in reconstituted membranes using atomic force microscopy. *FEBS Lett.*, 392, 110-113.

Tsunoda, S.P., Aggeler, R., Yoshida, M. and Capaldi, R.A. (2001) Rotation of the c subunit oligomer in fully functional F_1F_0 ATP synthase. *Proc. Natl. Acad. Sci. U.S.A.*, 98, 898-902.

Valiyaveetil, F., Hermolin, J. and Fillingame, R.H. (2002) pH dependent inactivation of solubilized F_1F_0 ATP synthase by dicyclohexylcarbodiimide: pK(a) of detergent unmasked aspartyl-61 in *Escherichia coli* subunit c. *Biochim. Biophys. Acta*, 1553, 296-301.

Velasco-Guillen, I., Corbalan-Garcia, S., Gomez-Fernandez, J.C. and Teruel, J.A. (1998) Location of N-cyclohexyl-N'-(4-dimethyl-amino-alpha-naphthyl)carbodiimide- binding site in sarcoplasmic reticulum Ca^{2+}-transporting ATPase. *Eur. J. Biochem.*, 253, 339-344.

von Ballmoos, C., Appoldt, Y., Brunner, J., Granier, T., Vasella, A. and Dimroth, P. (2002) Membrane topography of the coupling ion binding site in Na⁺-translocating F_1F_0 ATP synthase. *J. Biol. Chem.*, 277, 3504-3510.

Vonck, J., Krug von Nidda, T., Meier, T., Matthey, U., Mills, D.J., Kühlbrandt, W. and Dimroth, P. (2002) Molecular architecture of the undecameric rotor of a bacterial Na⁺-ATP synthase. *submitted*.

Ward, A., Sanderson, N.M., O'Reilly, J., Rutherford, N.G., Poolman, B. and Henderson, P.J.F. (2000) *The amplified expression, identification, purification, assay, and properties of hexahistidine-tagged bacterial membrane transport proteins.* University Press, Oxford.

Weber, J. and Senior, A.E. (1997) Catalytic mechanism of F_1-ATPase. *Biochim. Biophys. Acta*, **1319**, 19-58.

Yoshida, M., Muneyuki, E. and Hisabori, T. (2001) ATP synthase--a marvellous rotary engine of the cell. *Nat. Rev. Mol. Cell. Biol.*, **2**, 669-677.

Zucker, S.D., Goessling, W., Bootle, E.J. and Sterritt, C. (2001) Localization of bilirubin in phospholipid bilayers by parallax analysis of fluorescence quenching. *J. Lipid. Res.*, **42**, 1377-1388.

5. The ion channel of F-ATP synthase is the target of toxic organotin compounds

Christoph von Ballmoos[1], Josef Brunner[2] and Peter Dimroth[1]

[1]Institut für Mikrobiologie der Eidgenössischen Technischen Hochschule, ETH Zentrum, CH-8092 Zürich, Switzerland; [2]Institut für Biochemie der Eidgenössischen Technischen Hochschule, ETH-Hönggerberg, CH-8093 Zürich, Switzerland

5.1 Abstract

ATP is the universal energy currency of living cells and the majority of it is synthesized by the F_1F_0 ATP synthase. Inhibitors of this enzyme are therefore potentially detrimental for all life forms. Tributyltin chloride (TBT-Cl) inhibits ATP hydrolysis by the Na^+-translocating ATP synthase of *Ilyobacter tartaricus* or the H^+-translocating counterpart of *Escherichia coli* with apparent K_i of 200 nM. To target the site of this inhibition, we synthesized a tritium labeled derivative of TBT-Cl in which one of the butyl groups was replaced by a photoactivatable aryldiazirine residue. Upon illumination, subunit a of the ATP synthase becomes specifically modified and this labeling is suppressed in the presence of the original inhibitor. In case of the Na^+ ATP synthase, labeling is also suppressed in the presence of Na^+ ions, suggesting an interference in Na^+ or TBT-Cl binding to subunit a. This interference is corroborated by the protection of ATP hydrolysis from TBT-Cl inhibition by 105 mM Na^+. TBT-Cl strongly inhibits Na^+ exchange by the reconstituted *Ilyobacter tartaricus* ATP synthase. Taken together these results indicate that the subunit a ion channel is the target site for ATPase inhibition by toxic organotin compounds. TBT-Cl is the first known inhibitor interacting specifically with this site.

5.2 Introduction

Organotin compounds are of widespread use in many different areas since more than 60 years. Tributyltin is broadly used as a preserving agent mainly for wood and textiles, and in antifouling paints on ships leading to severe contamination of aquatic ecosystems. Triphenyltin is applied in agriculture as a pesticide. Dioctyl-, mono- and dibutyltin serve as stabilizers in plastics (e.g. PVC) and are therefore found in many products of daily use (Fent, 1996; Fent, 2003).

The general toxicity of organotin compounds is complex and not well understood. In higher organisms, the immune system and production of steroid hormones are affected, e.g. through inhibition of aromatase leading to masculinization (Heidrich et al., 2001; Omura et al., 2001). Although organotins have been known for decades to act as potent inhibitors of the F_1F_0 ATP synthase, this property has received remarkable little attention and the mechanism of interaction has remained enigmatic (Cain and Griffiths, 1977; Matsuno-Yagi and Hatefi, 1993; Selwyn, 1976). This is the more astonishing as the release of an efficient F-ATP synthase inhibitor into the environment may be critical for all life forms. F-ATP synthases

play a fundamental role in cellular energy metabolism and are therefore an important constituent of nearly every living cell from bacteria to man.

The ATP synthases are rotary enzymes composed of two motors that are connected by a common shaft to exchange energy with one another (Boyer, 1997). During ATP synthesis, the membrane embedded F_0 motor converts energy from an electrochemical transmembrane gradient of protons or Na^+ ions into torque. Rotation is transmitted by the shaft to the water exposed F_1 motor where it drives the synthesis of ATP from ADP and phosphate. While the structure and function of the F_1 motor is well established (Abrahams *et al.*, 1994; Capaldi and Aggeler, 2002; Noji *et al.*, 1997) knowledge of the F_0 motor trails behind (Dimroth *et al.*, 2003). An effective approach to gain mechanistic insight into the workings of the F_0 motor are studies with specific inhibitors that target this portion of the F-ATP synthase. A well characterized inhibitor of the F-ATP synthases is dicyclohexylcarbodiimide (DCCD), which covalently modifies the ion binding site residues glutamate or aspartate on the c subunits, effectively disabling the F_0 motor from rotation by sterical hindrance. Some 45 years ago, Aldridge described the toxic effect of organotin substances on oxidative phosphorylation in mitochondria (Aldridge, 1958). This was the beginning of a variety of investigations that showed that all known ATP synthases from bacteria, yeast, and chloroplast to mammalian mitochondria are susceptible to these substances at comparable concentrations. Thereby, tributyltin chloride (TBT-Cl) turned out to be an especially potent inhibitor, although only representing the large variety of organotin compounds, which all act in the same manner (Cain and Griffiths, 1977; Selwyn, 1976). TBT-Cl affects the enzyme at levels 10 to 100 times lower and faster than DCCD. However, as TBT-Cl reacts non-covalently with the enzyme, the site for its interaction is not clear. We reasoned that determination of the binding site could provide important insights into the molecular features of the ATP synthase that are crucial for biological function and at the same time reveal a molecular basis for the toxicology of organotin compounds.

5.3 Experimental procedures

All chemicals were purchased from Fluka, Buchs, Switzerland, or the Sigma-Aldrich company.

Purification of F_1F_0 ATP synthase

The F_1F_0 ATP synthase was purified from wild-type *I. tartaricus* or *E. coli* cells by fractionated precipitation with polyethyleneglycol (Neumann *et al.*, 1998; von Ballmoos *et al.*, 2002b). The ATP synthase was resuspended in 10 mM Tris-HCl, pH 8.0, and stored in liquid N_2.

Purification of the c_{11} ring from *Ilyobacter tartaricus*

The c oligomer of the F_1F_0 ATP synthase from *I. tartaricus* was purified as described (Meier *et al.*, 2003).

Determination of ATP hydrolyzing activity

ATP hydrolyzing activity was determined with the coupled spectrophotometric assay as described (Laubinger and Dimroth, 1988).

Na^+-exchange experiments

The Na^+-exchange measurements were performed as described (Kluge and Dimroth, 1992).

Photoaffinity labeling experiments with photoactivatable organotin analogue

Incubation mixtures of 100 µl contained 20 µg of purified F_1F_0 ATP synthase or 10 µg of purified c_{11} from *Ilyobacter tartaricus* in 50 mM Tris/ HCl, pH 8.0, 5 mM $MgCl_2$, and 0.05% Triton X-100. In competition experiments samples were either incubated with DCCD for 30 min, or with Na^+ and organotin derivatives for 60 s before the addition of the tritium marked photoprobe ($[^3H]$-4-[3-(trifluoromethyl)-3*H*-diazirin-3-yl]benzyloxymethyl-dibutyltin chloride; 1µM; 1.875 µCi).The mixed sample was then mounted 10 cm in front of a Hg-lamp and immediately (60 s handling time) irradiated for 45 s at $\lambda > 320$ nm and 280 W (350 W Hg-Lamp, SUSS LH 1000 lamp house). An unirradiated sample was kept at 4°C as a control.

Workup of photolabeling experiments and $[^3H]$-autoradiography/fluorography

The samples were mixed with SDS to 1% final concentration, and subsequently overlaid with 1.2 ml of diisopropyl ether and shaken by hand for 2 min to remove unbound photolabel from the aqueous solution. The upper organic phase was discarded and the aqueous phase mixed with 5x loading buffer without SDS. An amount of 25 µl (5 µg protein) was then subjected to SDS PAGE on a 13.2 % gel. The gel was fixed for 30 min (10% acetic acid, 30% 2-propanol,

60% water) and subsequently incubated for 15 min with enhancer solution (Amersham). The gel was dried in a heat drier system (BioRad) on Whatman paper while the other side was covered with water impermeable foil, which could be removed after drying. Radioactively marked proteins were fluorographically detected using Hyperfilm MP (Amersham) in a cassette with intensifying screen, which was kept at –80° C for 12-50 h before development. The gels were afterwards removed from the Whatman paper and stained with silver.

Chemical synthesis

General methods

Thin layer chromatography was performed on Merck silica gel 60F-254 plates. Intermediates and tin-containing substances were detected by fluorescence quenching in UV-light (254 nm) or with an organotin reaction spray (1. decomposition of the metallorganic substances by UV light; 2. spray plates with a 0.1% (w/v) solution of pyrocatecholviolet in ethanol to stain tin containing bands in bright blue color). Flash chromatography was performed with Merck 60 (0.04-0.063 mm) silica gel in various solvent mixtures. UV spectra (λ_{max} in nm (log ε)) were recorded in a 1 cm quartz cell. IR spectra were recorded from a 3% $CHCl_3$ solution. ^{1}H-NMR (300 MHz) and ^{13}C-NMR (75 MHz) were recorded on a Varian Gemini system. Chemical shifts δ are in ppm and coupling constants J in Hz.

Strategy

The chemical synthesis of the photoactivatable organotin derivative (DDBT-Cl) is depicted in Figure 1-1. Briefly, we prepared dibutylphenyltin methyl iodide *4* from commercially available dibutyltin dichloride *1* via Grignard reaction, halogenation and subsequent conversion with Simmons-Smith reagent ICH_2ZnI. The methyl iodide *4* was further coupled to a photoactivatable aryldiazirinylmethyl alcohol *5* and the protecting phenyl group was removed by halogenation to obtain the active photolabeling compound *7*. Insertion of a tritium label was obtained by a back-to-back oxidation/reduction reaction of the aryldiazirinylmethyl alcohol *5* with labeled $NaB[^3H]_4$ as described for the synthesis of a photoactivatable cholesterol analogue (Thiele *et al.*, 2000).
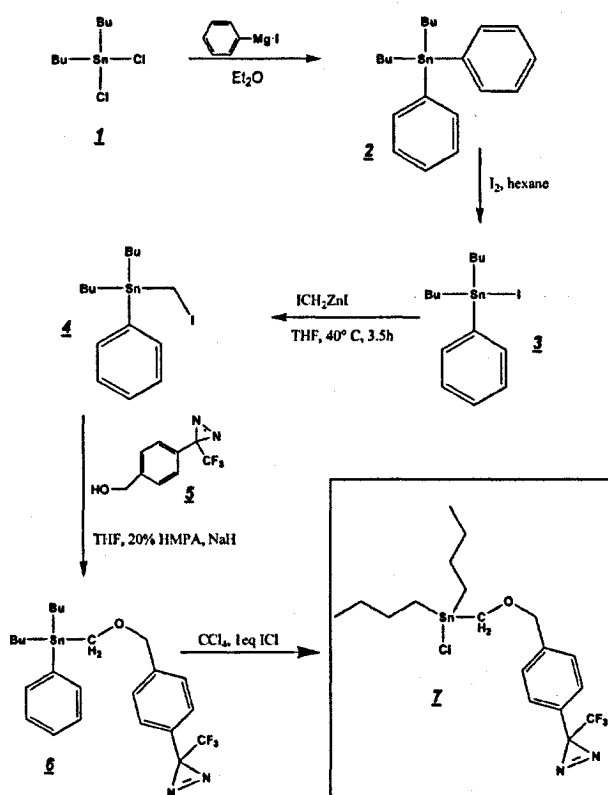
Figure 5-1. Chemical synthesis of the photoactivatable organotin derivative _7_ (DDBT-Cl).
Dibutylphenyltin iodide _3_ was prepared as described in the literature via Grignard reaction and subsequent halogenation. Synthesis of _4_ was obtained after conversion with Simmons-Smith reagent ICH₂ZnI, which was further coupled to an aryldiazirinylmethyl alcohol _5_ in the presence of sodium hydride and hexamethylphosphoramide (HMPA). Deprotection of the product _6_ was obtained after stoichiometric treatment with iodine monochloride in carbon tetrachloride.

Preparation of dibutylphenyltin methyliodide _4_

Dibutylphenyltin iodide _3_ was prepared via dibutyldiphenyltin _2_ from commercially available dibutyltin dichloride _1_ as described (Marr *et al.*, 1988). Synthesis of _4_, which has not been described in the literature, was performed in analogy to the method of Seyferth and Andrews (Seyferth and Andrews, 1971). The zinc copper couple was prepared by the method of Le Goff (LeGoff, 1964). In a 100 ml three-necked, round bottomed flask, 40 mg of cupric acetate was dissolved in 4 ml hot acetic acid using a steam bath. To this solution, 2.6 g of granular zinc was added, and the hot mixture was shaken for 2 min. The solvent was decanted and replaced by 4 ml of acetic acid and the process repeated. The cooled couple was then washed three times with 8 ml of diethyl ether and dried under a stream of nitrogen. The apparatus was completed by a magnetic stir bar, a 50 ml dropping funnel, reflux condenser and a gas inlet tube. The complete apparatus was dried by heat and strictly kept under nitrogen atmosphere. After cooling to room temperature, 7 ml of dry tetrahydrofuran (THF) was added to the

couple and the dropping funnel was loaded with 10.2 g of diiodomethane in 7 ml of dry THF. The reaction was started by the addition of a few drops of the diiodomethane solution and slight warming by a heat gun, which could be followed by an exothermic reaction and the formation of a purple color. The reaction mixture was diluted with two volumes of dry THF, while addition of diiodomethane was completed at 40° C. The reaction was allowed to continue for additional 150 min, with mild heating (50° C) over the last hour, by which time most of the couple was consumed.

The mixture was cooled to 0° C and the turbid, grayish suspension was filtered under nitrogen into a dried apparatus similar as described above. The dropping funnel was loaded with 5.6 g (11.5 mmol) _3_ in 12 ml THF and the solution added slowly within 1 h to the mixture kept at 40° C. The reaction was allowed to continue for additional 120 min.

The cooled reaction mixture was treated with 50 ml benzene and extracted four times each with 40 ml 5% hydrochloric acid. The organic phase was dried with $MgSO_4$, concentrated and Kugelrohr distilled to obtain a colorless liquid (4.5 g, 83%; 90% purity as estimated by thin layer chromatography (TLC)). Further purification was performed with flash chromatography using pure hexane.

^{1}H-NMR ($CDCl_3$): 0.9 (t, $(CH_2)_3CH_3$, 6H); 1.2-1.6 (m, $(CH_2)_3CH_3$, 12H); 2.18 (t, $SnCH_2I$, 2H); 7.35 (d, J= 8.1, 2H); 7.47 (m, 3H). ^{13}C-NMR ($CDCl_3$): 54.15; 127.19; 128.7; 129.38; 137.5. Mass spectrometry (positive electron impact): found m/z= 394.9 (45%) (expected m/z= 394.9 for [M-Bu]$^+$); found m/z= 338.8 (27%) (expected m/z= 338.8 for [M-Bu$_2$]$^+$); found m/z= 196.9 (100%) (expected m/z= 196.9 for [M-Bu2PhCH$_2$I]$^+$)

Preparation of 4-[3-(trifluoromethyl)-3H-diazirin-3-yl]benzyloxymethyl- dibutyl-phenyltin _6_

Synthesis of _6_ was done as described by Still (Still, 1978) with the following modifications. Sodium hydride (55-65% dispersion in oil, 50 mg, 1 mmol) was washed three times with pentane and suspended in 7 ml dry THF in a two-necked round bottomed flask. 170 mg of diazirine-alcohol _5_, dissolved in 5 ml THF, was added dropwise to the stirred suspension. After gas evolution had ceased, 384 mg of _4_ in 6 ml THF were added and the reaction mixture completed with the addition of 4 ml hexamethylphosphoramide (HMPA). The reaction was stirred for 150 min, and then quenched with H_2O (10 ml). The mixture was extracted with diethyl ether (3x 20 ml) and the combined organic phases washed with brine (20 ml), dried

over Na_2SO_4 and concentrated under reduced pressure. Flash chromatography (hexane/ethyl acetate 20:1) yielded 340 mg (75%) of **6** as colorless oil.

^{1}H-NMR (CDCl$_3$): 0.9 (m, (CH$_2$)$_3$CH$_3$, 6H); 1.2-1.6 (m, (CH$_2$)$_3$CH$_3$, 12H); 2.18 (t, SnCH$_2$I, 2H); 7.35 (d, J= 8.1, 2H); 7.47 (d, J= 8.1, 2H). ^{19}F-NMR (CDCl$_3$): -65.0 (s, CF$_3$). ^{13}C-NMR (CDCl$_3$): 54.15; 127.19; 128.7; 129.38; 137.5.

Preparation of 4-[3-(trifluoromethyl)-*3H*-diazirin-3-yl]benzyloxymethyl-dibutyltin chloride **7**

Halogenation of compound **6** was performed as described (Bähr and Pawlenko, 1978). A solution of 16.7 mg ICl in 825 μl CCl$_4$ was added dropwise to 50 mg of **6** dissolved in 11 ml CCl$_4$ while stirring at 0° C. After warming up to room temperature (10 min) CCl$_4$ was evaporated under reduced pressure without heating. The slightly purple (iodine) oil was dried under high vacuum for 12 h to remove iodobenzene to yield 38 mg (80%) of **7** as colorless oil. The sample was free from iodobenzene as checked by ^{1}H-NMR and was not further purified.

Preparation of [^{3}H]-4-[3-(trifluoromethyl)-3*H*-diazirin-3-yl]benzyloxymethyl-dibutyltin chloride **8**

A solution of **5** (530 mg, 2.31 mmol) in 20 ml dichloromethane and Dess-Martin periodinane (1.3 g, 3.23 mmol, 1.4 x) was added at room temperature (Fang *et al.*, 1998; Weber and Brunner, 1995). After stirring for 20 min, the mixture was poured into a mixture of 1 M Na$_2$SO$_3$ (5 ml) and aqueous saturated NaHCO$_3$ (5 ml), and subsequently extracted with dichloromethane (3x 10 ml). The combined organic solution was concentrated *in vacuo* and the residual oil was purified by flash chromatography (hexane/ethyl acetate 4:1) and 140 mg (30%) of diazirine aldehyde **8** was obtained as colorless oil. Since the boiling point of the aldehyde is considerably lower than that of the alcohol, most of the material was lost during drying under high vacuum.

To 0.5 ml solution of pure aldehyde **8** (1 mg, 4.6 μmol) in isopropanol, a solution of 25 mCi of [^{3}H] NaBH$_4$ (0.33 μmol) in 0.1 M NaOH was added and the mixture was stirred at room temperature for 6 h. 300 μl of 1 M HCl was added, and after 15 min the mixture was extracted with 2 x 1 ml ethyl acetate. The combined organic solution was dried by filtering it through a Pasteur pipette containing MgSO$_4$ and concentrated to a volume of 0.5 ml. The solution was subjected to column chromatography, yielding 11.5 mCi (46%) of [^{3}H]-labeled alcohol **5**. The sample was of high purity according to analysis by TLC and autoradiography.

5.4 Results and Discussion

Inhibition characteristics of membrane-bound and solubilized ATP synthases

We investigated the effect of TBT-Cl on the Na^+-translocating F-ATP synthase of *Ilyobacter tartaricus* and the H^+-translocating ATP synthase from *Escherichia coli* in parallel. Sodium ion translocating F-ATP synthases are close relatives of their proton translocating counterparts with unique experimental options to explore features of the ion translocation mechanism (Dimroth *et al.*, 2003). In the ATP hydrolysis mode, both enzymes displayed a similar response to TBT-Cl yielding apparent K_i values of 200 nM, comparable to studies with ATPases from other organisms (Linnett and Beechey, 1979) (Figure 5-2B). Inhibition characteristics were the same for the membrane-bound and detergent-purified enzymes. However, with F_1 alone or after disrupting energy coupling with excess detergent (1.5 % Triton X-100), the inhibition was abolished, indicating that TBT-Cl affects the F_0 part of the enzyme complex.

Synthesis and application of a photoactivatable organotin derivative (DDBT-Cl)

In order to define the site of TBT-Cl interaction we chose a photoaffinity labeling strategy (von Ballmoos *et al.*, 2002a). We chemically synthesized a tritium labeled derivative of TBT-Cl in which one of the butyl groups was replaced by an aryldiazirine residue (Figure 5-2A, for details see Figure 5-1 and Experimental procedures). Upon illumination with UV light, the diazirine is converted into a highly reactive carbene which forms a covalent photolabeling product with any nearby molecule. The inhibition characteristics of the photoprobe were very similar (Figure 5-2B) to those of TBT-Cl indicating that the site of interaction with the ATP synthase was the same for both compounds.
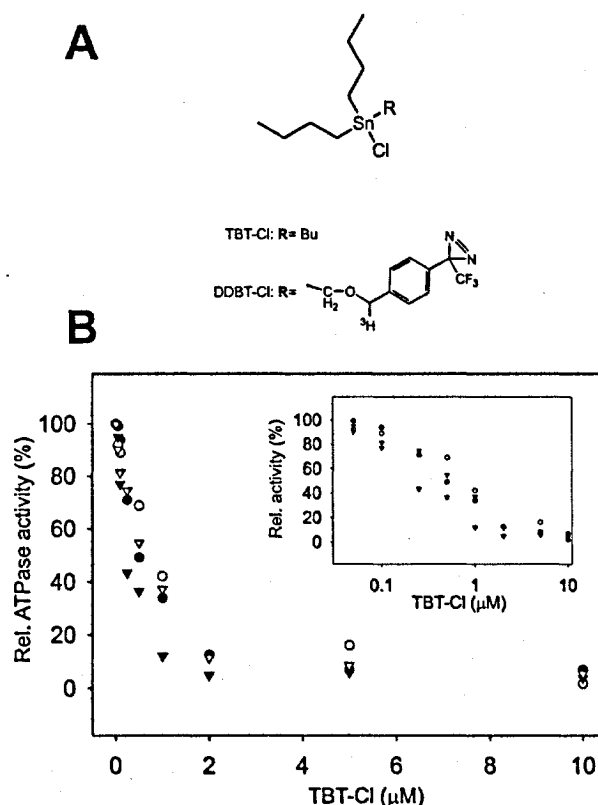
Figure 5-2. Chemical structures of TBT-Cl derivatives and inhibition of ATPases. A.) Structure of trisubstituted organotin compounds used in this study. TBT-Cl: tributyltin chloride; [^{3}H]-DDBT-Cl: [^{3}H]-diazirinedibutyltin chloride. **B.)** Inhibition of ATPase by TBT-Cl derivatives. TBT-Cl and detergent purified ATP synthase from *I. tartaricus* (black triangles). TBT-Cl and membrane associated ATP synthase from *I. tartaricus* (black circles). TBT-Cl and membrane associated ATP synthase from *E. coli* (open circles). DDBT-Cl and detergent purified ATP synthase from *I. tartaricus* (open triangles). Inset: logarithmic plot.

Photoaffinity labeling of ATP synthase and c-oligomer with DDBT-Cl

In a typical photolabeling experiment, 20 µg of the purified sodium F-ATP synthase of *Ilyobacter tartaricus* was mixed with 1 µM of radioactive photolabel and illuminated for 45 s with UV light. Analysis of the sample by SDS-PAGE and subsequent fluorography revealed only two radioactive products, which were barely seen in the non-irradiated control (Figure 5-3). Clearly, the main product was formed with subunit a and significantly weaker labeling was found in the oligomeric c ring (c$_{11}$), despite its relative abundance. However, when the sample was pretreated with 50 µM of TBT-Cl or the non radioactive photoprobe, labeling of subunit a was almost completely suppressed while that of c$_{11}$ was not affected. No change in subunit a modification was observed if the sodium binding sites of the c$_{11}$ ring were partially

modified with DCCD. Preincubation of the ATP synthase with 50 mM NaCl showed reduced labeling of the a subunit.
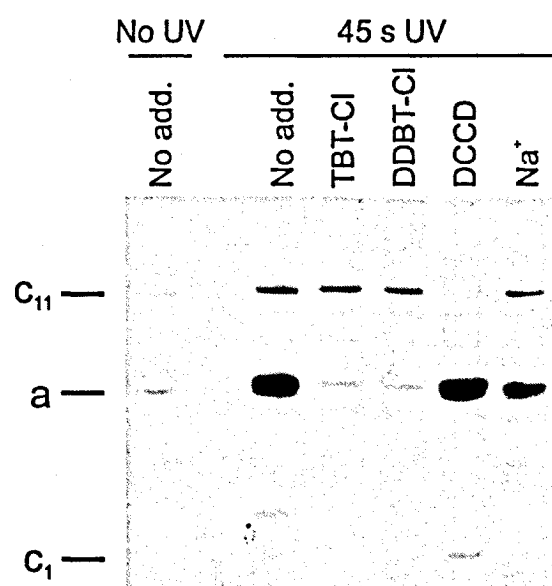

Figure 5-3. Photoaffinity labeling experiments reveal specific interaction of organotins with subunit a. Fluorogram of SDS-PAGE analysis of photoaffinity studies with the ATP synthase from *I. tartaricus*. F- ATP synthase (20 µg, 0.2 mg/ml) in 50 mM Tris/HCl, pH 8.0, 5 mM MgCl$_2$ and 0.05% Triton X-100 was mixed with 1 µM of [^{3}H]-DDBT-Cl and irradiated for 45 s with UV light. An unirradiated sample shows that product formation requires photoactivation by UV light. Samples were incubated as indicated with TBT-Cl, DDBT-Cl (50 µM) and NaCl (50 mM) 1 min prior to addition of the radioactive photolabel, whereas DCCD (50 µM) was added 30 min before the radioactive photolabel.

This prompted us to perform a more detailed analysis on the interaction of Na$^+$ with the binding of TBT-Cl to subunit a (see below). Photolabeling experiments were repeated with the enzyme reconstituted into lipid bilayers, revealing the same labeling characteristics. Since only modification of subunit a is affected by the addition of competitors, we conclude that the photoprobe specifically binds to subunit a and that the observed weak interaction with subunit c is of a non-specific nature. Since the diazirine group is about 7 Å apart from the central tin ion, one has to consider the possibility that the organotin binding site resides on subunits b or c and that the observed labeling of subunit a is due to bridging the distance by the diazirine-containing side chain. Such a scenario is however unlikely to cause massive labeling of subunit a side by side with no labeling at all of subunit b and only poor unspecific labeling of subunit c. Furthermore, the ion channel is blocked effectively with low concentrations of

TBT-Cl which does not contain the diazirine compound. Therefore a site in proximity to the subunit a channel evidently binds DDBT-Cl with high affinity causing specific autolabeling of this subunit upon irradiation. This conclusion is fully in accord with binding studies performed with the isolated c_{11} ring from *I. tartaricus*. Similar to the binding studies with the enzyme complex described above, the labeling of c subunits of c_{11} was of unspecific nature not being competed by the addition of tributyltin chloride or by Na^+ ions (data not shown). These findings are in accordance to early photolabeling experiments of the ATP synthase with hydrophobic diazirine compounds where products were formed preferentially with subunit c (Hoppe *et al.*, 1984).

Interaction studies of TBT with the Na^+ ion binding site on the c-oligomer

From earlier experiments, subunit c was regarded as the primary target for organotins (Cain and Griffiths, 1977; Partis *et al.*, 1984). However, these experiments were unable to exploit the use of a covalent protein-inhibitor complex as reported here. Additional investigations performed at low pH, where the tin chloride bond is broken and a hydrophobic cation is the dominant species in solution (Tobias *et al.*, 1966), indicated that this species binds to the c oligomer and prevents its modification by DCCD. This is probably due to non-specific ion pairing of the positive organotin and the negative DCCD binding amino acid (pK~7) in the hydrophobic environment of the membrane. Prevention of carbodiimide modification however, could not be found at pH values above 7 (data not shown).

Influence of Na^+ concentration on organotin inhibition

Subunit a harbors the ion channel that provides access to the binding site on the c_{11} ring in the middle of the membrane from the periplasmic surface (von Ballmoos *et al.*, 2002b). The channel is essential for the enzyme's operation since mutants in which the channel is blocked are completely inactive in both the ATP synthesis and/ or coupled ATP hydrolysis mode (Kaim and Dimroth, 1998a). The channel of subunit a could therefore be the target for the inhibitory organotin compounds. In strong support of this hypothesis is the reduced binding of the photolabel in the presence of Na^+ ions as described above (Figure 5-3). Further acceptance of this notion is provided by a comparison of ATPase inhibition by TBT-Cl at varying Na^+ concentrations. The results of Figure 5-4A show a remarkable shift of the apparent K_i of TBT-Cl from 0.2 to 1.5 µM if the Na^+ concentration was increased from 5 to 105 mM, indicating competition between TBT-Cl and Na^+ for a common binding site on subunit a. The competition between Na^+ and TBT-Cl binding was corroborated at a constant inhibitor

concentration and varying Na^+ concentrations. ATPase inhibition by TBT-Cl decreased from 90% to 30% if the Na^+ concentration was raised from 5 to 300 mM. In contrast, no effect was observed with similar concentrations of LiCl or RbCl.
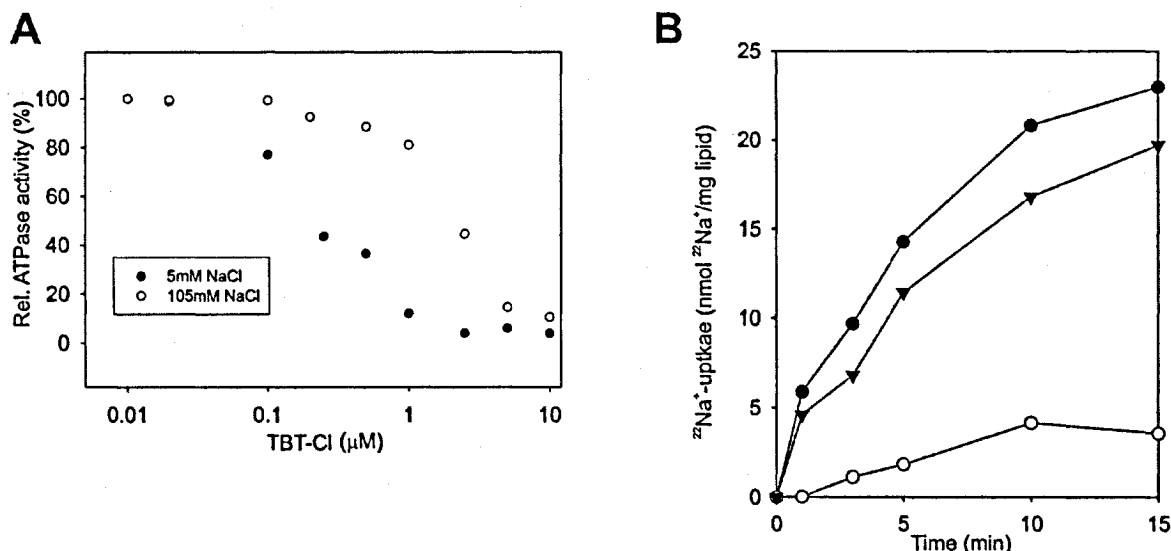

Figure 5-4. Evidence for competition between Na^+ and TBT-Cl for binding to the ATP synthase. A.) Protection of ATPase from TBT-Cl inhibition by 105 mM NaCl. ATPase activities were determined with the purified enzyme from *I. tartaricus* in the presence of TBT-Cl and NaCl concentrations indicated. **B.)** TBT-Cl blocks the Na^+ channel. $^{22}Na^+/Na^+$-exchange experiments with ATP synthase from *I. tartaricus* reconstituted into liposomes. Control without inhibitor (black circles). ATP synthase preincubated 30 min with 50 μM DCCD (black triangles). Exchange in presence of 50 μM TBT-Cl (open circles).

Na^+ transport studies in proteoliposomes

A recognition site for Na^+ ions in subunit a of the *Propionigenium modestum* (a close relative from *I. tartaricus*) ATP synthase was anticipated from earlier studies when the ion specificity was restricted by mutagenesis to Li^+ and H^+ and ATP hydrolysis was specifically inhibited by Na^+ due to the impaired permeability of the subunit a ion channel for this alkali ion (Kaim *et al.*, 1998). Similar to this mutant phenotype is the inhibition of ATPase activity of the wild type enzyme by TBT-Cl indicating that TBT-Cl could act as a specific blocker of the subunit a ion channel. The results described above on the specific binding of DDBT-Cl to subunit a and the competition between TBT-Cl and Na^+ for a common binding site are completely compatible with this supposition. To investigate the effect of TBT-Cl on Na^+ translocation directly, we took advantage of a convenient property of the ATP synthase. In absence of an external energy source (membrane potential or ATP), the enzyme rests in an idling mode, which is characterized by back and forth movements of the rotor against the stator within a

narrow angle, catalyzing a 1:1 exchange of Na^+ ions between the two reservoirs separated by the membrane (Kaim and Dimroth, 1998b). This exchange can therefore be followed by the uptake of $^{22}Na^+$ into proteoliposomes, if the radioactive tracer is present at the outside and unlabeled Na^+ is present at the inside. During exchange, every Na^+ traversing the membrane must pass through the subunit a channel. Hence, if the channel is blocked by TBT-Cl, this should abolish $^{22}Na^+$ uptake into the proteoliposomes via $^{22}Na^+_{out}/ Na^+_{in}$ exchange. The results of Figure 5-4B show that this is indeed the case. In control experiments without TBT-Cl, the enzyme catalyzes rapid uptake of $^{22}Na^+$ into the proteoliposomes. This exchange is not significantly affected by modifying part of the binding sites on c_{11} with DCCD in accord with previous measurements (Kaim and Dimroth, 1998b). In these studies it was shown that modifying part of the rotor sites with DCCD inhibits the rotor sterically from full revolutions but allows back and forth movements within a narrow angle which is sufficient for Na^+ exchange via stator (subunit a) (Kaim and Dimroth, 1998b) and rotor (c_{11}) channels (Meier et al., 2003; von Ballmoos et al., 2002b) across the membrane. Prevention of Na^+ exchange by TBT-Cl treatment indicates direct interference with the ion translocation pathway and is therefore completely compatible with the proposed action of this compound as a blocker of the subunit a ion channel.

Models for ion translocation through the F_0 part

Two different models have been envisaged for ion translocation through the F_0 motor domain of the Na^+ or H^+ F-ATP synthase, respectively. Sodium ion translocation through the F_0 motor is proposed to proceed via the subunit a channel (inlet channel) from the periplasm to the binding site on the c_{11} rotor ring in the middle of the membrane. After moving the site out of the interface with subunit a by rotation, the ion can diffuse through its intrinsic rotor channel (outlet channel) into the cytoplasmic reservoir, a process which is facilitated by the positive stator charge (R227) at the reentry of the interface (Dimroth et al., 2003). Evidence for the inlet channel was obtained by a subunit a triple mutant (Kaim et al., 1998a), which specifically abolished Na^+ transport through the channel while retaining transport capacity of Li^+ and H^+, and by the inhibitor studies reported in this communication. Evidence for the intrinsic rotor channels was obtained by demonstrating access of Na^+ or H^+ to the binding sites of the isolated c_{11} ring in solution or in reconstituted in liposomes, respectively (Meier et al., 2003; von Ballmoos et al., 2002b).

The model for H^+ translocation through the E. coli F_0 motor postulates that both the inlet and the outlet channel are located in subunit a and denies any rotor intrinsic channels (Junge et al.,

1997; Vik and Antonio, 1994). Hence, both models agree with respect to the inlet channel and evidence for it has recently been presented by accessibility studies with engineered cysteine residues in subunit a (Angevine *et al.*, 2003). The outlet channel has also been probed by the same technique, but only residues near the cytoplasmic surface could be reached by the aqueous probes. Until now, clear evidence for a cytoplasmic outlet channel on subunit a or on the rotor ring is therefore not available.

5.5 Concluding remarks

Organotin compounds are under intense debate since they have been recognized in the 1990's for a variety of disastrous effects in the marine ecosystem. Thereby, the well known tributyltin, which is used in huge amounts in antifouling paints for large ships, has been called "the most toxic chemical ever deliberately released into the seas" (WWF). Whereas the toxicity towards higher organisms includes a variety of effects, in bacteria, inhibition of the phosphorylation cascade for ATP synthesis seems to be a primary target. About 45 years ago, TBT-Cl has been described as a powerful inhibitor for ATP synthases from different organisms, mostly H^+-translocating enzymes from mitochondrial, chloroplast and bacterial origin (Aldridge, 1958; Linnett and Beechey, 1979). This universal inhibitory capacity implies a common structural arrangement conserved among these enzymes. The site of interaction could, however, never be elucidated due to the non covalent nature of the interaction. Using a photoaffinity labeling strategy, we could define the site of interaction to be the membrane embedded a subunit. Subunit a provides a half channel from the periplasmic reservoir to the middle of the membrane through which coupling ions are gated to reach the binding site on the oligomeric c subunit. We show that in the sodium F-ATP synthase inhibition can be suppressed by high sodium ion concentrations, indicating competition between inhibitor and Na^+ binding.

Summing up, we envisage at the entrance of the subunit a channel a hydrophilic environment, allowing hydrated ions to approach. A recognition site allows the Na^+ ion to shed part of its hydration shell. This process acts as a selectivity filter, comparable to the mechanism in the potassium channel, where the size of the hydrated potassium ion is crucial (Doyle *et al.*, 1998). TBT-Cl is proposed to bind near the selectivity filter and to prevent Na^+ ions to pass through the channel. Conversely, Na^+ binding to the recognition site interferes with TBT-Cl binding, since the recognition sites for the two compounds are structurally overlapping (Figure 5-5). The interaction of organotins on the periplasmic channel in subunit a is

compatible with proposed mechanisms for ion translocation in different species in spite of their discrepancies described above. This is the first documentation of an ATPase inhibitor that interacts specifically with subunit a. The periplasmic channel is blocked by TBT-Cl with concomitant inhibition of ATP synthesis or hydrolysis activities. This novel tool will allow directed experiments to unravel details of the ion transport mechanism across the membrane, which may shed light on the mechanism of torque generation by the F_0 motor. The successful application of a photoactivatable organotin analogue should be of considerable interest for research towards organotin toxicity in every investigated organism.
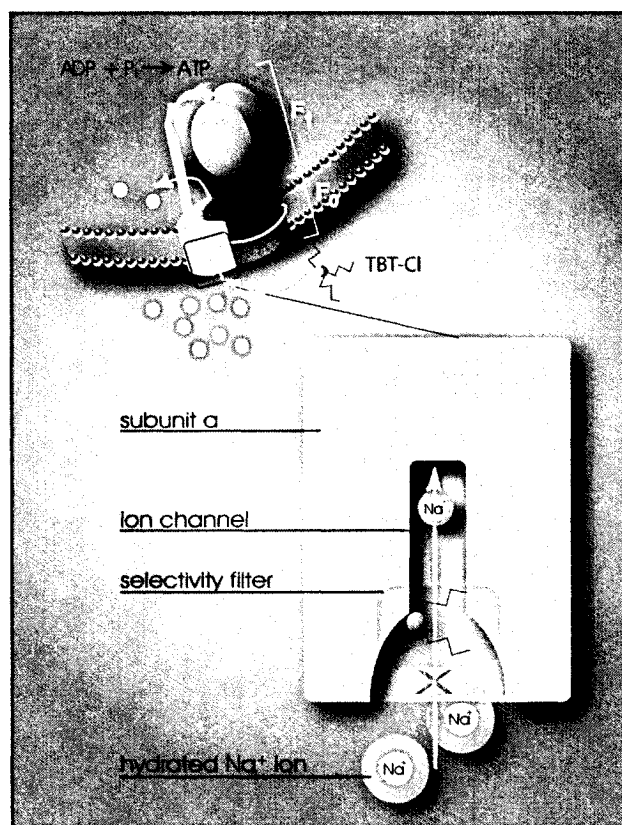
Figure 5-5. Model for the interaction of organotin compounds with F-ATP synthases. ATP synthesis from ADP and phosphate (P_i) is coupled to the downhill flux of ions across the membrane-bound F_0 portion. The lower part shows a section through the subunit a channel along the membrane normal. During ATP synthesis hydrated ions enter the mouth of the channel and stripe off part of their hydration shell at the selectivity filter (only Na^+ ions can pass the filter). If hydrophobic organotin compounds are present they accumulate within the membrane and easily penetrate into the entrance of the channel. Here, they interact with a site near the selectivity filter which disables incoming ions to shed their hydration shell. As a consequence, the ions do not proceed through the channel and ATP synthesis is blocked.

Acknowledgements

5.6 References and Notes

Abrahams, J.P., Leslie, A.G., Lutter, R. and Walker, J.E. (1994) Structure at 2.8 A resolution of F_1-ATPase from bovine heart mitochondria. *Nature*, 370, 621-628.

Aldridge, W.N. (1958) The biochemistry of organotin compounds: trialkyltins and oxidative phosphorylation. *Biochem. J.*, 69, 367-376.

Angevine, C.M., Herold, K.A. and Fillingame, R.H. (2003) Aqueous access pathways in subunit a of rotary ATP synthase extend to both sides of the membrane. *Proc. Natl. Acad. Sci. U.S.A.*, 100, 13179-13183.

Bähr, G. and Pawlenko, S. (1978) Organozinn-halogenide bzw. -pseudeohalogenide. *Houben-Weyl*, 13, 265-288.

Boyer, P.D. (1997) The ATP synthase- a splendid molecular machine. *Annu. Rev. Biochem.*, 66, 717-749.

Cain, K. and Griffiths, D.E. (1977) Studies of energy-linked reactions. Localization of the site of action of trialkyltin in yeast mitochondria. *Biochem. J.*, 162, 575-580.

Capaldi, R.A. and Aggeler, R. (2002) Mechanism of the F_1F_0-type ATP synthase, a biological rotary motor. *Trends. Biochem. Sci.*, 27, 154-160.

Dimroth, P., von Ballmoos, C., Meier, T. and Kaim, G. (2003) Electrical power fuels rotary ATP synthase. *Structure (Camb.)*, 11, 1469-1473.

Doyle, D.A., Morais Cabral, J., Pfuetzner, R.A., Kuo, A., Gulbis, J.M., Cohen, S.L., Chait, B.T. and MacKinnon, R. (1998) The structure of the potassium channel: molecular basis of K^+ conduction and selectivity. *Science*, 280, 69-77.

Fang, K., Hashimoto, M., Jockusch, S., Turro, N.J. and Nakanishi, K. (1998) A bifunctional photoaffinity probe for ligand/receptor interaction studies. *J. Amer. Chem. Soc.*, 120, 8543-8544.

Fent, K. (1996) Ecotoxicology of organotin compounds. *Crit. Rev. Toxicol.*, 26, 1-117.

Fent, K. (2003) Ecotoxicological problems associated with contaminated sites. *Toxicol. Lett.*, 140-141, 353-365.

Heidrich, D.D., Steckelbroeck, S. and Klingmuller, D. (2001) Inhibition of human cytochrome P450 aromatase activity by butyltins. *Steroids*, 66, 763-769.

Hoppe, J., Brunner, J. and Jorgensen, B.B. (1984) Structure of the membrane-embedded F_0 part of F_1F_0 ATP synthase from *Escherichia coli* as inferred from labeling with 3-(Trifluoromethyl)-3-(m-[125I]iodophenyl)diazirine. *Biochemistry*, 23, 5610-5616.

Junge, W., Lill, H. and Engelbrecht, S. (1997) ATP synthase: an electrochemical transducer with rotatory mechanics. *Trends Biochem. Sci.*, 22, 420-423.

Kaim, G. and Dimroth, P. (1998a) A triple mutation in the a subunit of the *Escherichia coli/Propionigenium modestum* F_1F_0 ATPase hybrid causes a switch from Na^+ stimulation to Na^+ inhibition. *Biochemistry*, 37, 4626-4634.

Kaim, G. and Dimroth, P. (1998b) Voltage-generated torque drives the motor of the ATP synthase. *EMBO J.*, 17, 5887-5895.

Kaim, G., Matthey, U. and Dimroth, P. (1998) Mode of interaction of the single a subunit with the multimeric c subunits during the translocation of the coupling ions by F_1F_0 ATPases. *EMBO J.*, 17, 688-695.

Kluge, C. and Dimroth, P. (1992) Studies on Na^+ and H^+ translocation through the F_0 part of the Na^+-translocating F_1F_0 ATPase from *Propionigenium modestum*: discovery of a membrane potential dependent step. *Biochemistry*, 31, 12665-12672.

Laubinger, W. and Dimroth, P. (1988) Characterization of the ATP synthase of *Propionigenium modestum* as a primary sodium pump. *Biochemistry*, 27, 7531-7537.

LeGoff, E. (1964) Cyclopropanes from an easily prepared, highly active zinc-copper couple, dibromomethane, and olefins. *J. Org. Chem.*, 29, 2048-2050.

Linnett, P.E. and Beechey, R.B. (1979) Inhibitors of the ATP synthetase system. *Methods Enzymol.*, 55, 472-518.

Marr, I.L., Rosales, D. and Wardell, J.L. (1988) Preparation and properties of unsymmetrical tetraorganotin compounds. *J. Organomet. Chem.*, 349, 65- 74.

Matsuno-Yagi, A. and Hatefi, Y. (1993) Studies on the mechanism of oxidative phosphorylation. ATP synthesis by submitochondrial particles inhibited at F_0 by venturicidin and organotin compounds. *J. Biol. Chem.*, 268, 6168-6173.

Meier, T., Matthey, U., von Ballmoos, C., Vonck, J., Krug von Nidda, T., Kühlbrandt, W. and Dimroth, P. (2003) Evidence for structural integrity in the undecameric c-rings isolated from sodium ATP synthases. *J. Mol. Biol.*, **325**, 389-397.

Neumann, S., Matthey, U., Kaim, G. and Dimroth, P. (1998) Purification and properties of the F_1F_0 ATPase of *Ilyobacter tartaricus*, a sodium ion pump. *J. Bacteriol.*, **180**, 3312-3316.

Noji, H., Yasuda, R., Yoshida, M. and Kinosita, K., Jr. (1997) Direct observation of the rotation of F_1-ATPase. *Nature*, **386**, 299-302.

Omura, M., Ogata, R., Kubo, K., Shimasaki, Y., Aou, S., Oshima, Y., Tanaka, A., Hirata, M., Makita, Y. and Inoue, N. (2001) Two-generation reproductive toxicity study of tributyltin chloride in male rats. *Toxicol. Sci.*, **64**, 224-232.

Partis, M.D., Griffiths, D.G. and Beechey, R.B. (1984) Discrimination between the binding sites of modulators of the H^+-translocating ATPase activity in rat liver mitochondrial membranes. *Arch. Biochem. Biophys.*, **232**, 610-615.

Selwyn, M.J. (1976) Triorganotin compounds as ionophores and inhibitors of ion translocating ATPases. *Adv. Chem.*, **157**, 204-226.

Seyferth, D. and Andrews, B.S. (1971) Halomethyl-Metal compounds L. Preparation of monohalomethyl derivatives of germanium, tin, lead and mercury via halomethylzinc halides. *J. Organomet. Chem.*, **30**, 151-166.

Still, C.W. (1978) Stannylation/Destannylation. Preparation of alpha-alkoxy organolithium reagents and synthesis of dendrolasin via a carbinyl carbanion equivalent. *J. Amer. Chem. Soc.*, **100**, 1484-1487.

Thiele, C., Hannah, M.J., Fahrenholz, F. and Huttner, W.B. (2000) Cholesterol binds to synaptophysin and is required for biogenesis of synaptic vesicles. *Nat. Cell. Biol.*, **2**, 42-49.

Tobias, R.S., Farrer, H.N., Hughes, M.B. and Nevett, B.A. (1966) Hydrolysis of the aquo ions R_3Sn^+ and R_2Sn^{2+}: Steric effects on the dissociation of aquo acids. *Inorg. Chem.*, **5**, 2052-2055.

Vik, S.B. and Antonio, B.J. (1994) A mechanism of proton translocation by F_1F_0 ATP synthases suggested by double mutants of the a subunit. *J. Biol. Chem.*, **269**, 30364-30369.

von Ballmoos, C., Appoldt, Y., Brunner, J., Granier, T., Vasella, A. and Dimroth, P. (2002a) Membrane topography of the coupling ion binding site in Na^+-translocating F_1F_0 ATP synthase. *J. Biol. Chem.*, **277**, 3504-3510.

von Ballmoos, C., Meier, T. and Dimroth, P. (2002b) Membrane embedded location of Na^+ or H^+ binding sites on the rotor ring of F_1F_0 ATP synthases. *Eur. J. Biochem.*, **269**, 5581-5589.

Weber, T. and Brunner, J. (1995) 2-(Tributylstannyl)-4-3-(trifluoromethyl)-3*H*-diazirin-3-yl-benzyl alcohol: A building block for photolabeling and crosslinking reagents of very high specific radioactivity. *J. Amer. Chem. Soc.*, **117**, 3084-3095.

6. A continuous fluorescent method to measure Na$^+$ transport

Christoph von Ballmoos and Peter Dimroth

Institut für Mikrobiologie der Eidgenössischen Technischen Hochschule, ETH Zentrum, CH-8092 Zürich, Switzerland

6.1 Introduction

In the past decades, various primary sodium pumps have been found which play important roles in the metabolism of different organisms (Dimroth, 1997). Examples are the ubiquitous Na$^+$/K$^+$ ATPases of eukaryotic cells and the bacterial Na$^+$-translocating decarboxylases, ATP synthases and NADH: ubiquinone oxidoreductase of the Nqr and complex I type (Dimroth *et al.*, 2003; Gemperli *et al.*, 2002). The measurement of Na$^+$ transport across a biological membrane is an important experimental tool to investigate specific properties of these catalysts (as an example, see ref. (Kluge and Dimroth, 1992)). Unlike H$^+$-transport, which can be followed by pH change in a particular compartment, the measurement of Na$^+$ into proteoliposomes is more difficult and laborious. Methods, which have been used previously, have a common drawback. Since only the Na$^+$ content entrapped in the interior compartment should be measured, this has to be separated afore from external Na$^+$ ions. This separation is usually performed by passing the liposome suspension through a column of the strong cation exchanger DOWEX50, K$^+$, which adsorbs all Na$^+$ ions except those entrapped in the inner lumen of the liposomes. The incorporated sodium content is then easily measured by means of radioactive ^{22}Na$^+$ or by atomic absorption spectroscopy. Both methods, however, have the disadvantage of being discontinuous, since for every data point the separation procedure described above has to be included. Moreover, the usage of the strong radioactive ^{22}Na$^+$ (γ radiation) is inconvenient.

Although a number of Na$^+$ fluorophores are commercially available, their application has so far been restricted to the detection of sodium ions within whole cells (as an example, see ref. (Despa *et al.*, 2000)). Here we present a facile method to qualitatively measure sodium ion uptake into proteoliposomes by the Na$^+$-specific fluorophore Sodium Green, which is commercially available.

6.2 Material and Methods

Reagents

The two sodium specific fluorophores, SBFI, tetraammonium salt (S-1262) and Sodium Green, tetra (tetramethyl) ammonium salt (S-6900) were from Molecular Probes, Inc. (Leiden, NL). Phosphatidylcholine from soy bean (Type II S) was from Sigma. Other reagents were from Fluka (Buchs, Switzerland).

The fluorophores were dissolved in dimethylsulfoxide (20 mg/ ml) and stored at -20° C in the dark.

Reconstitution of F_1F_0 ATP synthase into lipid vesicles

Method A

The reconstitution of F-type ATP synthase from *Ilyobacter tartaricus* into liposomes was performed with minor modifications as described (Kluge and Dimroth, 1992). Liposomes were formed by vortexing of a suspension of 30 mg phosphatidylcholine and 20 μg of a Na^+-specific fluorophore in 0.9 ml 50 mM potassium phosphate, pH 7.0, 1 mM dithioerythritol, 1 mM NaCl to homogeneity (5 min) and subsequent sonication for 2 x 30 s in a tip sonicator (MSE Soniprep 150 homogenizer, Sanyo). The purified F_1F_0 ATP synthase from *Ilyobacter tartaricus* (0.3 mg protein) in 0.1 ml 5 mM potassium phosphate, pH 8.0, 2.5 mM $MgCl_2$ was added to the preformed liposomes and the suspension was incubated at room temperature for 10 min with occasional shaking. The mixture was frozen in liquid nitrogen, kept there for 10 min and subsequently thawed in a water/ ice mixture which lasted about 1 h. The proteoliposomes were sonicated for 3 x 5 s with the tip sonicator. To remove the external fluorophore, the proteoliposomes were subjected to gel filtration on a NAP-10 column (Amersham Biosciences) in 50 mM potassium phosphate, 2.5 mM $MgCl_2$. The turbid fractions were collected and directly used for transport measurement.

Method B

Liposomes were formed after a modified protocol as described (Knol *et al.*, 1996). Soy bean phosphatidylcholine (30 mg), dissolved in $CHCl_3$:MeOH (2:1, v:v) in a round-bottomed flask were flushed with nitrogen. The solvent was removed under reduced pressure first in a rotary evaporator and then in high vacuum for 4 h. The lipids and 20 μg of the fluorophore were resuspended in 0.9 ml buffer (50 mM potassium phosphate, pH 7.0, 1 mM dithioerythritol, 1 mM NaCl) and subjected to seven freeze-thaw cycles in liquid N_2 and at 37°C with short vigorous shaking after each cycle. In order to gain unilamellar vesicles of defined size, the suspension was passed 15 times through a membrane (100, 200, or 400 nm) using a liposome extruder (LiposoFast Pneumatic, Avestin, Canada). The preformed liposomes were further utilized as described in Method A.

Determination of Na^+ transport into proteoliposomes

All measurements were performed on a RF-5001PC spectrofluorometer (Shimadzu) in a 300 μl quartz cuvette. Typically, 50 μl of the proteoliposomes were mixed with 250 μl of the assay mixture (50 mM potassium phosphate, pH 7.0, 2.5 mM $MgCl_2$, 6 mM phosphoenolpyruvate, 10 U pyruvate kinase). Subsequently, 1 μM of valinomycin was added and the fluorescence emission was recorded (Sodium green: 540 nm/ 488 nm excitation; SBFI 505 nm/ 333 nm

excitation). Na$^+$-uptake into proteoliposomes was initiated with the addition of 1 mM Na$_2$ATP. The dicyclohexylcarbodiimide (DCCD) treated sample was incubated with 50 µM of the inhibitor at pH 6.5 30 min prior to measurement. Tributyltin chloride (50 µM) was added directly into the final solution without prior incubation.

6.3 Results and Discussion

Formation of proteoliposomes

Both fluorophores used in this study have been applied to detect sodium ions in whole cell studies (Despa *et al.*, 2000). Initial experiments were performed with both fluorophores, but only the results with Sodium Green are presented here, since this compound turned out to be more suitable. The only advantage of SFBI over Sodium Green is its easier quantification via relative emission at two wavelengths. Both compounds are available in a membrane permeable and an impermeable form, which was chosen for this study. As stated in the product sheet from Molecular Probes (Haugland, 2002), Sodium Green consists of a fluorescein analogue linked to each of the nitrogens of a crown ether with a cavity size that confers selectivity for the Na$^+$ ion and can detect small changes (< 1mM) of Na$^+$ in solution (Figure 6-1). As compared to SBFI, Sodium Green exhibits greater selectivity for Na$^+$ than for K$^+$ (41-fold versus 18-fold) and displays a much higher quantum yield in Na$^+$-containing solutions. Its dissociation constant (K$_d$) for Na$^+$ is about 6 mM at 22°C in potassium-free solution, and about 21 mM at 22°C in solutions containing both Na$^+$ and K$^+$ (with a total ion concentration of 135 mM) (Haugland, 2002).

Since the inner volume of the liposomes is almost negligible compared to that of the surrounding medium, the amount of fluorophore incorporated into the proteoliposomes is intuitively important for the sensitivity of the transport assay. In a first series of experiments, we tested how we can influence the amount of incorporated fluorophore by different reconstitution techniques. We varied the size of the liposomes, the time point and the amount of added fluorophore. Afterwards, we removed the external fluorophore by gel filtration and measured the fluorophore incorporated.
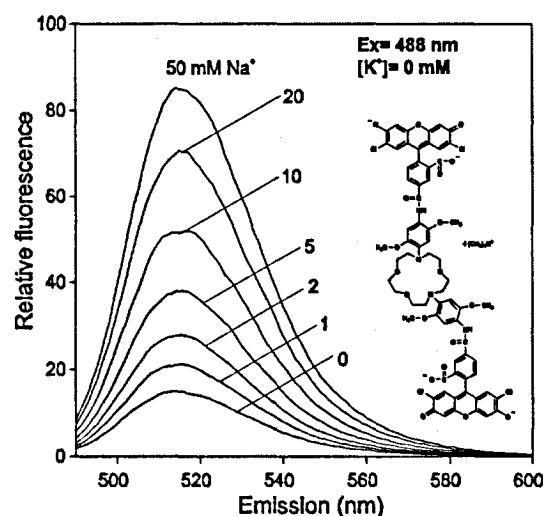
Figure 6-1. Fluorescence emission spectra of the Na⁺ specific fluorophore Sodium Green in K⁺ free solution at the Na⁺ concentrations indicated. The excitation wavelength was set at 488 nm. Inset: Chemical structure of the Na⁺ specific fluorophore Sodium Green, tetra (tetramethyl) ammonium salt (S-6900, Molecular Probes, Inc.).

This was accomplished by measuring the fluorescence emission of the proteoliposomes in a Na⁺ free buffer solution. As summarized in Table 6.1, the size of the liposomes had a notable effect, whereas the amount of added fluorophore showed no significant influence, underlining the importance of the vesicle volume. Vesicles with an average volume of 400 nm showed a 2.2 fold or a 20-fold higher incorporation of the fluorophore as vesicles with 150-300 nm or 100 nm. For efficient incorporation of the fluorophore, this has to be added before vortexing the solution. Experiments with a later addition showed a massive reduction in the amount of incorporated fluorophore.

TABLE 1			
Incorporation of Sodium Green into lipid vesicles during reconstitution			
Addition of fluorophore	Vesicles diameter (nm)	Fluorophore added (µg/ 30 mg lipid)	Amount incorporated (%)
A Before vortexing (standard)	150-300	20	100
A Before vortexing	150-300	40	107
A Before vortexing	150-300	60	116
A After vortexing, but before sonication	150-300	20	26
A After sonication	150-300	20	12
B Before resuspension	100	20	10
B Before resuspension	200	20	76
B Before resuspension	400	20	220

Note: Reconstitution method A and B as described in Material and Methods. Emission was measured at 540 nm (excitation wavelength= 488 nm).

Measurement of ATP driven Na$^+$ uptake

Although the vesicles with 400 nm diameter formed by the extrusion method yielded the best results, the following data were produced with proteoliposomes formed with the less time consuming sonication method. We have tested ATP driven Na$^+$ uptake by the F_1F_0 ATP synthase from *Ilyobacter tartaricus*, reconstituted into liposomes, a procedure often used for functional studies in the field (Figure 6-2). After Na$_2$ATP addition, an immediate shift in fluorescence was observed, mainly due to the reaction of the added Na$^+$ with the remainder of external fluorophore. This shift however, was not enzyme dependent, since it could also be observed by the addition of a similar amount of Na$_2$ADP (not shown). After this initial shift, the fluorescence increased, representing the uptake of Na$^+$ into the proteoliposomes. As expected, no uptake could be observed experiments where the ATPase was blocked by the well known inhibitors DCCD or tributyltin chloride. The measurements with the same material were repeated the next day, yielding comparable results.

Limitations of the method

Direct quantification of the uptake rate is rather difficult, since the calibration of such a system is laborious. Furthermore, the determination of initial rates is critical, since the fluorescence response is non linear at Na$^+$ concentrations above 5 mM. To avoid the initial fluorescence increase, sodium free chemicals should be used to start the

transport process (K$_2$ATP is much less stable than Na$_2$ATP and was therefore not used in this study).
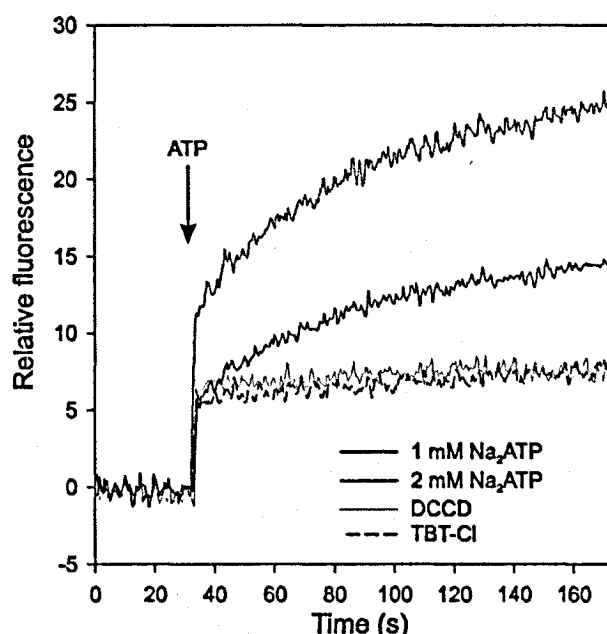
Figure 6-2. ATP driven Na⁺- uptake into proteoliposomes reconstituted with Na⁺-F ATP synthase of *Ilyobacter tartaricus* and containing Sodium Green. After 30 s, the uptake was initiated by the addition of 1 mM Na_2ATP or 2 mM Na_2ATP, respectively. Fluorescence emission was recorded at 540 nm (excitation: 488 nm). Sample without inhibitor (black continuous line; black pointed line), sample preincubated with 50 µM DCCD for 30 min (grey continuous line), sample in presence of 50 µM tributyltin chloride (black dashed line).

6.4 Conclusion

The method presented is ideally suited for rapid continuous measurements of Na^+ transport in reconstituted systems. It provides several advantages over established procedures, mainly based on radioactive $^{22}Na^+$, which is unpleasant to handle and cumbersome in decontamination. A novelty is the fact, that Na^+ transport can be followed continuously, providing important information about the initial phase of the transport. The fluorophore incorporation step is compatible with most popular reconstitution methods and the removal of the external fluorophore can be accomplished in a rapid gel filtration step. If a more concentrated sample is required, the liposomes can be collected by ultracentrifugation. Due to the low reagent price per experiment, the assay is also economically advantaged over radioactive procedures. We have demonstrated the usefulness of the new method to follow Na^+ pumping into proteoliposomes containing sodium F-ATP synthase and we expect that it can also be used to determine Na^+ transport by other primary Na^+ translocating enzymes.

Acknowledgement

6.5 References

Despa, S., Vecer, J., Steels, P. and Ameloot, M. (2000) Fluorescence lifetime microscopy of the Na$^+$ indicator Sodium Green in HeLa cells. *Anal. Biochem.*, **281**, 159-175.

Dimroth, P. (1997) Primary sodium ion translocating enzymes. *Biochim. Biophys. Acta*, **1318**, 11-51.

Dimroth, P., von Ballmoos, C., Meier, T. and Kaim, G. (2003) Electrical power fuels rotary ATP synthase. *Structure (Camb.)*, **11**, 1469-1473.

Gemperli, A.C., Dimroth, P. and Steuber, J. (2002) The respiratory complex I (NDH I) from Klebsiella pneumoniae, a sodium pump. *J. Biol. Chem.*, **277**, 33811-33817.

Haugland, R.P. (2002) *Handbook of Fluorescent Probes and Research Products*. Molecular Probes, Eugene, US.

Kluge, C. and Dimroth, P. (1992) Studies on Na$^+$ and H$^+$ translocation through the F_0 part of the Na$^+$-translocating F_1F_0 ATPase from *Propionigenium modestum*: discovery of a membrane potential dependent step. *Biochemistry*, **31**, 12665-12672.

Knol, J., Veenhoff, L., Liang, W.J., Henderson, P.J., Leblanc, G. and Poolman, B. (1996) Unidirectional reconstitution into detergent-destabilized liposomes of the purified lactose transport system of Streptococcus thermophilus. *J. Biol. Chem.*, **271**, 15358-15366.

7. Evidence for hydronium ion binding in H+-translocating F1F0 ATP synthases

Christoph von Ballmoos[1], Dirk Bakowies[2], Wilfried van Gunsteren[2] und Peter Dimroth[1]

[1]Institut für Mikrobiologie der Eidgenössischen Technischen Hochschule, ETH Hönggerberg, CH-8093 Zürich, Switzerland; [2]Institut für Physikalische Chemie der Eidgenössischen Technischen Hochschule, ETH-Hönggerberg, CH-8093 Zürich, Switzerland

7.1 Abstract

The synthesis of ATP by F_1F_0 ATP synthases is tightly coupled to the transport of protons or Na^+ ions across the membrane. Ion transport is mediated through the membrane-embedded F_0 subunits a and the oligomeric c_{10-15}. Basically, the ion is transported through two half channels, which are functionally connected through the ion binding sites on the c ring. Features of these sites mediate ion transfer into one or the other channel entrances. Some 10 years ago, it was suggested, that H^+-depending ATP synthases may coordinate their proton together with a water molecule as hydronium ion analogously to Na^+ ion coordination, instead of a group protonation of the conserved acidic residue of subunit c.

Here we report the characterization of the ion binding site from several organisms by monitoring the covalent modification with the specific inhibitor dicyclohexylcarbodiimide (DCCD). We prepared native membranes from the bacteria of *Ilyobacter tartaricus*, *Escherichia coli*, spinach chloroplast and bovine mitochondria and tested their reactivity towards DCCD in a pH dependent manner. The amount of modification was quantified with MALDI mass spectroscopy. The Na^+-dependent enzyme of *I. tartaricus* shows a strong pH dependence of the reaction as expected for a model of group protonation in the absence of Na^+. The pH profile for the H^+-dependent enzymes, however, is bell shaped and does not obey the expectations of a group protonation, but rather resembles the pH profile of enzyme. The results are discussed in respect to a binding mechanism including hydronium ion coordination.

7.2 Introduction

The majority of cellular ATP is manufactured from ADP and phosphate by the ATP synthase using a transmembrane electrochemical ion gradient as energy source. A proton motive force derived from photosynthesis or respiration drives ATP synthesis in chloroplasts, mitochondria and most bacteria (Boyer, 1997). Some anaerobic bacteria convert the energy of a chemical decarboxylation event into an electrochemical gradient of sodium ions, which serves a Na^+-translocating F_1F_0 ATP synthase as energy source (Dimroth *et al.*, 2003; Laubinger and Dimroth, 1987). The H^+- and Na^+-translocating F_1F_0 ATP synthases are phylogenetically related and both groups of enzymes share many common structural and functional features. They are most convincingly documented by the formation of functional hybrids harboring subunits from the Na^+- and H^+-translocating ATP synthase families (Laubinger *et al.*, 1990).

All ATP synthases are composed of two rotary motors, the membrane embedded F_0 motor which translocates the coupling ions and the extrinsic F_1 motor, which synthesizes the ATP. The two motors are connected by a central and a peripheral stalk to exchange energy with each other (Capaldi and Aggeler, 2002). The F_0 motor consists of a ring of c subunits which is abutted laterally by the a subunit and a dimer of b subunits. Each c subunit harbors a binding site for the coupling ion which is located in the middle of the membrane (Girvin et al., 1998; von Ballmoos et al., 2002a; von Ballmoos et al., 2002b). Therefore an entrance channel leading from the periplasmic surface to the binding site is necessary to load the site with the ion and an exit channel leading to the cytoplasmic surface is necessary to release the ion. There is general agreement for the location of the entrance channel in subunit a, but the location of the exit channel is still under debate. For the H$^+$-ATP synthase from E. coli the exit channel is thought to be localized on subunit a as well (Angevine and Fillingame, 2003). In contrast, various experiments documented a direct route for Na$^+$ ions to the membrane embedded binding sites within the c_{11} ring of the I. tartaricus or P. modestum ATP synthases in the absence of subunit a (Meier et al., 2003; von Ballmoos et al., 2002b).

The most obvious difference between the two enzyme species, however, is the chemical nature of the ion binding site on the oligomeric subunit c ring, which functions as junction in the ion pathway across the membrane through the entrance and exit channels. In both cases, a conserved acidic residue (cE65 in P. modestum and I. tartaricus; cD61 in E. coli) is located in the middle of the lipid bilayer, which is indispensable for overall enzyme function and for ion binding. Whereas in the H$^+$-translocating ATP synthases the acidic residue is thought to be sufficient for ion binding, mutational studies have shown, that at least three residues are involved in the recognition and binding of the Na$^+$ ion in the Na$^+$-translocating counterparts (Kaim et al., 1997).

A conserved property of the acidic residue from all ATP synthases is its ability to covalently react with the organic molecule dicyclohexylcarbodiimide (DCCD). Figure 7-1 depicts the reaction mechanism as proposed by Khorana (Khorana, 1953). In the first step, the protonated form of the acidic residue polarizes the C=N bond in the carbodiimide and induces the formation of a hydrogen bond between the proton and the nitrogen on the carbodiimide (1). Subsequently, the nucleophilic carboxylic oxygen binds to the carbodiimide carbon and forms an unstable O-acyl-urea derivative (2). In absence of a nucleophile, the two molecules can rearrange to form the stable N-acyl urea derivative (3). Whereas the formation of the reactive intermediate in the first partial reaction is controlled by the pH, the rearrangement reaction (3) is independent from the substrate concentration (Balcom, 1989). The requirement of an

exchangeable proton for the first partial reaction implies a strong pH dependency for the modification of the ATP synthase by DCCD. This can easily be followed with the enzyme of *P. modestum*, where a proton is bound to the carboxylic acid in the absence of sodium as formulated in Figure 7-1. The reaction velocity has its maximum in the acidic range and decreases with increasing pH with a sigmoid dependency and an inflection point around pH 7. This reflects the pK_a of the glutamic residue in the hydrophobic environment of the membrane. As a consequence, the addition of Na^+ decreases the velocity of the modification due to the competition of Na^+ binding to the acidic residue and the concomitant displacement of the proton (Kluge and Dimroth, 1993; Meier *et al.*, 2003). Interestingly, a similar pH dependence has not been observed for the H^+-translocating enzyme of *E. coli* (Valiyaveetil *et al.*, 2002). This was explained by deeply membrane buried binding sites, which are completely inaccessible to the surrounding medium. The binding sites of the Na^+-dependent enzyme, however, are located at the same position within the membrane, but strongly responds towards the pH of the surrounding medium (Meier *et al.*, 2003; von Ballmoos *et al.*, 2002b).
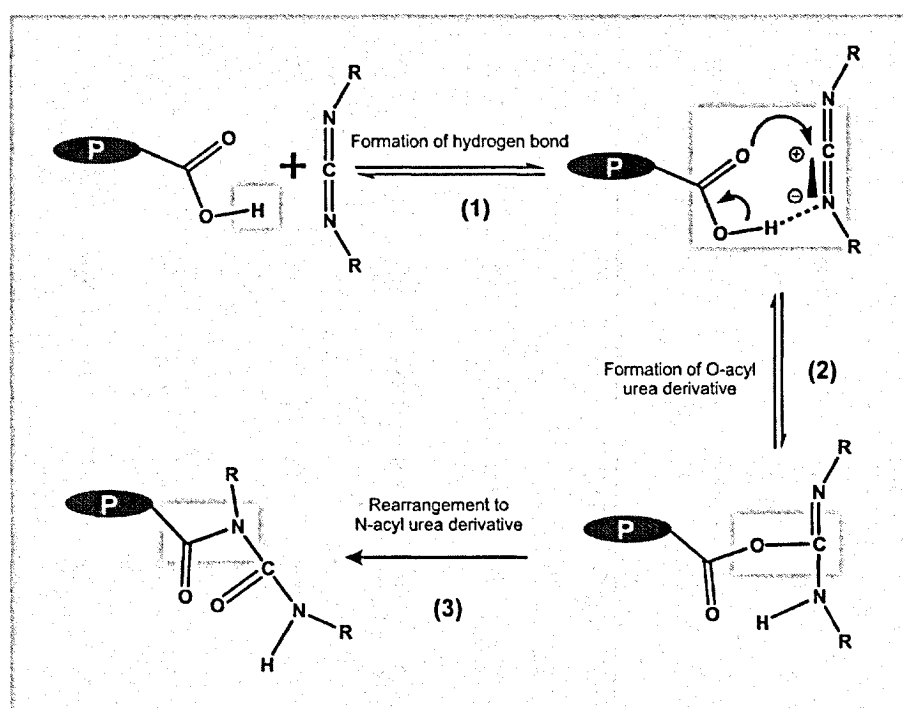
Figure 7-1. Proposed mechanism for the modification of the conserved carboxylic acid on subunit c with DCCD. In a first step, the carboxylic acid forms a hydrogen bond to one of the nitrogen atoms of the carbodiimide (1). Electron rearrangement leads to the formation of the unstable O-acyl urea derivative (2). In the absence of a nucleophile, rearrangement of the molecule leads to the formations of the stable N-acyl urea derivative (3).

To further investigate this ambiguity, we compared the pH dependence of c subunit modification from the enzymes of *I. tartaricus*, *E. coli*, spinach chloroplast and bovine mitochondria by DCCD. To cover a broad pH range MALDI mass spectroscopy was applied to directly monitor the amount of c-subunit modification.. The simple abnalytical method also allowed to perform the DCCD labeling studies in native membranes without prior purification. The results are discussed in respect to an alternative ion binding mechanism involving hydronium ion coordination.

7.3 Materials and Methods

Bacterial growth and tissue origin

E. coli atp deletion strain DK8 was transformed with plasmid pBWU13 carrying the *atp* operon except for *atpI* (Moriyama *et al.*, 1991). Cells were grown on LB medium, harvested in the late exponential phase and stored at -80 °C. *I. tartaricus* cells were grown under anaerobic conditions as described (Neumann *et al.*, 1998). Spinach (*spinacia oleracea*) leaves were obtained from the local market. Bovine heart was obtained from the local slaughterhouse, and was kept at 4°C for 16 h between slaughter and homogenization.

Preparative procedures

The preparation of *E. coli* membranes and their solubilization with cholate/ deoxycholate in presence of 1M KCl was performed as described (Fillingame and Foster, 1986; von Ballmoos *et al.*, 2002b). Membranes from *I. tartaricus* cells were prepared and solubilized with Triton X-100 as described (Neumann *et al.*, 1998).

A total of 1.5 to 2 kg of spinach leaves were homogenized in a sucrose-containing buffer with a Waring blender. Subsequent filtration and centrifugation steps were performed to obtain a thylakoid membrane preparation (chlorophyll concentration of 5 mg/ ml) and the samples were stored at -20 °C as described (Turina *et al.*, 2003). The ATP synthase was solubilized from the membranes, fractionated by ammonium sulphate precipitation and subsequent sucrose density gradient centrifugation as described (Turina *et al.*, 2003). The purified protein samples (5 mg protein/ ml) were stored in liquid nitrogen.

A total of 0.9 to 1 kg bovine heart was used to prepare mitochondria as described (Smith, 1967). The protein content of the collected mitochondria was adjusted to 20 mg/ ml and the preparation was stored at -20 °C. Solubilization of bovine mitochondria with dodecyl maltoside was performed as described (Buchanan and Walker, 1996).

For DCCD labeling experiments, all materials except enriched chloroplast ATP synthase were freshly prepared prior to usage.

Modification of the c subunit with DCCD

A 50 μl sample of membrane preparation or the detergent extracted enzyme was diluted into 450 μl of incubation buffer. For the pH range from 5 to 9 MMT (100 mM MES, 100 mM MOPS, 100 mM Tricine, 5 mM MgCl₂, adjusted to the desired pH with 5 M KOH) was used, whereas for more alkaline pH, Tricine was replaced by glycine. DCCD was added at the desired concentration using stock solutions prepared in ethanol with the volume of ethanol added being ≤ 1% of the total reaction volume. At the desired time points, samples of 30 μl were taken and mixed with 20 μl of 1 M ammonium acetate to adjust the pH to near 7. The samples were immediately mixed with 500 μl of chloroform: methanol (1: 1) and shaken vigorously. The subsequent addition of 100 μl H₂O induced a phase separation, which was completed by centrifugation. The c subunit containing samples in the organic solvent were stored at -80 °C prior to MALDI measurements.

MADLI TOF measurements

Molecular masses were determined on a Perseptive Biosystems Voyager Elite System, or a 4700 Proteomics Analyzer from Applied Biosystems, both MALDI-TOF instruments, equipped with reflector. Different matrices were used, but if not otherwise stated, a 100 mg/ ml solution of dihydroxybenzoic acid (DHB) in acetonitrile: H₂O (0.1% TFA) = 2: 1 was used. An amount of 0.7 μl was placed onto the target plate and allowed to dry before 0.5- 1 μl of the chloroform phase of the DCCD modified samples was applied onto the matrix coated spot. Measurements were performed in the linear mode in order to minimize sample decomposition as observed (von Ballmoos *et al.*, 2002a).

pH profile of hydrolysis activity of the *E. coli* ATP synthase

Purified *E. coli* ATP synthase was prepared as described (von Ballmoos *et al.*, 2002b). ATPase activity was determined with the coupled enzyme assay with the following modifications as described (Laubinger and Dimroth, 1988). Instead of potassium phosphate buffer, assay solution was buffered with the desired pH with 50 mM MES, 50 mM MOPS and 50 mM Tricine (pH 5 to pH 9) or 50 glycine (pH 9.5 to pH 11) and adjusted with KOH.

Semiempirical calculations

Semiempirical calculations were performed with the method OM2, as described by Weber and Thiel (Weber, 1996; Weber and Thiel, 2000).

7.4 Results

MALDI TOF as a quantitative tool for analysis of subunit c labelling by DCCD

Dicyclohexylcarbodiimide (DCCD) is well known to react with the ATP synthase by specifically modifying a conserved acidic residue of subunit c. This reaction has either been followed by the inhibition of ATP hydrolysis activity or by the incorporation of radioactivity from ^{14}C-DCCD. However, these methods are laborious and not applicable to conveniently monitor the modification reaction. In the assays described below we took advantage of the unique property of subunit c to become highly enriched from any kind of sample by a chloroform/ methanol extraction and subsequent phase separation. The subunit c- containing organic phase can be easily applied to MALDI mass spectroscopy. Mass spectroscopy is generally difficult to calibrate for quantitative measurements. However, our system contains a built-in internal standard in the form of the unmodified c subunit. Subunit c labelling can therefore be related to the ratio of labelled to unlabelled c subunit in individual measurements. To test this presumption different ratios of labelled and non-labelled c-monomer were mixed in the organic solvent and applied to mass spectroscopy. The results in Figure 7-2 show a good accordance between the measured and the calculated ratios.
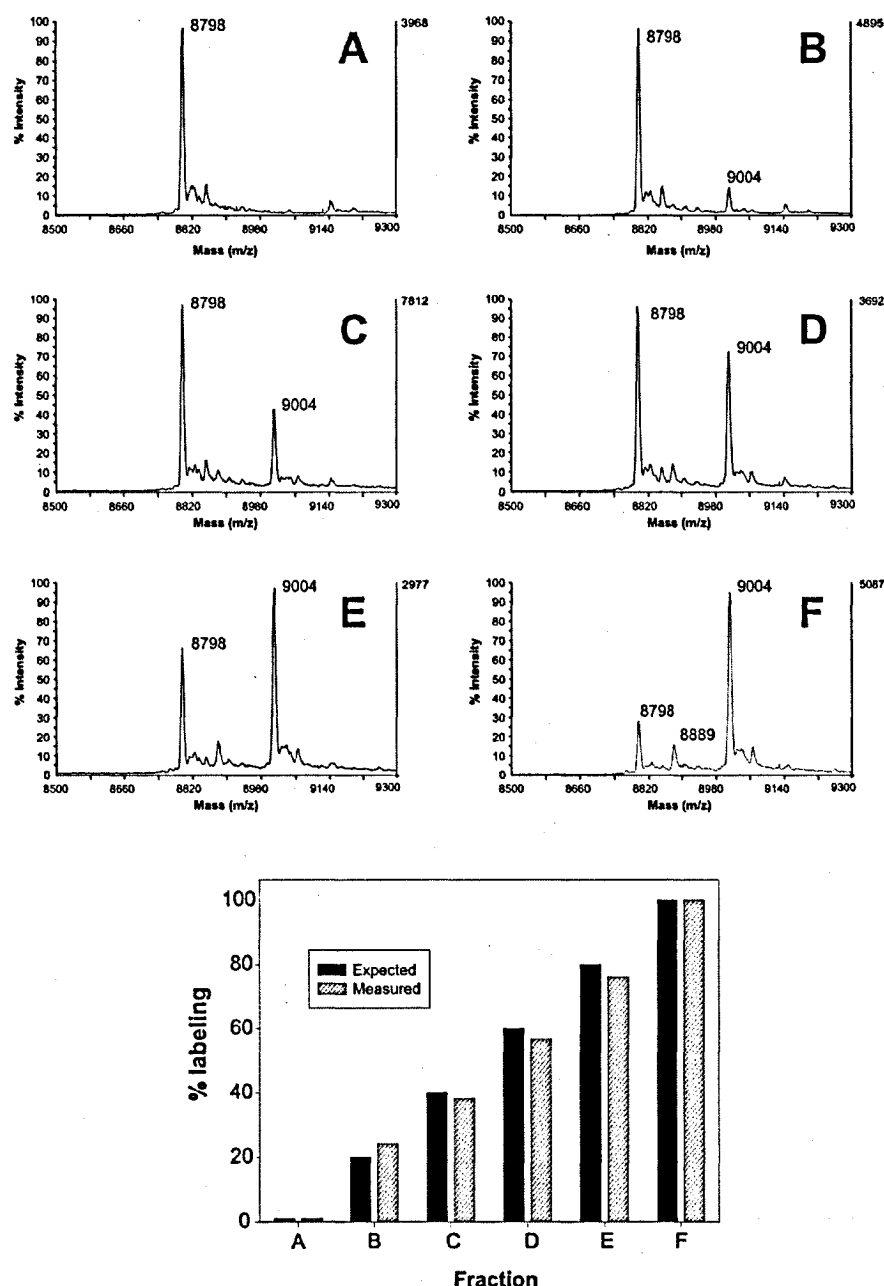
Figure 7-2. MALDI TOF spectra of mixtures between DCCD-modified and unmodified c subunits. Top: The c subunits were modified by incubation of the isolated c_{11} ring of the *I. tartaricus* enzyme and the modified c subunits (M) were extracted with organic solvent. The unmodified c subunits (U) were prepared the same way from c_{11} which was not treated with DCCD. The two sampled were mixed in the ratios (U:M) indicated below and subjected to MALDI mass spectroscopy. A, (100:0); B, (80:20); C, (60:40); D, (40:60); E, (20:80); F, (0:100). Bottom: The intensities of the peaks from these measurements (Figure 7-2A-F) were used to calculate the relative amount of c subunit modification. These values are compared with the expected ratios.

The pH dependence of subunit c labelling from different ATP synthases by DCCD

In a first series of experiments, the new method was applied to measure subunit c labelling of the *I. tartaricus* ATP synthase by DCCD in dependence of the pH. From previous studies

with the active enzyme or the isolated c ring it was known that the pH profile for the modification reaction follows a titration curve with an inflection point around pH 7. This is thought to represent the pK_a of the glutamic acid which becomes modified by DCCD. In our assays either isolated membranes from *I. tartaricus* (Figure 7-3A) or the ATP synthase solubilized from the membranes by detergent or the purified enzyme (data not shown), were incubated with DCCD at the pH values indicated as described in Materials and Methods. To stop the modification an aliquot of the reaction was rapidly mixed with an excess of chloroform-methanol followed by phase separation by addition of water. One µl of the lower organic phase was then directly applied onto a layer of dried matrix on the target plate for mass spectroscopy. The results from all three ATP synthase preparations were very similar and showed the expected pH dependency of the modification (Figure 7-3A). For practical reasons, only two time points were measured, and it is therefore important to point out, that the representations in Figure 7-3 do not reflect the initial reaction rates, but rather a comparison of reaction velocities at different pH values.

Being satisfied with the method, similar experiments were performed with the crude and detergent solubilized (Na+-cholate/ deoxycholate, 1M KCl) membrane fraction from *E. coli*. The reaction of DCCD with the *E. coli* ATP synthase is slower than that with the *I. tartaricus* enzyme. The incubation time was therefore adjusted to reach similar modification levels in the different experiments. This standardisation is important for an accurate comparison because not every c subunit in the ring may be modified with the same rate. Generally, we adjusted the incubation time with DCCD to obtain labelling rates of 50 %.

The pH profile for the modification of subunit c from *E. coli* membranes is shown in Figure 7-3B. Measurements with detergent solubilized membranes produced essentially the same results (data not shown). The profile is entirely different form that found with *I. tartaricus* ATP synthase, showing an increase in the labelling velocity between pH 5.5 and 8.0, almost a plateau between pH 8.0 and pH 10 and a strong decrease between pH 10 and pH 12. The plateau in the near alkaline pH range might explain the finding of Valiyaveetil and Fillingame, that the modification is not sensitive to the pH of the medium (Valiyaveetil *et al.*, 2002). The significant decrease of the modification rate at lower pH is unexpected and not compatible with a mechanism which requires the protonation the acidic amino acid prior to its modification (see Introduction). The low modification at acidic pH is not due to protein harming effects, since after a transient low pH treatment the membrane preparation is still enzymatically active (data not shown).

This unexpected finding prompted us to extend our studies to H⁺-translocating enzymes from other organisms. We isolated thylakoid membranes (Th) from spinach, and purified the ATP synthase by ammonium sulphate precipitation (AS) and sucrose density gradient centrifugation (SD) as described (Turina *et al.*, 2003). The DCCD labelling properties of the enzyme in the solubilized thylakoid membranes (sTh) was compared with those after each purification step. The results obtained with enzyme after sucrose density centrifugation (SD) are depicted in Figure 7-3C.
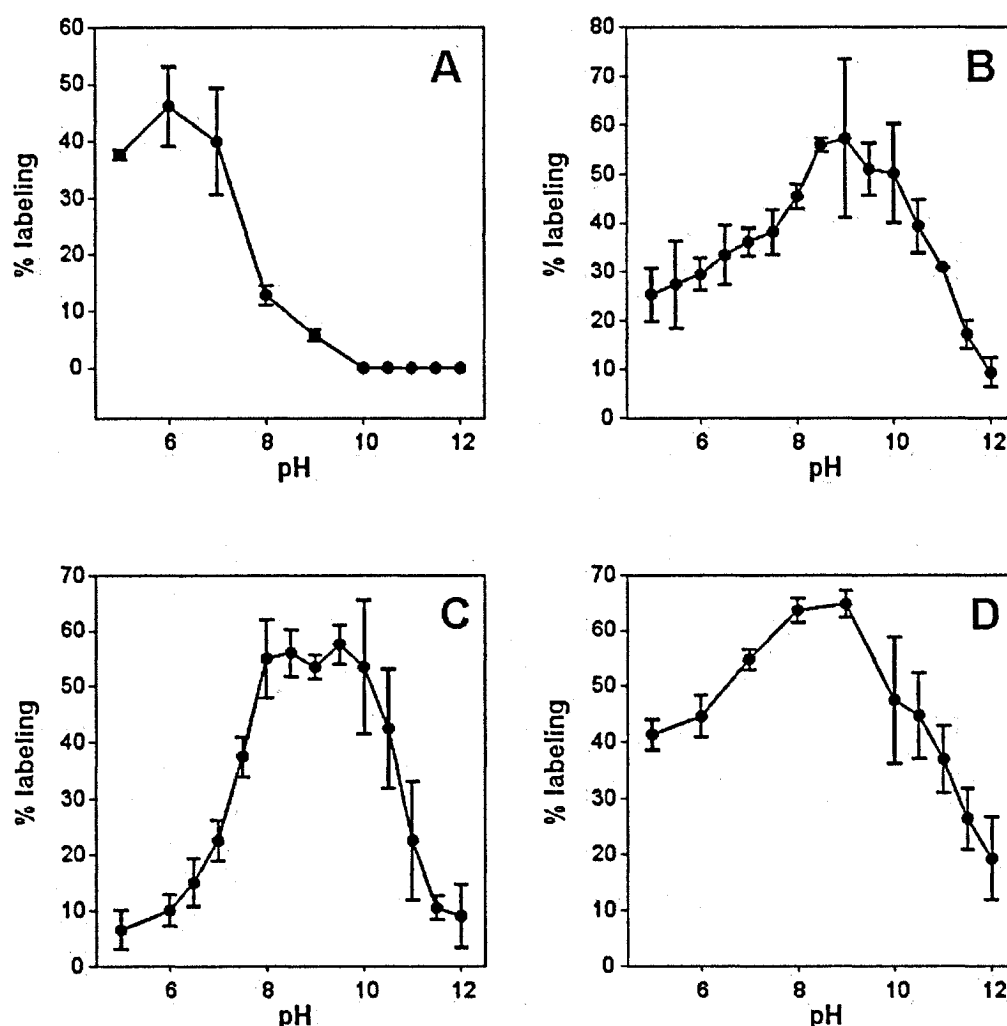
Figure 7-3. pH dependence for the modification of different c-subunits by DCCD. A. Membranes of *I. tartaricus* cells were prepared and incubated with DCCD at different pH values as described. Peak intensities from labelled (L) and unlabelled (U) c-subunits were used to determine the ratio (L/ (U+L), which was plotted against the pH values indicated. Depicted are the mean values and the standard deviations of at least two measurements. **B.** Like *A*, but with isolated membranes of *E. coli* cells. **C.** Like *A*, but with sucrose density gradient purified F₁F₀ ATP synthase from spinach chloroplasts. **D.** Like *A*, but with isolated mitochondria from bovine heart.

The pH profile of DCCD labelling of the chloroplast ATP synthase is rather similar to that of the *E. coli* enzyme, except for a more pronounced decrease in the labelling rate in the acidic pH range. In contrast to the *E. coli* ATP synthase that from chloroplasts hardly reacts at all at pH 5 and the rate increase between pH 5 and 8 is approximately 10-fold for the chloroplast enzyme but only 2-fold for that of *E. coli*. The DCCD labelling experiments were also performed with the ATP synthase from bovine heart mitochondria. For this purpose, the mitochondria were isolated and the ATP synthase extracted with detergent. With both fractions similar pH profiles for the DCCD labelling were obtained which are shown for the isolated mitochondria in Figure 7-3D. The pH profile closely resembles that found with the *E. coli* enzyme, showing significant labelling at pH 5 and a small increase in the labelling rate on increasing the pH to 8, A plateau is reached between pH 8 and 9 and the rate of DCCD labelling decreases again if the pH is raised further into the alkaline range. Tpyical MALDI spectra for all organisms kind are depicted in the supplementary material (Figure 7-7).

Initial kinetic studies on the modification of the chloroplast enzyme

The obvious discrepancy between our findings compared to those of Valiyaveetil and Fillingame could result from the different analytical methods applied to follow the rate of labelling of subunit c with DCCD. In the former study, the rate of labelling was followed by residual enzyme activity measurements. This monitors the modification of a single subunit within the ring, since this is sufficiently to completely impair activity. In contrast, we followed the chemical modification of approximately 50% of all c subunits directly, and might therefore have missed to monitor the initial modification rate, which is crucial for the results obtained with the enzymatic assay. To investigate this possibility, we followed the kinetics of the chloroplast enzyme at pH 7 and at pH 9, since a high discrepancy was expected from the results of Figure 7-3C. We incubated the purified enzyme in buffered solutions with DCCD, and stopped the modification at different time points as described above. The results in Figure 7-4 depict an interesting finding. It seems that the initial rate of the two reactions is similar (which is guided by the modification of the first subunit), but that the modification of further subunits seems to be strongly pH dependent as observed in Figure 7-3C. This finding· might reflect the possibility, that not all DCCD accessible binding sites have a similar chemical environment.
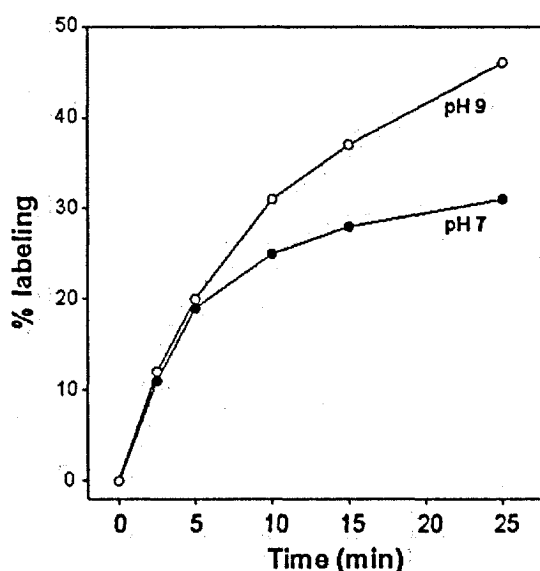
Figure 7-4. Kinetics of c subunit modification of chloroplast ATP synthase by DCCD. Purified F_1F_0 ATP synthase from spinach chloroplast was incubated with DCCD at pH 7 and pH 9, respectively. At the time points indicated, the modification was stopped and analysed by MALDI mass spectroscopy as described in Materials and Methods.

pH dependence of the hydrolysis activity of the *E. coli* ATP synthase

To gain information about the pH range at which the *E. coli* ATPase is functional the pH profile of the enzyme was determined. For this purpose the ATP hydrolysis activities were measured with the coupled assay at different pH values and the relative hydrolysis activities were plotted against the pH (Figure 7-6). The resulting curve had a bell shaped appearance, comparable to that of the *P. modestum* under Na^+ saturation, with a sharp increase from pH 6 to 8. Maximal rates are found in a rather broad pH range from pH 7.5 to 9.5, which is slightly shifted to the alkaline range compared to the *P. modestum* enzyme. Below pH 6.5 and above pH 10, only minor hydrolysis activities were detected.

Semiempirical computational investigation of the proton binding mechanism in H⁺-translocating enzymes

As pointed out in the Discussion of this chapter, the commonly proposed group protonation mechanism for H⁺-translocation could not explain the results summarized in Figure 7-3. An alternative mechanism might involve coordination of a hydronium ion (H_3O^+) by several amino acids instead of the group protonation of the conserved acidic residue as already proposed by Boyer. The coordination by multiple residues would provide several advantages over the common model in respect to enzyme activity and stability (see Discussion). To examine whether H_3O^+ binding might be an option, a semiempirical calculation of the two

possible scenarios was performed. We created a simple system, harbouring the acidic residue (imitated by a formic acid molecule), a proton and a water molecule. Furthermore, the existence of possible ligands for the hydronium ion was imitated by the addition of two formaldehyde molecules (Figure 7-5A). We set initial geometries for ideal liganding (H-bridges) of the water molecule by the two carbonyls and the proton with the water molecule. As a variable, we set the distance between the carboxylate and the protonated water molecule. The proton is expected to be strongly attracted by the carboxylate if the two molecules are close to each other. However, at longer distances, it may be favourable for the proton to stay on the water molecule and be coordinated by multiple residues. This would reflect a rather charge-separated state. Using semiempirical quantum chemical calculations we determined the reaction coordinate for the distance between the formic acid and the water molecule. We also used much more accurate (and computer time consuming) *ab initio* calculations to test, whether semi empirical calculation are accurate enough for further investigations with more complex systems
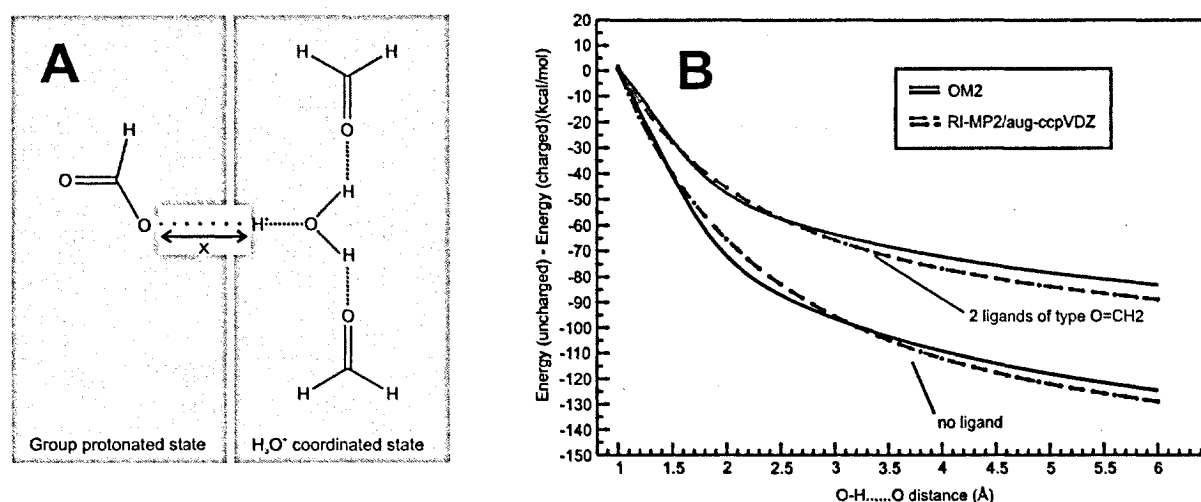
Figure 7-5. Semiempirical and *ab initio* calculations of the reaction coordinate for charge separation. A. Cartoon of the simplified system for the discrimination of group protonated or hydronium ion coordinated state in H⁺-translocating enzymes, which was used for semi empiric calculations. For details, see text. **B.** Energy difference profile between the uncharged and the charged proton binding states in respect to the distance of the proton from the carboxylic oxygen. Compared are the energy profiles without (grey lines) and with two formaldehyde ligands (black lines), calculated using the semiempirical method OM2 (straight lines) and the more accurate *ab initio* method (line with dots).

In Figure 7-5B, the difference between the energy of the uncharged (reflecting group protonation) and the charged (reflecting hydronium ion) is depicted. At a distance of 1 Å, the

two states are identical and the energy difference must therefore be 0. It can be easily seen, that in both scenarios (with or without formaldehyde ligands), the group protonated charge is energetically more favourable. The addition of two ligands however decreases the energy difference between the two states significantly. Furthermore, it is obvious, that semi empirical calculation and accurate *ab initio* calculations produce similar results.

7.5 Discussion

It is generally believed that the mechanism of proton translocation by the H$^+$-coupled F_1F_0 ATP synthases includes the protonation of the conserved acidic amino acid residue in subunit c in the C-terminal helix near the centre of the membrane. Such a group protonation step would be dissimilar to the mechanism of Na$^+$ translocation by the Na$^+$-coupled ATP synthases which bind the alkali ion through coordination with multiple ligands (Kaim *et al.*, 1997). Inspired by this mechanism and based on a similar coordination sphere for Na$^+$ and H$_3$O$^+$ by crown ethers, Boyer came up with the idea that hydronium ion binding should be considered as a potential mechanism for the H$^+$-coupled ATP synthases (Boyer, 1988). As no direct means are available to discriminate between protonation of the carboxylate and the coordination of a hydronium ion more indirect methods had to be considered to discern between these options. We reasoned that for optimal group protonation the pH must be more acidic than the pK$_a$ of the carboxylic acid but hydronium ion binding requires the carboxylate species and should therefore have its optimum in the more alkaline pH range. It has been well documented that ATP hydrolysis of the Na$^+$ dependent ATP synthase is Na$^+$ dependent which implies that the Na$^+$ binding sites must be occupied to allow ATP-driven rotation. A rationale for this observation would be an unbearable energy barrier to move a negatively charged rotor site through a hydrophobic sector of the interface with the stator (Dimroth *et al.*, 2003). Further in accord with this model is the observation of Na$^+$-independent ATP hydrolysis at acidic pH values, i.e. under conditions where the carboxylate becomes protonated (Kluge and Dimroth, 1992). With this knowledge in mind we measured the ATP hydrolysis activity of the *E. coli* ATP synthase in the dependence to pH. Interestingly enough, the activity was quite low at pH 6 and below where the cD61 sites are expected to be protonated and increased significantly at alkaline pH values. Maximal activity was observed at pH 9 and significant activities were still found at pH 10 and above. These values are 3 orders of magnitude above the pK$_a$ of cD61 and hence only approximately 0.1 % of this residue would be protonated. This degree of protonation cannot explain the observed hydrolysis activities if we assume that

H^+ and Na^+ ATP synthases operate basically by the same mechanism. This is reasonable, however, since any ATP driven rotation without ion binding notoriously lead to uncoupling. Hence, these data are not compatible with a group protonation mechanism but they might be explained with hydronium ion binding to a coordination sphere including the deprotonated cD61. Substantial support for H_3O^+ binding to the ATP synthases from *E. coli*, spinach chloroplasts and bovine mitochondria was obtained from the pH dependence of DCCD labelling experiments. The compound specifically reacts with the acidic amino acid of the subunit c binding site and the reaction requires a proton as described in the Introduction. In spite of this requirement the reaction is much faster at pH 8- 10 than at pH 5- 7 where the carboxylate can be expected to exist in the protonated form. In contrast, the pH profile for the modification of the Na^+-dependent ATP synthase from *I. tartaricus* by DCCD follows the expected titration curve with the highest rates at pH <6 , half maximal rates at pH 7 and no detectable labelling at pH 8.5 and above. This difference in the pH dependence of DCCD labelling by Na^+ and H^+-dependent ATP synthase most likely reflects different proton donors for the modification reaction. The pH behaviour of the Na^+ ATP synthase is completely compatible with a mechanism where the proton for the reaction stems from the protonated carboxylate while that of the H^+ ATP synthases must rely on a different proton donor close to the same site. An obvious candidate is a hydronium ion which would be coordinated by the unprotonated carboxylate and additional ligands. It is clear that the binding of a hydronium ion at pH 8- 10 requires a high affinity binding site. This must not be present in the Na^+-translocating ATP synthase with their 5 orders of magnitude lower Na^+ binding affinities. An advantage of hydronium ion binding over group protonation may be a significant extension of the pH range at which the enzyme is functional. While group protonation is restricted to environmental pH values near the pK_a of the protonatable group or below, a hydronium ion binding site could cover a broader pH range especially in the alkaline region. Indeed, the *I. tartaricus* ATP synthase operates at narrow pH in its H^+-translocating activity (Kluge and Dimroth, 1992) whereas the *E. coli* ATP synthase exhibits significant activity over a pH range of more than 3 units (Figure 7-6).
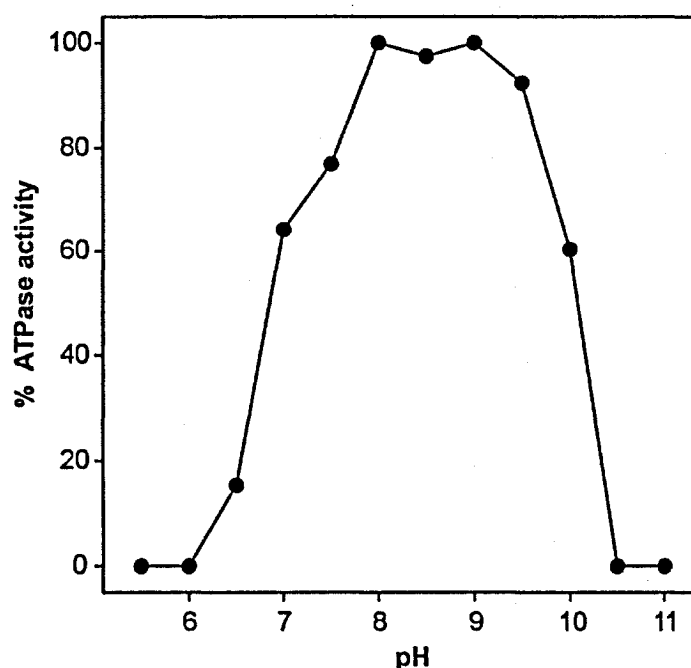
Figure 7-6. pH profile of the purified F$_1$F$_0$ ATP synthase of *E. coli*. Purified *E. coli* ATP synthase was prepared as described (von Ballmoos *et al.*, 2002b). ATP hydrolysis activity was determined with the coupled enzyme assay with the following modifications as described (Laubinger and Dimroth, 1988). Instead of potassium phosphate buffer, assay solutions were buffered with 50 mM MES, 50 mM MOPS and 50 mM Tricine (pH 5 to pH 9) or 50 glycine (pH 9.5 to pH 11) and adjusted with KOH to the desired pH. Depicted are the mean values of two measurements from the same preparation.

Another aspect of this work relates to potential models for proton translocation through the F$_0$ motor. Based on different NMR structures from monomeric subunit c of *E. coli* at pH 5 and 8 protonation of cD61 was proposed to induce conformational changes within subunit c which were envisaged to play an important role in the rotational mechanism. However, with hydronium ion binding instead of group protonation the pH induced conformational change would not be part of the physiological reaction mechanism of the enzyme.

7.6 Concluding remarks

This work provides for the fist time experimental evidence for an alternative proton binding mechanism in the H$^+$-translocating ATP synthases. Although, no direct observation of the hydronium ion species is possible, the data of this report indicate strongly, that group protonation is not a feasible explanation for the observed modification behaviour. Further experiments should address the involvement of other amino acid residues in hydronium ion coordination. A point mutation of a hydronium ion ligand should alter the pH profile of ATP

hydrolysis activity and of the modification with DCCD significantly. Such observations would strongly support the existence of a coordination of the hydronium ion by several amino acids. The mutational approach might fail however, if the backbone of polypeptide chain is involved in the coordination. A participation of backbone carbonyls has been proposed for a P-type H⁺-ATPase through homology modelling (Bukrinsky *et al.*, 2001).

A second approach to the problem is the presented application of semi empirical calculations. In a first series, we could justify the application of semi empirical calculation compared to time consuming *ab initio* calculations. Further studies will involve different liganding geometries and ligands such as additional water molecules to further decrease the energy difference between the two states. However, a real modelling of the binding site will only be possible, if a high resolution structure of the c-ring of *E. coli* is available.

7.7 Supplementary material
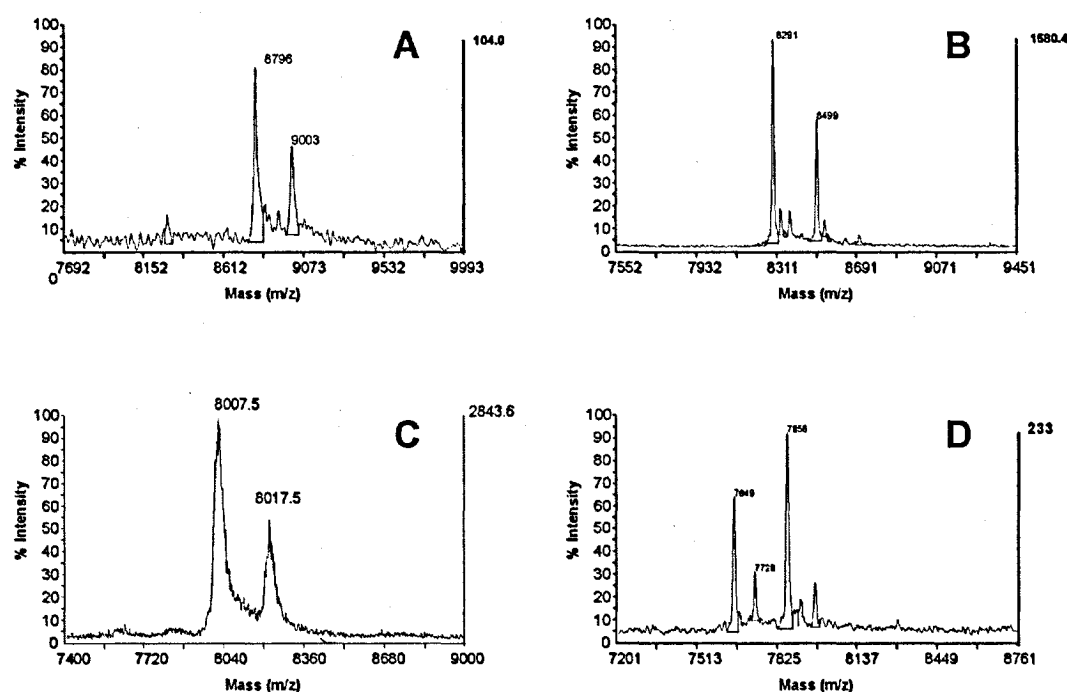
Figure 7-7. MALDI TOF analysis of c-subunit modification by DCCD from different organisms. All samples were incubated with DCCD and submitted to MALDI mass spectroscopy as described in Materials and Methods. Shown are typical spectra obtained after these procedures for **A.** *Ilyobacter tartaricus*, **B.** *E. coli*, **C.** spinach chloroplast, **D.** bovine mitochondria. All the masses for labelled and unlabelled c-subunits were in the accuracy range of 0.1%.

7.8 References

Angevine, C.M. and Fillingame, R.H. (2003) Aqueous access channels in subunit a of rotary ATP synthase. *J. Biol. Chem.*, **278**, 6066-6074.

Balcom, B.J., Petersen, N.O. (1989) Solvent Dependence of Carboxylic Acid Condensations with Dicyclohexylcarbodiimide. *J. Org. Chem.*, **54**, 1922-1927.

Boyer, P.D. (1988) Bioenergetic coupling to protonmotive force: should we be considering hydronium ion coordination and not group protonation? *Trends Biochem. Sci.*, **13**, 5-7.

Boyer, P.D. (1997) The ATP synthase- a splendid molecular machine. *Annu. Rev. Biochem.*, **66**, 717-749.

Buchanan, S.K. and Walker, J.E. (1996) Large-scale chromatographic purification of F$_1$F$_0$-ATPase and complex I from bovine heart mitochondria. *Biochem. J.*, **318**, 343-349.

Bukrinsky, J.T., Buch-Pedersen, M.J., Larsen, S. and Palmgren, M.G. (2001) A putative proton binding site of plasma membrane H$^+$-ATPase identified through homology modelling. *FEBS Lett.*, **494**, 6-10.

Capaldi, R.A. and Aggeler, R. (2002) Mechanism of the F$_1$F$_0$-type ATP synthase, a biological rotary motor. *Trends. Biochem. Sci.*, **27**, 154-160.

Dimroth, P., von Ballmoos, C., Meier, T. and Kaim, G. (2003) Electrical power fuels rotary ATP synthase. *Structure (Camb.)*, **11**, 1469-1473.

Fillingame, R.H. and Foster, D.L. (1986) Purification of F$_1$F$_0$ H(+)-ATPase from *Escherichia coli*. *Methods Enzymol.*, **126**, 545-557.

Girvin, M.E., Rastogi, V.K., Abildgaard, F., Markley, J.L. and Fillingame, R.H. (1998) Solution structure of the transmembrane H$^+$-transporting subunit c of the F$_1$F$_0$ ATP synthase. *Biochemistry*, **37**, 8817-8824.

Kaim, G., Wehrle, F., Gerike, U. and Dimroth, P. (1997) Molecular basis for the coupling ion selectivity of F$_1$F$_0$ ATP synthases: probing the liganding groups for Na$^+$ and Li$^+$ in the c subunit of the ATP synthase from *Propionigenium modestum*. *Biochemistry*, **36**, 9185-9194.

Khorana, H.G. (1953) The Chemistry of Carbodiimides. *Chem. Rev.*, **53**, 145.

Kluge, C. and Dimroth, P. (1992) Studies on Na$^+$ and H$^+$ translocation through the F$_0$ part of the Na$^+$-translocating F$_1$F$_0$ ATPase from *Propionigenium modestum*: discovery of a membrane potential dependent step. *Biochemistry*, **31**, 12665-12672.

Kluge, C. and Dimroth, P. (1993) Specific protection by Na$^+$ or Li$^+$ of the F$_1$F$_0$-ATPase of *Propionigenium modestum* from the reaction with dicyclohexylcarbodiimide. *J. Biol. Chem.*, **268**, 14557-14560.

Laubinger, W., Deckers-Hebestreit, G., Altendorf, K. and Dimroth, P. (1990) A hybrid adenosinetriphosphatase composed of F$_1$ of *Escherichia coli* and F$_0$ of *Propionigenium modestum* is a functional sodium ion pump. *Biochemistry*, **29**, 5458-5463.

Laubinger, W. and Dimroth, P. (1987) Characterization of the Na$^+$-stimulated ATPase of *Propionigenium modestum* as an enzyme of the F$_1$F$_0$ type. *Eur. J. Biochem.*, **168**, 475-480.

Laubinger, W. and Dimroth, P. (1988) Characterization of the ATP synthase of *Propionigenium modestum* as a primary sodium pump. *Biochemistry*, **27**, 7531-7537.

Meier, T., Matthey, U., von Ballmoos, C., Vonck, J., Krug von Nidda, T., Kühlbrandt, W. and Dimroth, P. (2003) Evidence for structural integrity in the undecameric c-rings isolated from sodium ATP synthases. *J. Mol. Biol.*, **325**, 389-397.

Moriyama, Y., Iwamoto, A., Hanada, H., Maeda, M. and Futai, M. (1991) One-step purification of Escherichia coli H(+)-ATPase (F$_0$F$_1$) and its reconstitution into liposomes with neurotransmitter transporters. *J. Biol. Chem.*, **266**, 22141-22146.

Neumann, S., Matthey, U., Kaim, G. and Dimroth, P. (1998) Purification and properties of the F$_1$F$_0$ ATPase of *Ilyobacter tartaricus*, a sodium ion pump. *J. Bacteriol.*, **180**, 3312-3316.

Smith, A.L. (1967) Preparation, Properties, and Conditions for Assay of Mitochondria: Slaughterhouse Material, Small-scale. *Methods Enzymol.*, **10**, 81-86.

Turina, P., Samoray, D. and Gräber, P. (2003) H$^+$/ATP ratio of proton transport-coupled ATP synthesis and hydrolysis catalysed by CF$_0$F$_1$-liposomes. *EMBO J.*, **22**, 418-426.

Valiyaveetil, F., Hermolin, J. and Fillingame, R.H. (2002) pH dependent inactivation of solubilized F$_1$F$_0$ ATP synthase by dicyclohexylcarbodiimide: pK(a) of detergent unmasked aspartyl-61 in *Escherichia coli* subunit c. *Biochim. Biophys. Acta*, **1553**, 296-301.

von Ballmoos, C., Appoldt, Y., Brunner, J., Granier, T., Vasella, A. and Dimroth, P. (2002a) Membrane topography of the coupling ion binding site in Na$^+$-translocating F$_1$F$_0$ ATP synthase. *J. Biol. Chem.*, **277**, 3504-3510.

von Ballmoos, C., Meier, T. and Dimroth, P. (2002b) Membrane embedded location of Na$^+$ or H$^+$ binding sites on the rotor ring of F$_1$F$_0$ ATP synthases. *Eur. J. Biochem.*, **269**, 5581-5589.

Weber, W. (1996) *Ein neues semiempirisches NDDO-Verfahren mit Orthogonalisierungskorrekturen: Entwicklung des Modells, Implementierung, Parametrisierung und Anwendungen.* Hartung-Gorre Verlag Konstanz.

Weber, W. and Thiel, W. (2000) Orthogonalization corrections for semiempirical methods. *Theor. Chem. Acc.*, **103**, 495-50.

8. Purification and mass spectroscopy analysis of subunit a from Na⁺-translocating ATP synthase

Christoph von Ballmoos and Peter Dimroth

Institut für Mikrobiologie der Eidgenössischen Technischen Hochschule, ETH Zentrum, CH-8092 Zürich, Switzerland

A part of this work has been published in

Complete DNA sequence of the *atp* operon of the sodium-dependent F_1F_0 ATP synthase from *Ilyobacter tartaricus* and identification of the encoded subunits.

Meier T, von Ballmoos C, Neumann S, Kaim G

8.1 Introduction

The F-type ATP synthase is organized in two domains. The cytoplasmic, soluble F_1 domain harbors the nucleotide binding sites and the central stalk, which transmits the rotational energy between the two domains (Capaldi and Aggeler, 2002). The membrane embedded F_0 part is responsible for the coupling ion transfer across the membrane, which is intimately coupled with the synthesis or hydrolysis of ATP in the F_1 part (Dimroth et al., 2003). Compared to the water soluble F_1 part, the subunits of the F_0 part, and especially subunit a, are difficult to over express and purify. The purification of heterologously expressed subunits is however a prerequisite for functional studies with the Na⁺-translocating enzyme of P. modestum, since a convenient genetic system for this organism is not available, and the functional expression of the whole enzyme complex in E. coli has failed so far (Wehrle et al., 2002). Whereas subunit b can rather easily be expressed and purified by classical means, the purification of the hydrophobic subunit c is somewhat surprising. More than twenty years ago, subunit c was recognized to be extracted together with lipid, when biological samples were treated with chloroform: methanol, and was therefore called proteolipid. The purification of subunit a has shown to be the most difficult, resulting in samples of unsatisfied purity or yield (Arechaga et al., 2003). In this work, we present a similar approach for subunit a as it is used for the proteolipid, by means of extraction into an organic solvent mixture.

8.2 Material and Methods

ATP synthases from P. modestum and I. tartaricus were purified as described (Laubinger and Dimroth, 1987; Neumann et al., 1998). Subunit a with N-terminal His_{10}-tag and without tag was expressed as described (Wehrle et al., 2002).

Extraction of subunit a and c from purified ATP synthase by organic solvents

Typically, a sample of 100 µl purified ATP synthase (400 µg) in 10 mM potassium phosphate, pH 7, 2.5 mM $MgCl_2$ was mixed with a 1 ml of chloroform: methanol (1: 1) and shaken for 20 s. The precipitated proteins were collected by centrifugation (1 min, 13'200 rpm) and the supernatant transferred to a new test tube. The supernatant was then mixed with 200 µl of 5% citric acid in aqueous solution and shaken by hand for 20 s. The phase separation was induced by a short centrifugation and the lower organic phase, containing subunits a and c, was taken and mixed with 50 µl of methanol to clarify the solution. SDS gel chromatography was used to analyze the extracted samples. If not otherwise stated, an aliquot of the extract was mixed

with 5 µl of 10% SDS, evaporated in a Speed-Vac and resuspended in 50 mM Tris buffer, pH 8.

Extraction of subunit a and c other proteins from crude membrane fractions

The protocol described above was also used, to enrich subunit a and other hydrophobic proteins from crude subunit a or ATP synthase-containing samples. If subunit a was expressed in *E. coli*, membranes were prepared and solubilized with 1% lauryl sarcosine as described (Wehrle *et al.*, 2002). Extraction of hydrophobic proteins from the soluble fraction was performed in similar organic solvent mixtures as described above.

Intact cells of *I. tartaricus* were mixed with Triton X-100 (1% final concentration) and stirred for 30 min at 37 °C. The sample was centrifuged (200'000 g, 30 min, 4°C) and the supernatant used as starting material for the extraction with organic solvents as described above.

Isolation of subunit a by weak cation exchange chromatography

As a weak cationic exchange chromatography material, we used Fractogel EMD-COO (20-40 µm) from MERCK. The column material was washed twice with deionized water, three times with methanol and than equilibrated with the running buffer chloroform: methanol: H_2O= 4: 4: 1. Depending on the sample size, different columns were used. For analytical purpose, we used Pasteur pipettes, sealed with glass wool. After sample loading, the column was washed with the running buffer, before the protein was eluted by elution buffer (running buffer with ammonium acetate). For larger scale samples, bigger columns or HPLC separation were used. The samples were analyzed with SDS-PAGE as described above.

Alternatively, the protein was bound to the column as described above, but was then washed with methanol: trifluoroethanol= 1:1 and then eluted with formic acid: ethanol: trifluoroethanol: H_2O= 1: 2.8: 1: 1. This buffer is fully miscible with aqueous buffer systems and was used to dialyze the samples after elution.

Identification of subunit a by tryptic digestion and MALDI mass spectroscopy

Subunit a was purified as described above and submitted to SDS-PAGE. The gel was stained with Coomassie and the band for subunit a excised from the gel. In-gel digestion was performed as described (Shevchenko *et al.*, 1996) and analyzed on a Perseptive Biosystems voyager Elite system, a MALDI TOF with reflector as described (Meier *et al.*, 2003).

MALDI TOF analysis of the entire subunit a

Subunit a was purified as described above and prepared for MALDI mass spectroscopy by two different strategies. Analogously as described (von Ballmoos *et al.*, 2002), the sample was evaporated to dryness, redissolved in methanol: formic acid= 1: 1 and spotted it onto the MALDI target consisting a layer of sinapic acid. Alternatively, subunit a in elution buffer was mixed with 5% acetic acid to chloroform: methanol: H$_2$O= 4: 4: 3. One µl of the lower organic phase was directly spotted onto the MALDI target as described above.

8.3 Results and Discussion

During purification of subunit c, the aqueous sample is extracted with chloroform: methanol to precipitate insoluble material. Usually, this fraction is never considered to be analyzed, since a subsequent phase separation is performed to further enrich subunit c. If purified ATP synthase from *I. tartaricus* is the starting sample, one however observes a second prominent band after the monophasic extraction with organic solvents, which runs with the expected mobility for subunit a in SDS-PAGE (Figure 8-1A, lane 1-3). This observation was the starting point for the following experiments. Similar to synthetic organic chemistry, we used aqueous solutions with different chemical properties to induce the phase separation. The starting material (lane 1) in chloroform: methanol: buffer= 4: 4: 1 was mixed with two units of either water (data not shown), saturated sodium chloride solution (lane 2+3), saturated ammonium hydrogen carbonate solution (lane 4+5) or 3 % citric acid (lane 6+7) and the aqueous and the organic phases were analyzed on SPS-PAGE. Whereas water and the basic carbonate did only extract subunit c into the organic phase, in the case of NaCl and under acidic conditions, also subunit a was observed in the organic phase (Figure 8-1). We further concentrated on the acidic conditions, since the phase separation was much easier to handle compared to the salt condition (e.g. large precipitate of NaCl in the inter/ upper phase). As a rationale, we propose, that the acidic treatment competes with several charged residues in subunit a, which are responsible for its insolubility in chloroform. Around pH 7, charged residues mainly stem from acidic glutamic and aspartic acid residues. They are however neutralized under more acidic conditions provided by the presence of citric acid. We tested this hypothesis and included different concentrations of acetic acid solutions. Acetic acid would be advantageous over citric acid because of its volatility. Starting solution (Figure 8-1, lane 1) was mixed with either 3 % citric (lane 2+5), 1% acetic acid (lane 3+6) or 5% acetic acid (lane 4+7) and the two phases were analyzed on SDS-PAGE.
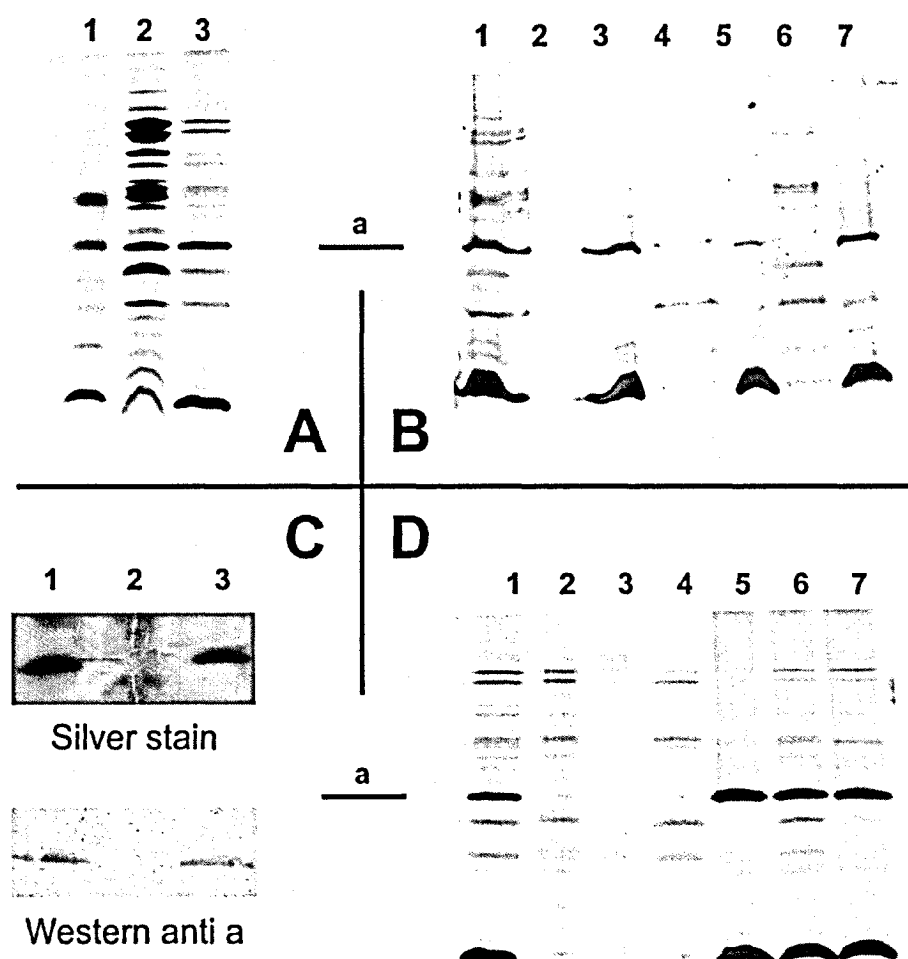
Figure 8-1. Extraction of subunit a of the ATP synthase from *I. tartaricus* by organic solvents

A. Extraction of purified ATP synthase from I. tartaricus. Lane 1: Marker (second band from top is subunit a); lane 2: purified ATP synthase from *I. tartaricus*; lane 3: supernatant after treatment of purified ATP synthase with chloroform: methanol as described in the text.

B. Phase separation with different aqueous solutions. Lane 1: supernatant after extraction with chloroform: methanol; lane 2: empty; lane 3: organic phase after phase separation with saturated NaCl solution; lane 4: aqueous phase after phase separation with NaHCO$_3$; lane 5: organic phase after phase separation with NaHCO$_3$; lane 6: aqueous phase after phase separation with 3% citric acid; lane 7: organic phase after phase separation with citric acid

C. Western blot analysis of subunit a extraction. Lane 1: supernatant after treatment with chloroform: methanol; lane 2: aqueous phase after phase separation with 3% citric acid; lane 3: organic phase after phase separation with citric acid

D. Comparison of different acids to induce phase separation. Lane 1: supernatant after extraction with chloroform: methanol; lane 2: aqueous phase after phase separation with 3% citric acid; lane 3: aqueous phase after phase separation with 1% acetic acid; lane 4: aqueous phase after phase separation with 5% acetic acid; lane 5: organic phase after phase separation with 3% citric acid; lane 6: organic phase after phase separation with 1% acetic acid; lane 4: organic phase after phase separation with 5% acetic acid

The best results were obtained with citric acid, where almost all the subunits except a and c can be observed in the aqueous phase. The subunit distribution is less clear with acetic acid, although subunit a can be nicely enriched under all three conditions employed. The presence of subunit a in the samples was verified with Western blotting using a specific antibody against subunit a from *P- modestum* (Figure 8-1C). For further purification of subunit a, we followed the strategy of ion chromatography in mixed organic solvents, which was already successfully applied for subunit c. Pilot experiments with a weak anion exchanger indicated that it was unable to bind subunit a (data not shown). Further experiments with a a weak cation exchange material (carboxymethyl) indicated, that subunit a was bound to the column material. The protein was the stepwise eluted with ammonium acetate in the same solvent system which resulted in the separatation of subunit a from subunit c (Figure 8-2).
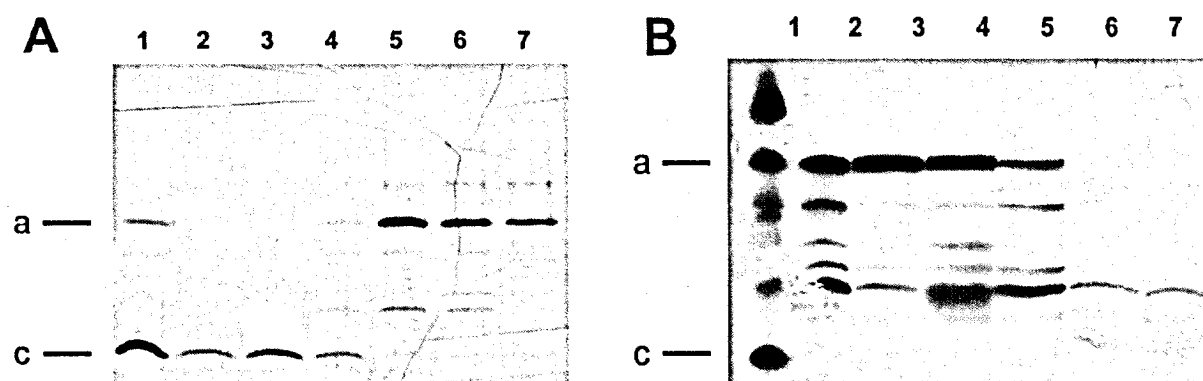

Figure 8-2. Purification of subunit a in organic solvents.

A. SDS-PAGE analysis of cation exchange chromatography of extracted protein sample. Lane 1: Flow trough of the applied sample; lane 2: wash with chloroform: methanol: H₂O= 4: 4: 1; lane 3: elution with 10 mM ammonium acetate in chloroform: methanol: H₂O= 4: 4: 1; lane 4: elution with 25 mM ammonium acetate; lane 5: elution with 25 mM ammonium acetate; lane 6: elution with 50 mM ammonium acetate; lane 7: elution with 100 mM ammonium acetate.

B. SDS-PAGE analysis of dialyzed sample after chromatography. Lane 1: Marker; lane 2: sample applied to cation exchange chromatography; lane 3+4: elution of cation exchange chromatography with formic acid: ethanol: trifluoroethanol: H₂O= 1: 2.8: 1: 1 ; lane 5: addition of SDS and subsequent evaporation of solvent, lane 6+7: dialyzed samples in 50 mM Tris, pH 7, 100 mM NaCl, 10% glycerol, 1% lauryl sarcosine.

MALDI TOF analysis of subunit a

Subunit c was eluted during the wash steps and subunit a was specifically eluted with ammonium acetate concentrations above 25 mM. The obtained samples were further analyzed by MALDI mass spectroscopy and the expected mass of 32'367 Da for subunit a was verified

by the measurement yielding m/z= 32'382 (Figure 8-3). This finding could elucidate the initiation of transcription, which is not clear from the DNA sequence, since two possible starting regions are found in the sequence of subunit a of *I. tartaricus*. Further analyses were performed by tryptic digestion and subsequent MALDI mass spectroscopy of the protein and could univocally identify it as subunit a (Meier *et al.*, 2003). The extraction and purification protocol described above could also be applied to purify subunit a of *P. modestum* from an appropriate *E. coli* expression host, as shown by SDS PAGE and MALDI mass spectroscopy (data not shown).

Protein transfer from organic solvents into aqueous solution

Since after purification, subunit a is present in an organic solvent mixture, which is incompatible with functionality, we tried to exchange the organic solvent by a detergent solution, in order to achieve the functional reconstitution of the protein. In a first attempt, we added the detergent solution to the purified sample, evaporated the solvents and resuspended the sample with buffer solution. Except for the strong ionic detergents lauryl sarcosine and SDS, this method was not successful and was abandoned. Lyophilisation is known as a mild method to remove liquids from protein samples. The used organic solvent mixture is however not suited for this procedure, since the freezing point is too high. Therefore, we mixed the sample with dioxane (melting point: 12 °C, boiling point: 101 °C), which is fully miscible with the solvent mixture. Again, the results were only satisfying with strong detergents, which are not suited for reconstitution experiments. Some 20 years ago, Khorana delipidated and purified bacteriorhodopsin by means of organic solvents (Huang *et al.*, 1981) and brought the protein back into aqueous solution by dialysis for 48h. To adapt his protocol to our system the protein was eluted from the ion exchange column with a mixture of formic acid: ethanol: trifluoroethanol: H₂O= 1: 2.8: 1: 1. This solvent mixture has the advantage of being fully miscible with water and is therefore suited for dialysis. After elution, detergent was added and the sample subsequently dialyzed against the desired buffer solution containing the same detergent. Lane 2 and 3+4 in Figure 8-2B show the sample before and after exchange chromatography, eluted with the mixture described above, respectively. While addition of SDS and subsequent evaporation of the solvent was successful (lane 5), the samples after dialysis did not contain any subunit a (lane 6+7). Leakage of the dialysis tube could be excluded, since the contaminant with a lower molecular weight was retained.
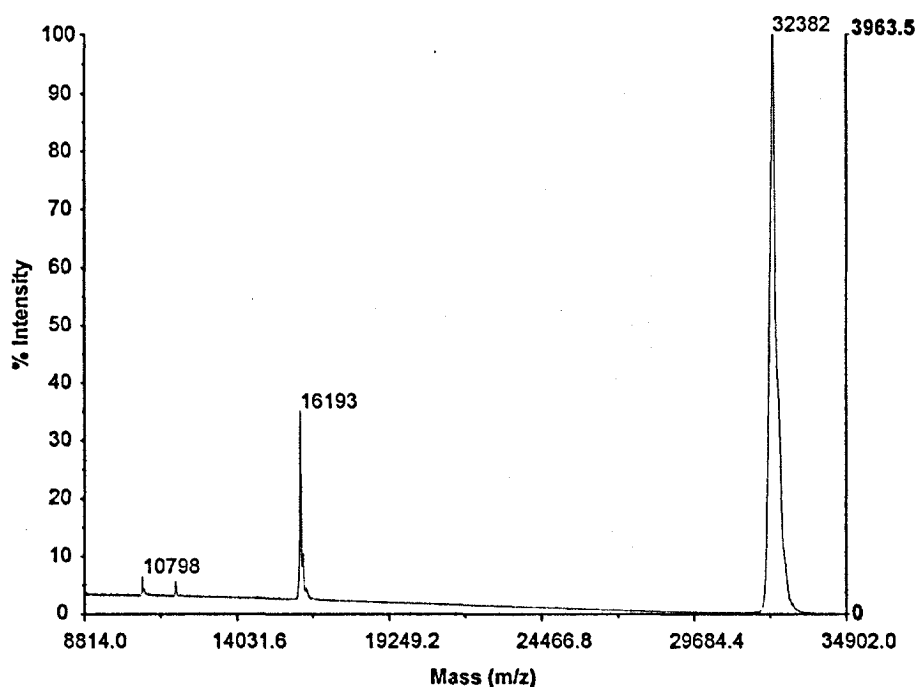
Figure 8-3. MALDI-TOF mass spectroscopy of purified subunit a. The sample was prepared for MALDI mass spectroscopy by mixing subunit a in elution buffer (chloroform: methanol: H_2O= 4:4:1) with 5% acetic acid (aq) to reach chloroform: methanol: H_2O= 4:4:3. One µl of the lower organic phase was directly spotted onto the MALDI target, which before was coated with saturated sinapic acid solution in acetonitrile: H_2O (0.1% trifluoroacetic acid)= 2:1. Measurements were performed in the linear mode using external standard, where an accuracy of 0.1% can be expected.

8.4 Concluding remarks

The presented method to extract subunit a into organic solvents is generally applicable to proteins from different organisms (e.g *E. coli*, not shown). The acidification of the sample increases the solubility of membrane proteins in organic solvents significantly. The method could therefore be extended to other hydrophobic proteins. The presence of organic solvents may prevent the aggregation of the hydrophobic proteins in aqueous solutions and increase their solubility. Furthermore, proteins are obtained in a very pure environment, lacking detergent and salts. This property allowed the first analysis of the intact subunit a with MALDI mass spectroscopy, since all measurement from aqueous solutions have failed before. In parallel to our studies, very similar experiments were independently performed with the subunit a from *E. coli* in order to analyze the structures by NMR analogously to subunit c in the mixed organic solvent (Dmitriev *et al.*, 2004). The problem of incompatibility with aqueous systems was circumvented by mixing subunit a together with lipids before evaporation of the solvent and subsequent functional reconstitution. This shows that the protein is not irreversibly misfolded during treatment with organic solvents.

8.5 References

Arechaga, I., Miroux, B., Runswick, M.J. and Walker, J.E. (2003) Over-expression of *Escherichia coli* F_1F_0-ATPase subunit a is inhibited by instability of the uncB gene transcript. *FEBS Lett.*, **547**, 97-100.

Capaldi, R.A. and Aggeler, R. (2002) Mechanism of the F_1F_0-type ATP synthase, a biological rotary motor. *Trends. Biochem. Sci.*, **27**, 154-160.

Dimroth, P., von Ballmoos, C., Meier, T. and Kaim, G. (2003) Electrical power fuels rotary ATP synthase. *Structure (Camb.)*, **11**, 1469-1473.

Dmitriev, O.Y., Altendorf, K. and Fillingame, R.H. (2004) Subunit A of the *E. coli* ATP synthase: reconstitution and high resolution NMR with protein purified in a mixed polarity solvent. *FEBS Lett.*, **556**, 35-38.

Huang, K.S., Bayley, H., Liao, M.J., London, E. and Khorana, H.G. (1981) Refolding of an integral membrane protein. Denaturation, renaturation, and reconstitution of intact bacteriorhodopsin and two proteolytic fragments. *J. Biol. Chem.*, **256**, 3802-3809.

Laubinger, W. and Dimroth, P. (1987) Characterization of the Na⁺-stimulated ATPase of *Propionigenium modestum* as an enzyme of the F_1F_0 type. *Eur. J. Biochem.*, **168**, 475-480.

Meier, T., von Ballmoos, C., Neumann, S. and Kaim, G. (2003) Complete DNA sequence of the atp operon of the sodium-dependent F_1F_0 ATP synthase from *Ilyobacter tartaricus* and identification of the encoded subunits. *Biochim. Biophys. Acta.*, **1625**, 221-226.

Neumann, S., Matthey, U., Kaim, G. and Dimroth, P. (1998) Purification and properties of the F_1F_0 ATPase of *Ilyobacter tartaricus*, a sodium ion pump. *J. Bacteriol.*, **180**, 3312-3316.

Shevchenko, A., Wilm, M., Vorm, O. and Mann, M. (1996) Mass spectrometric sequencing of proteins silver-stained polyacrylamide gels. *Anal. Chem.*, **68**, 850-858.

von Ballmoos, C., Appoldt, Y., Brunner, J., Granier, T., Vasella, A. and Dimroth, P. (2002) Membrane topography of the coupling ion binding site in Na⁺-translocating F_1F_0 ATP synthase. *J. Biol. Chem.*, **277**, 3504-3510.

Wehrle, F., Appoldt, Y., Kaim, G. and Dimroth, P. (2002) Reconstitution of F_0 of the sodium ion translocating ATP synthase of *Propionigenium modestum* from its heterologously expressed and purified subunits. *Eur. J. Biochem.*, **269**, 2567-2573.

9. Discussion

On the role of the membrane potential for torque generation in F-type ATP synthases

An "objective" view on three different mechanistic models

Insights into the molecular mechanism of rotation in the F_0 sector of ATP synthase.
Aksimentiev A, Balabin IA, Fillingame RH, Schulten K.
Biophysical Journal, 86(3), 1332-44, (2004).

The proton-driven rotor of ATP synthase: ohmic conductance (10 fS), and absence of voltage gating
Feniouk BA, Kozlova MA, Knorre DA, Cherepanov DA, Mulkidjanian AY, Junge W.
Biophysical Journal, 86(6):4094-109, (2004).

Torque generation by the F_0 motor of the sodium ATPase.
Xing J, Wang H, von Ballmoos C, Dimroth P, Oster G.
Biophysical Journal, 87(4):2148-63, (2004).

9.1 Introduction

Ten years after the first high resolution structure of the F_1 ATPase (Abrahams *et al.*, 1994), many speculations and assumptions derived from biochemical data could be confirmed through the atomic picture of the enzyme. Vice versa, the interpretation of the structural data led to new biochemical experiments which in turn tested the hypothesis. This smooth collaboration of structural and functional investigations allowed building of a nearly complete picture of the mechanism of the F_1 motor. The absence of any high resolution structure of the F_0 motor impedes a similar progress for the membrane-embedded part of the enzyme. Although much effort has been taken to understand the interactions of the F_0 subunits, no conclusive mechanistic model has emerged until today (see Chapter 1). In recent years, computational models gained importance to understand the molecular mechanism of this biological motor. It is therefore not surprising, that three different research groups published their computational investigations about the F_0 motor of the ATP synthase within a very short time period.

However, the works differ in respect to the taken assumptions for the computational work. The work of Aksimentiev *et al.* (2004) is an all atom simulation of the a subunit and the c_{10} ring of the ATP synthase of *E. coli*, based on structural models, which were derived from NMR and mutational analyses. In contrary, the report of Feniouk *et al.* (2004) bases on fast kinetic measurements with F_1 depleted chromatophores of *Rhodobacter capsulatus*. The results of the work are therefore less precise but rely on actual measurements. Finally, Xing *et al.* (2004) present a model for torque generation in Na^+-translocating ATP synthase, which is based on dynamical experimental observations from many functional and mutational studies. Structural constraints are implemented according to the available structural data. This discussion will shortly introduce the three proposed models and compare them with respect to their critical aspects.

9.2 Insights into the molecular mechanism of rotation in the F_0 sector of ATP synthase (Aksimentiev *et al.*, 2004)

9.2.1 Introduction and setup of parameters

The report of Aksimentiev *et al.* (2004) describes so called steered molecular simulations and mathematical modeling of the a subunit and the c_{10} ring, placed into a phosphatidyl ethanolamine bilayer. The structural model is based on the ac_{12} model (Rastogi and Girvin,

1999), which combines NMR investigations of the subunit c monomer in mixed organic solvents, disulfide crosslinking data and analyses of suppressor mutations. The number of c subunits was corrected to 10 and the structure replaced by the more recent c_{10} model of the *E. coli* c-ring (Dmitriev *et al.*, 1999; Fillingame *et al.*, 2000a; Jiang *et al.*, 2001). Furthermore, the parameters rely on the observed different subunit c monomer conformations at acidic and neutral pH, which were interpreted as large helical movements (Rastogi and Girvin, 1999). This movement is thought to characterize the protonation and deprotonation of Asp61, while entering and leaving the interface with subunit a, where the ion exchange of the two reservoirs takes place through two half channels (Angevine and Fillingame, 2003).
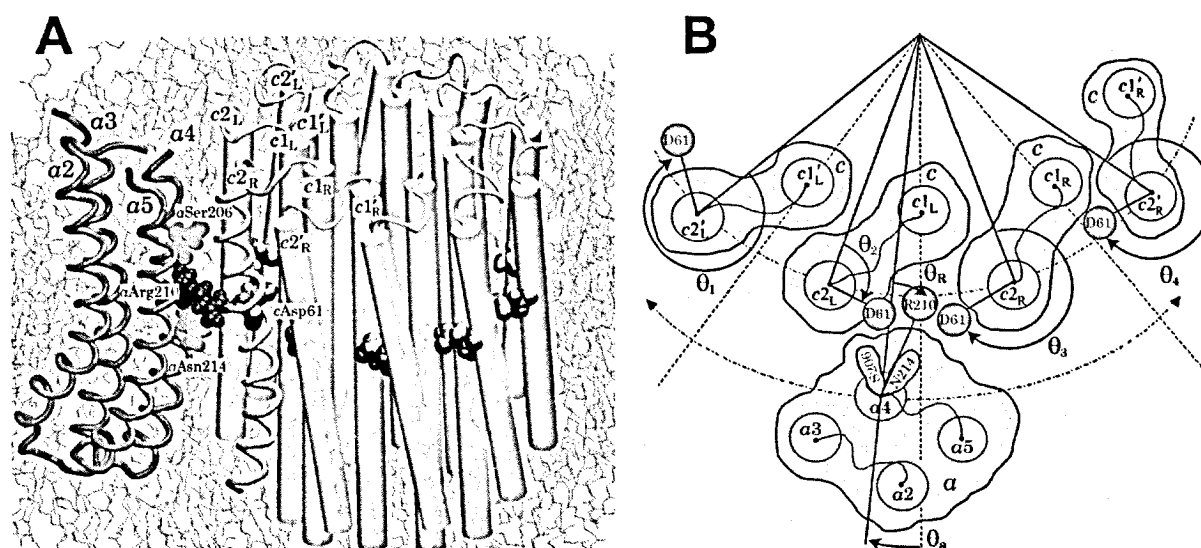

Figure 9-1. A. Microscopic model of F_0 ATPase composed of a four-helix bundle of subunit a and an oligomer of 10 c-subunits. The conserved acidic residues (cAsp61) in the c-ring are depicted in red, whereas the conserved stator charge (aArg210) is shown in blue. Additional important residues for the model are aSer206 and aAsn214 which are shown in green. **B. Stochastic model for F_0 (view from cytoplasm).** Four out of 10 c-subunits and the a-subunit are shown. The c_{10} complex is fixed, and the a-subunit can move in either direction (angle θ_a). This is equivalent to the more natural choice of a fixed subunit a and a moving c_{10} complex. The second transmembrane helix (c2) of each c-subunit can rotate independently (described by angles θ_1, θ_2, θ_3, and θ_4), thereby moving the key cAsp61 residues, which are the proton-binding sites. The c1 helices do not rotate. Similarly, only the fourth helix of the a-subunit (a4) can rotate (angle θ_R), moving the aArg210 residue; helices a2, a3, and a5 do not rotate. Proton transfer occurs between the terminal residue of the periplasmic channel (aAsn214) and the cAsp61 binding site on helix $c2_R$, and between the terminal residue of the cytoplasmic channel (aSer206) and the cAsp61 binding site on $c2_L$. Motions are confined to the plane of the figure. The system is fully described by helix orientations θ_1, θ_2, θ_3, and θ_4 (c-subunits), θ_R (a4), rotor angle θ_a, and protonation state of the two aspartates (cAsp61) on helices $c2_L$ and $c2_R$.

Since the time scale of Molecular Dynamics (MD) simulations are in the order of picoseconds, they do not match the millisecond timescale of the rotational enzyme. The timescales were bridged by combining a mathematical model of the overall millisecond function of F_0 with nanosecond MD simulations. The model assumes that the F_0 motor operates as molecular ratchet, in which the proton-motive force biases the rotational diffusion of the c-oligomer. In other words, the conformational changes which are obtained after nanoseconds are irreversible in respect of the rotational direction of the c-ring. Mechanistically, several constraints and approximations were taken. It was assumed, that only the outer helices of two c subunits and TMH4 of subunit a are involved in the ion translocation. Only these helices were allowed to rotate, whereas the others were fixed. Moreover, the pathways of the ions from the reservoirs to the binding sites were explicitly specified. And most importantly, it was assumed, that all key residues (aArg210, aSer206, aAsn214 and two cAsp61) are approximately located in a horizontal plane. The flexibility of side chains was neglected.

9.2.2 Results and Discussion

A key feature of the applied stochastic model is the involvement of a 180° helical rotation of the outer TMH of subunit c upon protonation or deprotonation as described (Fillingame et al., 2000a; Rastogi and Girvin, 1999). The transported ions are delivered through subunit a intrinsic half channels, whereby the terminus of the cytoplasmic half channel is denoted as aSer206 and the terminus of the periplasmic half channel is assumed to be aAsn214. Both residues are part of aTMH-4 and are expected to lie in a vertical plane with the conserved aArg210. Since in the structural model of subunit c, the outer helix forms an angle of ~17° with the inner TMH (Girvin and Fillingame, 1993), rotation of the outer TMH along the helical axis shifts the group of cAsp61 also in the vertical direction for around 3 Å. If the site is deprotonated, the side chain of cAsp61 is closer to the cytoplasmic half channel (aSer206), whereas a 180° rotation brings the side chain into proximity of aAsn214, which reflects the entrance of the periplasmic channel.

Another new aspect of the model is the presence of two c subunits in the interface with subunit a. At least one cAsp61 of these subunits is deprotonated, thereby building a salt bridge with aArg210. The deprotonation of Asp61 on the second subunit induces a 180° rotation of its C-terminal helix and thereby brings its Asp61 side chain almost face to face to the other acidic residue, and both acidic residues share the salt bridge with aArg210. More

precisely, it is assumed, that one Asp61 residue forms a salt bridge with aArg210, while the second Asp61 is stabilized by the generated dipole of the salt bridge. Calculations of this event showed only a small difference in the potential energy between the dimeric "two charged" and the trimeric "three charged" situation. This finding implies that the salt bridge can readily change between the subunits. This is the key feature of the proposed sequence of events during functional rotation, which are depicted in Figure 9-2 (For details, see legend). As a starting situation, both binding sites ($c2_L$ and $c2_R$) are deprotonated and are in the trimeric state with aArg210 as described above. The sequence is initiated by the transfer of a periplasmic proton from aAsn214 to the binding site of a c subunit ($c2_R$). The salt bridge between $c2_R$ and aArg210 is lost and $c2_L$ is the remaining partner. This event rotates the newly protonated $c2_R$ out of the interface and the c ring moves relative to subunit a. The salt bridge between $c2_L$ and aArg210 stays intact and the movement of the c-ring rotates back the $c2_L$ to its initial conformation. When subunit a approaches the protonated $c2_L$', this helix begins to swivel for 180°C in either direction and transfers its proton onto the aSer206 of the cytoplasmic channel. The now deprotonated $c2_L$' faces $c2_L$ and aArg210 and the trimeric starting conformation is regenerated, but with the c_{10} oligomer advanced by 36°.

The main difference of the described mechanism to that proposed by Girvin, Fillingame and their co-workers is that the rotation of c_{10} is induced by the cooperative interaction of two adjacent c-subunits with TMH-4 of subunit a, whereby cAsp61 of one of the c subunits is always deprotonated (Rastogi and Girvin, 1999; Fillingame et al., 2000b). The direction in which the c_{10} oligomer can rotate depends on the protonation states of the binding sites and is therefore controlled by the proton motive force, which determines the probability of the binding sites' protonation or deprotonation.

The described mechanism is not the result of a single simulation, but rather the sum of different simulations, where the substeps have been investigated. Unknown processes, like the transport of the protons from the reservoir through the channels to the binding site, have been omitted. Instead of that, the direction of proton flux was simulated through protonation or deprotonation of the "relay" residues aAsn214 or aSer206, respectively.
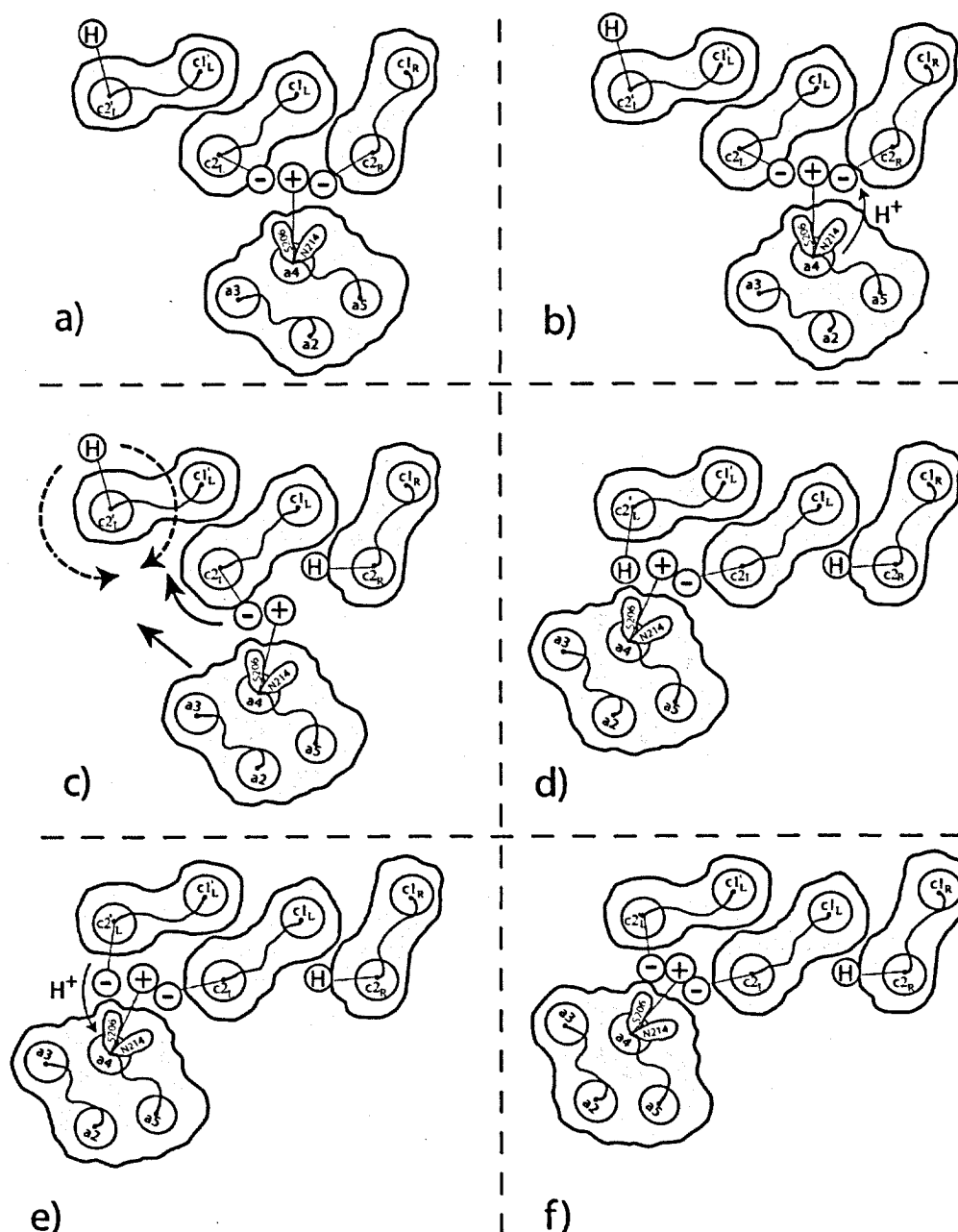
Figure 9-2. Schematic representation of the sequence of suggested events. These events, labelled *a–f*, occur during rotation of the c_{10} oligomer by $2\pi/10$ in the synthesis direction, viewed here from the cytoplasm. (*a*) In the starting conformation, two residues *c*Asp61 are deprotonated and form a dual salt bridge with *a*Arg210, *c*Asp61ʹ–*a*Arg210–*c*Asp61ʺ. (*b*) A proton is transferred from the terminal residue of the periplasmic proton channel, *a*Asn214, to *c*Asp61 on helix *c*2$_R$. (*c*) Subunit *a* rotates clockwise with respect to the c_{10} oligomer in concert with a clockwise rotation of helix *c*2$_L$. When subunit *a* approaches helix *c*2$_L$ʹ, *c*Asp61 on that helix rotates by 180°. The latter rotation may proceed in either clockwise or counterclockwise direction. (*d*) The concerted rotation of subunit *a* and helix *c*2$_L$ are completed: *c*Asp61 on helix *c*2$_L$ʹ has rotated by 180° toward subunit *a*. (*e*) A proton is transferred to the terminal residue of the cytoplasmic proton channel, *a*Ser206. (*f*) The system returns to the starting conformation *a*, but with the c_{10} oligomer advanced by an angle $2\pi/10$. The processes depicted are of stochastic nature, and, hence, do not necessarily obey strictly the sequence shown.

9.3 The proton-driven rotor of ATP synthase: ohmic conductance (10 fS), and absence of voltage gating (Feniouk *et al.*, 2004)

9.3.1 Introduction and setup of parameters

The experimental system of the Junge group is unique in the ATP synthase research field. The use of intact chromatophores of the photosynthetic bacteria *Rhodobacter capsulatus* provides interesting advantages. The chromatophores are closed vesicles (comparable to the chloroplasts of plants) harbouring photosynthetic reaction centres (RC), respiratory enzymes and the ATP synthase. An advantage of this system is its simple and fast preparation, which ensures a high functionality of the vesicles. Vesicles of a defined size (~30 nm) were produced to ensure only a single copy of ATP synthase per vesicle, whereas about 11 RC's are present in the same compartment (Feniouk *et al.*, 2002). The disadvantage of the system is the fact, that other membrane proteins are present, which may influence the outcome of the experiment. Therefore, control experiments have to be carefully performed to enable the interpretation of the results restricted to the ATP synthase. The chromatophores are treated in low buffer and salt conditions at high pH to strip off the F_1 part of the ATP synthase. An advantage of the system is the ease to establish a transmembrane potential. This is accomplished by a short laser treatment of the chromatophores to activate the reaction centres, which are then establish a transmembrane potential. The course of the electrical potential can then be monitored by electrochromic transients of intrinsic carotenoids and the proton flow by pH-indicating dyes. The principle of the measurements is depicted in Figure 9-3.
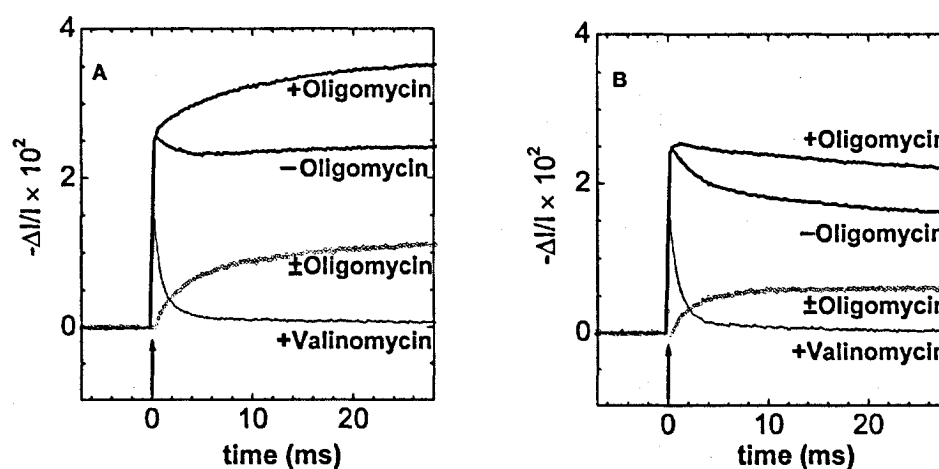

Figure 9-3. Electrochromic absorption transients at a wavelength of 522 nm in F_1-depleted chromatophores as caused by a short flash of light. The upper traces were obtained without and with blocking of F_0 by 3 μM oligomycin, respectively. The difference trace ($\pm$ *oligomycin*) represents

the charge flow across F_0 (*A*) without and (*B*) with 3 μM myxothiazol added to deactivate the electrogenic and proton pumping activity of the cytochrome bc_1 complex. The actinic flash is indicated by an arrow. The bottom traces were obtained in the presence of 1 μM valinomycin to enhance the ion conductance of all chromatophores in the sample.

The activating flash is indicated by an arrow, and a transmembrane potential is established immediately. In the presence of valinomycin, the trace is rapidly decaying. Valinomycin is a potassium specific ionophore and abolishes the membrane potential. This decay reveals the magnitude of the electrochromic response to the transmembrane electric field. The upper traces were recorded in the presence or in the absence of the F_0 specific inhibitor oligomycin, as well as the difference of the two traces ($\pm$oligomycin), corresponding to the cumulative charge flow through F_0. In the presence of oligomycin (no proton flux through F_0), the fast charge separation in the RC is followed by a further slow increase of the transmembrane potential. This is attributed to the electrogenic reaction in the bc_1 complex. This slow phase was abolished upon the addition of the bc_1 inhibitor myxothiazol (Figure 9-3, right panel). Since the activity of the bc_1 complex is hindered by a large $\Delta\mu_H^+$, the inhibition of the F_0 complex influences the pumping rate of the bc_1 complex. Therefore, only the $\pm$oligomycin trace in the presence of myxothiazol (right panel) reflects the effective transport activity of the F_0 complex. Calibration of the system was achieved by the measurement of the electrochromic absorption transients after KCl/ valinomycin generated diffusion potentials of different magnitudes. A saturating flash of light therefore generated a transmembrane voltage of 70 $\pm$15 mV.

9.3.2 Results and Discussion

In a first series of experiments, Feniouk and coworkers investigated the pH dependence of the electric relaxation constant of the F_0 transport as described above. They found an astonishingly independent behaviour with an almost unchanged rate between the pH values of 6.5 and 10 (data in the original report, not shown here).

In their next experiment, they varied the flash energy and therefore the initial voltage jump and accordingly, the F_0 motors conducted fewer protons across the membrane. However, when they normalized the initial step of absorption of a 100% and a 33% saturating flash, they found, that the kinetics of the relaxation perfectly superimposed (Figure 9-4A). The relaxation was monoexponential and independent from the initial voltage jump. This voltage independent relaxation describes the discharge of a capacitor by an ohmic resistor. Therefore,

it could be concluded, that the F_0 channel behaves as an ohmic conductor and is not voltage gated. The shortest relaxation time implied a transport rate of 6500 protons per second at a 100 mV steady driving force, which is about ten times faster than in the coupled enzyme. In a further experiment, they monitored the pH on the two sides of the chromatophores by two pH sensitive dyes (Cresol red and Neutral red) (Figure 9-4B).
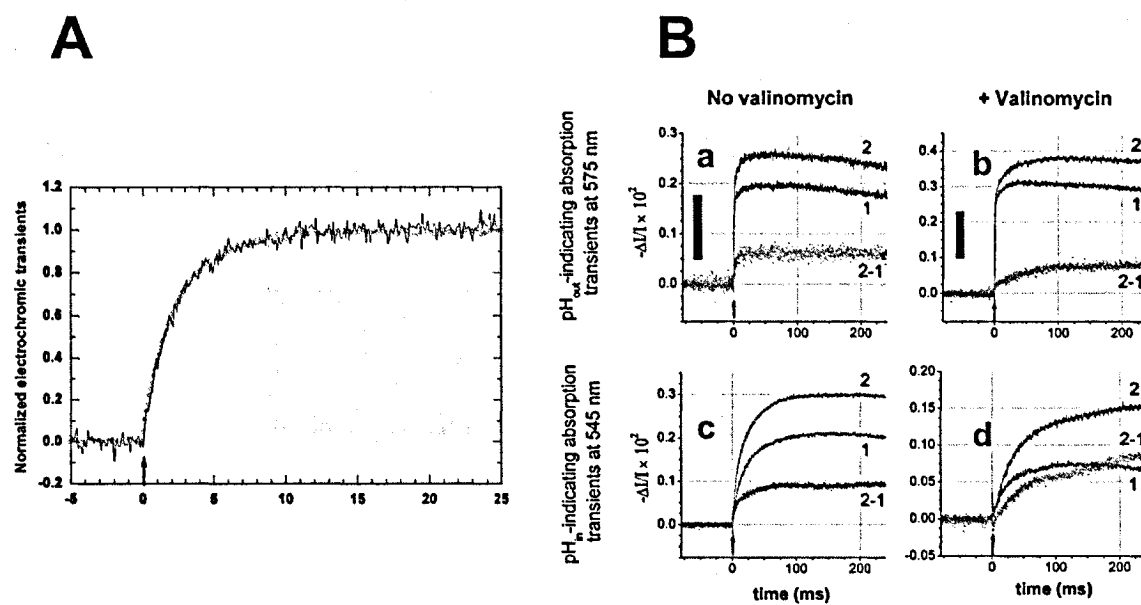

Figure 9-4 A. Transient charge transfer through F_0 in the presence of 3 μM myxothiazol as inhibitor of cytochrome-bc$_1$. Two transients of charge flow through F_0, both electrochromic differences ($\pm$ *oligomycin*) as the bottom trace in Figure 9-3. (o), the transient recorded under excitation with a flash of saturating energy. Noisy line, the transient recorded at attenuated excitation flash energy to produce 33% signal saturation. The extent after the flash was normalized to unity.

B. Proton transfer through F_0 as monitored by two pH indicators reporting pH transients from either side of the chromatophore membrane, (a, b) from the n-side (Cresol red, at a wavelength of 575 nm), and (c, d) from the p-side (Neutral red, at 545 nm). Traces in parts a and c were recorded in the absence, and traces b and d in the presence of the ionophore valinomycin (2 μM). In the latter case the transmembrane voltage was collapsed by the valinomycin-mediated K^+ current in <3 ms (see Figure 9-3). The relaxation of the pH difference was then entirely due to the entropic driving force (ΔpH).

Again, a fast relaxation of the charge separation can be observed by both dyes. However, if valinomycin is added, the relaxation slows clearly. The presence of valinomycin destroys the membrane potential and the ΔpH is the only remaining driving force for the F_0 motor. However, since the membrane potential is abolished within a few milliseconds (Figure 9-3), this experiment shows, that ΔpH is sufficient to drive rotational proton transport in the F_0 part

of *Rhodobacter capsulatus*. The obvious discrepancy to the earlier finding of a voltage-dependent mechanism of the intact enzymes of several organisms is rationalized by the conclusion, that the membrane potential affects the interaction of the two enzyme parts, F_0 and F_1 (Junge, 1970; Junge *et al.*, 1970; Kaim and Dimroth, 1999).

Based on these findings, Feniouk *et al.* designed a kinetic model for proton conduction by F_0 that fits the framework of an earlier published model (Elston *et al.*, 1998; Junge *et al.*, 1997). The molecular basis of this model is the Brownian rotary motion of the c-ring relative to subunit a, two non collinear access channels for protons from either side, and two electrostatic constraints, namely the glutamic acid residue (cAsp61 in *E. coli*) in the middle of the hairpin of subunit c being deprotonated when in contact with subunit a and protonated when facing the core of the membrane (Figure 9-5). The fit of experimental data yielded a low pK_a of 5–6 for the proton-accepting group of the input half-channel and an alkaline pK_a of 8 for the output group. This was in accord with the earlier observation, that in energized membranes, the pK values of the relay groups tend to match the ambient pH of the corresponding side of the membrane. This would allow higher turnover number of F_0, even against back pressure as found in alkaliphilic bacteria (Cherepanov *et al.*, 1999). The observed weak pH-dependence of the F_0 motor follows from this model. The effect of the transmembrane potential was introduced by adjusting the pK_a values of the acceptor/donor groups, weighted by their respective z-position in the membrane dielectric and the missing parameters were optimized by numerical integration (for further details, see (Feniouk *et al.*, 2004)).

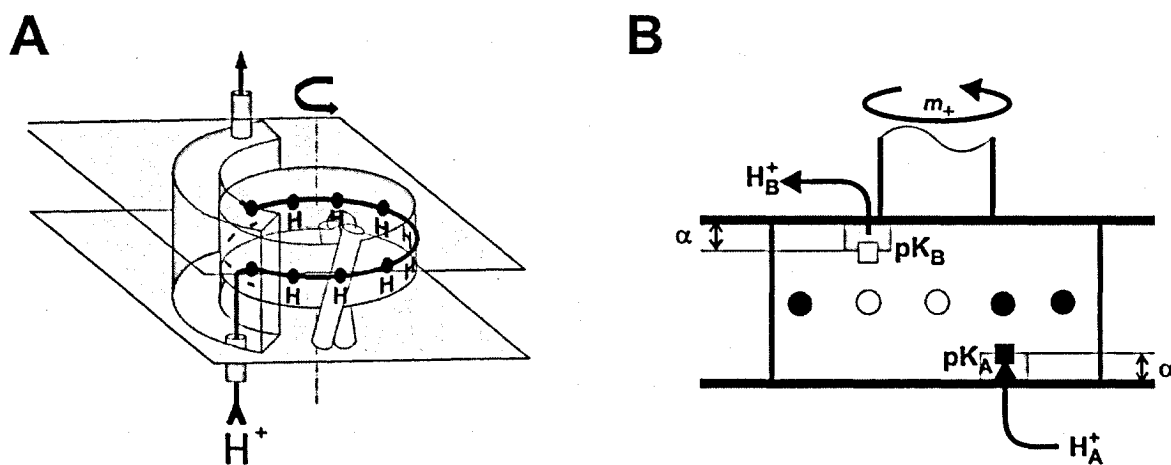**Figure 9-5. Functional model of F_0. A.** Schematic illustration of F_0 operation with a rotary c ring and two non-collinear half channels in subunit a. **B.** Simple model for proton transfer. Depicted are the membrane embedded binding sites (circles; open for deprotonated, closed for protonated) and the putative proton acceptor and donor groups close to the membrane surface. See text for further details.

The practical result of the calculation is an estimate of the distance of the two relay groups in the membrane. Assuming a constant permittivity across the whole membrane (4 nm), the topological distance of the two groups would be >3.4 nm. The permittivity is however strongly influenced by the chemical environment and may therefore differ substantially. Such effects could reduce the distance of the two groups <1.8 nm, but would also imply a deviation from an Ohmic behaviour. The model concludes that proton transport across the membrane through two non coaxial half channels is mediated by at least two residues closely located at the membrane / water interface. Furthermore, the very high observed proton specificity can be attributed to acid/ base groups as selectivity filter. It excludes water-wire without such groups and a self diffusion of protons in form of H_3O^+ and OH^-.

9.4 Torque generation by the F_0 motor of the sodium ATPase (Xing *et al.*, 2004)

9.4.1 Introduction and setup of parameters

The paper of Xing *et al.* describes a more intuitive approach to build a theoretical and mathematical model of the F_0 motor. Its principle is explained in the original text as follows: "Abstractly, the dynamical behavior of a system is governed by its free-energy profiles along some set of reaction and geometric coordinates. Thus theoretical studies frequently begin by constructing plausible free-energy functions and then comparing experimental observations with the dynamical behavior predicted by traversing the coordinates driven by these free-energy functions. In principle, this task can be carried out by molecular dynamics simulations; however, this requires accurate force fields and the complete molecular structure. Here we illustrate an approach to modeling using the inverse procedure. We use incomplete available structural data to construct empirical free-energy profiles from experimental measurements. These are refined by adjusting structural dimensions to fit further experimental data. The method demonstrates how mathematical modeling can provide a way to combine structural information with biochemical, mutation, and mechanical measurements to elucidate the basic operating principles for a mechanoenzyme."

In contrary to the two studies described above, this work deals with the sodium dependent ATP synthase of *Propionigenium modestum*. Firstly, functional properties and constraints derived from kinetic and mutational analyses were listed to define the functional framework of the system.

1. In the Na^+ dependent enzyme of *P. modestum*, it was shown that the electric membrane potential is indispensable for rotational function of the ATP synthase. In 1992, Kluge *et al.* determined that a potential threshold of ~40 mV is observed to initiate $\Delta\psi$-driven Na^+-uptake through F_0 into liposomes (Kluge and Dimroth, 1992). This threshold corroborated well with the found value in the intact enzyme during synthesis (Kaim and Dimroth, 1999). Neither the ATP synthase nor the F_0 part alone could be driven by a ΔpNa alone.

2. In the absence of any driving force ($\Delta\psi$ or ATP), the enzyme is in its idling mode, where small fluctuations of the c-ring allow the exchange of Na^+ ions between the two sides of the membrane. This transport is bidirectional without any net charge transfer. The channels are therefore not voltage gated, but the continuous rotation of the enzyme is.

3. ATP hydrolysis is dependent on Na^+ concentration. In absence of Na^+, the empty rotor site can not be transported into the a/ c interface.

4. Through mutational analysis, the functional role of the essential arginine 227 (aArg227, stator charge) could be assigned as a tool to strip off Na^+ ions from the incoming rotor binding sites (both directions). The positive charge is the essential feature of the residue, whereby the delocalized charge of the arginine is favored over the more localized charges of lysine and histidine (Wehrle *et al.*, 2002). Furthermore, an exchange of the stator arginine to a hydrophobic alanine allowed directed Na^+ transport in absence of $\Delta\psi$ by ΔpNa alone (see point 1).

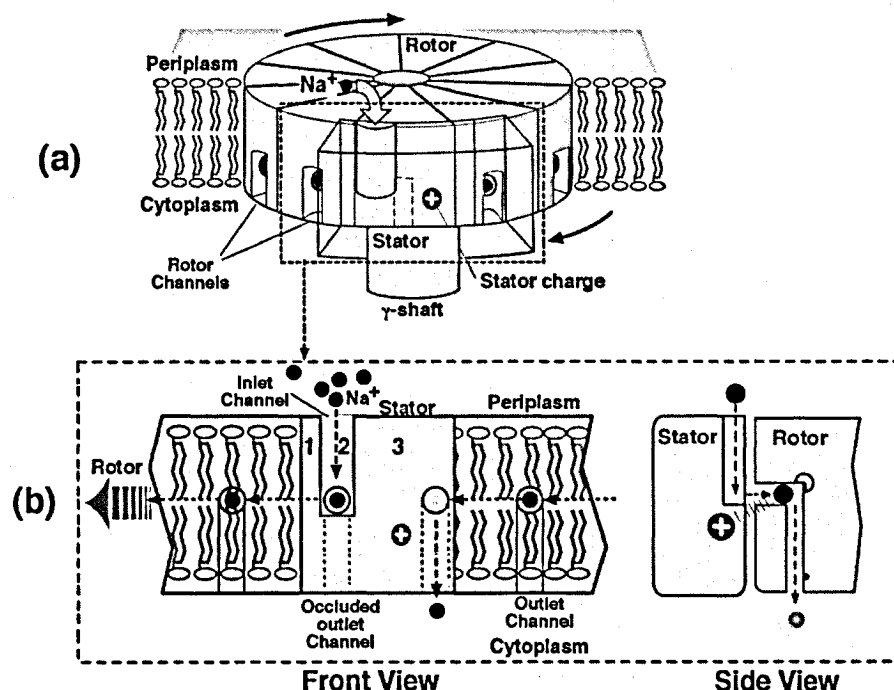The structural outline of the model is depicted as cartoon in Figure 9-6.

Figure 9-6. Cartoon structure (*panel a*) and front/side views (*panel b*) of the F_o rotor-stator assembly. The stator-rotor (*a-c*) interface is divided into three regions labeled *1*, *2*, and *3* (see *panel b*). In the ATP synthesis direction, a rotor site enters the interface from the right and, upon encountering the repulsive force from the positive stator charge in region 3, discharges its bound ion through the outlet channel to the cytoplasm. The rotor then diffuses carrying the site into the inlet channel (region 2), where it binds an ion from the periplasm. The nearly neutral site then leaves the interface through region 1. The inlet channel is connected to the rotor site via a short horizontal channel (*side view* in *panel b*), and the outlet channel is closed in region 2 to prevent ion leakage.

9.4.2 Results and Discussion

9.4.2.1 Push and pull

The principle of potential curves and how they are interpreted is demonstrated with the working principle of the wild type enzyme in the ATP synthesis direction (Figure 9-7). The potential curve along a reaction coordinate (in our case the angle of rotation θ) is described by the energy of the system at the defined moment. Low potentials are more favored than high potentials, which often need additional activation energy (kinetic energy) for being reached. The potential curves in Figure 7 describe the free energy profiles (and therefore also the probability) of an empty rotor site (red) and Na^+ occupied rotor site (blue) during its passage through the interface with subunit a. It is apparent, that an empty rotor site is generally more favoured, which is in accordance to the fact that release and binding of Na^+ ions takes place during this interface passage (for a detailed description of the events, please refer to the legend.) The chain of events can be rationalized by a push and pull mechanism which is rather

synchronized than clearly split into two different events. The pull event occurs during the solvation of the empty binding site within the stator channel (4→5), indicated by sharp decrease of the empty potential. This energy can be used to pull the occupied rotor site into the interface, where it faces the positive stator charge. The Na$^+$ ion is released and the now negatively charged binding residue is attracted by the stator charge (events 2→3). This forced rotation pushes the next empty site into the stator channel, where it is solvated as described above. The c-ring has now rotated for an angle of 360°/11.
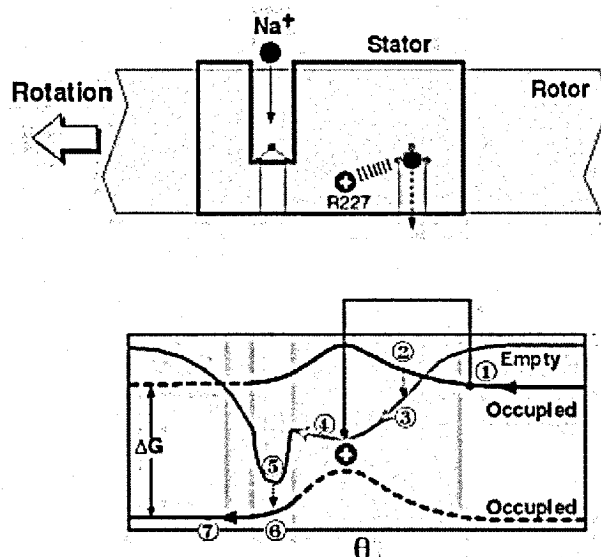

Figure 9-7. The operating principle of the F_0 motor at physiological conditions. The upper panel illustrates the events occurring in F_0 during ATP synthesis. A Na$^+$ ion enters the a/ c interface the periplasmic channel leaves the interface by rotating to the left. After almost a full revolution, the occupied binding site re-enters the interface and is forced to strip off the Na$^+$ ion by the stator charge Arg227. The lower panel describes the relative energy potential during this sequence of events. An occupied rotor site sees an occupied potential (blue), and an unoccupied site sees the empty potential (red). An empty site lies in the Coulomb well due to the stator charge (4), and an occupied rotor site is about to enter into the a-c interaction region (1). The rotor diffuses until the left site moves into the input channel, where it solvates, preventing it from leaving the channel (4→5). This motion pulls the right-hand site into the a-c interface (1→2). The left site binds a sodium ion from the periplasm to be neutralized and switches to the occupied potential (5→6). Meanwhile, the right-hand site loses its ion to the cytoplasm and switches to the empty potential curve (2→3). The empty right-hand site is then pulled into apposition with the stator charge (3→4), and pushes the left-hand site out of the interface (6→7). After one cycle, the rotor site has carried an ion from the periplasm to the cytoplasm, resulting in a free-energy decrease $\Delta G = e\Delta\psi + k_BT \times ln([Na^+]_p/[Na^+]_c)$. The sodium ions lose free energy twice: once when binding to an empty site (5→6) and again when being released into the cytoplasm (2→3). Both events take place while the corresponding rotor sites interact with the stator and are torque-generating steps. Thus the occupied potential for the rotor site emerging from the left side of the stator is ΔG lower than the occupied site entering the right side of the stator.

During ATP hydrolysis, the direction of rotation is reversed and the stator charge has now to dislodge the incoming Na^+ ions into the stator channel. To explain the experimental observations, it is needed, that the stator charge is moved slightly closer to the stator channel compared to the ATP synthesis direction.

9.4.2.2 Torque generation for ATP synthesis and the role of the membrane potential

The membrane potential comes into play in two ways. First, it must move the stator charge from its resting position (idling, hydrolysis) to a position more advantageous for attracting the incoming rotor charge (synthesis). Second, if the stator channel is partially aqueous, then only a portion of the potential drop across the membrane will take place between the cytoplasmic channel entrance and the middle of the membrane where the stator channel terminates. The rest of the potential drop must occur horizontally between the end of the stator channel and the top of the rotor channel (Dimroth et al., 1999). This portion of the membrane potential contributes an electrostatic driving force to the motion of the rotor, namely to pull the negatively charged binding site through the interface towards the stator channel (Figure 9-7, $3 \rightarrow 4 \rightarrow 5$).

The mathematical model built is able to explain all experimental data. Whereas the rough framework was established on available structural information and physical constraints, the fine tuning of the parameters was obtained by fitting a wealth of experimental data from the wild type and the mutant enzymes. Although quite a few parameters are used, none of them is extremely sensitive but rather robust towards changes, which implies a balanced set of parameters. The mathematical model was then used to calculate different information like the energy released through F_0 rotation, the membrane potential threshold or the calculated rotational speed of the system. All these data fitted well with the expected torque load for the F_1 part or the physiological ATP synthesis rate (for more information, please see (Xing et al., 2004)).

9.4.2.3 Na^+ dependency of ATP hydrolysis: Model and experiment

In the ATP hydrolysis mode, the F_1 motor drives F_0 in reverse and pumps ions from the cytoplasmic side to the periplasmic side. According to the model (Figure 9-6), a rotor site, loaded with a Na^+ ion, rotates to the right through region 1 into the rotor-stator interface. As it approaches the stator charge, electrostatic repulsion dislodges the ion into the stator input channel. For a wild-type F_0 motor, an occupied rotor is forced to give up its ion to the stator channel by the Coulomb repulsion between the stator charge and the binding ion. Laubinger et

al. (Laubinger and Dimroth, 1987; Laubinger and Dimroth, 1988) found that ATP hydrolysis requires the presence of Na^+ ions. The model predicts that the ATP hydrolysis rate increases with increasing Na^+ ion concentration, reaching a maximum at ~20 mM, then decreases at higher Na^+ concentrations. This prediction was subsequently confirmed by experiments, as shown in Figure 9-8.
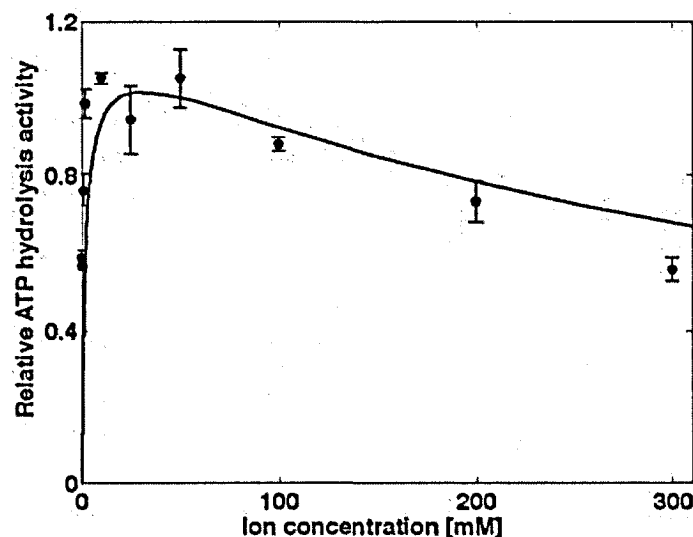

Figure 9-8. The ATP hydrolysis activity of the F_1F_0 complex as a function of the ion concentration with no membrane potential. The solid circles are experimental data and the curve is the computed prediction of the model.

9.5 General discussion

The discovery of a rotary mechanism of the ATP synthase more than 10 years ago established an entirely new class of enzymes (Abrahams *et al.*, 1996; Boyer, 1993). For the first time, not only conformational changes but integral rotation of an entire protein complex could be assigned to enzyme function. This outstanding facet has attracted attention to researchers from multiple disciplines. Next to biochemistry and molecular biology assays, the ATP synthase has been investigated by a variety of other methods like NMR, X-ray crystallography and in recent years by single molecule spectroscopy, including several imaging techniques (for a review, see (Capaldi and Aggeler, 2002)). Last but not least, the elegant rotary mechanism of the enzyme tempted physicians and mathematicians to build theoretical models, which account for the function of the enzyme (Oster and Wang, 2003).

As pointed out in the introduction of this chapter, the F_1 part of the enzyme is far better understood than its membrane embedded F_0 counterpart. However, available biochemical data in corroboration with the rotation were used to build simple mechanistic models of the F_0 motor. The formulation of the so called "two channel model" was a first important step

towards a valid working model (Junge *et al.*, 1997; Vik and Antonio, 1994). Basically, for the first time, this model combined the structural prerequisites with a few experimental findings. The essential acidic residue is assigned as a shuttle residue between the channels, which mediate the transport of the coupling ion across the membrane. Since then, a variety of changes were implemented into the working models from different research groups, mostly to adapt it optimally to their own data (Dimroth *et al.*, 2000; Fillingame *et al.*, 2003). It is therefore not surprising that 10 years later, no conclusive working model for all ATP synthases is formulated, which is commonly accepted (Dimroth *et al.*, 2003).

9.5.1 To not see the forest for the trees

The work of Aksimentiev *et al.* reports for the first time an all atom simulation of the ATP synthase F_0 motor. This model reveals more details of the process than the two other approaches by obtaining missing parameters from molecular dynamics simulation. However, the approach holds some dangers, which should be kept in mind.

1. The structural assumptions are massive. The NMR structure of a single c subunit from *E. coli* in mixed organic solvents is unlikely representing the actual conformation of the side chains in the membrane embedded ring structure (Girvin and Fillingame, 1993). Similar investigations with the *P. modestum* subunit c in the same solvent mixture as well as in detergent solution have drawn a different picture, which advises caution to the above interpretation (e.g. the assumption, that the helical structure of the amino acid chain is continuous) (Matthey *et al.*, 2002; Matthey *et al.*, 1999). Literally no real structural information is available about subunit a, except from crosslinking studies between aTMH-4 and cTMH-2 (Jiang and Fillingame, 1998). To minimize these problems, only these TMH's were allowed to rotate along their vertical axis. The proposed tilt of 17° between cTMH-1 and 2, which plays an important role in the mechanistic model, is neither observed in the medium resolution (6Å) structure of the entire c-ring of *I. tartaricus* nor in the structure of the yeast F_1-c_{10} structure (Stock *et al.*, 1999; Vonck *et al.*, 2002).

2. The so called "steered molecular dynamics" performed on the F_0 motor is largely depending on mechanistic assumptions. In other words, the mechanistic model, or the functional mode of the enzyme, was already specified. The simulation was used to calculate accurate parameters of different substeps, which however remained mechanistically the same. The uptake/ release of an ion onto a rotor binding site could

not be freely calculated, but was simulated through the protonation of the "predefined" relay residues aSer206 and aAsn214. If however such a step is actually occurring during enzyme action is highly hypothetical.

3. In a recent report of Müller *et al.* (Müller *et al.*, 2004), a contradiction between a MD simulation and an earlier experimental finding about the unwinding of an F_1 subunit was treated experimentally. Thereby, the MD simulation proved to be unable to correctly predict the enzyme's function. Obviously, the pico- to nanosecond time scale of MD simulations can not be easily transferred to the microsecond time range, which is found during enzyme function. To allow such a transfer for the observed helical rotation of cTMH-2, they introduced a ratchet function which impedes a reversible motion of the helix. Again, a strong mechanical constraint was introduced, which originated from an empirical interpretation.

4. The mathematical model is not able to predict results (or at least was not used for), which might be verified experimentally. Furthermore the question of energetization is neglected. Their interpretation, that the direction of rotation is solely determined by the relay residue's probability of being protonated is ignoring several energetic investigations about the influence of the membrane potential. Furthermore, a membrane potential was not applied separately but treated equivalently to the proton gradient as proton motive force (pmf).

Besides these objections, molecular dynamics simulations are an elegant tool to address questions, which are experimentally inaccessible. The supplied movies illustrate descriptively how molecular processes might occur (http://www.ks.uiuc.edu/Research/f0atpase/movies/). However, all atom molecular dynamic simulations are extremely computing time expensive and therefore, only a short time scale can be calculated, which might be more valuable for sub steps of a general mechanism. One has to keep in mind, that next to a high resolution structure of all components, an assured general mechanism is a prerequisite for this kind of investigation.

9.5.2 A drop in the bucket

The report of Feniouk *et al.* describes a completely different approach to investigate the mechanism of torque generation in the F_0 motor of the ATP synthase. Their elegant system to investigate the enzyme complex in an almost native environment answers several questions satisfyingly. Firstly, they determined the rate of proton transport through F_0 alone ($\sim 6'500\ H^+$

s^{-1} at a $\Delta\psi= 100$ mV) and found it to be about ten times faster as with the load of F_1 during ATP synthesis. The observed rate is in good accordance with a recent result for the *E. coli* enzyme (3100 ± 500 H^+ s^{-1}) (Franklin *et al.*, 2004). Earlier results from Junge and other groups on the rate of the proton flux were highly contradictory and the values deviated by several orders of magnitude (Lill *et al.*, 1986; Negrin *et al.*, 1980). Second, the F_0 motor is not voltage gated nor is a minimal electrical threshold necessary to drive the transport of protons. Moreover, the behaviour of the enzyme is ohmic and the transport rate is proportional to the applied proton motive force. This behaviour is in accordance to the behaviour of the F_0 enzyme of the thermophilic bacterium PS3 (Okamoto *et al.*, 1977), but in clear contradiction to the voltage gated F_0 part of *P. modestum* (see below) (Kluge and Dimroth, 1992). The importance of the membrane potential, which has been observed for enzymes from different organism during ATP synthesis is therefore attributed to the interaction of the F_0 with the F_1 part, but is not further discussed in the work (Junge, 1970; Kaim and Dimroth, 1999). The implementation of these results into a mathematical model however allows only a limited gain of new insights from a mechanistic point of view. The introduction of two relay residues into the lipid bilayer, which accommodate for the uptake and release of the coupling proton from the surrounding bulk medium is comparable to the two channel gates aSer206 and aAsn214 (Aksimentiev *et al.*, 2004). The calculation of the relative distance of these two residues within the membrane could be calculated. Thereby, the expected distance of at least 2 nm up to 3.4 nm is however far too large to be attributed to the distance of the two residues (1.2 nm) mentioned above. A critical discussion of this obvious contradiction is omitted and postponed for further investigations.

Nevertheless, this report describes valuable results with an elegant experimental system. The obtained kinetic data match the expected data of the enzyme *in vivo*, which makes this system superior to other *in vitro* systems. However, a critical debate of the results with published biochemical data of potentially important amino acid residues in subunits a and c is as well missed as a sophisticated explanation to the obvious dilemma of the obligatory role of the electrical potential. Nevertheless, if the system of *Rhodobacter capsulatus* would be accessible to genetic tools, further investigations would allow even more valuable insights into the basic mechanism of torque generation.

9.5.3 To compare apples with oranges?

Finally, the report of Xing *et al.* describes the development of a balanced model based on many observed experimental data. Mutational studies as well as structural information were used to build a model to explain all actual data. In contrary to the two other studies, this work focuses on Na^+-translocating enzymes.

Roughly, the model is built on conclusions and restrictions from mechanistic interpretations of the experimental data. This allowed drawing of empirical energy profiles of the transport processes, which were afterwards used to build the mathematical model. The model was then used to calculate several critical parameters of the enzyme function, e.g. the influence of the membrane potential on the rotation rate or of the Na^+ concentration on the transport processes, which could be validated through experiments (see (Xing *et al.*, 2004) and references therein). Furthermore, the model sets for the first time a theoretical basis for the obligatory role of the membrane potential (Kaim and Dimroth, 1998a; Kaim and Dimroth, 1999; Kluge and Dimroth, 1992). It proposes, that an applied membrane potential orients the stator charge in the direction of an incoming Na^+ ion in order to trigger its release from the binding site. Furthermore, the horizontal part of the membrane potential confines the direction of rotation during ATP synthesis. In absence of a $\Delta\psi$, the position of the stator charge is relaxed and closer to the stator channel. During ATP hydrolysis, this allows an optimized release of the incoming Na^+ ions through the stator channel. In both cases, the stator charge acts as a tool for an efficient release of the ion from the incoming binding site. This model further explains the intriguing finding that the strictly conserved arginine of the stator charge can be replaced by lysine and histidine in the Na^+- but not in the H^+-translocating enzymes: The guanidine structure of the arginine residue reflects a somehow delocalized charge compared to the more localized charges of lysine and histidine. This finding is corroborated by the calculation that the effective point charge on aArg227 is about 0.75 e (Xing *et al.*, 2004) . In other words, the effective charge of histidine and lysine deviated too much from this optimized value. This could be compensated by a variation of the outside pH to a lower (histidine) or a higher (lysine) pH value, respectively (Wehrle *et al.*, 2002). Taking this together, new experiments can be formulated, which may manifest the direct interaction of the membrane potential and the stator charge. In 1992, Kluge *et al.* showed, that the uptake of Na^+ ions by the F_0 motor alone is voltage gated and that a minimal threshold of $\Delta\psi= 40$ mV is necessary to drive ion transport (Kluge and Dimroth, 1992). If such an experiment would be repeated with the stator

charge replaced by histidine or lysine, a direct influence of $\Delta\psi$ on the stator charge would be reflected by a shift of the $\Delta\psi$ dependency profile of Na^+ uptake.

9.5.4 Irregularities and regularities

A comparison of the three presented models allows drawing some rationales, which might be attributed to a common mechanism.

There is general agreement, that the interface of the rotating c-ring with the membrane embedded a subunit seems to cover at least two binding sites on the c-ring. The report of Aksimentiev *et al.* as well as the report of Xing *et al.* proposes a neat collaboration of two binding sites, with one of them being in a non ion-bound form (Aksimentiev *et al.*, 2004; Xing *et al.*, 2004). From a structural point of view, these assumptions are in accordance to electron microscopy data from the entire enzyme (Mellwig and Böttcher, 2003; Rubinstein *et al.*, 2003). All models propose an ion conductive half channel from the periplasmic reservoir to the binding site through subunit a. Furthermore, the release of the coupling ion to the cytoplasm is proposed to take place immediately before the entrance of the biding site into the a/ c interface. Although there is disagreement about the localization of the cytoplasmic half channel (c intrinsic in Na^+ enzymes and non coaxial in subunit a in H^+-enzymes), the models can not distinguish between these properties (Angevine *et al.*, 2003; von Ballmoos *et al.*, 2002). In this context, the approaches of Feniouk *et al.* and Xing *et al.* produce more convincing data, since their models are built strongly on experimental findings and less on hypothetical structural data. However, at a time point, when high resolution data from the interface of the a subunit and the c-ring are available, the method of Aksimentiev *et al.* will be of primary interest to resolve interaction of the two subunits on a molecular level.

Next to all these common properties, these reports reinforce the raise of a fundamental question. The work of Feniouk *et al.* clearly shows that the behaviour of the F_0 motor in the absence of a coupled F_1 part is not voltage gated and furthermore can be driven by a ΔpH alone. These data are well corroborated with the H^+-translocating enzyme of the thermophilic bacterium PS3 (Okamoto *et al.*, 1977). However, the report of Kluge *et al.* shows with the same clarity, that the F_0 motor of the Na^+ depending enzyme of *P. modestum* is strictly dependent on $\Delta\psi$ and can never be driven by a ΔpNa alone (Kluge and Dimroth, 1992). This contradiction inevitably raises the question, if these two enzymes work with a different mechanism.

9.5.5 Na$^+$- translocating ATP synthases – a freak of nature?

To compare the Na$^+$ and the H$^+$ ATP synthases, a closer look was taken at their kinetic rates. Roughly independently from the source organism, the hydrolysis rate of the ATP synthase is found to be around 200 to 300 ATP s^{-1} (Etzold *et al.*, 1997; Neumann *et al.*, 1998). If however, the ATP synthesis rates are compared, a large discrepancy is observed. Whereas the measured rates of the H$^+$-translocating enzymes of *E. coli* and spinach chloroplast can reach comparables values of 270 ATP s^{-1} and up to 400 ATP s^{-1}, respectively, the rates of the Na$^+$ translocating enzyme of *P. modestum* is as low as 0.5- 1 ATP s^{-1} (Etzold *et al.*, 1997; Kaim and Dimroth, 1998b). Even more interestingly, the Na$^+$ transport rates of the F$_0$ motor alone (Kluge and Dimroth, 1992) matches the Na$^+$ transport rates calculated from ATP synthesis (Kaim and Dimroth, 1998b). The report of Feniouk *et al.* however describes a ten times faster transport in the absence of the load of the F$_1$ motor. To summarize, the ATP synthase of *P. modestum* can hydrolyze as fast as any other ATP synthase, but synthesizes ATP at a much lower rate under the *in vitro* conditions employed. Furthermore, the rate limiting step seems to be intrinsic in F$_0$ and independent from the load of the F$_1$ part.

To estimate, if an enzyme with such a low synthesis rate would be sufficient for bacterial growth, a closer look at the physiological data of *P. modestum* was taken. Some 20 years ago, the discovery of a Na$^+$ dependent ATP synthase in the strictly anaerobic bacterium of *P. modestum* represented a unique metabolism in nature (Hilpert *et al.*, 1984; Schink and Pfennig, 1982). Since the conversion of the substrate succinate to propionate and CO_2, which is the primary reaction, only yields insufficient energy for substrate level phosphorylation, it remained unclear, how this organism was able to grow on this carbon source. The discovery of a membrane bound Na$^+$- dependent decarboxylase, which establishes a membrane potential, and the subsequent characterization of a Na$^+$-dependent ATP synthase, which can use the electrochemical gradient, provided an elegant solution to this dilemma. Basically, the minimal biological energy unit was thereby reduced to the energy required for the transport of a Na$^+$ ion across the membrane through the F$_1$F$_0$ ATP synthase. The stoichiometric ratio of the two motors (3.6 Na$^+$ ions are transported for 1 ATP) allows the synthesis of an ATP molecule despite the lack of a sufficient energy equivalent for the phosphorylation of ADP (Hilpert *et al.*, 1984).

	P. modestum	E. coli
Substrate measured	succinate	O_2
Growth rate	0.154	0.2
Yield (dry cells)/ mol substrate	2.1	-
Substrate consumption (mmole/ h/ g cells)	73	15
Ratio substrate: ATP	4	0.5
ATP consumption (mmole/ h/ g cells)	18.25	30
ATP synthase per g cells (mg)	8	10
ATP synthesis rate (s^{-1})	316	416
in vitro measured ATP synthesis rate (s^{-1})	~0.5- 1	270

Table 9-1 Calculation of the theoretical ATP synthase rate for the enzymes of P. modestum and E. coli. Data used for calculation derive from published data (Marr, 1991; Schink and Pfennig, 1982), except the amount of E. coli enzyme, which is set comparable to the amount of enzyme in P. modestum.

The table depicts a rough calculation of the theoretical ATP synthase activity during growth on minimal medium. Whereas the ATP synthesis rates for E. coli in vivo are in the same range as those determined in vitro, these rates deviated by more than two orders of magnitude for the P. modestum system.

Although the calculated data represent only a rough estimate, it is obvious, that the reported values of either ATP synthesis or $\Delta\psi$-driven Na^+-uptake of by the P. modestum ATP synthase represent only a minor fraction of the enzyme's capacity in vivo. It is therefore the more astonishing, that ATP hydrolysis activity at full speed (~350 ATP s^{-1}) is monitored easily, and the coupling of ATP hydrolysis to Na^+-transport can be verified by inhibition with F_0 specific compounds (unpublished data). These findings suggest, that the experimental system for ATP synthesis is not yet fully developed in order to obtain comparable ATP synthesis rates in vitro and in vivo.

9.5.6 Outlook

From a mechanistic point of view, it is of primary interest to resolve the conflicting results described above. A side by side investigation of these two kinds of enzyme has to be performed to reveal the basis of their functional difference.

1. The F_0 motor of the E. coli enzyme should be tested for its ohmic behaviour on the response to the membrane potential. This would definitely manifest the fundamental

difference between H^+ and Na^+ dependent enzymes. The available genetic tools in *E. coli* should furthermore allow investigating the molecular basis of this difference.

2. Since it can not be ruled out, that the measured Na^+ transport with reconstituted *P. modestum* enzyme yields low rates under the experimental conditions employed, great efforts should be taken to clarify this point. ATP synthesis experiments have to be optimized and new methods for well-defined Na^+ transport have to be developed.

3. Last but not least, the raised question on the working point of the membrane potential in H^+-translocating enzymes should be addressed. A first approach might include the comparison of $\Delta\psi$ and ΔpH as driving forces. If they were equivalent not only from a thermodynamic but also kinetic point of view, rates of proton flux should be comparable. However, Figure 9-4B from the work of Feniouk *et al.* implies a delayed uptake rate for ΔpH driven uptake, although not additionally treated in the text. This investigation should also be paralleled with the enzyme of *P. modestum*, in which Wehrle *et al.* found a ΔpNa driven Na^+ transport, if the stator charge aArg227 was replaced by an uncharged alanine (Wehrle *et al.*, 2002).

9.6 References

Abrahams, J.P., Buchanan, S.K., Van Raaij, M.J., Fearnley, I.M., Leslie, A.G. and Walker, J.E. (1996) The structure of bovine F_1-ATPase complexed with the peptide antibiotic efrapeptin. *Proc. Natl. Acad. Sci. USA*, **93**, 9420-9424.

Abrahams, J.P., Leslie, A.G., Lutter, R. and Walker, J.E. (1994) Structure at 2.8 A resolution of F_1-ATPase from bovine heart mitochondria. *Nature*, **370**, 621-628.

Aksimentiev, A., Balabin, I.A., Fillingame, R.H. and Schulten, K. (2004) Insights into the molecular mechanism of rotation in the F_0 sector of ATP synthase. *Biophys. J.*, **86**, 1332-1344.

Angevine, C.M. and Fillingame, R.H. (2003) Aqueous access channels in subunit a of rotary ATP synthase. *J. Biol. Chem.*, **278**, 6066-6074.

Angevine, C.M., Herold, K.A. and Fillingame, R.H. (2003) Aqueous access pathways in subunit a of rotary ATP synthase extend to both sides of the membrane. *Proc. Natl. Acad. Sci. U.S.A.*, **100**, 13179-13183.

Boyer, P.D. (1993) The binding change mechanism for ATP synthase - some probabilities and possibilities. *Biochim. Biophys. Acta*, **1140**, 215-250.

Capaldi, R.A. and Aggeler, R. (2002) Mechanism of the F_1F_0-type ATP synthase, a biological rotary motor. *Trends. Biochem. Sci.*, **27**, 154-160.

Cherepanov, D.A., Mulkidijanian, A.Y. and Junge, W. (1999) Transient accumulation of elastic energy in proton translocating ATP synthase. *FEBS Lett.*, **449**, 1-6.

Dimroth, P., Matthey, U. and Kaim, G. (2000) Critical evaluation of the one- versus the two-channel model for the operation of the ATP synthase's F(o) motor. *Biochim. Biophys. Acta*, **1459**, 506-513.

Dimroth, P., von Ballmoos, C., Meier, T. and Kaim, G. (2003) Electrical power fuels rotary ATP synthase. *Structure (Camb.)*, **11**, 1469-1473.

Dimroth, P., Wang, H., Grabe, M. and Oster, G. (1999) Energy transduction in the sodium F-ATPase of *Propionigenium modestum*. *Proc. Natl. Acad. Sci. U.S.A.*, **96**, 4924-4929.

Dmitriev, O.Y., Jones, P.C. and Fillingame, R.H. (1999) Structure of the subunit c oligomer in the F_1F_0 ATP synthase: model derived from solution structure of the monomer and cross-linking in the native enzyme. *Proc. Natl. Acad. Sci. USA*, **96**, 7785-7790.

Elston, T., Wang, H. and Oster, G. (1998) Energy transduction in ATP synthase. *Nature*, **391**, 510-513.

Etzold, C., Deckers-Hebestreit, G. and Altendorf, K. (1997) Turnover number of *Escherichia coli* F_0F_1 ATP synthase for ATP synthesis in membrane vesicles. *Eur. J. Biochem.*, **243**, 336-343.

Feniouk, B.A., Cherepanov, D.A., Voskoboynikova, N.E., Mulkidjanian, A.Y. and Junge, W. (2002) Chromatophore vesicles of *Rhodobacter capsulatus* contain on average one F_0F_1-ATP synthase each. *Biophys. J.*, **82**, 1115-1122.

Feniouk, B.A., Kozlova, M.A., Knorre, D.A., Cherepanov, D.A., Mulkidjanian, A.Y. and Junge, W. (2004) The proton-driven rotor of ATP synthase: ohmic conductance (10 fS), and absence of voltage gating. *Biophys. J.*, **86**, 4094-4109.

Fillingame, R.H., Angevine, C.M. and Dmitriev, O.Y. (2003) Mechanics of coupling proton movements to c-ring rotation in ATP synthase. *FEBS Lett.*, **555**, 29-34.

Fillingame, R.H., Jiang, W. and Dmitriev, O.Y. (2000a) Coupling H(+) transport to rotary catalysis in F-type ATP synthases: structure and organization of the transmembrane rotary motor. *J. Exp. Biol.*, **203 Pt 1**, 9-17.

Fillingame, R.H., Jiang, W. and Dmitriev, O.Y. (2000b) The oligomeric subunit c rotor in the fo sector of ATP synthase: unresolved questions in our understanding of function. *J. Bioenerg. Biomembr.*, **32**, 433-439.

Franklin, M.J., Brusilow, W.S. and Woodbury, D.J. (2004) Determination of proton flux and conductance at pH 6.8 through single F_0 sectors from *Escherichia coli*. *Biophys. J.*, **87**, 3594-3599.

Girvin, M.E. and Fillingame, R.H. (1993) Helical structure and folding of subunit c of F_1F_0 ATP synthase: 1H NMR resonance assignments and NOE analysis. *Biochemistry*, **32**, 12167-12177.

Hilpert, W., Schink, B. and Dimroth, P. (1984) Life by a new decarboxylation-dependent energy conservation mechanism with Na^+ as coupling ion. *EMBO J.*, **3**, 1665-1670.

Jiang, W. and Fillingame, R.H. (1998) Interacting helical faces of subunits a and c in the F_1F_0 ATP synthase of *Escherichia coli* defined by disulfide cross-linking. *Proc. Natl. Acad. Sci. U.S.A.*, **95**, 6607-6612.

Jiang, W., Hermolin, J. and Fillingame, R.H. (2001) The preferred stoichiometry of c subunits in the rotary motor sector of *Escherichia coli* ATP synthase is 10. *Proc. Natl. Acad. Sci. U.S.A.*, **98**, 4966-4971.

Junge, W. (1970) The critical electric potential difference for photophosphorylation. Its relation to the chemiosmotic hypothesis and to the triggering requirements of the ATPase system. *Eur. J. Biochem.*, **14**, 582-592.

Junge, W., Lill, H. and Engelbrecht, S. (1997) ATP synthase: an electrochemical transducer with rotatory mechanics. *Trends Biochem. Sci.*, **22**, 420-423.

Junge, W., Rumberg, B. and Schroder, H. (1970) The necessity of an electric potential difference and its use for photophosphorylation in short flash groups. *Eur. J. Biochem.*, **14**, 575-581.

Kaim, G. and Dimroth, P. (1998a) ATP synthesis by the F_1F_0 ATP synthase of *Escherichia coli* is obligatorily dependent on the electric potential. *FEBS Lett.*, **434**, 57-60.

Kaim, G. and Dimroth, P. (1998b) Voltage-generated torque drives the motor of the ATP synthase. *EMBO J.*, **17**, 5887-5895.

Kaim, G. and Dimroth, P. (1999) ATP synthesis by F-type ATP synthase is obligatorily dependent on the transmembrane voltage. *EMBO J*, **18**, 4118-4827.

Kluge, C. and Dimroth, P. (1992) Studies on Na^+ and H^+ translocation through the F_0 part of the Na^+-translocating F_1F_0 ATPase from *Propionigenium modestum*: discovery of a membrane potential dependent step. *Biochemistry*, **31**, 12665-12672.

Laubinger, W. and Dimroth, P. (1987) Characterization of the Na^+-stimulated ATPase of *Propionigenium modestum* as an enzyme of the F_1F_0 type. *Eur. J. Biochem.*, **168**, 475-480.

Laubinger, W. and Dimroth, P. (1988) Characterization of the ATP synthase of *Propionigenium modestum* as a primary sodium pump. *Biochemistry*, **27**, 7531-7537.

Lill, H., Engelbrecht, S., Schonknecht, G. and Junge, W. (1986) The proton channel, CF_0, in thylakoid membranes. Only a low proportion of CF_1-lacking CF_0 is active with a high unit conductance (169 fS). *Eur. J. Biochem.*, **160**, 627-634.

Marr, A.G. (1991) Growth rate of *Escherichia coli*. *Microbiol. Rev.*, **55**, 316-333.

Matthey, U., Braun, D. and Dimroth, P. (2002) NMR investigations of subunit c of the ATP synthase from Propionigenium modestum in chloroform/methanol/water (4: 4: 1). *Eur. J. Biochem.*, **269**, 1942-1946.

Matthey, U., Kaim, G., Braun, D., Wüthrich, K. and Dimroth, P. (1999) NMR studies of subunit c of the ATP synthase from *Propionigenium modestum* in dodecylsulfate micelles. *Eur. J. Biochem.*, **261**, 459-467.

Mellwig, C. and Böttcher, B. (2003) A unique resting position of the ATP-synthase from chloroplasts. *J. Biol. Chem.*, **278**, 18544-18549.

Müller, M., Gumbiowski, K., Cherepanov, D.A., Winkler, S., Junge, W., Engelbrecht, S. and Pänke, O. (2004) Rotary F_1-ATPase. Is the C-terminus of subunit gamma fixed or mobile? *Eur. J. Biochem.*, **271**, 3914-3922.

Negrin, R.S., Foster, D.L. and Fillingame, R.H. (1980) Energy-transducing H^+-ATPase of *Escherichia coli*. Reconstitution of proton translocation activity of the intrinsic membrane sector. *J. Biol. Chem.*, **255**, 5643-5648.

Neumann, S., Matthey, U., Kaim, G. and Dimroth, P. (1998) Purification and properties of the F_1F_0 ATPase of *Ilyobacter tartaricus*, a sodium ion pump. *J. Bacteriol.*, **180**, 3312-3316.

Okamoto, H., Sone, N., Hirata, H., Yoshida, M. and Kagawa, Y. (1977) Purified proton conductor in proton translocating adenosine triphosphatase of a thermophilic bacterium. *J. Biol. Chem.*, **252**, 6125-6131.

Oster, G. and Wang, H. (2003) Rotary protein motors. *Trends Cell. Biol.*, **13**, 114-121.

Rastogi, V.K. and Girvin, M.E. (1999) Structural changes linked to proton translocation by subunit c of the ATP synthase. *Nature*, **402**, 263-268.

Rubinstein, J.L., Walker, J.E. and Henderson, R. (2003) Structure of the mitochondrial ATP synthase by electron cryomicroscopy. *EMBO J.*, **22**, 6182-6192.

Schink, B. and Pfennig, N. (1982) *Propionigenium modestum* gen. nov. sp. nov. a new strictly anaerobic, nonsporing bacterium growing on succinate. *Arch. Microbiol.*, **133**, 209-216.

Stock, D., Leslie, A.G. and Walker, J.E. (1999) Molecular architecture of the rotary motor in ATP synthase. *Science*, **286**, 1700-1705.

Vik, S.B. and Antonio, B.J. (1994) A mechanism of proton translocation by F_1F_0 ATP synthases suggested by double mutants of the a subunit. *J. Biol. Chem.*, **269**, 30364-30369.

von Ballmoos, C., Appoldt, Y., Brunner, J., Granier, T., Vasella, A. and Dimroth, P. (2002) Membrane topography of the coupling ion binding site in Na^+-translocating F_1F_0 ATP synthase. *J. Biol. Chem.*, **277**, 3504-3510.

Vonck, J., Krug von Nidda, T., Meier, T., Matthey, U., Mills, D.J., Kühlbrandt, W. and Dimroth, P. (2002) Molecular architecture of the undecameric rotor of a bacterial Na^+-ATP synthase. *submitted*.

Wehrle, F., Kaim, G. and Dimroth, P. (2002) Molecular mechanism of the ATP synthase's F_0 motor probed by mutational analyses of subunit a. *J. Mol. Biol.*, **322**, 369-381.

Xing, J., Wang, H., von Ballmoos, C., Dimroth, P. and Oster, G. (2004) Torque generation by the F_0 motor of the sodium ATPase. *Biophys. J.*, **87**, 2148-2163.

Appendix

3D- visualization of the rotary mechanism of Na^+-dependent ATP synthase

The application 3dsmax, version 6 (Discreet) was used to create the animation of the enzyme. A trial version of the application (with a 30 days period of validity) was downloaded from the official homepage and installed. The animation was created within these 30 days and is not suited for commercial purpose.

The movie can be downloaded from the homepage of the Peter Dimroth group.

http://www.micro.biol.ethz.ch/re/re_dimroth/movie10x7.avi

Additional information:

http://www.discreet.com

Curriculum vitae

Christoph von Ballmoos

Born, 26th of July, 1974 in Bern, Switzerland
Citizen of Heimiswil (BE), Switzerland

1981-84	Primary education in Lyssach (BE)
1985-86	Secondary education in Kirchberg (BE)
1987-94	Gymnasium in Burgdorf (BE); Final examination: Matura Typus C
1995-2000	Studies of biology at the Swiss Federal Institute of Technology (ETH), Zürich Diploma thesis in the Institute of Biochemistry
2001-2005	Assistant researcher at the Institute of Microbiology, ETH Zürich Ph.D. thesis

List of publications

von Ballmoos C., Appoldt Y., Brunner J., Granier T., Vasella A., and Dimroth P. (2002). Membrane topography of the coupling ion binding site in Na$^+$-translocating F$_1$F$_0$ ATP synthase. *J. Biol. Chem.* 277(5):3504-10.

von Ballmoos C., Meier T., Dimroth P. (2002). Membrane embedded location of Na$^+$ or H$^+$ binding sites on the rotor ring of F$_1$F$_0$ ATP synthases. *Eur. J. Biochem.*, 269(22):5581-9.

Meier T., Matthey U., von Ballmoos C., Vonck J., Krug von Nidda T., Kühlbrandt W. and Dimroth P. (2003). Evidence for structural integrity in the undecameric c-rings isolated from sodium ATP synthases. *J. Mol. Biol.*, 325(2):389-97.

Meier T., von Ballmoos C., Neumann S. and Kaim G. (2003). Complete DNA sequence of the *atp* operon of the sodium-dependent F$_1$F$_0$ ATP synthase from *Ilyobacter tartaricus* and identification of the encoded subunits. *Biochim. Biophys. Acta.,* 1625(2):221-6.

Cook G.M., Keis S., Morgan H.W., von Ballmoos C., Matthey U., Kaim G. and Dimroth P. (2003). Purification and biochemical characterization of the F$_1$F$_0$-ATP synthase from thermoalkaliphilic *Bacillus* sp. strain TA2.A1. *J. Bacteriol.,* 185(15):4442-9.

Dimroth P., von Ballmoos C., Meier T., and Kaim G. (2003). Electrical power fuels rotary ATP synthase. *Structure (Camb).*;11(12):1469-73. *Review.*

von Ballmoos C., Brunner J. and Dimroth P. (2004). The ion channel of F-ATP synthase is the target of toxic organotin compounds. *Proc.Natl.Acad.Sci.U.S.A.,*101(31):11239-44.

Xing J., Wang H., von Ballmoos C., Dimroth P. and Oster G. (2004). Torque generation by the F$_0$ motor of the sodium ATPase. *Biophys. J.,* 87(4):2148-63.

von Ballmoos C., and Dimroth P. (2004). A continuous fluorescent method for measuring Na$^+$ transport. *Anal. Biochem.* 335(2):334-7.

von Ballmoos C. und Dimroth P. (2004). Partnersuche im Energiekraftwerk der Zelle. *ETH Bulletin,* 295:44-47